



Universiteit
Leiden
The Netherlands

Thromboinflammation in high-risk human populations

Yuan, L.

Citation

Yuan, L. (2023, November 7). *Thromboinflammation in high-risk human populations*. Retrieved from <https://hdl.handle.net/1887/3656071>

Version: Publisher's Version

License: [Licence agreement concerning inclusion of doctoral thesis in the Institutional Repository of the University of Leiden](#)

Downloaded from: <https://hdl.handle.net/1887/3656071>

Note: To cite this publication please use the final published version (if applicable).

Thromboinflammation in high-risk human populations

Lushun Yuan

ISBN: 978-94-93289-33-8

Cover design: Manon Zuurmond and Lushun Yuan

Layout and printing: printsupport4u.nl

Copyright © Lushun Yuan, 2023

All rights reserved. No part of this publication may be reproduced, stored in a retrieval system, or transmitted, in any form or by any means, electronically, mechanically, by photocopying, recording or otherwise, without the prior written permission of the author.

Thromboinflammation in high-risk human populations

Proefschrift

er verkrijging van

de graad van doctor aan de Universiteit Leiden,
op gezag van rector magnificus prof.dr.ir. H. Bijl,
volgens besluit van het college voor promoties
te verdedigen op dinsdag 7 november 2023

klokke 13.45 uur

door

Lushun Yuan

geboren te Shanghai, China

in 1992

Promotor

Prof. Dr. T.J. Rabelink

Co-promotor

Dr. B.M. van den Berg

Promotiecommissie

Prof. Dr. P.C.N. Rensen

Dr. M.S. Arbous

Prof. Dr. J.A.P. Willems van Dijk

Prof. Dr. B.J. van den Born *Amsterdam UMC, University of Amsterdam*

Prof. Dr. F.L.J. Visseren *University Medical Center Utrecht*

The studies presented in this thesis were carried out at the Department of Internal Medicine, Division of Nephrology, Leiden University Medical Center, the Netherlands. The works were supported by ZonMW (The Enabling Technologies Hotels program, grant: 435005003, 2019), the China Scholarship Council grant to Lushun Yuan (CSC no. 201806270262) and BEAT-COVID funding by Leiden University Medical Center.

Contents

Chapter 1: General introduction and outline of the thesis

Chapter 2: Sex-specific association between microvascular health and coagulation parameters: the Netherlands Epidemiology of Obesity (NEO) Study

Chapter 3: Altered HDL composition is associated with risk for complications in type 2 diabetes mellitus in South Asian descendants: a cross-sectional, case-control study on lipoprotein subclass profiling

Chapter 4: Diacylglycerol abnormalities in diabetic nephropathy in Dutch South Asians and Dutch white Caucasians with type 2 diabetes mellitus: lipidomic phenotyping of plasma in a cross-sectional study

Chapter 5: Heparan sulfate mimetic fucoidan restores the endothelial glycocalyx and protects against dysfunction induced by serum of COVID-19 patients in the intensive care unit

Chapter 6: High-density lipoprotein composition related to endothelial dysfunction is associated with disease outcome in COVID-19 patients

Chapter 7: Summary, general discussion, and future perspectives

Chapter 8: Nederlandse Samenvatting, algemene discussie en toekomstperspectieven

Curriculum Vitae

List of Publications

Acknowledgements

CHAPTER

1

General introduction and outline of the thesis

1. Endothelium: a key regulator in inflammation and Coagulation

The biological systems of coagulation and inflammation are intricately intertwined and delicately balanced, with a great deal of crosstalk between each other. Whereby inflammation not only leads to coagulation activation, but coagulation also considerably affects inflammatory activity. When any one component is out of balance, the entire balance is thrown off, resulting in a wide range of disorders with varying degrees of excess inflammation and thrombosis.

The endothelium is the fundamental regulator in both systems. Quiescent endothelial cells reveal an anti-coagulant surface phenotype by repressing tissue factor (TF) expression and releasing anti-thrombogenic factors (e.g, TF pathway inhibitor). Endothelial cells become activated and rapidly shift in response to inflammation in either acute illnesses such as sepsis and COVID-19 or chronic inflammatory states such as diabetes and obesity, disrupting the hemostatic balance which could lead to a procoagulant state [1]. TF plays a critical role in procoagulant phenotype switching and endothelial dysfunction. In experimental *in vitro* situations, a wide range of inflammatory cytokines, including tumor necrosis factor (TNF)- α , IL-1, and IFN-I beta, together with C-reactive protein (CRP) and lipopolysaccharides (LPS) have been shown to increase TF expression in endothelial cells [2-5]. Such an increase in TF initiates the extrinsic coagulation pathway which allows complex forming with circulating factor VIIa, enhancing the catalytic activity of the latter and triggering coagulation by activating coagulation factor X [6, 7] and participating in the prothrombinase complex (FVa: FXa). The prothrombinase complex (FVa: FXa) activates prothrombin (PT) to thrombin. Once the generated thrombin concentration exceeds a threshold beyond physiological conditions, it leads to a pro-inflammatory state and triggers a wide spectrum of endothelial responses [8]. This includes the induction of adhesion molecules that facilitate leukocyte binding and transmigration, such as E-selectin, P-selectin, intracellular cell adhesion molecule-1 (ICAM-1), and vascular cell adhesion molecule-1 (VCAM-1), as well as the disruption of the endothelial barrier function, the release of proinflammatory cytokines and complement activation [9-13].

Additionally, previous studies showed that the TF-FVIIa complex could stimulate proteinase-activated receptor (PAR) signaling, which induces the release of inflammatory cytokines and chemokines [14].

Endothelial cells of all blood vessels are covered with an endothelial glycocalyx, a tight matrix of glycosaminoglycans, such as heparan sulfate (HS) and chondroitin sulfate (CS) anchored in the cell membrane by a protein backbone, together as proteoglycans, and intertwined with hyaluronan (HA), a glycosaminoglycan not covalently linked [15, 16]. The endothelial glycocalyx together with associated proteins, such as lipase, growth factors, and chemokines, forming a bioactive surface layer [17], and plays a critical role in maintaining vascular integrity and homeostasis, regulating endothelial mechanotransduction, vascular permeability, coagulation, and inflammation [18, 19].

Under physiological conditions, the endothelial glycocalyx composition inhibits blood coagulation. For example, 3-O sulfate modification of HS inhibits Factor Xa activity, and further blocks thrombin generation [20]; besides, other components such as syndecan-1 and hyaluronic acid also interfere with clot formation (inhibits both intrinsic and extrinsic pathway) and affect fibrin polymerization [21]. Tissue factor pathway inhibitor (TFPI) in turn, binds to endothelial cells via HS and as such prevents initiation of coagulation by blocking the actions of the FVIIa-TF complex. HS binding and sequestering protein anti-thrombin III (ATIII) to the cell surface is capable of inhibiting thrombin activity produced by the coagulation cascade, whereas thrombomodulin (TM), also bound to HS binds thrombin, inhibiting fibrin generation. Subsequently, thrombin-TM complexes activate protein C, and activated protein C (APC) inactivates coagulation factors Va and VIIIa, thereby inhibiting further thrombin generation [22]. Intracellular Weibel-Palade bodies (WPB) in endothelial cells store von Willebrand factor (vWF), a protein enhancing the interaction with platelets. HS chains are reported to act as a relevant binding factor for vWF fibers at the endothelial cell surface [23]. In addition to its anti-coagulation function, the endothelial glycocalyx is involved in inflammation. As HS compositional changes can induce binding and signaling in inflammatory conditions, numerous studies have shown

that HS, via its protein-binding properties, regulates inflammatory responses [24-27]. For example, CCL2 is a well-known proinflammatory chemokine, playing a critical role in macrophage recruitment and polarization during inflammation [28]. HS, particularly 3-O-sulfated HS domains, can interact with C-C Motif Chemokine Ligand 2 (CCL2), which further regulates vascular integrity and homeostasis through the CCL2/CCR2 signaling pathway [29, 30]. Also, N- and 6-O-sulfated HS domains were remarkably increased on glomerular endothelium under inflammatory conditions, enhancing leukocyte adhesion *in vitro* [31]. Finally, loss of HA could lead to impaired microvascular perfusion and endothelial stability via disturbed angiotensin1- TEK receptor tyrosine kinase (TIE2) signaling, stabilizing VE-cadherin cell-cell interactions [32].

Impairment of the endothelial glycocalyx during various pathological conditions, therefore, can result in the initiation of both the inflammation and coagulation system which results in thromboinflammation. Thromboinflammation, the activating interplay of thrombosis and inflammation not only drives cardiovascular disease but also induces acute severe illness, such as sepsis, acute respiratory distress syndrome (ARDS), and disseminated intravascular coagulation (DIC). In the current thesis, I specifically will discuss the role of thromboinflammation in the participants of the Netherlands Epidemiology of Obesity (NEO) study and high-risk patient populations during the COVID-19 pandemic and South-Asian Surinamese participants with type 2 diabetes mellitus (T2DM).

2. Thromboinflammation and gender

Accumulating evidence shows that sex-specific pathophysiological mechanisms play a growing role in the development of cardiovascular disease (CVD). Thromboinflammation, as one of the risk factors for CVD, also exhibits certain sex differences.

C-reactive protein (CRP), the most studied inflammatory marker, is primarily released from the liver following cytokine stimulation [33]. CRP has been shown to predict cardiovascular events in both men and women independently [34, 35]. However, various groups have reported remarkable sex differences in CRP, in which the CRP concentration in women is much higher than in men [36-42]. The well-documented sex differences in body fat distribution and sex hormone concentrations might be key determinants in sex dimorphism [43, 44]. For instance, CRP concentration was found to be higher in premenopausal women than in men, owing to the increasing effect of estrogens [36]. Meanwhile, the use of oral contraceptive drugs and postmenopausal hormone replacement therapy was also able to raise CRP levels [45, 46]. CRP is tightly correlated with both subcutaneous and visceral adipose tissue. Postmenopausal and perimenopausal women have more ectopic fat accumulation (i.e., visceral adipose tissue) than premenopausal women, and women have more subcutaneous fat than men, which contributes to higher CRP concentrations in women [47].

Women not only appear to have higher plasma levels of inflammatory factors, but they also have higher fibrinogen plasma levels than men of the same age and ethnic group [48], pushing the balance from fibrinolysis to clotting [49]. Plasma fibrinogen was reported to be associated with morbidity and mortality in coronary heart disease (CHD) patients [50-52] and to the extent of coronary atherosclerosis [53]. Besides, the levels of coagulation factors II, VII, X, IX, XI, and XII are higher in women than in men [54]. These elevated coagulation factors have been associated with an increased risk of CHD in multiple studies [55, 56].

Sex differences in presence of inflammatory- and coagulation factors therefore might lead to differences in microvascular health and contribute to a different clinical presentation and outcome of CVD. In previous decades, men were thought to be more susceptible to coronary heart disease (CHD) than women [57]. However, the risk of CHD in women is frequently underestimated due to the under-recognition of CHD and distinct clinical presentations, which eventually when discovered resulted in a poor prognosis [58].

Therefore, it is important to study the significance of microvascular dysfunction in the pathophysiology of CHD and how this may differ by sex.

3. Thromboinflammation and diabetes

T2DM is characterized by insulin resistance and insufficient compensatory insulin secretion, the mechanism of which varies by ethnicity.

Thromboinflammation is commonly observed in patients with diabetes [59]. A previous epidemiological study in the general population demonstrated that increased levels of fasting glucose, HbA1c, and postprandial glucose response were associated with higher activity of FVIII, FIX, and FXI, and to some extent also with increased concentration of fibrinogen, which provided some evidence between hyperglycemia and coagulation [60]. Another study revealed that platelets of patients with diabetes had an increased capacity of mediating microvascular thrombosis and inflammation during ischemia-reperfusion injury [61].

Several mechanisms might be involved in the diabetes-associated thromboinflammation process. One mechanism is associated with platelet aggregation/activation, such as platelet-derived chemokine C-X-C motif ligand 14 (CXCL14). CXCL14 is one of the potential players in the development of thromboinflammation in diabetes expressing proinflammatory properties through its involvement in thrombus formation, platelet migration, and monocyte migration [62, 63]. Besides, platelets can interact with inflammatory cells by regulating lipids in a paracrine manner [64]. A recent study showed that the platelet atypical chemokine receptor 3 (ACKR3)/ CXC-chemokine receptor 7 (CXCR7) interaction is capable of favoring antiplatelet lipids over an atherothrombotic lipidome and regulating thromboinflammation [65].

Another mechanism at play in diabetes involves the endothelial glycocalyx in platelet adhesion to the endothelium of damaged vessels [66]. Our previous study showed that loss of endothelial hyaluronan, a key component of the extracellular matrix, could lead to disturbed glomerular endothelial stabilization [18]. Besides, the endothelial glycocalyx is perturbed upon treatment with human diabetic serum [67]. The impaired endothelial glycocalyx could lead to increased ICAM1 and decreased eNOS expression [68], which might contribute to platelet activation [69, 70], thus forming a procoagulant cell surface and further promoting thromboinflammation.

Increasing studies investigate the biological functions of high-density lipoproteins (HDL) in pathophysiological conditions including cholesterol efflux mediation, capacity of anti-oxidation, anti-inflammation, and anti-thrombosis [71, 72]. Given the causal relationship between HDL function and diabetes [73-76], it may yet be another novel mechanism causing thromboinflammation in subjects with diabetes. Numerous epidemiological studies have shown that low levels of plasma HDL cholesterol (HDL-C) were associated with an elevated risk of T2DM and cardiovascular disease [77-79]. Also, the function of HDL was associated with incidence of cardiovascular disease and prognosis of heart failure [80-82]. Interestingly, accumulation of symmetric dimethylarginine, a marker associated with diabetes, could lead to HDL dysfunction, switching to an endothelial-damaging phenotype, and then mediating glycocalyx breakdown [83].

4. Thromboinflammation and COVID-19

Severe acute respiratory syndrome coronavirus-2 (SARS-CoV-2) infection caused the coronavirus disease 2019 (COVID-19), and its worldwide spreading led to a global pandemic since late 2019 [84]. Although the majority of COVID-19 patients are asymptomatic or only showed mild symptoms [85], it is worth noting that part of the patients suffered from respiratory illness in the early disease stage, and rapidly progressed

into respiratory failure [86, 87]. Additionally, there was an increased incidence of thromboembolism events during hospitalization in the intensive care unit (ICU) [88]. ARDS and coagulopathy are major contributors to the mortality of COVID-19 [89], while endothelial dysfunction is reported to participate in both ARDS and coagulopathy [90, 91]. Severe pulmonary endothelial damage was observed in autopsy of COVID-19 non-survivors [92], therefore, COVID-19 could be regarded as an endothelial disease. Endothelial dysfunction with subsequent COVID-19-related thromboinflammation might play a vital role in the pathogenesis of ARDS and coagulopathy.

Hyperinflammation is involved in the severe illness of COVID-19 resulting in a cytokine storm regarding to increased levels of pro-inflammatory cytokines [85, 93-97]. Although the observed cytokine storm in COVID-19 patients was lower than those with non-COVID-19 severe cases with ARDS, sepsis, and influenza virus infection [98, 99], COVID-19 patients exhibited decreased innate antiviral defenses accompanied by exploded inflammatory cytokine production [100]. NLR family pyrin domain containing 3 (NLRP3) inflammasome was activated by SARS-CoV-2 in the lungs of patients who died from COVID-19-associated ARDS. *In vitro* studies on primary human monocytes revealed that SARS-CoV-2 infection activated the NLRP3 inflammasome [101, 102]. Furthermore, IL-1 and IL-18, products of NLRP3 inflammasome, are elevated in the COVID-19 patients with critical illness and are associated with poor clinical outcomes [102].

In addition to the hyperinflammation, SARS-CoV-2 infection could also lead to a prothrombotic state. Patients with severe COVID-19 were associated with endogenous activation of coagulation and fibrinolysis; but different from sepsis-induced hypercoagulant status, patients with COVID-19 showed a loss of coagulation-initiating mechanisms [103]. Moreover, emerging evidence demonstrated that the complement system had a role in the maladaptive immune response that promotes hyperinflammation and thrombotic microangiopathy, increasing COVID-19 mortality [104]. SARS-CoV-2 was found to trigger complement-mediated endothelial damage, cause deregulations of the coagulation cascade, and further result in adverse clinical presentations [105-107]. Despite

the indirect effect of the complement activation, COVID-19-associated coagulopathy is also suggested to be caused by endothelial dysfunction. Endothelial activation markers such as von Willebrand factor (vWF) and Angiopoietin 2 (ANG2) were elevated in patients with SARS-CoV-2 infection and associated with disease severity [108, 109]. In COVID-19 patients, elevated circulating ANG2 levels have been linked to decreased respiratory function, hypercoagulable status, acute kidney injury, and increased mortality [109-112]. ANG2 also was shown to mediate the endothelial glycocalyx breakdown [113], and the MYSTIC study revealed that glycocalyx health, as measured by perfused boundary region (PBR), an inversed reflection of endothelial glycocalyx layer, was a prognostic predictor for COVID-19 and disease severity [109].

Early studies of lipid metabolism in patients revealed a role for high-density lipoproteins (HDL) protective factors in a variety of endothelial functions such as antioxidant, anti-inflammatory, anti-thrombotic, and even anti-infectious properties [114, 115]. Thromboinflammation in COVID-19 might be also induced by HDL dysregulation. Recently, it was observed that the metabolic lipid profile in COVID-19 patients in the ICU was different when compared to healthy controls or patients with cardiogenic shock in ICU [116]. It is worth noting that increasing evidence suggested that low serum HDL-cholesterol (HDL-C) levels at hospital admission are associated with disease severity and mortality in COVID-19 [117, 118]. However, other studies revealed that the HDL lipidome and proteome rather than quantitative HDL-C concentration play a more representative role in HDL function during disease [80, 119]. In addition to HDL-C concentrations in COVID-19, several studies showed significant inflammatory remodeling of the HDL proteome, associated with COVID-19 disease severity in both adult and pediatric COVID-19 patients [119-121].

Outline of this thesis

In this thesis, we address the role of thromboinflammation in different high-risk populations, such as women versus men in the general Dutch population, type 2 diabetes mellitus, and COVID-19 patients.

Recent research reveals that microvascular dysfunction more commonly in women is a growing determinant of sex difference in coronary heart disease. In **Chapter 2**, we examined the sex differences in the relationship between microvascular health and coagulation parameters in a middle-aged Dutch population and revealed a hitherto unreported sex-specific association between microcirculatory health and procoagulant status, which suggests considering microvascular health in the early development of coronary heart disease in women.

HDL particles exhibit large heterogeneity in size, density, and composition. The composition of HDL can partly affect various functions including mediating cholesterol efflux, anti-oxidation, anti-inflammation, and anti-thrombotic processes, which is becoming an important determinant in the development of microvascular complications in T2DM. In **Chapter 3**, we used ^1H nuclear magnetic resonance (NMR) spectroscopy and Bruker IVDr Lipoprotein Subclass Analysis (B.I.LISATM) software to determine the changes in plasma HDL (both particle size and lipid composition) in healthy individuals (Dutch white Caucasian [DwC], Dutch South Asian [DSA]) and individuals with T2DM. We also investigated the role of HDL in anti-thrombotic capacity, determined as the ability to suppress TNF- α induced thrombin generation in endothelial cells *in vitro*.

Lipids play an essential role in both the intrinsic and extrinsic pathways of prothrombin activation and dyslipidemia is one of the hallmarks of T2DM. Oxidized lipids could contribute to thrombus initiation and growth in oxidative stress-induced cardiovascular diseases. Following the previous study, in **Chapter 4**, we used the LC/MS-based LipidyzerTM platform to measure the same participants mentioned above to study the biological

mechanisms underlying the link between dyslipidemia and T2DM in different ethnic groups.

Evidence of pulmonary microvascular thrombosis and inflammation were found on autopsy of COVID-19 non-survivors, leading to the increasing concern on thromboinflammation in the disease pathogenesis. In **Chapter 5**, we explored how serum factors affect vascular integrity in patients with severe COVID-19 (glycocalyx function, barrier function, and anti-coagulation capacity). Serum from COVID-19 patients in the ICU could induce endothelial dysfunction, characterized by endothelial glycocalyx degradation, endothelial barrier failure, and hypercoagulable status, which could be targeted earlier in the disease by supplementation of heparin sulfate mimetics. As HDL has both anti-inflammatory and anti-thrombotic capacity regarding thromboinflammation, therefore, in **Chapter 6**, we measured blood HDL subclasses and lipid content concentrations in longitudinally collected serum samples from ICU and non-ICU, together with age-matched healthy controls using ^1H NMR spectroscopy and the validated B.I.LISATM software to identify HDL composition concerning disease progression, and endothelial function, and investigate whether specific HDL compositional changes could lead to different outcomes in the course of the disease.

In **Chapter 7**, we summarize and discuss the observations in this thesis, as well as future perspectives.

References

- 1 Szotowski B, Antoniak S, Poller W, Schultheiss HP, Rauch U. Procoagulant soluble tissue factor is released from endothelial cells in response to inflammatory cytokines. *Circ Res*. 2005; **96**: 1233-9. 10.1161/01.RES.0000171805.24799.fa.
- 2 Eisenreich A, Bogdanov VY, Zakrzewicz A, Pries A, Antoniak S, Poller W, Schultheiss HP, Rauch U. Cdc2-like kinases and DNA topoisomerase I regulate alternative splicing of tissue factor in human endothelial cells. *Circ Res*. 2009; **104**: 589-99. 10.1161/CIRCRESAHA.108.183905.

- 3 Napoleone E, Di Santo A, Lorenzet R. Monocytes upregulate endothelial cell expression of tissue factor: a role for cell-cell contact and cross-talk. *Blood*. 1997; **89**: 541-9.
- 4 Cirillo P, Golino P, Calabro P, Cali G, Ragni M, De Rosa S, Cimmino G, Pacileo M, De Palma R, Forte L, Gargiulo A, Corigliano FG, Angri V, Spagnuolo R, Nitsch L, Chiariello M. C-reactive protein induces tissue factor expression and promotes smooth muscle and endothelial cell proliferation. *Cardiovasc Res*. 2005; **68**: 47-55. 10.1016/j.cardiores.2005.05.010.
- 5 Chen Y, Wang J, Yao Y, Yuan W, Kong M, Lin Y, Geng D, Nie R. CRP regulates the expression and activity of tissue factor as well as tissue factor pathway inhibitor via NF-kappaB and ERK 1/2 MAPK pathway. *FEBS Lett*. 2009; **583**: 2811-8. 10.1016/j.febslet.2009.07.037.
- 6 Morrissey JH. Tissue factor interactions with factor VII: measurement and clinical significance of factor VIIa in plasma. *Blood Coagul Fibrinolysis*. 1995; **6 Suppl 1**: S14-9.
- 7 Yuan L, Cheng S, Sol W, van der Velden AIM, Vink H, Rabelink TJ, van den Berg BM. Heparan sulfate mimetic fucoidan restores the endothelial glycocalyx and protects against dysfunction induced by serum of COVID-19 patients in the intensive care unit. *ERJ Open Res*. 2022; **8**. 10.1183/23120541.00652-2021.
- 8 Popovic M, Smiljanic K, Dobutovic B, Syrovets T, Simmet T, Isenovic ER. Thrombin and vascular inflammation. *Mol Cell Biochem*. 2012; **359**: 301-13. 10.1007/s11010-011-1024-x.
- 9 Cheng S, Wu D, Yuan L, Liu H, Ei-Seedi HR, Du M. Crassostrea gigas-Based Bioactive Peptide Protected Thrombin-Treated Endothelial Cells against Thrombosis and Cell Barrier Dysfunction. *J Agric Food Chem*. 2022; **70**: 9664-73. 10.1021/acs.jafc.2c02435.
- 10 Papadaki S, Sidiropoulou S, Moschonas IC, Tselepis AD. Factor Xa and thrombin induce endothelial progenitor cell activation. The effect of direct oral anticoagulants. *Platelets*. 2021; **32**: 807-14. 10.1080/09537104.2020.1802413.
- 11 Giri H, Srivastava AK, Naik UP. Apoptosis signal-regulating kinase-1 regulates thrombin-induced endothelial permeability. *Vascul Pharmacol*. 2022; **145**: 107088. 10.1016/j.vph.2022.107088.
- 12 Durigutto P, Macor P, Pozzi N, Agostinis C, Bossi F, Meroni PL, Grossi C, Borghi MO, Planer W, Garred P, Tedesco F. Complement Activation and Thrombin Generation by MBL Bound to beta2-Glycoprotein I. *J Immunol*. 2020; **205**: 1385-92. 10.4049/jimmunol.2000570.
- 13 Puy C, Pang J, Reitsma SE, Lorentz CU, Tucker EI, Gailani D, Gruber A, Lupu F, McCarty OJT. Cross-Talk between the Complement Pathway and the Contact Activation System of Coagulation: Activated Factor XI Neutralizes Complement Factor H. *J Immunol*. 2021; **206**: 1784-92. 10.4049/jimmunol.2000398.

- 14 Kondreddy V, Wang J, Keshava S, Esmon CT, Rao LVM, Pendurthi UR. Factor VIIa induces anti-inflammatory signaling via EPCR and PAR1. *Blood*. 2018; **131**: 2379-92. 10.1182/blood-2017-10-813527.
- 15 Boels MG, Lee DH, van den Berg BM, Dane MJ, van der Vlag J, Rabelink TJ. The endothelial glycocalyx as a potential modifier of the hemolytic uremic syndrome. *Eur J Intern Med*. 2013; **24**: 503-9. 10.1016/j.ejim.2012.12.016.
- 16 Wang G, Tiemeier GL, van den Berg BM, Rabelink TJ. Endothelial Glycocalyx Hyaluronan: Regulation and Role in Prevention of Diabetic Complications. *Am J Pathol*. 2020; **190**: 781-90. 10.1016/j.ajpath.2019.07.022.
- 17 Reitsma S, Slaaf DW, Vink H, van Zandvoort MA, oude Egbrink MG. The endothelial glycocalyx: composition, functions, and visualization. *Pflugers Arch*. 2007; **454**: 345-59. 10.1007/s00424-007-0212-8.
- 18 van den Berg BM, Wang G, Boels MGS, Avramut MC, Jansen E, Sol W, Lebrin F, van Zonneveld AJ, de Koning EJP, Vink H, Grone HJ, Carmeliet P, van der Vlag J, Rabelink TJ. Glomerular Function and Structural Integrity Depend on Hyaluronan Synthesis by Glomerular Endothelium. *J Am Soc Nephrol*. 2019; **30**: 1886-97. 10.1681/ASN.2019020192.
- 19 Rabelink TJ, van den Berg BM, Garsen M, Wang G, Elkin M, van der Vlag J. Heparanase: roles in cell survival, extracellular matrix remodelling and the development of kidney disease. *Nat Rev Nephrol*. 2017; **13**: 201-12. 10.1038/nrneph.2017.6.
- 20 Chopra P, Joshi A, Wu J, Lu W, Yadavalli T, Wolfert MA, Shukla D, Zaia J, Boons GJ. The 3-O-sulfation of heparan sulfate modulates protein binding and lyase degradation. *Proc Natl Acad Sci U S A*. 2021; **118**. 10.1073/pnas.2012935118.
- 21 Buchheim JI, Enzinger MC, Chouker A, Bruegel M, Holdt L, Rehm M. The stressed vascular barrier and coagulation - The impact of key glycocalyx components on in vitro clot formation. *Thromb Res*. 2020; **186**: 93-102. 10.1016/j.thromres.2019.12.015.
- 22 Ito T, Maruyama I. Thrombomodulin: protectorate God of the vasculature in thrombosis and inflammation. *J Thromb Haemost*. 2011; **9 Suppl 1**: 168-73. 10.1111/j.1538-7836.2011.04319.x.
- 23 Kalagara T, Moutsis T, Yang Y, Pappelbaum KI, Farken A, Cladder-Micus L, Vidal YSS, John A, Bauer AT, Moerschbacher BM, Schneider SW, Gorzelanny C. The endothelial glycocalyx anchors von Willebrand factor fibers to the vascular endothelium. *Blood Adv*. 2018; **2**: 2347-57. 10.1182/bloodadvances.2017013995.
- 24 Pum A, Ennemoser M, Gerlza T, Kungl AJ. The Role of Heparan Sulfate in CCL26-Induced Eosinophil Chemotaxis. *Int J Mol Sci*. 2022; **23**. 10.3390/ijms23126519.
- 25 Jain P, Shanthamurthy CD, Leviatan Ben-Arye S, Woods RJ, Kikkeri R, Padler-Karavani V. Discovery of rare sulfated N-unsubstituted glucosamine based heparan sulfate analogs selectively activating chemokines. *Chem Sci*. 2021; **12**: 3674-81. 10.1039/d0sc05862a.

- 26 Sawant KV, Sepuru KM, Lowry E, Penaranda B, Frevert CW, Garofalo RP, Rajarathnam K. Neutrophil recruitment by chemokines Cxcl1/KC and Cxcl2/MIP2: Role of Cxcr2 activation and glycosaminoglycan interactions. *J Leukoc Biol.* 2021; **109**: 777-91. 10.1002/JLB.3A0820-207R.
- 27 Vallet SD, Clerc O, Ricard-Blum S. Glycosaminoglycan-Protein Interactions: The First Draft of the Glycosaminoglycan Interactome. *J Histochem Cytochem.* 2021; **69**: 93-104. 10.1369/0022155420946403.
- 28 Dzenko KA, Song L, Ge S, Kuziel WA, Pachter JS. CCR2 expression by brain microvascular endothelial cells is critical for macrophage transendothelial migration in response to CCL2. *Microvasc Res.* 2005; **70**: 53-64. 10.1016/j.mvr.2005.04.005.
- 29 Winkler S, Derler R, Gesslbauer B, Krieger E, Kungl AJ. Molecular dynamics simulations of the chemokine CCL2 in complex with pull down-derived heparan sulfate hexasaccharides. *Biochim Biophys Acta Gen Subj.* 2019; **1863**: 528-33. 10.1016/j.bbagen.2018.12.014.
- 30 van Gemst JJ, Kouwenberg M, Rops A, van Kuppevelt TH, Berden JH, Rabelink TJ, Loeven MA, van der Vlag J. Differential binding of chemokines CXCL1, CXCL2 and CCL2 to mouse glomerular endothelial cells reveals specificity for distinct heparan sulfate domains. *PLoS One.* 2018; **13**: e0201560. 10.1371/journal.pone.0201560.
- 31 Rops AL, van den Hoven MJ, Baselmans MM, Lensen JF, Wijnhoven TJ, van den Heuvel LP, van Kuppevelt TH, Berden JH, van der Vlag J. Heparan sulfate domains on cultured activated glomerular endothelial cells mediate leukocyte trafficking. *Kidney Int.* 2008; **73**: 52-62. 10.1038/sj.ki.5002573.
- 32 Wang G, de Vries MR, Sol W, van Oeveren-Rietdijk AM, de Boer HC, van Zonneveld AJ, Quax PHA, Rabelink TJ, van den Berg BM. Loss of Endothelial Glycocalyx Hyaluronan Impairs Endothelial Stability and Adaptive Vascular Remodeling After Arterial Ischemia. *Cells.* 2020; **9**. 10.3390/cells9040824.
- 33 Baumann H, Gaudie J. Regulation of hepatic acute phase plasma protein genes by hepatocyte stimulating factors and other mediators of inflammation. *Mol Biol Med.* 1990; **7**: 147-59.
- 34 Ridker PM, Hennekens CH, Buring JE, Rifai N. C-reactive protein and other markers of inflammation in the prediction of cardiovascular disease in women. *N Engl J Med.* 2000; **342**: 836-43. 10.1056/NEJM200003233421202.
- 35 Ballantyne CM, Hoogeveen RC, Bang H, Coresh J, Folsom AR, Heiss G, Sharrett AR. Lipoprotein-associated phospholipase A2, high-sensitivity C-reactive protein, and risk for incident coronary heart disease in middle-aged men and women in the Atherosclerosis Risk in Communities (ARIC) study. *Circulation.* 2004; **109**: 837-42. 10.1161/01.CIR.0000116763.91992.F1.

- 36 Wener MH, Daum PR, McQuillan GM. The influence of age, sex, and race on the upper reference limit of serum C-reactive protein concentration. *J Rheumatol*. 2000; **27**: 2351-9.
- 37 Wang TJ, Nam BH, Wilson PW, Wolf PA, Levy D, Polak JF, D'Agostino RB, O'Donnell CJ. Association of C-reactive protein with carotid atherosclerosis in men and women: the Framingham Heart Study. *Arterioscler Thromb Vasc Biol*. 2002; **22**: 1662-7. 10.1161/01.atv.0000034543.78801.69.
- 38 McConnell JP, Branum EL, Ballman KV, Lagerstedt SA, Katzmann JA, Jaffe AS. Gender differences in C-reactive protein concentrations—confirmation with two sensitive methods. *Clin Chem Lab Med*. 2002; **40**: 56-9. 10.1515/CCLM.2002.011.
- 39 Wong ND, Pio J, Valencia R, Thakal G. Distribution of C-reactive protein and its relation to risk factors and coronary heart disease risk estimation in the National Health and Nutrition Examination Survey (NHANES) III. *Prev Cardiol*. 2001; **4**: 109-14. 10.1111/j.1520-037x.2001.00570.x.
- 40 Ford ES, Giles WH, Mokdad AH, Myers GL. Distribution and correlates of C-reactive protein concentrations among adult US women. *Clin Chem*. 2004; **50**: 574-81. 10.1373/clinchem.2003.027359.
- 41 Khera A, McGuire DK, Murphy SA, Stanek HG, Das SR, Vongpatanasin W, Wians FH, Jr., Grundy SM, de Lemos JA. Race and gender differences in C-reactive protein levels. *J Am Coll Cardiol*. 2005; **46**: 464-9. 10.1016/j.jacc.2005.04.051.
- 42 Lakoski SG, Cushman M, Criqui M, Rundek T, Blumenthal RS, D'Agostino RB, Jr., Herrington DM. Gender and C-reactive protein: data from the Multiethnic Study of Atherosclerosis (MESA) cohort. *Am Heart J*. 2006; **152**: 593-8. 10.1016/j.ahj.2006.02.015.
- 43 Kvist H, Chowdhury B, Grangard U, Tuyen U, Sjostrom L. Total and visceral adipose-tissue volumes derived from measurements with computed tomography in adult men and women: predictive equations. *Am J Clin Nutr*. 1988; **48**: 1351-61. 10.1093/ajcn/48.6.1351.
- 44 Sjostrom L, Kvist H. Regional body fat measurements with CT-scan and evaluation of anthropometric predictions. *Acta Med Scand Suppl*. 1988; **723**: 169-77. 10.1111/j.0954-6820.1987.tb05941.x.
- 45 Rexrode KM, Pradhan A, Manson JE, Buring JE, Ridker PM. Relationship of total and abdominal adiposity with CRP and IL-6 in women. *Ann Epidemiol*. 2003; **13**: 674-82. 10.1016/s1047-2797(03)00053-x.
- 46 Ridker PM, Hennekens CH, Rifai N, Buring JE, Manson JE. Hormone replacement therapy and increased plasma concentration of C-reactive protein. *Circulation*. 1999; **100**: 713-6. 10.1161/01.cir.100.7.713.

- 47 Cartier A, Cote M, Lemieux I, Perusse L, Tremblay A, Bouchard C, Despres JP. Sex differences in inflammatory markers: what is the contribution of visceral adiposity? *Am J Clin Nutr*. 2009; **89**: 1307-14. 10.3945/ajcn.2008.27030.
- 48 Vorster HH. Fibrinogen and women's health. *Thromb Res*. 1999; **95**: 137-54. 10.1016/s0049-3848(99)00033-x.
- 49 Kim PY, Stewart RJ, Lipson SM, Nesheim ME. The relative kinetics of clotting and lysis provide a biochemical rationale for the correlation between elevated fibrinogen and cardiovascular disease. *J Thromb Haemost*. 2007; **5**: 1250-6. 10.1111/j.1538-7836.2007.02426.x.
- 50 Cortellaro M, Boschetti C, Cofrancesco E, Zanussi C, Catalano M, de Gaetano G, Gabrielli L, Lombardi B, Specchia G, Tavazzi L, et al. The PLAT Study: hemostatic function in relation to atherothrombotic ischemic events in vascular disease patients. Principal results. PLAT Study Group. Progetto Lombardo Atero-Trombosi (PLAT) Study Group. *Arterioscler Thromb*. 1992; **12**: 1063-70. 10.1161/01.atv.12.9.1063.
- 51 Thompson SG, Fehstrup C, Squire E, Heyse U, Breithardt G, van de Loo JC, Kienast J. Antithrombin III and fibrinogen as predictors of cardiac events in patients with angina pectoris. *Arterioscler Thromb Vasc Biol*. 1996; **16**: 357-62. 10.1161/01.atv.16.3.357.
- 52 Benderly M, Graff E, Reicher-Reiss H, Behar S, Brunner D, Goldbourt U. Fibrinogen is a predictor of mortality in coronary heart disease patients. The Bezafibrate Infarction Prevention (BIP) Study Group. *Arterioscler Thromb Vasc Biol*. 1996; **16**: 351-6. 10.1161/01.atv.16.3.351.
- 53 ECAT angina pectoris study: baseline associations of haemostatic factors with extent of coronary arteriosclerosis and other coronary risk factors in 3000 patients with angina pectoris undergoing coronary angiography. *Eur Heart J*. 1993; **14**: 8-17. 10.1093/eurheartj/14.1.8.
- 54 Favaloro EJ, Soltani S, McDonald J, Grezchnik E, Easton L. Cross-laboratory audit of normal reference ranges and assessment of ABO blood group, gender and age on detected levels of plasma coagulation factors. *Blood Coagul Fibrinolysis*. 2005; **16**: 597-605. 10.1097/01.mbc.0000187250.32630.56.
- 55 Olson NC, Cushman M, Judd SE, Kissela BM, Safford MM, Howard G, Zakai NA. Associations of coagulation factors IX and XI levels with incident coronary heart disease and ischemic stroke: the REGARDS study. *J Thromb Haemost*. 2017; **15**: 1086-94. 10.1111/jth.13698.
- 56 Zakai NA, Judd SE, Kissela B, Howard G, Safford MM, Cushman M. Factor VIII, Protein C and Cardiovascular Disease Risk: The REasons for Geographic and Racial Differences in Stroke Study (REGARDS). *Thromb Haemost*. 2018; **118**: 1305-15. 10.1055/s-0038-1655766.

- 57 Bots SH, Peters SAE, Woodward M. Sex differences in coronary heart disease and stroke mortality: a global assessment of the effect of ageing between 1980 and 2010. *BMJ Glob Health*. 2017; **2**: e000298. 10.1136/bmjgh-2017-000298.
- 58 Khamis RY, Ammari T, Mikhail GW. Gender differences in coronary heart disease. *Heart*. 2016; **102**: 1142-9. 10.1136/heartjnl-2014-306463.
- 59 Einarson TR, Acs A, Ludwig C, Panton UH. Prevalence of cardiovascular disease in type 2 diabetes: a systematic literature review of scientific evidence from across the world in 2007-2017. *Cardiovasc Diabetol*. 2018; **17**: 83. 10.1186/s12933-018-0728-6.
- 60 van der Toorn FA, de Mutsert R, Lijfering WM, Rosendaal FR, van Hylckama Vlieg A. Glucose metabolism affects coagulation factors: The NEO study. *J Thromb Haemost*. 2019; **17**: 1886-97. 10.1111/jth.14573.
- 61 Maiocchi S, Alwis I, Wu MCL, Yuan Y, Jackson SP. Thromboinflammatory Functions of Platelets in Ischemia-Reperfusion Injury and Its Dysregulation in Diabetes. *Semin Thromb Hemost*. 2018; **44**: 102-13. 10.1055/s-0037-1613694.
- 62 Witte A, Rohlfing AK, Dannenmann B, Dicenta V, Nasri M, Kolb K, Sudmann J, Castor T, Rath D, Borst O, Skokowa J, Gawaz M. The chemokine CXCL14 mediates platelet function and migration via direct interaction with CXCR4. *Cardiovasc Res*. 2021; **117**: 903-17. 10.1093/cvr/cvaa080.
- 63 Witte A, Chatterjee M, Lang F, Gawaz M. Platelets as a Novel Source of Pro-Inflammatory Chemokine CXCL14. *Cell Physiol Biochem*. 2017; **41**: 1684-96. 10.1159/000471821.
- 64 Manke MC, Ahrends R, Borst O. Platelet lipid metabolism in vascular thromboinflammation. *Pharmacol Ther*. 2022; **237**: 108258. 10.1016/j.pharmthera.2022.108258.
- 65 Cebo M, Dittrich K, Fu X, Manke MC, Emschermann F, Rheinlaender J, von Eysmond H, Ferreiros N, Sudman J, Witte A, Pelzl L, Borst O, Geisler T, Rath D, Bakchoul T, Gawaz M, Schaffer TE, Lammerhofer M, Chatterjee M. Platelet ACKR3/CXCR7 favors antiplatelet lipids over an atherothrombotic lipidome and regulates thromboinflammation. *Blood*. 2022; **139**: 1722-42. 10.1182/blood.2021013097.
- 66 Kohli S, Shahzad K, Jouppila A, Holthofer H, Isermann B, Lassila R. Thrombosis and Inflammation-A Dynamic Interplay and the Role of Glycosaminoglycans and Activated Protein C. *Front Cardiovasc Med*. 2022; **9**: 866751. 10.3389/fcvm.2022.866751.
- 67 Boels MG, Avramut MC, Koudijs A, Dane MJ, Lee DH, van der Vlag J, Koster AJ, van Zonneveld AJ, van Faassen E, Grone HJ, van den Berg BM, Rabelink TJ. Atrasentan Reduces Albuminuria by Restoring the Glomerular Endothelial Glycocalyx Barrier in Diabetic Nephropathy. *Diabetes*. 2016; **65**: 2429-39. 10.2337/db15-1413.
- 68 Wang G, Kostidis S, Tiemeier GL, Sol W, de Vries MR, Giera M, Carmeliet P, van den Berg BM, Rabelink TJ. Shear Stress Regulation of Endothelial Glycocalyx Structure Is

- Determined by Glucobiosynthesis. *Arterioscler Thromb Vasc Biol.* 2020; **40**: 350-64. 10.1161/ATVBAHA.119.313399.
- 69 Loscalzo J. Nitric oxide insufficiency, platelet activation, and arterial thrombosis. *Circ Res.* 2001; **88**: 756-62. 10.1161/hh0801.089861.
- 70 Kong J, Yao C, Dong S, Wu S, Xu Y, Li K, Ji L, Shen Q, Zhang Q, Zhan R, Cui H, Zhou C, Niu H, Li G, Sun W, Zheng L. ICAM-1 Activates Platelets and Promotes Endothelial Permeability through VE-Cadherin after Insufficient Radiofrequency Ablation. *Adv Sci (Weinh).* 2021; **8**: 2002228. 10.1002/advs.202002228.
- 71 Mineo C, Shaul PW. Novel biological functions of high-density lipoprotein cholesterol. *Circ Res.* 2012; **111**: 1079-90. 10.1161/CIRCRESAHA.111.258673.
- 72 Jialal I, Jialal G, Adams-Huet B. The platelet to high density lipoprotein -cholesterol ratio is a valid biomarker of nascent metabolic syndrome. *Diabetes Metab Res Rev.* 2021; **37**: e3403. 10.1002/dmrr.3403.
- 73 Constantinou C, Karavia EA, Xepapadaki E, Petropoulou PI, Papakosta E, Karavyraki M, Zvintzou E, Theodoropoulos V, Filou S, Hatziri A, Kalogeropoulou C, Panayiotakopoulos G, Kypreos KE. Advances in high-density lipoprotein physiology: surprises, overturns, and promises. *Am J Physiol Endocrinol Metab.* 2016; **310**: E1-E14. 10.1152/ajpendo.00429.2015.
- 74 Xepapadaki E, Nikdima I, Sagiadinou EC, Zvintzou E, Kypreos KE. HDL and type 2 diabetes: the chicken or the egg? *Diabetologia.* 2021; **64**: 1917-26. 10.1007/s00125-021-05509-0.
- 75 Ebtehaj S, Gruppen EG, Parvizi M, Tietge UJF, Dullaart RPF. The anti-inflammatory function of HDL is impaired in type 2 diabetes: role of hyperglycemia, paraoxonase-1 and low grade inflammation. *Cardiovasc Diabetol.* 2017; **16**: 132. 10.1186/s12933-017-0613-8.
- 76 Heier M, Borja MS, Brunborg C, Seljeflot I, Margeirsdottir HD, Hanssen KF, Dahl-Jorgensen K, Oda MN. Reduced HDL function in children and young adults with type 1 diabetes. *Cardiovasc Diabetol.* 2017; **16**: 85. 10.1186/s12933-017-0570-2.
- 77 Schmidt MI, Duncan BB, Bang H, Pankow JS, Ballantyne CM, Golden SH, Folsom AR, Chambless LE, Atherosclerosis Risk in Communities I. Identifying individuals at high risk for diabetes: The Atherosclerosis Risk in Communities study. *Diabetes Care.* 2005; **28**: 2013-8. 10.2337/diacare.28.8.2013.
- 78 Wilson PW, Meigs JB, Sullivan L, Fox CS, Nathan DM, D'Agostino RB, Sr. Prediction of incident diabetes mellitus in middle-aged adults: the Framingham Offspring Study. *Arch Intern Med.* 2007; **167**: 1068-74. 10.1001/archinte.167.10.1068.
- 79 Sacks FM, Hermans MP, Fioretto P, Valensi P, Davis T, Horton E, Wanner C, Al-Rubeaan K, Aronson R, Barzon I, Bishop L, Bonora E, Bunnag P, Chuang LM, Deerochanawong C, Goldenberg R, Harshfield B, Hernandez C, Herzlinger-Botein S, Itoh H,

Jia W, Jiang YD, Kadowaki T, Laranjo N, Leiter L, Miwa T, Odawara M, Ohashi K, Ohno A, Pan C, Pan J, Pedro-Botet J, Reiner Z, Rotella CM, Simo R, Tanaka M, Tedeschi-Reiner E, Twum-Barima D, Zoppini G, Carey VJ. Association between plasma triglycerides and high-density lipoprotein cholesterol and microvascular kidney disease and retinopathy in type 2 diabetes mellitus: a global case-control study in 13 countries. *Circulation*. 2014; **129**: 999-1008. 10.1161/CIRCULATIONAHA.113.002529.

80 Jia C, Anderson JLC, Gruppen EG, Lei Y, Bakker SJL, Dullaart RPF, Tietge UJF. High-Density Lipoprotein Anti-Inflammatory Capacity and Incident Cardiovascular Events. *Circulation*. 2021; **143**: 1935-45. 10.1161/CIRCULATIONAHA.120.050808.

81 Ajala ON, Demler OV, Liu Y, Farukhi Z, Adelman SJ, Collins HL, Ridker PM, Rader DJ, Glynn RJ, Mora S. Anti-Inflammatory HDL Function, Incident Cardiovascular Events, and Mortality: A Secondary Analysis of the JUPITER Randomized Clinical Trial. *J Am Heart Assoc*. 2020; **9**: e016507. 10.1161/JAHA.119.016507.

82 Emmens JE, Jia C, Ng LL, van Veldhuisen DJ, Dickstein K, Anker SD, Lang CC, Filippatos G, Cleland JGF, Metra M, Voors AA, de Boer RA, Tietge UJF. Impaired High-Density Lipoprotein Function in Patients With Heart Failure. *J Am Heart Assoc*. 2021; **10**: e019123. 10.1161/JAHA.120.019123.

83 Hesse B, Rovas A, Buscher K, Kusche-Vihrog K, Brand M, Di Marco GS, Kielstein JT, Pavenstadt H, Linke WA, Nofer JR, Kumpers P, Lukasz A. Symmetric dimethylarginine in dysfunctional high-density lipoprotein mediates endothelial glycocalyx breakdown in chronic kidney disease. *Kidney Int*. 2020; **97**: 502-15. 10.1016/j.kint.2019.10.017.

84 Cascella M, Rajnik M, Aleem A, Dulebohn SC, Di Napoli R. Features, Evaluation, and Treatment of Coronavirus (COVID-19). *StatPearls*. Treasure Island (FL), 2022.

85 Huang C, Wang Y, Li X, Ren L, Zhao J, Hu Y, Zhang L, Fan G, Xu J, Gu X, Cheng Z, Yu T, Xia J, Wei Y, Wu W, Xie X, Yin W, Li H, Liu M, Xiao Y, Gao H, Guo L, Xie J, Wang G, Jiang R, Gao Z, Jin Q, Wang J, Cao B. Clinical features of patients infected with 2019 novel coronavirus in Wuhan, China. *Lancet*. 2020; **395**: 497-506. 10.1016/S0140-6736(20)30183-5.

86 Ferrando C, Suarez-Sipmann F, Mellado-Artigas R, Hernandez M, Gea A, Arruti E, Aldecoa C, Martinez-Palli G, Martinez-Gonzalez MA, Slutsky AS, Villar J, Network C-SI. Clinical features, ventilatory management, and outcome of ARDS caused by COVID-19 are similar to other causes of ARDS. *Intensive Care Med*. 2020; **46**: 2200-11. 10.1007/s00134-020-06192-2.

87 Grasselli G, Zangrillo A, Zanella A, Antonelli M, Cabrini L, Castelli A, Cereda D, Coluccello A, Foti G, Fumagalli R, Iotti G, Latronico N, Lorini L, Merler S, Natalini G, Piatti A, Ranieri MV, Scandroglio AM, Storti E, Cecconi M, Pesenti A, Network C-LI. Baseline Characteristics and Outcomes of 1591 Patients Infected With SARS-CoV-2 Admitted to ICUs of the Lombardy Region, Italy. *JAMA*. 2020; **323**: 1574-81. 10.1001/jama.2020.5394.

- 88 Cui S, Chen S, Li X, Liu S, Wang F. Prevalence of venous thromboembolism in patients with severe novel coronavirus pneumonia. *J Thromb Haemost.* 2020; **18**: 1421-4. 10.1111/jth.14830.
- 89 Zhou F, Yu T, Du R, Fan G, Liu Y, Liu Z, Xiang J, Wang Y, Song B, Gu X, Guan L, Wei Y, Li H, Wu X, Xu J, Tu S, Zhang Y, Chen H, Cao B. Clinical course and risk factors for mortality of adult inpatients with COVID-19 in Wuhan, China: a retrospective cohort study. *Lancet.* 2020; **395**: 1054-62. 10.1016/S0140-6736(20)30566-3.
- 90 Vassiliou AG, Kotanidou A, Dimopoulou I, Orfanos SE. Endothelial Damage in Acute Respiratory Distress Syndrome. *Int J Mol Sci.* 2020; **21**. 10.3390/ijms21228793.
- 91 Vallet B, Wiel E. Endothelial cell dysfunction and coagulation. *Crit Care Med.* 2001; **29**: S36-41. 10.1097/00003246-200107001-00015.
- 92 Ackermann M, Verleden SE, Kuehnel M, Haverich A, Welte T, Laenger F, Vanstapel A, Werlein C, Stark H, Tzankov A, Li WW, Li VW, Mentzer SJ, Jonigk D. Pulmonary Vascular Endothelialitis, Thrombosis, and Angiogenesis in Covid-19. *N Engl J Med.* 2020; **383**: 120-8. 10.1056/NEJMoa2015432.
- 93 Bonaventura A, Vecchie A, Wang TS, Lee E, Cremer PC, Carey B, Rajendram P, Hudock KM, Korbee L, Van Tassell BW, Dagna L, Abbate A. Targeting GM-CSF in COVID-19 Pneumonia: Rationale and Strategies. *Front Immunol.* 2020; **11**: 1625. 10.3389/fimmu.2020.01625.
- 94 Buckley LF, Wohlford GF, Ting C, Alahmed A, Van Tassell BW, Abbate A, Devlin JW, Libby P. Role for Anti-Cytokine Therapies in Severe Coronavirus Disease 2019. *Crit Care Explor.* 2020; **2**: e0178. 10.1097/CCE.0000000000000178.
- 95 Li J, Gong X, Wang Z, Chen R, Li T, Zeng D, Li M. Clinical features of familial clustering in patients infected with 2019 novel coronavirus in Wuhan, China. *Virus Res.* 2020; **286**: 198043. 10.1016/j.virusres.2020.198043.
- 96 Vecchie A, Bonaventura A, Toldo S, Dagna L, Dinarello CA, Abbate A. IL-18 and infections: Is there a role for targeted therapies? *J Cell Physiol.* 2021; **236**: 1638-57. 10.1002/jcp.30008.
- 97 Zanza C, Romenskaya T, Manetti AC, Franceschi F, La Russa R, Bertozzi G, Maiese A, Savioli G, Volonnino G, Longhitano Y. Cytokine Storm in COVID-19: Immunopathogenesis and Therapy. *Medicina (Kaunas).* 2022; **58**. 10.3390/medicina58020144.
- 98 Kox M, Waalders NJB, Kooistra EJ, Gerretsen J, Pickkers P. Cytokine Levels in Critically Ill Patients With COVID-19 and Other Conditions. *JAMA.* 2020; **324**: 1565-7. 10.1001/jama.2020.17052.
- 99 Leisman DE, Ronner L, Pinotti R, Taylor MD, Sinha P, Calfee CS, Hirayama AV, Mastroiani F, Turtle CJ, Harhay MO, Legrand M, Deutschman CS. Cytokine elevation in severe and critical COVID-19: a rapid systematic review, meta-analysis, and comparison

with other inflammatory syndromes. *Lancet Respir Med.* 2020; **8**: 1233-44. 10.1016/S2213-2600(20)30404-5.

100 Blanco-Melo D, Nilsson-Payant BE, Liu WC, Uhl S, Hoagland D, Moller R, Jordan TX, Oishi K, Panis M, Sachs D, Wang TT, Schwartz RE, Lim JK, Albrecht RA, tenOever BR. Imbalanced Host Response to SARS-CoV-2 Drives Development of COVID-19. *Cell.* 2020; **181**: 1036-45 e9. 10.1016/j.cell.2020.04.026.

101 Toldo S, Bussani R, Nuzzi V, Bonaventura A, Mauro AG, Cannata A, Pillappa R, Sinagra G, Nana-Sinkam P, Sime P, Abbate A. Inflammasome formation in the lungs of patients with fatal COVID-19. *Inflamm Res.* 2021; **70**: 7-10. 10.1007/s00011-020-01413-2.

102 Rodrigues TS, de Sa KSG, Ishimoto AY, Becerra A, Oliveira S, Almeida L, Goncalves AV, Perucello DB, Andrade WA, Castro R, Veras FP, Toller-Kawahisa JE, Nascimento DC, de Lima MHF, Silva CMS, Caetite DB, Martins RB, Castro IA, Pontelli MC, de Barros FC, do Amaral NB, Giannini MC, Bonjorno LP, Lopes MIF, Santana RC, Vilar FC, Auxiliadora-Martins M, Luppino-Assad R, de Almeida SCL, de Oliveira FR, Batah SS, Siyuan L, Benatti MN, Cunha TM, Alves-Filho JC, Cunha FQ, Cunha LD, Frantz FG, Kohlsdorf T, Fabro AT, Arruda E, de Oliveira RDR, Louzada-Junior P, Zamboni DS. Inflammasomes are activated in response to SARS-CoV-2 infection and are associated with COVID-19 severity in patients. *J Exp Med.* 2021; **218**. 10.1084/jem.20201707.

103 Bouck EG, Denorme F, Holle LA, Middelton EA, Blair AM, de Laat B, Schiffman JD, Yost CC, Rondina MT, Wolberg AS, Campbell RA. COVID-19 and Sepsis Are Associated With Different Abnormalities in Plasma Procoagulant and Fibrinolytic Activity. *Arterioscler Thromb Vasc Biol.* 2021; **41**: 401-14. 10.1161/ATVBAHA.120.315338.

104 Skendros P, Mitsios A, Chrysanthopoulou A, Mastellos DC, Metallidis S, Rafailidis P, Ntinopoulou M, Sertaridou E, Tsiironidou V, Tsigalou C, Tektonidou M, Konstantinidis T, Papagoras C, Mitroulis I, Germanidis G, Lambris JD, Ritis K. Complement and tissue factor-enriched neutrophil extracellular traps are key drivers in COVID-19 immunothrombosis. *J Clin Invest.* 2020; **130**: 6151-7. 10.1172/JCI141374.

105 Yu J, Yuan X, Chen H, Chaturvedi S, Braunstein EM, Brodsky RA. Direct activation of the alternative complement pathway by SARS-CoV-2 spike proteins is blocked by factor D inhibition. *Blood.* 2020; **136**: 2080-9. 10.1182/blood.2020008248.

106 Yu J, Gerber GF, Chen H, Yuan X, Chaturvedi S, Braunstein EM, Brodsky RA. Complement dysregulation is associated with severe COVID-19 illness. *Haematologica.* 2022; **107**: 1095-105. 10.3324/haematol.2021.279155.

107 Aiello S, Gastoldi S, Galbusera M, Ruggenenti P, Portalupi V, Rota S, Rubis N, Liguori L, Conti S, Tironi M, Gamba S, Santarsiero D, Benigni A, Remuzzi G, Noris M. C5a and C5aR1 are key drivers of microvascular platelet aggregation in clinical entities spanning from aHUS to COVID-19. *Blood Adv.* 2022; **6**: 866-81. 10.1182/bloodadvances.2021005246.

- 108 Schmaier AA, Pajares Hurtado GM, Manickas-Hill ZJ, Sack KD, Chen SM, Bhambhani V, Quadir J, Nath AK, Collier AY, Ngo D, Barouch DH, Shapiro NI, Gerszten RE, Yu XG, Collection MC-, Processing T, Peters KG, Flaumenhaft R, Parikh SM. Tie2 activation protects against prothrombotic endothelial dysfunction in COVID-19. *JCI Insight*. 2021; **6**. 10.1172/jci.insight.151527.
- 109 Rovas A, Osiaevi I, Buscher K, Sackarnd J, Tepasse PR, Fobker M, Kuhn J, Braune S, Gobel U, Tholking G, Groschel A, Pavenstadt H, Vink H, Kumpers P. Microvascular dysfunction in COVID-19: the MYSTIC study. *Angiogenesis*. 2021; **24**: 145-57. 10.1007/s10456-020-09753-7.
- 110 Vassiliou AG, Keskinidou C, Jahaj E, Gallos P, Dimopoulou I, Kotanidou A, Orfanos SE. ICU Admission Levels of Endothelial Biomarkers as Predictors of Mortality in Critically Ill COVID-19 Patients. *Cells*. 2021; **10**. 10.3390/cells10010186.
- 111 Henry BM, de Oliveira MHS, Cheruiyot I, Benoit JL, Cooper DS, Lippi G, Le Cras TD, Benoit SW. Circulating level of Angiotensin-2 is associated with acute kidney injury in coronavirus disease 2019 (COVID-19). *Angiogenesis*. 2021; **24**: 403-6. 10.1007/s10456-021-09782-w.
- 112 Smadja DM, Guerin CL, Chocron R, Yatim N, Boussier J, Gendron N, Khider L, Hadjadj J, Goudot G, Debuc B, Juvin P, Hauw-Berlemont C, Augy JL, Peron N, Messas E, Planquette B, Sanchez O, Charbit B, Gaussem P, Duffy D, Terrier B, Mirault T, Diehl JL. Angiotensin-2 as a marker of endothelial activation is a good predictor factor for intensive care unit admission of COVID-19 patients. *Angiogenesis*. 2020; **23**: 611-20. 10.1007/s10456-020-09730-0.
- 113 Lukasz A, Hillgruber C, Oberleithner H, Kusche-Vihrog K, Pavenstadt H, Rovas A, Hesse B, Goerge T, Kumpers P. Endothelial glycocalyx breakdown is mediated by angiotensin-2. *Cardiovasc Res*. 2017; **113**: 671-80. 10.1093/cvr/cvx023.
- 114 Tanaka S, Couret D, Tran-Dinh A, Duranteau J, Montravers P, Schwendeman A, Meilhac O. High-density lipoproteins during sepsis: from bench to bedside. *Crit Care*. 2020; **24**: 134. 10.1186/s13054-020-02860-3.
- 115 Tran-Dinh A, Diallo D, Delbosc S, Varela-Perez LM, Dang QB, Lapergue B, Burillo E, Michel JB, Levoe A, Martin-Ventura JL, Meilhac O. HDL and endothelial protection. *Br J Pharmacol*. 2013; **169**: 493-511. 10.1111/bph.12174.
- 116 Schmelter F, Foh B, Mallagaray A, Rahmoller J, Ehlers M, Lehrian S, von Kopylow V, Kunsting I, Lixenfeld AS, Martin E, Ragab M, Meyer-Saraei R, Kreutzmann F, Eitel I, Taube S, Kading N, Jantzen E, Graf T, Sina C, Gunther UL. Metabolic and Lipidomic Markers Differentiate COVID-19 From Non-Hospitalized and Other Intensive Care Patients. *Front Mol Biosci*. 2021; **8**: 737039. 10.3389/fmolb.2021.737039.

117 Mahat RK, Rathore V, Singh N, Singh N, Singh SK, Shah RK, Garg C. Lipid profile as an indicator of COVID-19 severity: A systematic review and meta-analysis. *Clin Nutr ESPEN*. 2021; **45**: 91-101. 10.1016/j.clnesp.2021.07.023.

118 Chidambaram V, Shanmugavel Geetha H, Kumar A, Majella MG, Sivakumar RK, Voruganti D, Mehta JL, Karakousis PC. Association of Lipid Levels With COVID-19 Infection, Disease Severity and Mortality: A Systematic Review and Meta-Analysis. *Front Cardiovasc Med*. 2022; **9**: 862999. 10.3389/fcvm.2022.862999.

119 Souza Junior DR, Silva ARM, Rosa-Fernandes L, Reis LR, Alexandria G, Bhosale SD, Ghilardi FR, Dalcoquio TF, Bertolin AJ, Nicolau JC, Marinho CRF, Wrenger C, Larsen MR, Siciliano RF, Di Mascio P, Palmisano G, Ronsein GE. HDL proteome remodeling associates with COVID-19 severity. *J Clin Lipidol*. 2021; **15**: 796-804. 10.1016/j.jacl.2021.10.005.

120 Stadler JT, Mangge H, Rani A, Curcic P, Herrmann M, Pruller F, Marsche G. Low HDL Cholesterol Efflux Capacity Indicates a Fatal Course of COVID-19. *Antioxidants (Basel)*. 2022; **11**. 10.3390/antiox11101858.

121 Mietus-Snyder M, Suslovic W, Delaney M, Playford MP, Ballout RA, Barber JR, Otvos JD, DeBiasi RL, Mehta NN, Remaley AT. Changes in HDL cholesterol, particles, and function associate with pediatric COVID-19 severity. *Front Cardiovasc Med*. 2022; **9**: 1033660. 10.3389/fcvm.2022.1033660.

CHAPTER

2

Sex-specific association between microvascular health and coagulation parameters: the Netherlands Epidemiology of Obesity (NEO) Study

Lushun Yuan¹, Jihee Han², Anouk I.M. van der Velden¹, Hans Vink^{3,4}, Renée de Mutsert², Frits R. Rosendaal², Astrid van Hylckama Vlieg², Ruifang Li-Gao^{2,5}, T.J Rabelink¹, Bernard M. van den Berg¹

¹*Eindhoven Laboratory for Vascular and Regenerative Medicine, department of Internal Medicine, Nephrology, Leiden University Medical Center, Leiden, the Netherlands.*

²*Department of Clinical Epidemiology, Leiden University Medical Center, Leiden, the Netherlands.*

³*Department of Physiology, Cardiovascular Research Institute Maastricht, Maastricht, the Netherlands.*

⁴*MicroVascular Health Solutions LLC, Alpine, Utah, USA.*

⁵*Metabolon Inc., Morrisville, North Carolina, USA*

Abstract

Background: Microvascular dysfunction is a growing determinant of sex difference in coronary heart disease (CHD). The dysregulation of the coagulation system is involved in CHD pathogenesis and can be induced by endothelial glycocalyx (EG) perturbation. However, little is known about the link between EG function and coagulation parameters in population-based studies on sex specificity.

Objectives: We sought to examine sex differences in the relationship between EG function and coagulation parameters in a middle-aged Dutch population.

Methods: Using baseline measurements of 771 participants from the Netherlands Epidemiology of Obesity (NEO) study (age: 56 [IQR: 51-61] years, 53% women, BMI: 27.9 [IQR: 25.1-30.9] kg/m²), associations between glycocalyx-related perfused boundary region (PBR) derived from sidestream dark-field imaging and coagulation parameters (factor VIII/IX/XI, thrombin generation parameters, and fibrinogen) were investigated using linear regression analyses, adjusting for possible confounders (including CRP, leptin, and GlycA), followed by sex-stratified analyses.

Results: There was a sex difference in the associations between PBR and coagulation parameters. Particularly in women, one SD PBR (both total and feed vessel, indicating poorer glycocalyx status) was associated with higher FIX activity (1.8%, 95% CI: 0.3-3.3, and 2.0%, 95% CI: 0.5-3.4) and plasma fibrinogen levels (5.1 mg/dL, 95% CI: 0.4-9.9, and 5.8 mg/dL, 95% CI: 1.1-10.6). Furthermore, one SD PBR_{capillary} was associated with higher FVIII activity (3.5%, 95% CI: 0.4-6.5) and plasma fibrinogen levels (5.3 mg/dL, 95% CI: 0.6-10.0).

Conclusion: We revealed a sex-specific association between microcirculatory health and procoagulant status, which suggests considering microvascular health in the early development of CHD in women.

Keywords: coagulation factors, thrombin generation, fibrinogen, endothelial glycocalyx (EG), perfused boundary region (PBR)

Essentials

- Little is known about the link between microvascular health and coagulation parameters in population-based studies on sex specificity.
- We studied sex differences in relation between endothelial glycocalyx function and coagulation parameters in a middle-aged Dutch population.
- Particularly in women, associations between endothelial glycocalyx health and coagulation parameters were observed.
- Microcirculatory changes together with coagulation factors provide possible cues to prevent development of CHD in women.

Introduction

In previous decades, men were thought to be more susceptible to coronary heart disease (CHD) than women [1]. However, the risk of CHD in women is frequently underestimated due to the under-recognition of CHD and distinct clinical presentations, which resulted in a poor prognosis [2]. Nowadays, the systemic non-obstructive microvascular dysfunction, causing problems in small blood vessels feeding the muscular tissue, which can result in CHD, is believed to be more common in women than men. Therefore, this type of dysfunction is becoming a growing determinant of sex difference in CHD patients with normal or near normal coronary angiographic assessment [3, 4].

Previously, we examined endothelial surface perturbation using the non-invasive sidestream dark-field (SDF) imaging technique in a subpopulation of the Netherlands Epidemiology of Obesity (NEO) study [5-7]. While SDF imaging provides high contrast images of the sublingual microvasculature allowing to determine lateral red blood cell (RBC) movement within the vessels of interest, with the newly developed software automatic analysis of RBC velocity allows to include flow changes between feed vessels (10-25 μ m) and capillaries (< 10 μ m) to be coupled to the perfused boundary region (PBR), vessel density, and capillary blood volume [8, 9]. Already in various studies, it was previously shown that the detected changes in PBR, inversely related to the endothelial glycocalyx thickness, correlated with glycocalyx degradation products including circulating Syndecan-1, heparan sulfate (HS), hyaluronan, and soluble thrombomodulin and endothelial activation markers such as E-selection, soluble angiotensin-2, and soluble Tie-2 [10-13]. It was also found to be negatively correlated with coronary flow reserve (CFR), an assessment to evaluate coronary microvascular dysfunction (CMD). Besides, according to miCROvascular rarefaction in vasCUlar Cognitive Impairment and heArt failUre (CRUCIAL) study protocol [14], SDF imaging technique will be used to quantify microvascular health of cerebral and cardiac microvasculature, suggesting that this technique is a valid surrogate for cardiac microvasculature health examination [15].

The endothelial glycocalyx (EG) is a negatively charged gel-like surface matrix of proteoglycans and covalently bound glycosaminoglycans, glycoproteins, and glycolipids [16], and exerts an anti-inflammatory and antithrombotic role by covering various glycoprotein adhesion receptors for leukocytes [17], and platelets [18], or aiding in the sequestration of anti-adhesion factors [19]. EG perturbation acts as a representative of impaired microvascular function [6, 9, 20, 21]. In particular, several EG-bound proteins including specific sulfation patterns of HS proteoglycans or HS binding proteins such as anti-thrombin III (ATIII) and tissue factor pathway inhibitor (TFPI) could prevent the coagulation cascade *in vitro* and *in vivo* [22-24]. In disease cases such as nephrotic syndrome, sepsis, brain injury, and severe COVID-19, derangement of EG induced by microvascular dysfunction could accelerate hypercoagulation [8, 25-28].

Specifically, women were found to have already higher fibrinogen plasma levels than men of the same age and ethnic group [29]. Increased fibrinogen levels could push the balance from fibrinolysis to clotting [30] and have been reported as a potential risk factor for CHD [31-34]. Furthermore, other coagulation factors were also associated with increased risk of CHD [33, 35]. However, little is known about the link between EG function and coagulation parameters in population-based studies as well as whether a sex-specific determinant is present. Based on *in vitro* and *in vivo* evidence, we hypothesized that poorer endothelial glycocalyx function could lead to a procoagulant state in a population-based study, which might demonstrate sex specificity and be involved in the risk of CHD. The aim of our study was therefore to investigate the association between microvascular health, assessed by the new SDF imaging parameters, and levels of procoagulant factor activities (Factor VIII [FVIII], FIX, and FXI), fibrinogen concentration, and thrombin generation parameters in the general Dutch population and to further perform analyses stratified by sex, revealing sex differences in vascular vulnerability and its potential roles in the risk of CHD.

Materials and methods

Study population and study design

This study was performed in a population-based prospective cohort, the Netherlands Epidemiology of Obesity (NEO) study [7]. All 6,671 participants gave written informed consent, and the Medical Ethical Committee of the Leiden University Medical Center (LUMC) approved the study design. Initiated in 2008, the NEO study was designed to study pathways that lead to obesity-related diseases. Detailed information about the study design and data collection have been described elsewhere [7]. Briefly, men and women aged between 45 and 65 years with a self-reported body mass index (BMI) of 27 kg/m² or higher living in the greater area of Leiden (in the west of the Netherlands) were eligible to participate in the NEO study. In addition, all inhabitants aged between 45 and 65 years from one municipality (Leiderdorp) were invited irrespective of their BMI, representing the BMI distribution of the Dutch general population. Prior to their visits, participants completed questionnaires at home with demographic, lifestyle, and clinical information. At the baseline visit, fasting blood samples were drawn from the antecubital vein after the NEO participants had rested for 5 minutes. The present study is a cross-sectional analysis using a subpopulation of 918 NEO participants in whom SDF imaging was performed between January and October 2012, as part of the baseline visit at the Leiden University Medical Center NEO study center. Individuals were excluded from the analyses (Figure 1), when: 1) with missing SDF imaging parameters (n = 110); 2) with missing values of confounding factors (n = 8); 3) with current use of anticoagulant therapy (using vitamin K antagonists or heparin) (n = 7); 4) with missing values of coagulation parameters (n = 18); 5) with outliers values (z score > 5) in outcomes (i.e., coagulation factors and thrombin generation parameters) (n = 4), and 771 participants were included for all analyses using coagulation parameters as outcomes.

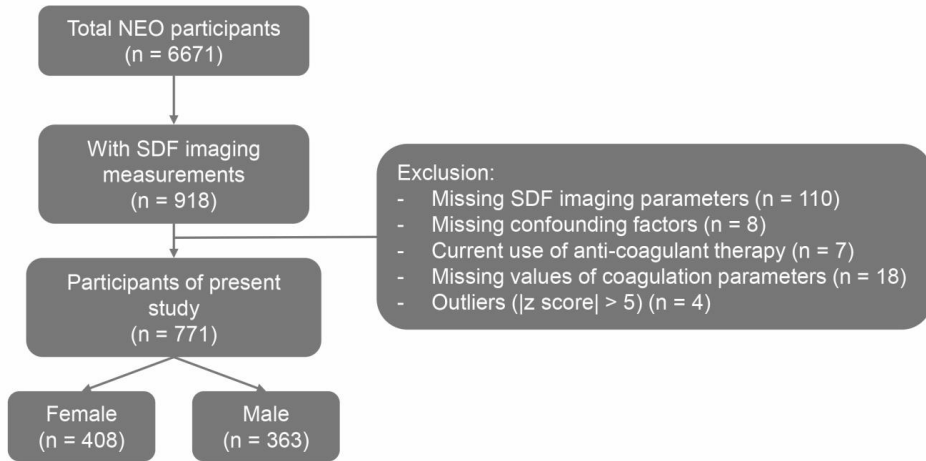


Figure 1. Study Flow chart.

SDF microcirculation imaging

Intravital microscopy was performed earlier on individuals in a supine position using an SDF camera (MicroVision Medical Inc., Wallingford, Pennsylvania) and acquired using Glycocheck software (Microvascular Health Solutions Inc., Salt Lake City, Utah) as described elsewhere [6, 9]. The software automatically identifies all available measurable microvessels distributed at a $1\mu\text{m}$ interval between $4\text{-}25\mu\text{m}$ and RBC velocity was included as a new parameter using the new software. After reanalyzing, the following validated parameters [8] were included in this study, divided into two categories: glycocalyx-related parameters, i.e., total PBR ($\text{PBR}_{\text{Total}}$, $4\text{-}25\mu\text{m}$), PBR feed vessel ($\text{PBR}_{\text{feed vessel}}$, $10\text{-}19\mu\text{m}$), and PBR capillary ($\text{PBR}_{\text{capillary}}$, $4\text{-}9\mu\text{m}$); microcirculatory-perfusion-related parameters, i.e., feed vessel RBC velocity ($\text{RBCV}_{\text{feed vessel}}$), capillary RBC velocity ($\text{RBCV}_{\text{capillary}}$), total valid vessel density (with measurable RBC velocity; D_{Total}), perfused feed vessel density ($D_{\text{feed vessel}}$), perfused capillary density ($D_{\text{capillary}}$), and capillary blood volume ($\text{CBV}_{\text{static}}$). Detailed

information about the new software used in the NEO study is described previously [8]. PBR_{Total} , $PBR_{feed\ vessel}$, and $PBR_{capillary}$ were expressed in μm . Levels of $RBCV_{feed\ vessel}$ and $RBCV_{capillary}$ were expressed in $\mu m/s$. Levels of D_{Total} , $D_{feed\ vessel}$, and $D_{capillary}$ were expressed in $\mu m/mm^2$. CBV_{static} was expressed in pL/mm^2 .

Coagulation factor activity

Blood samples for measurements of coagulation factors activity were collected and processed within 4 hours and drawn into tubes containing 0.106M trisodium citrate (Sarstedt, Etten Leur, the Netherlands) without the measurement of residual platelets, as discussed earlier [7]. Fasting fibrinogen levels were measured according to the method of Claus, as described earlier [36]. Fasting FVIII, FIX, and FXI activity were measured with a coagulometric clot detection method on an ACL TOP 700 analyzer (Werfen, Barcelona, Spain), and the Werfen plasma was used as reference plasma to calibrate factor measurements (Werfen). Levels of FVIII, FIX, and FXI activity were expressed in percentages (%). Levels of fibrinogen were expressed in mg/dL.

Thrombin generation

All blood samples were collected and processed within 4hrs. Tubes were centrifuged for 10 minutes at 2500g at 18°C and aliquoted plasma was stored at -80°C until further use, only after first time thawing for 3 min 37°C (waterbath), as discussed earlier [7]. Thrombin generation was measured according to the protocols earlier described by Hemker *et al.* [37]: calibrated automated thrombogram (CAT; Thrombinoscope BV, Maastricht, the Netherlands). Briefly, 20 μL of PPP-Reagent LOW (86194, TS31.00, STAGO, France) and thrombin calibrator (86192, TS30.00, STAGO, France) were dispensed into the wells of a round-bottom 96-well plate (#3655, Thermo Scientific, Uden, the Netherlands).

Thermostable inhibitor of contact activation (TICA, PS-0177-oxoxox, Maastricht, the Netherlands) was added to plasma samples from participants in the NEO study and normal pooled plasma (NPP, as an internal control for each plate). Then 80 μ L of mixed plasma was added to the plate and the plate was placed in the Fluorometer for a 10-minute, 37°C incubation. Thrombin formation was initiated by adding 20 μ L of the fluorogenic substrate with calcium (FluCa-kit, 86197, TS 50.00, STAGO, France). The final reaction volume was 120 μ L. Thrombin formation was determined every 10 seconds for 50 minutes and corrected for the calibrator using Thrombinscope software. Thrombin generation parameters included lag time, time to Peak (ttPeak), peak thrombin generation (Peak), endogenous thrombin potential (ETP), and thrombin generation velocity (VelIndex). Levels of lag time and ttPeak were expressed in minutes (min); levels of Peak height were expressed in nM; levels of ETP were expressed in nM \times min; levels of VelIndex were expressed in nM/min.

Serum inflammatory markers

Serum concentrations of C-reactive protein (CRP) were determined using a high sensitivity CRP assay (hs-CRP, TINA-Quant CRP HS system, Roche, Germany and Modular P800, Roche, Germany) [36]. Serum leptin concentration was measured using a human leptin competitive RadioImmunoAssay (RIA) (HL-81HK, Merck Millipore, Darmstadt, Germany). The leptin concentration was counted using a gamma counter, as described elsewhere [38]. Glycoprotein acetyls (GlycA) concentrations were measured in plasma that had undergone one previous freeze-thaw cycle, using a high-throughput proton nuclear magnetic resonance (NMR) spectroscopy (Nightingale Health Ltd., Helsinki, Finland) [39].

Statistical analyses

Descriptive baseline characteristics of the study population were expressed as median with interquartile range (IQR) for non-normally distributed variables, mean with standard deviation (SD) for normally distributed variables, or percentages (%) for dichotomous variables.

First, the distributions of confounding factors and SDF imaging parameters were evaluated, and z-transformation (i.e., with mean=0 and SD=1) was performed on age, BMI, and SDF imaging parameters. After checking the distributions of outcome variables, thrombin generation velocity (VelIndex) showed a right-skewed distribution and, \log_2 transformation was performed on VelIndex. Afterwards, linear regression analysis was used to investigate the associations between SDF imaging parameters (exposures) and pro-coagulation factors (i.e., FVIII, FIX, and FXI), fibrinogen, and thrombin generation parameters (outcomes). The analyses were adjusted for several potential confounding factors. First, crude analyses were performed (model 1). Second, we adjusted the models for the confounding factors age (unit: years, continuous variable) and sex (categories: women and men, dichotomous variable) (model 2). Third, models were adjusted for other confounding factors: BMI (unit: kg/m^2 , continuous variable), current smoking status (categories: current users and non-current users, dichotomous variable), menopausal status (categories: premenopausal and postmenopausal, dichotomous variable), current use of the oral contraceptive pill (categories: current users and non-current users, dichotomous variable), and current use of hormone replacement therapy (categories: current users and non-current users, dichotomous variable) (model 3). Fourth, we adjusted for serum C-reactive protein (CRP) (unit: mg/L , continuous variable), serum leptin concentration (unit: $\mu\text{g}/\text{L}$, continuous variable) and glycoprotein acetyls (GlycA, unit: mmol/L , continuous variable) in a separate model as these systemic inflammation markers might be potential confounders of the association between microvascular health and coagulation parameters (model 4). We calculated differences in the mean levels of fibrinogen, FVIII, FIX, FXI, and thrombin generation parameters, with 95% confidence intervals (CI), associated with SDF imaging

parameters. Furthermore, the association between SDF imaging parameters and coagulation factor levels was examined through sex-stratified analysis. Mean coagulation factor levels were calculated for sex-stratified SDF imaging parameters. As a sensitivity analysis, all analyses were performed separately in premenopausal and postmenopausal women.

To our knowledge, the present study is the first to investigate the association between the microvascular health index derived from SDF imaging and the levels of coagulation factors as well as the parameters of thrombin generation on a population level; we have no prior information on effect sizes to perform a power calculation. Noteworthy, most of previous studies with relatively small sample sizes have identified associations between the microvascular health index and disease outcomes, e.g., COVID-19 in 38 participants [13], coronary artery disease in 115 participants [40], and sepsis in 51 participants [8]. To address the power that we could achieve using 771 individuals, we used the following setting: significant level 0.05, power 80%, with the linear regression $PBR_{Total} \sim \text{fibrinogen}$ as an example; we may need 394, 54, and 24 samples for a small, medium and large effect size, respectively [41]. Therefore, a sample size of 771 individuals may have the statistical power to capture even small effect sizes.

Results

Participant characteristics

Table 1 shows the characteristics of individuals included in the present study. Of 771 included participants, 53% were women, with a median age of 56 years (interquartile range, 51–61 years), and 12.5% were current smokers. Participants had a median BMI of 27.9 kg/m² (interquartile range, 25.1–30.9). Among women, 84% had a postmenopausal status, 7.6% used oral contraceptives, and 3.4 % hormone replacement therapy. Apart from this, we observed a higher level of inflammatory markers and procoagulant status. While

capillary glycocalyx is very important for proper endothelial function, the PBR dimensions are measured in vessels with diameters ranging from 4 – 25 microns. Therefore the contribution of capillary glycocalyx to PBR_{total} is very limited. PBR_{total} is comparable to $PBR_{feed\ vessel}$ and both are the main parameters presenting possible disturbances of the endothelial surface layer, which in women are both significantly increased (median, women vs. men: PBR_{total} , 2.35 vs. 2.3; $PBR_{feed\ vessel}$, 2.31 vs. 2.24). The density of perfused capillaries is higher in women vs. men, as measured by both a higher capillary density ($D_{capillary}$) and higher capillary blood volume (CBV_{static}), which is associated with a lower capillary RBC velocity ($RBCV_{capillary}$), suggests a more advantages capillary presence in women.

Association between microvascular health and levels of coagulation parameters in the total population

Linear regression analyses were used to investigate the association between one standard deviation (SD) difference in microvascular parameters and the coagulation factors. In model 3 of the total population, both glycocalyx-related parameters, PBR_{Total} and $PBR_{feed\ vessel}$ were associated with higher fibrinogen levels (Table S1). Nevertheless, with an additional adjustment for systemic inflammatory markers (model 4), only the association of the $PBR_{feed\ vessel}$ remained (Table S1 and Figure S1) and we observed that one SD (i.e., $0.3\mu m$) in the $PBR_{feed\ vessel}$ was associated with an higher fibrinogen concentration of 3.2 mg/dL (95% CI: 0.02-6.4). Interestingly, the microcirculatory perfusion parameters, in particular all three vessel density parameters, were positively associated with the endogenous thrombin potential (ETP) in all models with very similar effect size estimations between model 3 and model 4 (Table S2 and Figure S2). In model 4 of the total population, one SD in vessel density (D_{Total} , $D_{feed\ vessel}$, $D_{capillary}$; 65.84, 42.17, 41.39 $\mu m/mm^2$, respectively), corresponded to higher ETP levels (31.9 nM \times min, 95% CI: 9.6-54.2; 23.7 nM \times min, 95% CI: 1.2-46.2; 25.2 nM \times min, 95% CI: 2.9-47.5, respectively).

Table 1. Characteristics of the study population

	Total (100%)	Women (53%)	Men (47%)
Demographic			
Age, y	56 (51-61)	56 (50.75-61)	57 (51-61)
BMI, kg/m ²	27.93 (25.08-30.91)	27.75 (24.52-31.25)	27.99 (25.73-30.59)
Tobacco smoking (% current user)	12.5	8.1	17.4
Menopause status (% of female postmenopausal/perimenopausal)	NA	83.8	NA
Medication (current use)			
Oral contraceptive pill (% of females)	NA	7.6	NA
HRT (% of female)	NA	3.4	NA
Systemic inflammatory markers			
C-reactive protein, mg/L	1.37 (0.74-3.06)	1.61 (0.8-3.5) ***	1.25 (0.64-2.26)
Leptin, µg/L	14.7 (8-27.15)	25.2 (16-37) ****	8.4 (5.55-12.9)
Glycoprotein acetyls, mmol/L	1.23 (1.13-1.34)	1.21 (1.11-1.32) *	1.24 (1.14-1.35)
Coagulation parameters			
Fibrinogen, mg/dL	289.32 (257.77-330.88)	300.55 (265.66-346.02) ****	278.98 (247.19-312.78)
Factor VIII (%)	122.98 (101.39-147.01)	123.53 (102.05-148.34)	122.98 (101.39-145.04)
Factor IX (%)	119.31 (108.41-134.28)	119.31 (107.27-136.11)	119.31 (110.74-131.41)
Factor XI (%)	116.77 (103.75-129.16)	120.02 (107.58-134.01) ****	111.56 (100.06-123.93)
Lag time, min	6.72 (6-7.75)	6.5 (5.75-7.58) ****	7.08 (6.17-7.92)
ttPeak, min	14.75 (13.46-16.08)	14.36 (13.19-15.75) ****	15.04 (13.83-16.33)
Peak, nM	83.27 (62.1-106.28)	84.77 (61.11-111.09)	81.69 (63.92-102.77)
ETP, nM-min	1149.22 (915.56-1396.66)	1175.06 (916.94-1439.8) *	1124.76 (914.49-1329.16)
VelIndex, nM/min	10.42 (7.47-14.63)	10.79 (7.36-15.32)	10.18 (7.76-13.8)
SDF imaging parameters			
PBR of total vessels, µm	2.33 (2.19-2.5)	2.35 (2.2-2.54) **	2.3 (2.17-2.44)
PBR of feed vessels, µm	2.28 (2.09-2.48)	2.31 (2.11-2.52) **	2.24 (2.06-2.44)
PBR of capillaries, µm	1.2 (1.13-1.27)	1.2 (1.14-1.27)	1.2 (1.13-1.26)
RBC velocity in feed vessels, µm/s	55.85 (43.93-68.91)	51.24 (39.7-64.4) ****	60.26 (49.5-73.13)
RBC velocity in capillaries, µm/s	55.74 (41.94-70.55)	50.77 (37.78-66.86) ****	60.45 (47.77-72.65)
Total vessel density, µm/mm ²	257.02 (209.81-309.06)	255.58 (206.18-309.23)	259.16 (213.37-306.45)
Feed vessel density, µm/mm ²	131.57 (107.1-160.52)	129.5 (103.51-158.26) *	134.83 (110.94-165.09)
Capillary density, µm/mm ²	100.71 (79.69-131.2)	104.25 (81.76-137.28) *	96.82 (74.81-121.83)
Capillary blood volume, pL/mm ²	2.52 (1.4-4.35)	2.81 (1.41-4.76) *	2.29 (1.38-3.92)

Data are shown as mean (± SD), median (25th percentile–75th percentile), or percentage.

Abbreviations: BMI, body mass index; ETP, endogenous thrombin potential; HRT, hormonal replacement therapy; NA, not applicable; PBR, perfused boundary region; Peak, peak thrombin generation; ttPeak, time to peak; VelIndex, thrombin generation velocity.

Non-paired t-test or Wilcoxon test were performed between women and men; * $p < 0.05$, ** $p < 0.01$, *** $p < 0.001$, **** $p < 0.0001$.

Effect modification by sex of the association between microvascular health and coagulation factors

After sex stratification, we observed differences between men and women between the glycocalyx-related parameters and coagulation factor levels (Figure 2 and Figure 3). Consistent associations were found between PBR_{Total} and $PBR_{feed\ vessel}$ and FIX activity as well as plasma fibrinogen concentration specifically in women, which remained after adjusting for inflammatory markers: one SD in PBR_{Total} or $PBR_{feed\ vessel}$ (0.25 μm and 0.3 μm , respectively) was associated with higher fibrinogen levels (5.1 mg/dL, 95% CI: 0.4-9.9 and 5.8 mg/dL, 95% CI: 1.1-10.6; respectively) and higher FIX activity (1.8%, 95% CI: 0.3-3.3 and 2.0%, 95% CI: 0.5-3.4; respectively) (Figure 2 and Table S3); while no associations were observed in men (Figure 3 and Table S4). For $PBR_{capillary}$, in addition to the association with fibrinogen concentration, $PBR_{capillary}$ was also associated with FVIII activity, which remained after further adjustment for systemic inflammatory markers (model 4): one SD in $PBR_{capillary}$ (0.11 μm) was associated with higher fibrinogen levels (5.3 mg/dL, 95% CI: 0.6-10.0) and FVIII activity (3.5%, 95% CI: 0.4-6.5) (Figure 2 and Table S3).

There were differences in the associations between microcirculatory-perfusion-related parameters and coagulation factor levels stratified by sex. For women, the associations between vessel density and ETP were observed in the crude and age- and sex-adjusted model (Figure S3 and Table S5); however, only $D_{capillary}$ was positively associated with ETP after further adjusting for demographic and lifestyle factors (model 3) and systemic inflammatory markers (model 4), in which one SD of $D_{capillary}$ (42.26 $\mu m/mm^2$) was associated with higher levels of ETP (32.0 nM \times min, 95% CI: 0.1-63.8). In men, only one consistent

negative association was observed between the $RBCV_{\text{feed vessel}}$ and thrombin generation parameter time to peak (ttPeak) (Figure S4 and Table S6), in which one SD of the $RBCV_{\text{feed vessel}}$ (61.52 $\mu\text{m/s}$) was associated with lower levels of ttPeak (-0.2, 95% CI: -0.4- -0.02). In addition, one SD of D_{Total} (68.08 $\mu\text{m/mm}^2$) was associated with higher ETP levels (31.9 $\text{nM} \times \text{min}$, 95% CI: 1.3-62.6).

Sensitivity analyses were performed to test the robustness. Using premenopausal women yielded even more notable results than the main analysis for total women that PBR difference was associated with higher fibrinogen concentration, higher FXI and FVIII activity, and higher thrombin generation parameters (ETP, peak, and VelIndex) (Figure S5, Table S7, Figure S7, and Table S9). However, the results in postmenopausal women were less significant but comparable to the main analysis for all women (Figure S6, Table S8, Figure S8, and Table S10).

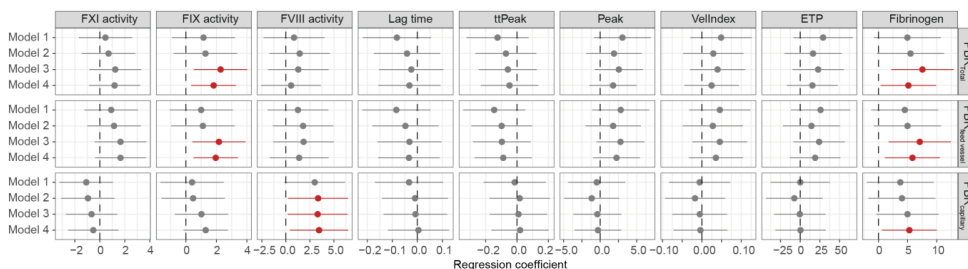


Figure 2. Association between glyocalyx-related SDF imaging parameters and levels of coagulation parameters in women. After sex stratification, differences in women between the glyocalyx-related parameters and coagulation factor levels can be observed. Model 1: crude model; Model 2 = model 1 + age; Model 3: model 2 + BMI, current smoking status, menopausal status, current use of the oral contraceptive pill, and current use of hormone replacement therapy; Model 4 = model 3 + serum CRP, serum leptin concentration, and serum GlycA concentration. The effect size and 95% confidence interval were depicted by a horizontal line with a dot. A non-significant association was represented by the color grey, and a substantial positive association was represented by the color red. Abbreviations: PBR_{Total} : PBR of total vessels from 4-25 μm ; $PBR_{\text{feed vessel}}$: PBR of feed vessels from 10-19 μm ; $PBR_{\text{capillary}}$: PBR of capillaries from 4-9 μm .

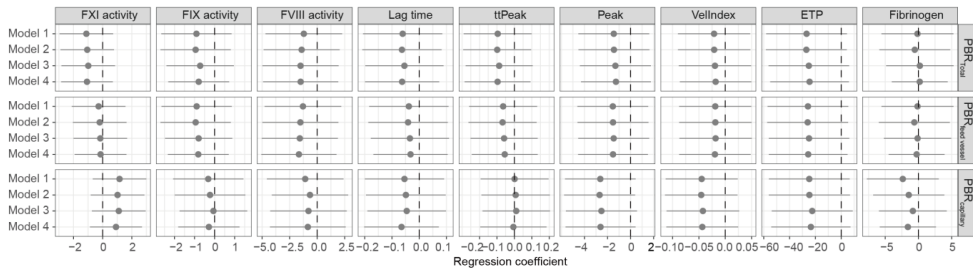


Figure 3. Association between glyocalyx-related SDF imaging parameters and levels of coagulation parameters in men. After sex stratification, differences in men between the glyocalyx-related parameters and coagulation factor levels can be observed. Model 1: crude model; Model 2: model 1 + age; Model 3: model 2 + BMI + current smoking status; Model 4: model 3 + serum CRP, serum leptin concentration, and serum GlycA concentration. The effect size and 95% confidence interval were depicted by a horizontal line with a dot. A non-significant association was represented by the color grey, and a substantial positive association was represented by the color red. Abbreviations: PBR_{Total}: PBR of total vessels from 4-25 μ m; PBR_{feed vessel}: PBR of feed vessels from 10-19 μ m; PBR_{capillary}: PBR of capillaries from 4-9 μ m.

Discussion

In this population-based cross-sectional study the PBR in feed vessels was positively associated with plasma fibrinogen levels in the total population. Remarkably, we discovered a sex difference in the associations between PBR and coagulation parameters, in which higher PBR (both total and feed vessel, indicating perturbed glyocalyx) was associated with higher FIX activity and plasma fibrinogen levels in women. Furthermore, in women, higher PBR_{capillary} (i.e., poorer glyocalyx status in capillaries) was associated with higher FVIII activity and fibrinogen levels and higher D_{capillary} was associated with higher levels of ETP, while none of these associations were present in men.

SDF imaging technique could provide two types of parameters concerning endothelial glyocalyx and microcirculatory perfusion function. We proposed that the change in the endothelial surface properties, i.e., the endothelial glyocalyx layer (PBR), is a likely functional unit that could present as a marker for microvascular dysfunction. In the present

study, we observed an association between early (pre-clinical) microvascular health changes and coagulation factor activation and discovered a striking sex difference in microvascular health, in which women showed a perturbed EG concomitant with a more pro-coagulable endothelial surface. This association was not observed in men. These findings highlight the importance of sex differences in microcirculatory perturbation in CHD.

Previously, studies reported the association between CHD and the underlying systemic presence of a hypercoagulable state [42-44]. Our results showed that in women, one SD in PBR_{Total} and $PBR_{feed\ vessel}$ was associated with a 5.1 and 5.8 mg/dL increase in fibrinogen concentration. Based on a large individual participant meta-analysis study that assessed the association between fibrinogen concentration and CHD risk [45], such increase in PBR would suggest a 12-14% increase in CHD risk in women, which could be clinically relevant. In line with our observations, Brands *et al.* reported that reduced endothelial glycocalyx barrier properties were only found in women with CHD, while not present in men [40]. In addition, in the REasons for Geographic and Racial Differences in Stroke Study (REGARDS), a large population-based observational study, higher levels of FVIII and FIX were associated with increased risk of CHD [35, 46]. According to these associations, per SD difference in PBR could correspond to a 2-5% increase in the risk of CHD in women. FVIII and vWF are two distinct but related glycoproteins that circulate in plasma as a tightly bound complex (FVIII/VWF) [47]. As one of the endothelial activation markers, vWF can bind to HS at the endothelial cell surface [26, 48]. Based on the observed tight correlation between FVIII and vWF in the Multiple Environmental and Genetic Assessment of risk factors for venous thrombosis (MEGA) study [49], we deduced an association between EG health and vWF in our present study, to further indicate the link between EG dysfunction and endothelial activation. Our current findings imply a role of microvascular health in CHD risk in women through the association between higher microvascular PBR (perturbed glycocalyx) and differences in both FIX and FVIII activity, together with the already high plasma fibrinogen levels (Figure 4).

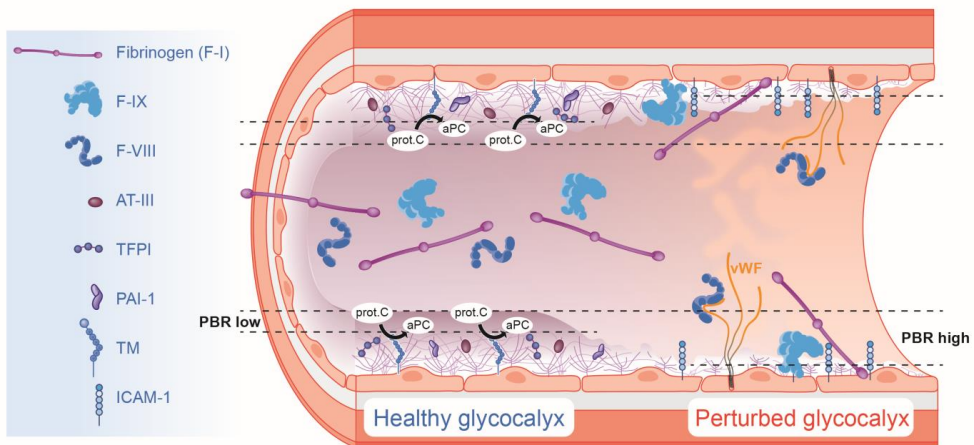


Figure 4. Proposed pathophysiologic concept on the association between microvascular health and endothelial response to coagulation. Here a healthy glycocalyx (i.e., PBR_{low}, marked by the arbitrary dotted lines) provides a robust anti-coagulant barrier through binding of AT-III [22], presence of thrombomodulin [26], PAI-1 [54] and TFPI [23] to HS proteoglycans [19]. The thrombin-TM complex activates protein C to produce APC, which inactivates factors VIIIa and Va in the presence of protein S, thereby inhibiting further thrombin (F-II) formation [55]. The pro-coagulant endothelial surface is a result of multiple mechanisms involving effects such as, gene transcription, protein expression and release. We hypothesized that in the event of a perturbed glycocalyx (i.e., PBR_{high}, marked by arbitrary dotted lines further apart), a pro-coagulant surface appears, with increasing binding possibilities of fibrinogen (interacting with ICAM1) [56, 57], FXI [58, 59] and F-VIII (to surface expressed von Willebrand factor, vWF) [47] and reduced presence of the anti-coagulant factors. While F-IX can bind directly to the cell surface or abluminal collagen, fibrinogen and F-VIII binding to the surface depends more on the activation state of the endothelial cells. This increased interaction of coagulation factor IX and VIII activity and fibrinogen concentration, as observed in the present study, together with possible diminished surface anti-coagulation pathways, would especially in women play a critical role in increased systemic microvascular dysfunction and development of coronary heart disease (CHD).

The present study also included various thrombin generation parameters which represent the global coagulation cascade in addition to coagulation factor activity. Interestingly, no associations were observed between the microvascular health parameters measured and

the dynamic parameters of thrombin generation (such as lag time and time to peak); except for an association between vessel density and ETP. Thrombin was found to be involved in both pro-thrombotic and inflammatory endothelial processes [50]. While previous studies reported an association between *in vivo* thrombin generation potential and severity of coronary vessel disease [51], increased thrombin generation potential was a characteristic in patients with clinically stable CHD [52]. Although we found sex differences in the association between vessel density and ETP, when we compared the findings in the total population, men, and women, we found that the associations in men and women were close to significance; therefore, this observation might reflect a general feature of microvascular health and thrombin formation rather than a sex specific feature. Furthermore, comparing with previous studies using thrombin generation assay, the participants in the present study were preclinical and did not have CHD yet, which might limit the effect of thrombin and findings related to thrombin generation. In the context with the associations between endothelial glycocalyx (PBR) and coagulation factors, the associations between vessel densities and ETP were very marginal.

To the best of our knowledge, this is the first study to show the association between microvascular health derived from SDF imaging and the levels of coagulation factors and thrombin generation parameters in a large population-based study. In addition, adjustment for extensive potential confounding factors including systemic inflammatory markers strongly suggested a sex-specific role in monitoring microvascular health change in women. Additionally, the present study used the new software with red blood cell (RBC) velocity being included as a new parameter to better quantify the microcirculatory difference.

Limitations of the present study should also be addressed. First, it is an observational, cross-sectional study and residual confounding may still be present. Second, the present study population is mainly comprised of European white participants in middle age (i.e., between 45 and 65 years). Therefore, it is not clear whether the results of the present study can be generalizable to other ethnicities or age groups. Third, the majority of women are postmenopausal; although sensitivity analysis revealed similar findings in premenopausal

women, future studies including more premenopausal women need to be done. Fourth, a recent study reported the variability of microcirculatory measurements in healthy volunteers [53] showing that when three consecutive measurements are averaged, SDF imaging with GlycoCheck software can be used with acceptable reliability and reproducibility for microcirculation measurements on a population level. In our current study, repeated measurement of SDF imaging was not performed for each participant and limited information was extracted from the smallest capillaries (diameter 4 μm). However, the measurement by itself is already an average from at least ten recordings on one individual at the same time point rather than averaging three consecutive measurements on the same individual, which could only lead to random error and subsequent underestimation of the effect size. Fifth, due to the technical limitation of the *ex vivo* thrombin generation assay, we could not avoid batch effects and this assay could not represent the real circumstances of the coagulation cascade in humans. Sixth, as a result of sample availability to measure the circulating EG disruption and EC activation markers, our study lacks possible mechanistic correlations between EG dysfunction, increased procoagulant state and increased CHD risk in females. Seventhly, although we focussed on the role of EG perturbation in coagulation in the present study, it is important to note that the formation of a pro-coagulant surface is a result of multiple mechanisms, among others, such as gene transcription changes and protein expression and release. Finally, in model 4 we adjusted for systemic inflammatory markers (such as CRP, leptin, and GlycA) in the association between microvascular health and coagulation factor levels. It should be noted that these systemic inflammatory markers could act as mediators instead of confounders in the estimated associations. If so, adjustment for systemic inflammatory markers could lead to an underestimation of the association between microvascular health and coagulation factor levels.

In conclusion, our data reveal a hitherto unreported sex-specific association between microcirculatory health and procoagulant status. Microcirculatory differences between men and women identified in our study implied that microvascular health changes might be

the earliest detectable clue prior to the general higher procoagulant status in women ultimately developing CHD, which is also independent of increased systemic inflammatory state (Figure 4). Our study suggested the potential clinical utility of monitoring microcirculatory change specifically in women to prevent the development of CHD.

Authors' contributions

The inclusion of participants for the NEO study, the study design of the NEO study, and the acquisition of data of the NEO study have been performed by Renée de Mutsert and Frits R. Rosendaal. Of the present study, the study concept and design was performed by Lushun Yuan, Jihee Han, Ruifang Li-Gao, T.J Rabelink and Bernard M. van den Berg. The analyses and interpretation of the data were performed by Lushun Yuan, Jihee Han, Anouk I.M. van der Velden, Hans Vink, Astrid van Hylckama Vlieg, Renée de Mutsert, Ruifang Li-Gao, T.J Rabelink and Bernard M. van den Berg. The draft of the manuscript and design of figures are performed by Lushun Yuan, Jihee Han, Ruifang Li-Gao, T.J Rabelink and Bernard M. van den Berg. All authors read and approved the final manuscript.

Acknowledgments

We express our gratitude toward all participants of the NEO study. Furthermore, we thank P.R. van Beelen and all research nurses for the data collection, P.J. Noordijk and her team for the handling and storage of the blood samples, and I. de Jonge for the data management.

Conflict of interest

Hans Vink works for MicroVascular Health Solutions LLC and Ruifang Li-Gao works for Metabolon Inc. All of the authors, including Lushun Yuan, Jihee Han, Anouk I.M. van der Velden, Hans Vink, Renée de Mutsert, Frits R. Rosendaal, Astrid van Hylckama Vlieg,

Ruifang Li-Gao, T.J Rabelink, Bernard M. van den Berg, hereby confirm that they have no conflict of interest and have nothing to disclose.

Funding

The NEO study is supported by the participating departments, the Division and the Board of Directors of the Leiden University Medical Centre, and by the Leiden University, Research Profile Area 'Vascular and Regenerative Medicine'. Coagulation factor analyses were funded by 'Stichting De Merel'. Stichting De Merel had no role in the study design, data collection, and analysis, decision to publish, or preparation, review, or approval of the manuscript. This work was supported by the China Scholarship Council grant to Lushun Yuan (CSC no. 201806270262).

Reference

- 1 Bots SH, Peters SAE, Woodward M. Sex differences in coronary heart disease and stroke mortality: a global assessment of the effect of ageing between 1980 and 2010. *BMJ Glob Health*. 2017; **2**: e000298. 10.1136/bmjgh-2017-000298.
- 2 Maas AH, Appelman YE. Gender differences in coronary heart disease. *Neth Heart J*. 2010; **18**: 598-602. 10.1007/s12471-010-0841-y.
- 3 Koller A. Perspectives: Microvascular endothelial dysfunction and gender. *Eur Heart J Suppl*. 2014; **16**: A16-A9. 10.1093/eurheartj/sut005.
- 4 Padro T, Manfrini O, Bugiardini R, Canty J, Cenko E, De Luca G, Duncker DJ, Eringa EC, Koller A, Tousoulis D, Trifunovic D, Vavlukis M, de Wit C, Badimon L. ESC Working Group on Coronary Pathophysiology and Microcirculation position paper on 'coronary microvascular dysfunction in cardiovascular disease'. *Cardiovasc Res*. 2020; **116**: 741-55. 10.1093/cvr/cvaa003.
- 5 Lekakis J, Abraham P, Balbarini A, Blann A, Boulanger CM, Cockcroft J, Cosentino F, Deanfield J, Gallino A, Ikonomidis I, Kremastinos D, Landmesser U, Protogerou A, Stefanadis C, Tousoulis D, Vassalli G, Vink H, Werner N, Wilkinson I, Vlachopoulos C. Methods for evaluating endothelial function: a position statement from the European Society of Cardiology Working Group on Peripheral Circulation. *Eur J Cardiovasc Prev Rehabil*. 2011; **18**: 775-89. 10.1177/1741826711398179.

- 6 Lee DH, Dane MJ, van den Berg BM, Boels MG, van Teeffelen JW, de Mutsert R, den Heijer M, Rosendaal FR, van der Vlag J, van Zonneveld AJ, Vink H, Rabelink TJ, group NEOs. Deeper penetration of erythrocytes into the endothelial glycocalyx is associated with impaired microvascular perfusion. *PLoS one*. 2014; **9**: e96477. 10.1371/journal.pone.0096477.
- 7 de Mutsert R, den Heijer M, Rabelink TJ, Smit JW, Romijn JA, Jukema JW, de Roos A, Cobbaert CM, Kloppenburg M, le Cessie S, Middeldorp S, Rosendaal FR. The Netherlands Epidemiology of Obesity (NEO) study: study design and data collection. *European journal of epidemiology*. 2013; **28**: 513-23. 10.1007/s10654-013-9801-3.
- 8 Rovas A, Sackarnd J, Rossaint J, Kampmeier S, Pavenstadt H, Vink H, Kumpers P. Identification of novel sublingual parameters to analyze and diagnose microvascular dysfunction in sepsis: the NOSTRADAMUS study. *Crit Care*. 2021; **25**: 112. 10.1186/s13054-021-03520-w.
- 9 van der Velden AIM, van den Berg BM, de Mutsert R, van der Vlag J, Jukema JW, Rosendaal FR, Rabelink TJ, Vink H. Microvascular differences in individuals with obesity at risk of developing cardiovascular disease. *Obesity*. 2021; **29**: 1439-44. 10.1002/oby.23222.
- 10 Drost CC, Rovas A, Kusche-Vihrog K, Van Slyke P, Kim H, Hoang VC, Maynes JT, Wennmann DO, Pavenstadt H, Linke W, Lukasz A, Hesse B, Kumpers P. Tie2 Activation Promotes Protection and Reconstitution of the Endothelial Glycocalyx in Human Sepsis. *Thromb Haemost*. 2019; **119**: 1827-38. 10.1055/s-0039-1695768.
- 11 Rovas A, Seidel LM, Vink H, Pohlkötter T, Pavenstadt H, Ertmer C, Hessler M, Kumpers P. Association of sublingual microcirculation parameters and endothelial glycocalyx dimensions in resuscitated sepsis. *Crit Care*. 2019; **23**: 260. 10.1186/s13054-019-2542-2.
- 12 Bol ME, Huckriede JB, van de Pas KGH, Delhaas T, Lorusso R, Nicolaes GAF, Sels JEM, van de Poll MCG. Multimodal measurement of glycocalyx degradation during coronary artery bypass grafting. *Front Med (Lausanne)*. 2022; **9**: 1045728. 10.3389/fmed.2022.1045728.
- 13 Rovas A, Osiaevi I, Buscher K, Sackarnd J, Tepasse PR, Fobker M, Kuhn J, Braune S, Gobel U, Tholking G, Groschel A, Pavenstadt H, Vink H, Kumpers P. Microvascular dysfunction in COVID-19: the MYSTIC study. *Angiogenesis*. 2021; **24**: 145-57. 10.1007/s10456-020-09753-7.
- 14 van Dinther M, Bennett J, Thornton GD, Voorter PHM, Ezponda Casajus A, Hughes A, Captur G, Holtackers RJ, Staals J, Backes WH, Bastarika G, Jones EAV, Gonzalez A, van Oostenbrugge R, Treibel TA. Evaluation of microvascular rarefaction in vascular Cognitive Impairment and heart failure (CRUCIAL): Study protocol for an observational study. *Cerebrovasc Dis Extra*. 2023; **13**: 18-32. 10.1159/000529067.
- 15 Ikonomidis I, Pavlidis G, Lambadiari V, Rafouli-Stergiou P, Makavos G, Thymis J, Kostelli G, Varoudi M, Katogiannis K, Theodoropoulos K, Katsimbri P, Parissis J, Papadavid

E. Endothelial glycocalyx and microvascular perfusion are associated with carotid intima-media thickness and impaired myocardial deformation in psoriatic disease. *J Hum Hypertens*. 2022; **36**: 1113-20. 10.1038/s41371-021-00640-2.

16 Dane MJ, van den Berg BM, Lee DH, Boels MG, Tiemeier GL, Avramut MC, van Zonneveld AJ, van der Vlag J, Vink H, Rabelink TJ. A microscopic view on the renal endothelial glycocalyx. *Am J Physiol Renal Physiol*. 2015; **308**: F956-F66. 10.1152/ajprenal.00532.2014.

17 Schmidt EP, Yang Y, Janssen WJ, Gandjeva A, Perez MJ, Barthel L, Zemans RL, Bowman JC, Koyanagi DE, Yunt ZX, Smith LP, Cheng SS, Overdier KH, Thompson KR, Geraci MW, Douglas IS, Pearse DB, Tudor RM. The pulmonary endothelial glycocalyx regulates neutrophil adhesion and lung injury during experimental sepsis. *Nature medicine*. 2012; **18**: 1217-23. 10.1038/nm.2843.

18 Reitsma S, Oude Egbrink MG, Heijnen VV, Megens RT, Engels W, Vink H, Slaaf DW, van Zandvoort MA. Endothelial glycocalyx thickness and platelet-vessel wall interactions during atherogenesis. *Thromb Haemost*. 2011; **106**: 939-46. 10.1160/TH11-02-0133.

19 Boels MG, Lee DH, van den Berg BM, Dane MJ, van der Vlag J, Rabelink TJ. The endothelial glycocalyx as a potential modifier of the hemolytic uremic syndrome. *Eur J Intern Med*. 2013; **24**: 503-9. 10.1016/j.ejim.2012.12.016.

20 de Jongh RT, Serne EH, RG IJ, de Vries G, Stehouwer CD. Impaired microvascular function in obesity: implications for obesity-associated microangiopathy, hypertension, and insulin resistance. *Circulation*. 2004; **109**: 2529-35. 10.1161/01.CIR.0000129772.26647.6F.

21 Vlahu CA, Lemkes BA, Struijk DG, Koopman MG, Krediet RT, Vink H. Damage of the endothelial glycocalyx in dialysis patients. *J Am Soc Nephrol*. 2012; **23**: 1900-8. 10.1681/ASN.2011121181.

22 Chopra P, Joshi A, Wu J, Lu W, Yadavalli T, Wolfert MA, Shukla D, Zaia J, Boons GJ. The 3-O-sulfation of heparan sulfate modulates protein binding and lyase degradation. *Proc Natl Acad Sci U S A*. 2021; **118**. 10.1073/pnas.2012935118.

23 Tinholt M, Stavik B, Louch W, Carlson CR, Sletten M, Ruf W, Skretting G, Sandset PM, Iversen N. Syndecan-3 and TFPI colocalize on the surface of endothelial-, smooth muscle-, and cancer cells. *PLoS one*. 2015; **10**: e0117404. 10.1371/journal.pone.0117404.

24 Rezaie AR, Giri H. Anticoagulant and signaling functions of antithrombin. *Journal of thrombosis and haemostasis : JTH*. 2020; **18**: 3142-53. 10.1111/jth.15052.

25 Uchimido R, Schmidt EP, Shapiro NI. The glycocalyx: a novel diagnostic and therapeutic target in sepsis. *Crit Care*. 2019; **23**: 16. 10.1186/s13054-018-2292-6.

26 Yuan L, Cheng S, Sol W, van der Velden AIM, Vink H, Rabelink TJ, van den Berg BM. Heparan sulfate mimetic fucoidan restores the endothelial glycocalyx and protects against

dysfunction induced by serum of COVID-19 patients in the intensive care unit. *ERJ Open Res.* 2022; **8**. 10.1183/23120541.00652-2021.

27 Rabelink TJ, van den Berg BM, Garsen M, Wang G, Elkin M, van der Vlag J. Heparanase: roles in cell survival, extracellular matrix remodelling and the development of kidney disease. *Nat Rev Nephrol.* 2017; **13**: 201-12. 10.1038/nrneph.2017.6.

28 Haeren RH, Vink H, Staals J, van Zandvoort MA, Dings J, van Overbeeke JJ, Hoogland G, Rijkers K, Schijns OE. Protocol for intraoperative assessment of the human cerebrovascular glycocalyx. *BMJ open.* 2017; **7**: e013954. 10.1136/bmjopen-2016-013954.

29 Vorster HH. Fibrinogen and women's health. *Thromb Res.* 1999; **95**: 137-54. 10.1016/s0049-3848(99)00033-x.

30 Kim PY, Stewart RJ, Lipson SM, Nesheim ME. The relative kinetics of clotting and lysis provide a biochemical rationale for the correlation between elevated fibrinogen and cardiovascular disease. *J Thromb Haemost.* 2007; **5**: 1250-6. 10.1111/j.1538-7836.2007.02426.x.

31 Hsieh CT, Chien KL, Hsu HC, Lin HJ, Su TC, Chen MF, Lee YT. Associations between fibrinogen levels and the risk of cardiovascular disease and all-cause death: a cohort study from the Chin-Shan community in Taiwan. *BMJ Open.* 2022; **12**: e054638. 10.1136/bmjopen-2021-054638.

32 Wilhelmsen L, Svardsudd K, Korsan-Bengtson K, Larsson B, Welin L, Tibblin G. Fibrinogen as a risk factor for stroke and myocardial infarction. *N Engl J Med.* 1984; **311**: 501-5. 10.1056/NEJM198408233110804.

33 Rudnicka AR, Mt-Isa S, Meade TW. Associations of plasma fibrinogen and factor VII clotting activity with coronary heart disease and stroke: prospective cohort study from the screening phase of the Thrombosis Prevention Trial. *J Thromb Haemost.* 2006; **4**: 2405-10. 10.1111/j.1538-7836.2006.02221.x.

34 Lee AJ, Lowe GD, Smith WC, Tunstall-Pedoe H. Plasma fibrinogen in women: relationships with oral contraception, the menopause and hormone replacement therapy. *Br J Haematol.* 1993; **83**: 616-21. 10.1111/j.1365-2141.1993.tb04699.x.

35 Olson NC, Cushman M, Judd SE, Kissela BM, Safford MM, Howard G, Zakai NA. Associations of coagulation factors IX and XI levels with incident coronary heart disease and ischemic stroke: the REGARDS study. *J Thromb Haemost.* 2017; **15**: 1086-94. 10.1111/jth.13698.

36 Dekkers IA, de Mutsert R, de Vries APJ, Rosendaal FR, Cannegieter SC, Jukema JW, le Cessie S, Rabelink TJ, Lamb HJ, Lijfering WM. Determinants of impaired renal and vascular function are associated with elevated levels of procoagulant factors in the general population. *Journal of thrombosis and haemostasis : JTH.* 2018; **16**: 519-28. 10.1111/jth.13935.

- 37 Hemker HC, Giesen P, Al Dieri R, Regnault V, de Smedt E, Wagenvoord R, Lecompte T, Beguin S. Calibrated automated thrombin generation measurement in clotting plasma. *Pathophysiol Haemost Thromb*. 2003; **33**: 4-15. 10.1159/000071636.
- 38 Buis DTP, Christen T, Smit RAJ, de Mutsert R, Jukema JW, Cannegieter SC, Lijfering WM, Rosendaal FR. The association between leptin concentration and blood coagulation: Results from the NEO study. *Thrombosis research*. 2020; **188**: 44-8. 10.1016/j.thromres.2020.01.021.
- 39 Huxley VH, Kemp SS. Sex-Specific Characteristics of the Microcirculation. *Adv Exp Med Biol*. 2018; **1065**: 307-28. 10.1007/978-3-319-77932-4_20.
- 40 Brands J, Hubel CA, Althouse A, Reis SE, Pacella JJ. Noninvasive sublingual microvascular imaging reveals sex-specific reduction in glycocalyx barrier properties in patients with coronary artery disease. *Physiol Rep*. 2020; **8**: e14351. 10.14814/phy2.14351.
- 41 Cohen J. *Statistical Power Analysis for the Behavioral Sciences*. 2nd ed. New York: Routledge, 1988.
- 42 Song CJ, Nakagomi A, Chandar S, Cai H, Lim IG, McNeil HP, Freedman SB, Geczy CL. C-reactive protein contributes to the hypercoagulable state in coronary artery disease. *J Thromb Haemost*. 2006; **4**: 98-106. 10.1111/j.1538-7836.2005.01705.x.
- 43 Tantry US, Bliden KP, Suarez TA, Kreutz RP, Dichiara J, Gurbel PA. Hypercoagulability, platelet function, inflammation and coronary artery disease acuity: results of the Thrombotic Risk Progression (TRIP) study. *Platelets*. 2010; **21**: 360-7. 10.3109/09537100903548903.
- 44 Bratseth V, Pettersen AA, Opstad TB, Arnesen H, Seljeflot I. Markers of hypercoagulability in CAD patients. Effects of single aspirin and clopidogrel treatment. *Thromb J*. 2012; **10**: 12. 10.1186/1477-9560-10-12.
- 45 Fibrinogen Studies C, Danesh J, Lewington S, Thompson SG, Lowe GD, Collins R, Kostis JB, Wilson AC, Folsom AR, Wu K, Benderly M, Goldbourt U, Willeit J, Kiechl S, Yarnell JW, Sweetnam PM, Elwood PC, Cushman M, Psaty BM, Tracy RP, Tybjaerg-Hansen A, Haverkate F, de Maat MP, Fowkes FG, Lee AJ, Smith FB, Salomaa V, Harald K, Rasi R, Vahtera E, Jousilahti P, Pekkanen J, D'Agostino R, Kannel WB, Wilson PW, Tofler G, Arocha-Pinango CL, Rodriguez-Larralde A, Nagy E, Mijares M, Espinosa R, Rodriguez-Roa E, Ryder E, Diez-Ewald MP, Campos G, Fernandez V, Torres E, Marchioli R, Valagussa F, Rosengren A, Wilhelmsen L, Lappas G, Eriksson H, Cremer P, Nagel D, Curb JD, Rodriguez B, Yano K, Salonen JT, Nyyssonen K, Tuomainen TP, Hedblad B, Lind P, Loewel H, Koenig W, Meade TW, Cooper JA, De Stavola B, Knottenbelt C, Miller GJ, Cooper JA, Bauer KA, Rosenberg RD, Sato S, Kitamura A, Naito Y, Palosuo T, Ducimetiere P, Amouyel P, Arveiler D, Evans AE, Ferrieres J, Juhan-Vague I, Bingham A, Schulte H, Assmann G, Cantin B, Lamarche B, Despres JP, Dagenais GR, Tunstall-Pedoe H, Woodward M, Ben-Shlomo Y, Davey Smith G, Palmieri V, Yeh JL, Rudnicka A, Ridker P, Rodeghiero F, Tosetto A, Shepherd J, Ford I,

Robertson M, Brunner E, Shipley M, Feskens EJ, Kromhout D, Dickinson A, Ireland B, Juzwishin K, Kaptoge S, Lewington S, Memon A, Sarwar N, Walker M, Wheeler J, White I, Wood A. Plasma fibrinogen level and the risk of major cardiovascular diseases and nonvascular mortality: an individual participant meta-analysis. *JAMA*. 2005; **294**: 1799-809. 10.1001/jama.294.14.1799.

46 Zakai NA, Judd SE, Kissela B, Howard G, Safford MM, Cushman M. Factor VIII, Protein C and Cardiovascular Disease Risk: The REasons for Geographic and Racial Differences in Stroke Study (REGARDS). *Thromb Haemost*. 2018; **118**: 1305-15. 10.1055/s-0038-1655766.

47 Federici AB. The factor VIII/von Willebrand factor complex: basic and clinical issues. *Haematologica*. 2003; **88**: EREPO2.

48 Kalagara T, Moutsis T, Yang Y, Pappelbaum KI, Farken A, Cladder-Micus L, Vidal YSS, John A, Bauer AT, Moerschbacher BM, Schneider SW, Gorzelanny C. The endothelial glycocalyx anchors von Willebrand factor fibers to the vascular endothelium. *Blood Adv*. 2018; **2**: 2347-57. 10.1182/bloodadvances.2017013995.

49 Rietveld IM, Lijfering WM, le Cessie S, Bos MHA, Rosendaal FR, Reitsma PH, Cannegieter SC. High levels of coagulation factors and venous thrombosis risk: strongest association for factor VIII and von Willebrand factor. *J Thromb Haemost*. 2019; **17**: 99-109. 10.1111/jth.14343.

50 Foley JH, Conway EM. Cross Talk Pathways Between Coagulation and Inflammation. *Circ Res*. 2016; **118**: 1392-408. 10.1161/CIRCRESAHA.116.306853.

51 Rho R, Tracy RP, Bovill EG, Ball SP, Becker RC. Plasma Markers of Procoagulant Activity Among Individuals with Coronary Artery Disease. *J Thromb Thrombolysis*. 1995; **2**: 239-43. 10.1007/BF01062716.

52 Tosi F, Micaglio R, Sandri M, Castagna A, Minguzzi D, Stefanoni F, Chiariello C, Franzese I, Luciani GB, Faggian G, Girelli D, Olivieri O, Martinelli N. Increased plasma thrombin potential is associated with stable coronary artery disease: An angiographically-controlled study. *Thromb Res*. 2017; **155**: 16-22. 10.1016/j.thromres.2017.04.021.

53 Bol ME, Broddin BEK, Delhaas T, Sels JEM, van de Poll MCG. Variability of microcirculatory measurements in healthy volunteers. *Sci Rep*. 2022; **12**: 19887. 10.1038/s41598-022-22947-x.

54 Dolleman SC, Agten SM, Spronk HMH, Hackeng TM, Bos MHA, Versteeg HH, van Zonneveld AJ, de Boer HC. Thrombin in complex with dabigatran can still interact with PAR-1 via exosite-I and instigate loss of vascular integrity. *J Thromb Haemost*. 2022; **20**: 996-1007. 10.1111/jth.15642.

55 Ikezoe T. Thrombomodulin/activated protein C system in septic disseminated intravascular coagulation. *J Intensive Care*. 2015; **3**: 1. 10.1186/s40560-014-0050-7.

- 56 Pluskota E, D'Souza SE. Fibrinogen interactions with ICAM-1 (CD54) regulate endothelial cell survival. *Eur J Biochem.* 2000; **267**: 4693-704. 10.1046/j.1432-1327.2000.01520.x.
- 57 Tsakadze NL, Zhao Z, D'Souza SE. Interactions of intercellular adhesion molecule-1 with fibrinogen. *Trends Cardiovasc Med.* 2002; **12**: 101-8. 10.1016/s1050-1738(01)00157-8.
- 58 Kossmann S, Lagrange J, Jackel S, Jurk K, Ehlken M, Schonfelder T, Weihert Y, Knorr M, Brandt M, Xia N, Li H, Daiber A, Oelze M, Reinhardt C, Lackner K, Gruber A, Monia B, Karbach SH, Walter U, Ruggeri ZM, Renne T, Ruf W, Munzel T, Wenzel P. Platelet-localized FXI promotes a vascular coagulation-inflammatory circuit in arterial hypertension. *Sci Transl Med.* 2017; **9**. 10.1126/scitranslmed.aah4923.
- 59 Shariat-Madar Z, Mahdi F, Schmaier AH. Factor XI assembly and activation on human umbilical vein endothelial cells in culture. *Thromb Haemost.* 2001; **85**: 544-51.

Supporting information

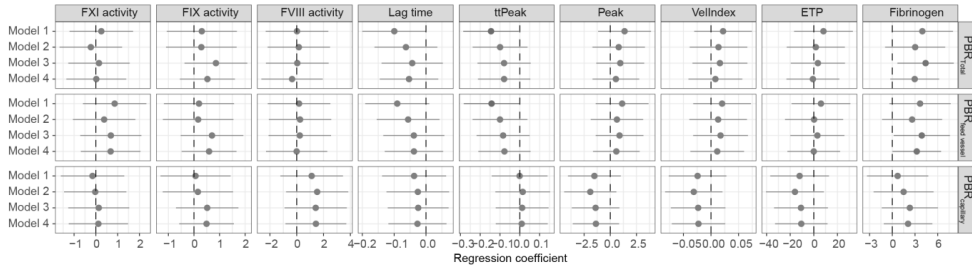


Figure S1. Association between glycoalyx-related SDF imaging parameters and levels of coagulation parameters in total population. Differences in the total population between the glycoalyx-related parameters and coagulation factor levels can be observed. Model 1: crude model; Model 2: model 1 + sex + age; Model 3: model 2 + BMI, current smoking status, menopausal status, current use of the oral contraceptive pill, and current use of hormone replacement therapy; Model 4: model 3 + serum CRP, serum leptin concentration, and serum GlycA concentration. The effect size and 95% confidence interval were depicted by a horizontal line with a dot. A non-significant association was represented by the color grey, and a substantial positive association was represented by the color red. Abbreviations: PBR_{Total}: PBR of total vessels from 4-25 μ m; PBR_{feed vessel}: PBR of feed vessels from 10-19 μ m; PBR_{capillary}: PBR of capillaries from 4-9 μ m.

Table S1. Association between glyocalyx-related SDF imaging parameters and levels of coagulation parameters in total population.

		FXI activity	FIX activity	FVIII activity	Lag time	ttPeak	Peak	ETP	VellIndex	Fibrinogen
PBR _{Total}	Model 1	0.3 (-1.2-1.7)	0.3 (-1.1-1.7)	0 (-2.3-2.4)	-0.1 (-0.2-0)	-0.1 (-0.3-0)	1.4 (-1.2-3.9)	8.2 (-16.7-33.1)	0 (0-0.1)	4 (-0.1-8)
	Model 2	-0.2 (-1.7-1.2)	0.3 (-1.1-1.7)	0.2 (-2.2-2.5)	-0.1 (-0.2-0)	-0.1 (-0.2-0)	0.8 (-1.7-3.3)	1.7 (-22.9-26.3)	0 (0-0.1)	3 (-0.9-7)
	Model 3	0.1 (-1.3-1.6)	0.9 (-0.4-2.1)	0 (-2.3-2.4)	0 (-0.1-0.1)	-0.1 (-0.2-0.1)	1 (-1.3-3.2)	3.4 (-19.5-26.4)	0 (0-0.1)	4.4 (0.7-8.1)
	Model 4	0 (-1.4-1.4)	0.5 (-0.5-1.6)	-0.3 (-2.6-1.9)	-0.1 (-0.1-0)	-0.1 (-0.2-0.1)	0.5 (-1.7-2.8)	-0.8 (-23.2-21.6)	0 (0-0.1)	3 (-0.3-6.2)
PBR _{feed vessel}	Model 1	0.9 (-0.6-2.3)	0.2 (-1.2-1.6)	0.2 (-2.2-2.5)	-0.1 (-0.2-0)	-0.1 (-0.3-0)	1.1 (-1.4-3.7)	6.1 (-18.8-31)	0 (0-0.1)	3.7 (-0.4-7.7)
	Model 2	0.4 (-1.1-1.8)	0.2 (-1.2-1.5)	0.2 (-2.1-2.6)	-0.1 (-0.2-0)	-0.1 (-0.2-0)	0.6 (-1.9-3.1)	0.2 (-24.4-24.9)	0 (0-0.1)	2.6 (-1.4-6.6)
	Model 3	0.7 (-0.7-2.1)	0.7 (-0.5-1.9)	0.2 (-2.1-2.6)	0 (-0.1-0.1)	-0.1 (-0.2-0)	0.9 (-1.4-3.2)	3 (-19.9-25.9)	0 (0-0.1)	3.9 (0.2-7.6)
	Model 4	0.7 (-0.7-2)	0.6 (-0.5-1.7)	0 (-2.3-2.3)	0 (-0.1-0.1)	-0.1 (-0.2-0.1)	0.6 (-1.6-2.8)	0 (-22.4-22.3)	0 (0-0.1)	3.2 (0-6.4)
PBR _{capillary}	Model 1	-0.2 (-1.6-1.3)	0.1 (-1.3-1.4)	1.1 (-1.2-3.5)	0 (-0.1-0.1)	0 (-0.1-0.1)	-1.5 (-4-1)	-12 (-36.9-12.9)	0 (-0.1-0)	0.7 (-3.3-4.8)
	Model 2	0 (-1.5-1.4)	0.2 (-1.2-1.5)	1.5 (-0.8-3.8)	0 (-0.1-0.1)	0 (-0.1-0.2)	-1.9 (-4.4-0.6)	-16 (-40.5-8.5)	0 (-0.1-0)	1.5 (-2.5-5.4)
	Model 3	0.1 (-1.3-1.5)	0.5 (-0.7-1.7)	1.4 (-0.9-3.7)	0 (-0.1-0.1)	0 (-0.1-0.1)	-1.4 (-3.7-0.9)	-10.9 (-33.7-11.9)	0 (-0.1-0)	2.3 (-1.4-6)
	Model 4	0.1 (-1.2-1.5)	0.5 (-0.6-1.6)	1.4 (-0.8-3.7)	0 (-0.1-0.1)	0 (-0.1-0.1)	-1.4 (-3.6-0.8)	-10.6 (-32.8-11.6)	0 (-0.1-0)	2.1 (-1.1-5.3)

Results are based on linear regression analyses of the general Dutch population. The beta coefficient (95% CI) can be interpreted as differences in coagulation parameter levels per SD change in PBR.

Model 1 = crude model.

Model 2 = model 1 + sex + age.

Model 3 = model 2 + BMI, current smoking status, menopausal status, current use of the oral contraceptive pill, and current use of hormone replacement therapy.

Model 4 = model 3 + serum CRP, serum leptin concentration, and serum GlycA concentration.

Abbreviation: PBR_{Total}: PBR of total vessels from 4-25µm; PBR_{feed vessel}: PBR of feed vessels from 10-19µm; PBR_{capillary}: PBR of capillaries from 4-9µm.

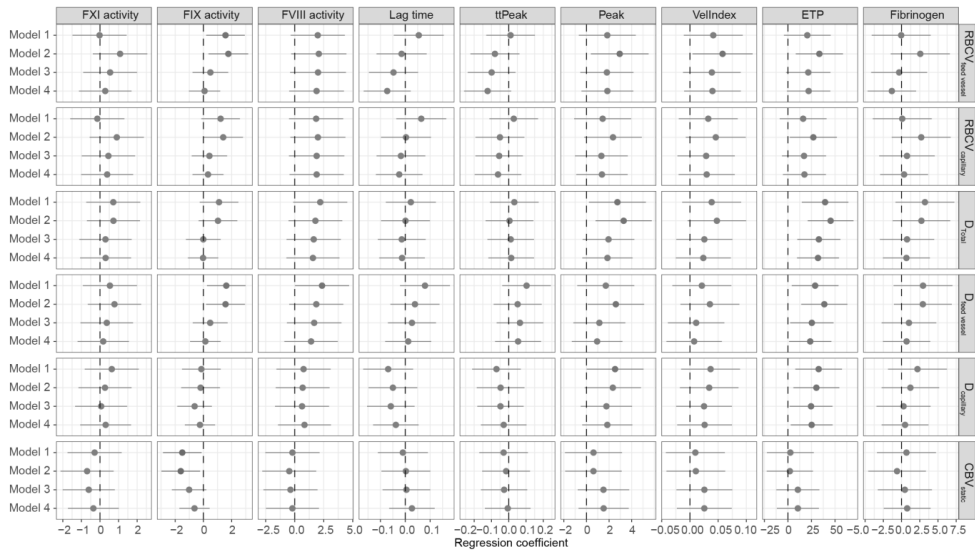


Figure S2. Association between microcirculatory-perfusion-related SDF imaging parameters and levels of coagulation parameters in total population. Differences in the total population between the microcirculatory-perfusion-related parameters and coagulation factor levels can be observed. Model 1: crude model; Model 2: model 1 + sex + age; Model 3: model 2 + BMI, current smoking status, menopausal status, current use of the oral contraceptive pill, and current use of hormone replacement therapy; Model 4: model 3 + serum CRP, serum leptin concentration, and serum GlycA concentration. The effect size and 95% confidence interval were depicted by a horizontal line with a dot. A non-significant association was represented by the color grey, and a substantial positive association was represented by the color red. Abbreviations: $RBCV_{feed\ vessel}$: feed vessel RBC velocity; $RBCV_{capillary}$: capillary RBC velocity; D_{Total} : total valid vessel density with measurable RBC velocity; $D_{feed\ vessel}$: perfused feed vessel density; $D_{capillary}$: perfused capillary density; CBV_{static} : capillary blood volume.

Table S2. Association between microcirculatory-perfusion-related SDF imaging parameters and levels of coagulation parameters in total population.

		FXI activity	FIX activity	FVIII activity	Lag time	ttPeak	Peak	ETP	VelIndex	Fibrinogen
RBCV _{feed vessel}	Model 1	0 (-1.5-1.4)	1.6 (0.2-2.9)	2 (-0.3-4.3)	0.1 (0-0.2)	0 (-0.1-0.2)	1.8 (-0.7-4.4)	20.6 (-4.3-45.4)	0 (0-0.1)	-0.1 (-4.1-4)
	Model 2	1.1 (-0.4-2.5)	1.8 (0.4-3.2)	2.1 (-0.3-4.5)	0 (-0.1-0.1)	-0.1 (-0.2-0.1)	2.9 (0.4-5.5)	33.4 (8.3-58.5)	0.1 (0-0.1)	2.6 (-1.5-6.6)
	Model 3	0.5 (-0.9-2)	0.5 (-0.8-1.8)	2 (-0.4-4.4)	0 (-0.1-0.1)	-0.1 (-0.2-0)	1.8 (-0.5-4.2)	21.6 (-2-45.2)	0 (0-0.1)	-0.3 (-4.2-3.5)
	Model 4	0.3 (-1.1-1.7)	0.1 (-1-1.2)	1.9 (-0.5-4.2)	-0.1 (-0.2-0)	-0.1 (-0.3-0)	1.8 (-0.4-4.1)	22 (-1.1-45)	0 (0-0.1)	-1.3 (-4.7-2)
RBCV _{capillary}	Model 1	-0.1 (-1.6-1.3)	1.2 (-0.1-2.6)	1.8 (-0.5-4.2)	0.1 (0-0.2)	0 (-0.1-0.2)	1.4 (-1.1-4)	16.1 (-8.7-41)	0 (0-0.1)	0.1 (-4-4.1)
	Model 2	0.9 (-0.6-2.4)	1.4 (0-2.8)	2 (-0.4-4.4)	0 (-0.1-0.1)	-0.1 (-0.2-0.1)	2.3 (-0.2-4.9)	27 (1.9-52)	0 (0-0.1)	2.7 (-1.3-6.7)
	Model 3	0.5 (-1.1-1.9)	0.4 (-0.8-1.7)	1.9 (-0.5-4.3)	0 (-0.1-0.1)	-0.1 (-0.2-0.1)	1.3 (-1-3.7)	17.1 (-6.3-40.5)	0 (0-0.1)	0.7 (-3.1-4.6)
	Model 4	0.4 (-1-1.8)	0.3 (-0.8-1.4)	1.9 (-0.4-4.2)	0 (-0.1-0.1)	-0.1 (-0.2-0.1)	1.4 (-0.9-3.6)	17.5 (-5.3-40.4)	0 (0-0.1)	0.4 (-2.9-3.6)
D _{Total}	Model 1	0.7 (-0.7-2.2)	1.1 (-0.3-2.5)	2.2 (-0.1-4.5)	0 (-0.1-0.1)	0 (-0.1-0.2)	2.7 (0.2-5.3)	39.5 (14.7-64.2)	0 (0-0.1)	3.2 (-0.8-7.3)
	Model 2	0.7 (-0.7-2.2)	1 (-0.3-2.4)	1.8 (-0.5-4.1)	0 (-0.1-0.1)	0 (-0.1-0.1)	3.3 (0.8-5.8)	45.3 (21-69.7)	0 (0-0.1)	2.7 (-1.2-6.7)
	Model 3	0.3 (-1.1-1.7)	0 (-1.2-1.2)	1.6 (-0.7-4)	0 (-0.1-0.1)	0 (-0.1-0.1)	1.9 (-0.3-4.2)	32.8 (10-55.7)	0 (0-0.1)	0.8 (-3-4.5)
	Model 4	0.3 (-1.1-1.7)	0 (-1.1-1.1)	1.6 (-0.7-3.9)	0 (-0.1-0.1)	0 (-0.1-0.1)	1.9 (-0.4-4.1)	31.9 (9.6-54.2)	0 (0-0.1)	0.7 (-2.6-3.9)
D _{feed vessel}	Model 1	0.5 (-0.9-2)	1.6 (0.3-3)	2.4 (0-4.7)	0.1 (0-0.2)	0.1 (0-0.2)	1.7 (-0.8-4.2)	28.9 (4.1-53.7)	0 (0-0.1)	2.9 (-1.1-7)
	Model 2	0.8 (-0.7-2.2)	1.6 (0.2-2.9)	1.9 (-0.5-4.2)	0 (-0.1-0.1)	0.1 (-0.1-0.2)	2.6 (0.1-5.1)	38.6 (14.1-63.1)	0 (0-0.1)	2.9 (-1-6.9)
	Model 3	0.4 (-1.1-1.8)	0.5 (-0.8-1.7)	1.7 (-0.7-4)	0 (-0.1-0.1)	0.1 (-0.1-0.2)	1.1 (-1.2-3.4)	25.4 (2.4-48.4)	0 (0-0.1)	1 (-2.7-4.8)
	Model 4	0.2 (-1.2-1.6)	0.2 (-0.9-1.2)	1.4 (-0.9-3.7)	0 (-0.1-0.1)	0.1 (-0.1-0.2)	0.9 (-1.3-3.2)	23.7 (1.2-46.2)	0 (0-0.1)	0.7 (-2.6-3.9)
D _{capillary}	Model 1	0.6 (-0.8-2.1)	-0.1 (-1.5-1.2)	0.8 (-1.6-3.1)	-0.1 (-0.2-0)	-0.1 (-0.2-0.1)	2.5 (0-5)	32.6 (7.8-57.4)	0 (0-0.1)	2.2 (-1.9-6.2)
	Model 2	0.3 (-1.2-1.7)	-0.2 (-1.6-1.2)	0.7 (-1.6-3)	0 (-0.1-0)	0 (-0.2-0.1)	2.3 (-0.2-4.8)	30.2 (5.8-54.6)	0 (0-0.1)	1.2 (-2.7-5.2)
	Model 3	0.1 (-1.3-1.5)	-0.6 (-1.8-0.6)	0.6 (-1.7-3)	-0.1 (-0.2-0)	0 (-0.2-0.1)	1.8 (-0.5-4)	24.5 (1.7-47.3)	0 (0-0.1)	0.3 (-3-4.4)
	Model 4	0.3 (-1.1-1.7)	-0.2 (-1.3-0.8)	0.8 (-1.4-3.1)	0 (-0.1-0.1)	0 (-0.2-0.1)	1.8 (-0.4-4.1)	25.2 (2.9-47.5)	0 (0-0.1)	0.5 (-2.7-3.7)
CBV _{static}	Model 1	-0.3 (-1.7-1.2)	-1.5 (-2.9-0.1)	-0.2 (-2.5-2.1)	0 (-0.1-0.1)	0 (-0.2-0.1)	0.6 (-1.9-3.1)	2.6 (-22.3-27.5)	0 (0-0.1)	0.7 (-3-4-4.7)
	Model 2	-0.7 (-2.1-0.7)	-1.6 (-3-0.2)	-0.5 (-2.8-1.9)	0 (-0.1-0.1)	0 (-0.2-0.1)	0.6 (-1.9-3.1)	2 (-22.5-26.6)	0 (0-0.1)	-0.6 (-4.6-3-3)
	Model 3	-0.6 (-2-0.8)	-1 (-2.2-0.2)	-0.4 (-2.7-2)	0 (-0.1-0.1)	0 (-0.2-0.1)	1.5 (-0.8-3.8)	10.5 (-12.3-33.4)	0 (0-0.1)	0.5 (-3-3-4.2)
	Model 4	-0.4 (-1.7-1)	-0.6 (-1.7-0.4)	-0.2 (-2.5-2.1)	0 (-0.1-0.1)	0 (-0.1-0.1)	1.5 (-0.7-3.7)	10.5 (-11.8-32.9)	0 (0-0.1)	0.8 (-2-4-4)

Results are based on linear regression analyses of the general Dutch population. The beta coefficient (95% CI) can be interpreted as differences in coagulation parameter levels per SD change in PBR.

Model 1 = crude model.

Model 2 = model 1 + sex + age.

Model 3 = model 2 + BMI, current smoking status, menopausal status, current use of the oral contraceptive pill, and current use of hormone replacement therapy.

Model 4 = model 3 + serum CRP, serum leptin concentration, and serum GlycA concentration.

Abbreviation: RBCV_{feed vessel}: feed vessel RBC velocity; RBCV_{capillary}: capillary RBC velocity; D_{Total}: total valid vessel density with measurable RBC velocity; D_{feed vessel}: perfused feed vessel density; D_{capillary}: perfused capillary density; CBV_{static}: capillary blood volume.

Table S3. Association between glyocalyx-related SDF imaging parameters and levels of coagulation parameters in women.

		FXI activity	FIX activity	FVIII activity	Lag time	ttPeak	Peak	ETP	VelIndex	Fibrinogen
PBR _{Total}	Model 1	0.4 (-1.7-2.6)	1.2 (-0.9-3.2)	0.8 (-2.3-4)	-0.1 (-0.2-0.1)	-0.1 (-0.3-0.1)	3 (-0.9-6.9)	29 (-8.6-66.7)	0 (0-0.1)	5 (-0.8-10.7)
	Model 2	0.7 (-1.5-2.8)	1.3 (-0.8-3.4)	1.4 (-1.7-4.6)	0 (-0.2-0.1)	-0.1 (-0.3-0.1)	1.9 (-1.9-5.7)	16.3 (-20-52.6)	0 (0-0.1)	5.5 (-0.3-11.3)
	Model 3	1.2 (-0.8-3.3)	2.3 (0.5-4)	1.3 (-1.9-4.5)	0 (-0.2-0.1)	-0.1 (-0.2-0.1)	2.6 (-0.7-5.9)	22.8 (-10-55.6)	0 (0-0.1)	7.5 (2.2-12.9)
	Model 4	1.2 (-0.9-3.2)	1.8 (0.3-3.3)	0.5 (-2.5-3.6)	0 (-0.2-0.1)	0 (-0.2-0.1)	1.8 (-1.5-5)	15.5 (-16.8-47.8)	0 (0-0.1)	5.1 (0.4-9.9)
PBR _{feed vessel}	Model 1	0.9 (-1.2-3.1)	1 (-1.1-3.1)	1.3 (-1.9-4.4)	-0.1 (-0.2-0.1)	-0.1 (-0.3-0.1)	2.8 (-1.1-6.7)	25.8 (-11.9-63.5)	0 (0-0.1)	4.5 (-1.2-10.3)
	Model 2	1.1 (-1-3.3)	1.1 (-1-3.2)	1.8 (-1.3-4.9)	0 (-0.2-0.1)	-0.1 (-0.3-0.1)	1.8 (-2-5.6)	14.3 (-21.9-50.6)	0 (0-0.1)	5 (-0.8-10.8)
	Model 3	1.7 (-0.4-3.7)	2.2 (0.4-3.9)	1.8 (-1.3-5)	0 (-0.2-0.1)	-0.1 (-0.3-0.1)	2.8 (-0.5-6.1)	24 (-8.7-56.7)	0 (0-0.1)	7.1 (1.7-12.4)
	Model 4	1.7 (-0.4-3.7)	2 (0.5-3.4)	1.4 (-1.7-4.5)	0 (-0.2-0.1)	-0.1 (-0.3-0.1)	2.2 (-1-5.4)	19 (-13.1-51)	0 (0-0.1)	5.8 (1.1-10.6)
PBR _{capillary}	Model 1	-1.1 (-3.2-1.1)	0.4 (-1.7-2.5)	3 (-0.1-6.2)	0 (-0.2-0.1)	0 (-0.2-0.2)	-0.5 (-4.4-3.4)	0.1 (-37.7-37.8)	0 (-0.1-0.1)	3.7 (-2-9.5)
	Model 2	-1 (-3.1-1.2)	0.5 (-1.6-2.6)	3.4 (0.2-6.5)	0 (-0.1-0.1)	0 (-0.2-0.2)	-1.2 (-4.9-2.6)	-7.5 (-43.6-28.6)	0 (-0.1-0.1)	4 (-1.7-9.8)
	Model 3	-0.7 (-2.7-1.4)	1 (-0.7-2.8)	3.3 (0.2-6.4)	0 (-0.1-0.1)	0 (-0.2-0.2)	-0.4 (-3.7-2.9)	-0.5 (-33.1-32.1)	0 (-0.1-0.1)	5 (-0.4-10.3)
	Model 4	-0.5 (-2.6-1.5)	1.3 (-0.2-2.8)	3.5 (0.4-6.5)	0 (-0.1-0.1)	0 (-0.2-0.2)	-0.3 (-3.5-2.9)	0.3 (-31.6-32.2)	0 (-0.1-0.1)	5.3 (0.6-10)

Results are based on linear regression analyses of the Dutch women population. The beta coefficient (95% CI) can be interpreted as differences in coagulation parameter levels per SD change in PBR.

Model 1 = crude model.

Model 2 = model 1 + age.

Model 3 = model 2 + BMI, current smoking status, menopausal status, current use of the oral contraceptive pill, and current use of hormone replacement therapy.

Model 4 = model 3 + serum CRP, serum leptin concentration, and serum GlycA concentration.

Abbreviation: PBR_{Total}: PBR of total vessels from 4-25µm; PBR_{feed vessel}: PBR of feed vessels from 10-19µm; PBR_{capillary}: PBR of capillaries from 4-9µm.

Table S4. Association between glyocalyx-related SDF imaging parameters and levels of coagulation parameters in men.

		FXI activity	FIX activity	FVIII activity	Lag time	ttPeak	Peak	ETP	VelIndex	Fibrinogen
PBR _{Total}	Model 1	-1.1 (-3-0.7)	-0.9 (-2.7-0.8)	-1.2 (-4.7-2.3)	-0.1 (-0.2-0.1)	-0.1 (-0.3-0.1)	-1.5 (-4.5-1.6)	-26.8 (-58.1-4.5)	0 (-0.1-0)	-0.1 (-5.6-5.3)
	Model 2	-1.1 (-2.9-0.8)	-0.9 (-2.7-0.8)	-1.4 (-4.9-2)	-0.1 (-0.2-0.1)	-0.1 (-0.3-0.1)	-1.4 (-4.5-1.6)	-27 (-58.4-4.4)	0 (-0.1-0)	-0.6 (-5.9-4.8)
	Model 3	-1 (-2.8-0.9)	-0.7 (-2.4-1)	-1.5 (-5-1.9)	-0.1 (-0.2-0.1)	-0.1 (-0.3-0.1)	-1.3 (-4.4-1.8)	-25.1 (-56.3-6.2)	0 (-0.1-0)	0.2 (-4.9-5.3)
	Model 4	-1.1 (-2.8-0.7)	-0.8 (-2.3-0.7)	-1.5 (-4.9-1.9)	-0.1 (-0.2-0.1)	-0.1 (-0.3-0.1)	-1.3 (-4.3-1.8)	-24.5 (-55-6)	0 (-0.1-0)	0.2 (-4-4.4)
PBR _{feed vessel}	Model 1	-0.3 (-2.1-1.6)	-0.9 (-2.6-0.9)	-1.3 (-4.8-2.2)	0 (-0.2-0.1)	-0.1 (-0.3-0.1)	-1.5 (-4.6-1.5)	-25.8 (-57.1-5.5)	0 (-0.1-0)	-0.1 (-5.6-5.3)
	Model 2	-0.2 (-2-1.6)	-0.9 (-2.7-0.8)	-1.5 (-5-1.9)	0 (-0.2-0.1)	-0.1 (-0.3-0.1)	-1.5 (-4.6-1.6)	-26 (-57.4-5.4)	0 (-0.1-0.1)	-0.6 (-6-4.7)
	Model 3	-0.2 (-2-1.7)	-0.8 (-2.5-0.9)	-1.6 (-5-1.9)	0 (-0.2-0.1)	-0.1 (-0.3-0.1)	-1.5 (-4.5-1.6)	-24.9 (-56.1-6.3)	0 (-0.1-0.1)	-0.1 (-5-2.5)
	Model 4	-0.1 (-1.9-1.6)	-0.8 (-2.3-0.7)	-1.7 (-5.1-1.8)	0 (-0.2-0.1)	-0.1 (-0.2-0.1)	-1.5 (-4.6-1.5)	-25.6 (-56.1-4.9)	0 (-0.1-0)	-0.3 (-4.5-3.9)
PBR _{capillary}	Model 1	1.2 (-0.7-3)	-0.3 (-2.1-1.4)	-1.1 (-4.6-2.4)	-0.1 (-0.2-0.1)	0 (-0.2-0.2)	-2.6 (-5.7-0.4)	-24.8 (-56.1-6.5)	0 (-0.1-0)	-2.4 (-7.8-3.1)
	Model 2	1 (-0.8-2.9)	-0.2 (-2-1.5)	-0.7 (-4.1-2.8)	0 (-0.2-0.1)	0 (-0.2-0.2)	-2.7 (-5.8-0.4)	-24.7 (-56.1-6.8)	0 (-0.1-0)	-1.5 (-6.8-3.9)
	Model 3	1.1 (-0.7-3)	-0.1 (-1.7-1.6)	-0.8 (-4.3-2.7)	0 (-0.2-0.1)	0 (-0.2-0.2)	-2.5 (-5.6-0.6)	-22.5 (-53.9-8.9)	0 (-0.1-0)	-0.8 (-5.9-4.3)
	Model 4	0.9 (-0.9-2.7)	-0.3 (-1.8-1.2)	-0.8 (-4.3-2.6)	-0.1 (-0.2-0.1)	0 (-0.2-0.2)	-2.6 (-5.6-0.4)	-23.5 (-54.2-7.2)	0 (-0.1-0)	-1.6 (-5.8-2.6)

Results are based on linear regression analyses of the Dutch men population. The beta coefficient (95% CI) can be interpreted as differences in coagulation parameter levels per SD change in PBR.

Model 1 = crude model.

Model 2 = model 1 + age.

Model 3 = model 2 + BMI + current smoking status.

Model 4 = model 3 + serum CRP, serum leptin concentration, and serum GlycA concentration.

Abbreviation: PBR_{Total}: PBR of total vessels from 4-25µm; PBR_{feed vessel}: PBR of feed vessels from 10-19µm; PBR_{capillary}: PBR of capillaries from 4-9µm.

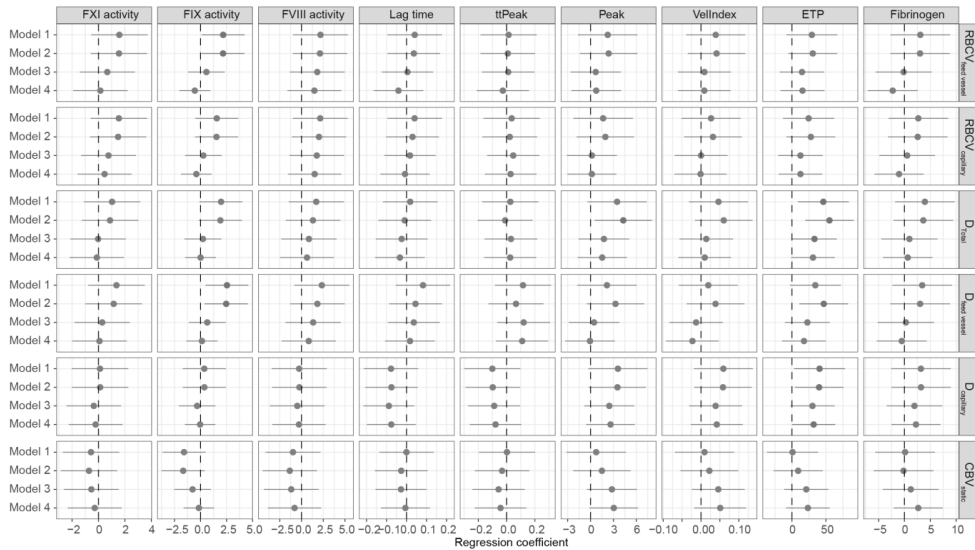


Figure S3. Association between microcirculatory-perfusion-related SDF imaging parameters and levels of coagulation parameters in women. After sex stratification, differences in women between the microcirculatory-perfusion-related parameters and coagulation factor levels can be observed. Model 1: crude model; Model 2: model 1 + age; Model 3: model 2 + BMI, current smoking status, menopausal status, current use of the oral contraceptive pill, and current use of hormone replacement therapy; Model 4: model 3 + serum CRP, serum leptin concentration, and serum GlycA concentration. The effect size and 95% confidence interval were depicted by a horizontal line with a dot. A non-significant association was represented by the color grey, and a substantial positive association was represented by the color red. Abbreviations: RBCV_{feed vessel}: feed vessel RBC velocity; RBCV_{capillary}: capillary RBC velocity; D_{Total}: total valid vessel density with measurable RBC velocity; D_{feed vessel}: perfused feed vessel density; D_{capillary}: perfused capillary density; CBV_{static}: capillary blood volume.

Table S5. Association between microcirculatory-perfusion-related SDF imaging parameters and levels of coagulation parameters in women.

		FXI activity	FIX activity	FVIII activity	Lag time	ttPeak	Peak	ETP	Vellindex	Fibrinogen
RBCV _{feed vessel}	Model 1	1.6 (-0.6-3.7)	2.2 (0.1-4.2)	2.2 (-1.5-3)	0 (-0.1-0.2)	0 (-0.2-0.2)	2.3 (-1.6-6.2)	29.3 (-8.3-67)	0 (0-0.1)	3.1 (-2.7-8.8)
	Model 2	1.6 (-0.6-3.7)	2.2 (0.1-4.2)	2.1 (-1.5-2)	0 (-0.1-0.2)	0 (-0.2-0.2)	2.4 (-1.4-6.1)	30.7 (-5.2-66.7)	0 (0-0.1)	3 (-2.7-8.8)
	Model 3	0.7 (-1.4-2.7)	0.6 (-1.2-2.3)	1.8 (-1.3-5)	0 (-0.1-0.1)	0 (-0.2-0.2)	0.7 (-2.6-4)	14.8 (-18-47.7)	0 (-0.1-0.1)	-0.2 (-5.6-5.3)
	Model 4	0.1 (-1.9-2.2)	-0.6 (-2-0.9)	1.5 (-1.6-4.6)	0 (-0.2-0.1)	0 (-0.2-0.2)	0.7 (-2.5-4)	15.6 (-16.9-48)	0 (-0.1-0.1)	-2.3 (-7.1-2.5)
RBCV _{capillary}	Model 1	1.5 (-0.6-3.7)	1.6 (-0.5-3.6)	2.2 (-1.5-3)	0 (-0.1-0.2)	0 (-0.2-0.2)	1.6 (-2.3-5.6)	24.6 (-13.1-62.3)	0 (-0.1-0.1)	2.7 (-3.1-8.5)
	Model 2	1.5 (-0.6-3.6)	1.5 (-0.5-3.6)	2 (-1.1-5.1)	0 (-0.1-0.2)	0 (-0.2-0.2)	1.9 (-1.8-5.7)	27.9 (-8.1-63.9)	0 (0-0.1)	2.6 (-3.2-8.3)
	Model 3	0.8 (-1.3-2.8)	0.3 (-1.5-2)	1.8 (-1.4-4.9)	0 (-0.1-0.1)	0 (-0.1-0.2)	0.2 (-3.1-3.5)	12.6 (-20.1-45.3)	0 (-0.1-0.1)	0.5 (-4.9-5.9)
	Model 4	0.5 (-1.6-2.5)	-0.4 (-1.9-1.1)	1.5 (-1.6-4.6)	0 (-0.1-0.1)	0 (-0.2-0.2)	0.2 (-3.1-3.4)	12.6 (-19.5-44.7)	0 (-0.1-0.1)	-1 (-5.8-3.7)
D _{Total}	Model 1	1 (-1.1-3.2)	2 (-0.1-4)	1.7 (-1.5-4.9)	0 (-0.1-0.2)	0 (-0.2-0.2)	3.5 (-0.4-7.4)	46.2 (8.7-83.7)	0 (0-0.1)	3.9 (-1.8-9.7)
	Model 2	0.9 (-1.3-3)	1.9 (-0.2-4)	1.3 (-1.8-4.5)	0 (-0.1-0.1)	0 (-0.2-0.2)	4.3 (0.5-8.1)	55.3 (19.5-91.1)	0.1 (0-0.1)	3.7 (-2.1-9.4)
	Model 3	0 (-2.1-2.1)	0.2 (-1.5-2)	0.9 (-2.3-4)	0 (-0.2-0.1)	0 (-0.2-0.2)	1.8 (-1.6-5.1)	33.2 (0.3-66.1)	0 (-0.1-0.1)	1 (-4.5-6.4)
	Model 4	-0.1 (-2.2-1.9)	0 (-1.5-1.5)	0.6 (-2.5-3.7)	0 (-0.2-0.1)	0 (-0.2-0.2)	1.5 (-1.7-4.8)	31 (-1.2-63.3)	0 (-0.1-0.1)	0.6 (-4.2-5.4)
D _{feed vessel}	Model 1	1.4 (-0.8-3.5)	2.5 (0.5-4.6)	2.3 (-0.8-5.5)	0.1 (-0.1-0.2)	0.1 (-0.1-0.3)	2.1 (-1.8-6)	34.4 (-3.2-72)	0 (-0.1-0.1)	3.4 (-2.3-9.2)
	Model 2	1.2 (-1-3.3)	2.5 (0.4-4.5)	1.8 (-1.3-5)	0 (-0.1-0.2)	0.1 (-0.1-0.3)	3.3 (-0.5-7.1)	46.9 (10.9-82.9)	0 (0-0.1)	3 (-2.8-8.8)
	Model 3	0.3 (-1.8-2.4)	0.6 (-1.1-2.4)	1.3 (-1.8-4.5)	0 (-0.1-0.2)	0.1 (-0.1-0.3)	0.5 (-2.9-3.8)	22.8 (-10.3-55.8)	0 (-0.1-0.1)	0.3 (-5.2-5.7)
	Model 4	0.1 (-2-2.1)	0.1 (-1.4-1.6)	0.8 (-2.3-3.9)	0 (-0.1-0.1)	0.1 (-0.1-0.3)	-0.1 (-3.3-3.2)	17.8 (-14.7-50.3)	0 (-0.1-0)	-0.5 (-5.3-4.3)
D _{capillary}	Model 1	0.1 (-2-2.3)	0.4 (-1.7-2.4)	-0.3 (-3.4-2.9)	-0.1 (-0.2-0.1)	-0.1 (-0.3-0.1)	3.6 (-0.3-7.5)	40.7 (3.1-78.3)	0.1 (0-0.1)	3.2 (-2.6-8.9)
	Model 2	0.1 (-2-2.3)	0.4 (-1.7-2.4)	-0.2 (-3.4-2.9)	-0.1 (-0.2-0.1)	-0.1 (-0.3-0.1)	3.5 (-0.2-7.3)	40 (4.2-75.9)	0.1 (0-0.1)	3.2 (-2.5-9)
	Model 3	-0.4 (-2.4-1.7)	-0.3 (-2.1-1.4)	-0.5 (-3.6-2.7)	-0.1 (-0.2-0)	-0.1 (-0.3-0.1)	2.5 (-0.8-5.7)	30.3 (-2-62.9)	0 (0-0.1)	1.9 (-3.4-7.3)
	Model 4	-0.2 (-2.3-1.8)	0 (-1.5-1.4)	-0.3 (-3.4-2.8)	-0.1 (-0.2-0)	-0.1 (-0.3-0.1)	2.6 (-0.6-5.8)	32 (0.1-63.8)	0 (0-0.1)	2.2 (-2.5-7)
CBV _{static}	Model 1	-0.6 (-2.7-1.6)	-1.6 (-3.7-0.5)	-1 (-4.1-2.2)	0 (-0.1-0.1)	0 (-0.2-0.2)	0.7 (-3.2-4.6)	0.9 (-36.9-38.7)	0 (-0.1-0.1)	0.1 (-5.6-5.9)
	Model 2	-0.7 (-2.9-1.4)	-1.7 (-3.7-0.4)	-1.3 (-4.5-1.8)	0 (-0.2-0.1)	0 (-0.2-0.2)	1.5 (-2.3-5.3)	9.1 (-27-45.3)	0 (-0.1-0.1)	-0.2 (-5.9-5.6)
	Model 3	-0.5 (-2.6-1.5)	-0.8 (-2.5-1)	-1.2 (-4.3-2)	0 (-0.2-0.1)	-0.1 (-0.2-0.1)	2.8 (-0.5-6.1)	21.1 (-11.5-53.8)	0 (0-0.1)	1.2 (-4.2-6.6)
	Model 4	-0.3 (-2.3-1.8)	-0.2 (-1.6-1.3)	-0.8 (-3.9-2.3)	0 (-0.1-0.1)	0 (-0.2-0.1)	3.1 (-0.1-6.2)	23.5 (-8.5-55.5)	0.1 (0-0.1)	2.7 (-2.1-7.4)

Results are based on linear regression analyses of the Dutch men population. The beta coefficient (95% CI) can be interpreted as differences in coagulation parameter levels per SD change in PBR.

Model 1 = crude model.

Model 2 = model 1 + age.

Model 3 = model 2 + BMI, current smoking status, menopausal status, current use of the oral contraceptive pill, and current use of hormone replacement therapy.

Model 4 = model 3 + serum CRP, serum leptin concentration, and serum GlycA concentration.

Abbreviation: RBCV_{feed vessel}: feed vessel RBC velocity; RBCV_{capillary}: capillary RBC velocity; D_{Total}: total valid vessel density with measurable RBC velocity; D_{feed vessel}: perfused feed vessel density; D_{capillary}: perfused capillary density; CBV_{static}: capillary blood volume.

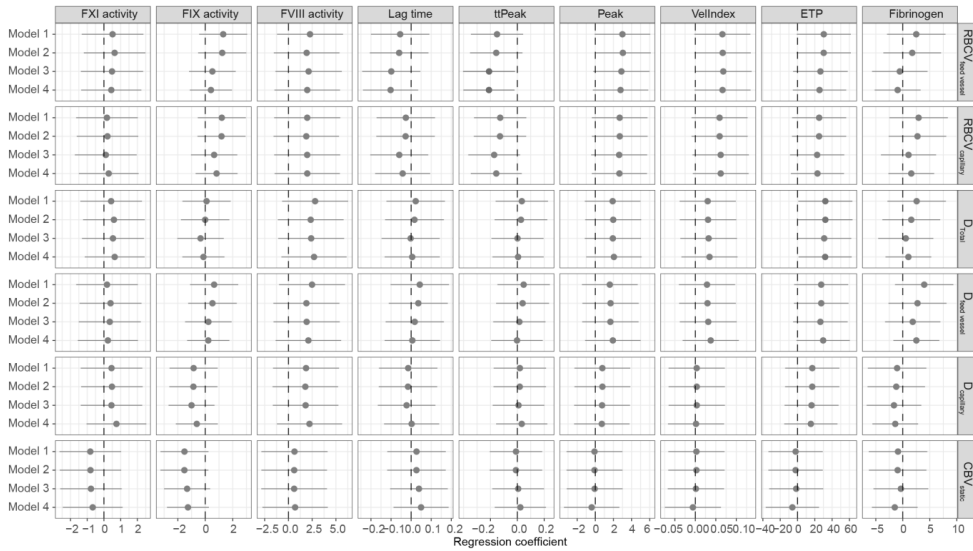


Figure S4. Association between microcirculatory-perfusion-related SDF imaging parameters and levels of coagulation parameters in men. After sex stratification, differences in men between the microcirculatory-perfusion-related parameters and coagulation factor levels can be observed. Model 1: crude model; Model 2: model 1 + age; Model 3: model 2 + BMI + current smoking status; Model 4: model 3 + serum CRP, serum leptin concentration, and serum GlycA concentration. The effect size and 95% confidence interval were depicted by a horizontal line with a dot. A non-significant association was represented by the color grey, and a substantial positive association was represented by the color red. Abbreviations: RBCV_{feed vessel}: feed vessel RBC velocity; RBCV_{capillary}: capillary RBC velocity; D_{Total}: total valid vessel density with measurable RBC velocity; D_{feed vessel}: perfused feed vessel density; D_{capillary}: perfused capillary density; CBV_{static}: capillary blood volume.

Table S6. Association between microcirculatory-perfusion-related SDF imaging parameters and levels of coagulation parameters in men.

		FXI activity	FIX activity	FVIII activity	Lag time	ttPeak	Peak	ETP	VelIndex	Fibrinogen
RBCV _{feed vessel}	Model 1	0.5 (-1.3-2.4)	1.3 (-0.4-3.1)	2.3 (-1.2-5.7)	-0.1 (-0.2-0.1)	-0.2 (-0.3-0)	3 (-0.1-6.1)	30.4 (-0.9-61.6)	0.1 (0-0.1)	2.5 (-2.9-7.9)
	Model 2	0.6 (-1.2-2.5)	1.2 (-0.5-3)	1.9 (-1.5-5.4)	-0.1 (-0.2-0.1)	-0.2 (-0.4-0)	3 (0-6.1)	30.3 (-1.1-61.7)	0.1 (0-0.1)	1.7 (-3.6-7.1)
	Model 3	0.5 (-1.4-2.3)	0.5 (-1.2-2.2)	2.1 (-1.4-5.6)	-0.1 (-0.2-0)	-0.2 (-0.4-0)	2.9 (-0.2-6)	26.5 (-5.1-58)	0.1 (0-0.1)	-0.6 (-5.7-4.6)
	Model 4	0.4 (-1.4-2.2)	0.4 (-1.1-1.9)	2 (-1.5-5.4)	-0.1 (-0.2-0)	-0.2 (-0.4-0)	2.8 (-0.3-5.8)	25.5 (-5.4-56.3)	0.1 (0-0.1)	-1 (-5.2-3.3)
RBCV _{capillary}	Model 1	0.2 (-1.7-2)	1.2 (-0.5-3)	2 (-1.5-5.5)	0 (-0.2-0.1)	-0.1 (-0.3-0.1)	2.7 (-0.4-5.8)	25 (-6.3-56.3)	0.1 (0-0.1)	2.9 (-2.5-8.3)
	Model 2	0.2 (-1.6-2.1)	1.2 (-0.6-2.9)	1.9 (-1.6-5.3)	0 (-0.2-0.1)	-0.1 (-0.3-0.1)	2.7 (-0.4-5.8)	25 (-6.4-56.3)	0.1 (0-0.1)	2.7 (-2.6-8)
	Model 3	0.1 (-1.7-2)	0.6 (-1-2.3)	2 (-1.5-5.4)	-0.1 (-0.2-0.1)	-0.2 (-0.4-0)	2.6 (-0.5-5.7)	22.7 (-8.7-54.1)	0.1 (0-0.1)	1.1 (-4-6.2)
	Model 4	0.3 (-1.5-2.1)	0.8 (-0.7-2.4)	2 (-1.5-5.4)	0 (-0.2-0.1)	-0.2 (-0.3-0)	2.7 (-0.4-5.7)	23 (-7.7-53.8)	0.1 (0-0.1)	1.6 (-2.7-5.8)
D _{Total}	Model 1	0.4 (-1.4-2.3)	0.1 (-1.7-1.8)	2.8 (-0.7-6.3)	0 (-0.1-0.2)	0 (-0.2-0.2)	1.9 (-1.2-5)	32.2 (0.9-63.4)	0 (0-0.1)	2.6 (-2.9-8)
	Model 2	0.6 (-1.3-2.4)	0 (-1.8-1.8)	2.3 (-1.1-5.8)	0 (-0.1-0.2)	0 (-0.2-0.2)	2 (-1.1-5.1)	32.2 (0.7-63.6)	0 (0-0.1)	1.6 (-3.8-6.9)
	Model 3	0.5 (-1.3-2.4)	-0.3 (-2-1.3)	2.4 (-1.1-5.9)	0 (-0.1-0.1)	0 (-0.2-0.2)	1.9 (-1.2-5)	30.8 (-5.5-62.2)	0 (0-0.1)	0.6 (-4.6-5.7)
	Model 4	0.6 (-1.1-2.4)	-0.1 (-1.7-1.4)	2.7 (-0.7-6.1)	0 (-0.1-0.1)	0 (-0.2-0.2)	2.1 (-1-5.1)	31.9 (1.3-62.6)	0 (0-0.1)	1 (-3.2-5.3)
D _{feed vessel}	Model 1	0.2 (-1.7-2)	0.6 (-1.1-2.4)	2.5 (-1-6)	0 (-0.1-0.2)	0 (-0.1-0.2)	1.6 (-1.5-4.7)	27.4 (-3.9-58.7)	0 (0-0.1)	4 (-1.4-9.4)
	Model 2	0.4 (-1.5-2.2)	0.5 (-1.2-2.3)	1.9 (-1.6-5.4)	0 (-0.1-0.2)	0 (-0.2-0.2)	1.7 (-1.4-4.8)	27.4 (-4.2-59)	0 (0-0.1)	2.7 (-2.7-8.1)
	Model 3	0.3 (-1.5-2.2)	0.2 (-1.5-1.9)	1.9 (-1.6-5.4)	0 (-0.1-0.2)	0 (-0.2-0.2)	1.7 (-1.4-4.8)	26.4 (-5.1-57.9)	0 (0-0.1)	1.8 (-3-3.7)
	Model 4	0.2 (-1.6-2)	0.2 (-1.3-1.8)	2.1 (-1.4-5.5)	0 (-0.1-0.1)	0 (-0.2-0.2)	1.9 (-1.1-5)	29.6 (-1.2-60.4)	0 (0-0.1)	2.5 (-1.7-6.8)
D _{capillary}	Model 1	0.5 (-1.4-2.3)	-0.8 (-2.6-0.9)	1.9 (-1.6-5.3)	0 (-0.2-0.1)	0 (-0.2-0.2)	0.8 (-2.3-3.9)	17.1 (-14.3-48.4)	0 (-0.1-0.1)	-1.1 (-6.5-4.4)
	Model 2	0.5 (-1.4-2.3)	-0.9 (-2.6-0.9)	1.8 (-1.7-5.2)	0 (-0.2-0.1)	0 (-0.2-0.2)	0.8 (-2.3-3.9)	17 (-14.4-48.4)	0 (-0.1-0.1)	-1.2 (-6.5-4.1)
	Model 3	0.4 (-1.4-2.3)	-1 (-2.7-0.7)	1.8 (-1.6-5.3)	0 (-0.2-0.1)	0 (-0.2-0.2)	0.7 (-2.3-3.8)	16.2 (-15-47.5)	0 (-0.1-0.1)	-1.6 (-6.7-3.4)
	Model 4	0.7 (-1-2.5)	-0.6 (-2.1-0.9)	2.2 (-1.2-5.6)	0 (-0.1-0.1)	0 (-0.2-0.2)	0.7 (-2.3-3.8)	15.4 (-15.4-46.2)	0 (-0.1-0.1)	-1.4 (-5.6-2.8)
CBV _{static}	Model 1	-0.8 (-2.7-1)	-1.5 (-3.3-0.2)	0.6 (-2.8-4.1)	0 (-0.1-0.2)	0 (-0.2-0.2)	-0.1 (-3.2-3)	-2.2 (-33.6-29.2)	0 (-0.1-0.1)	-0.9 (-6.3-4.5)
	Model 2	-0.8 (-2.6-1)	-1.5 (-3.3-0.2)	0.6 (-2.8-4.1)	0 (-0.1-0.2)	0 (-0.2-0.2)	-0.1 (-3.2-3)	-2.2 (-33.7-29.2)	0 (-0.1-0.1)	-1 (-6.3-4.4)
	Model 3	-0.8 (-2.6-1.1)	-1.3 (-3-0.4)	0.6 (-2.9-4.1)	0 (-0.1-0.2)	0 (-0.2-0.2)	-0.1 (-3.2-3)	-1.5 (-32.8-29.8)	0 (-0.1-0.1)	-0.4 (-5.4-4.7)
	Model 4	-0.7 (-2.5-1.1)	-1.3 (-2.8-0.3)	0.7 (-2.7-4.1)	0 (-0.1-0.2)	0 (-0.2-0.2)	-0.4 (-3.5-2.7)	-5.9 (-36.8-24.9)	0 (-0.1-0.1)	-1.5 (-5.7-2.7)

Results are based on linear regression analyses of the Dutch men population. The beta coefficient (95% CI) can be interpreted as differences in coagulation parameter levels per SD change in PBR.

Model 1 = crude model.

Model 2 = model 1 + age.

Model 3 = model 2 + BMI + current smoking status.

Model 4 = model 3 + serum CRP, serum leptin concentration, and serum GlycA concentration.

Abbreviation: RBCV_{feed vessel}: feed vessel RBC velocity; RBCV_{capillary}: capillary RBC velocity; D_{Total}: total valid vessel density with measurable RBC velocity; D_{feed vessel}: perfused feed vessel density; D_{capillary}: perfused capillary density; CBV_{static}: capillary blood volume.

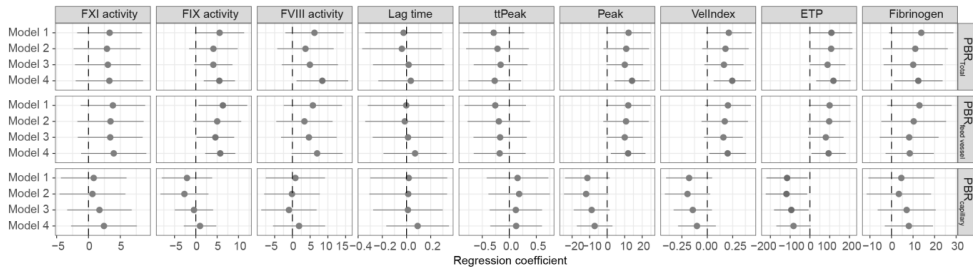


Figure S5. Association between glycoalyx-related SDF imaging parameters and levels of coagulation parameters in premenopausal women. After stratification for menopausal status, differences in premenopausal women between the glycoalyx-related parameters and coagulation factor levels can be observed. Model 1: crude model; Model 2: model 1 + age; Model 3: model 2 + BMI, current smoking status, current use of the oral contraceptive pill, and current use of hormone replacement therapy; Model 4: model 3 + serum CRP, serum leptin concentration, and serum GlycA concentration. The effect size and 95% confidence interval were depicted by a horizontal line with a dot. A non-significant association was represented by the color grey, and a substantial positive association was represented by the color red. Abbreviations: PBR_{Total}: PBR of total vessels from 4-25 μ m; PBR_{feed vessel}: PBR of feed vessels from 10-19 μ m; PBR_{capillary}: PBR of capillaries from 4-9 μ m.

Table S7. Association between glyocalyx-related SDF imaging parameters and levels of coagulation parameters in premenopausal women.

		FXI activity	FIX activity	FVIII activity	Lag time	ttPeak	Peak	ETP	VelIndex	Fibrinogen
PBR _{Total}	Model 1	3.3 (-1.8-8.4)	5.6 (-0.2-11.3)	6.2 (-2-14.4)	0 (-0.3-0.3)	-0.3 (-0.9-0.3)	12.2 (-0.5-24.9)	108.8 (4.1-213.5)	0.2 (0-0.4)	13.8 (-1.1-28.7)
	Model 2	2.9 (-2.3-8.1)	4.1 (-1.6-9.8)	3.7 (-4.3-11.6)	0 (-0.4-0.3)	-0.2 (-0.8-0.4)	10.9 (-2.1-23.9)	107.4 (-0.7-215.5)	0.2 (0-0.4)	11 (-4-26.1)
	Model 3	3 (-2.1-8.2)	4.1 (-0.4-8.6)	4.9 (-3-12.8)	0 (-0.3-0.3)	-0.2 (-0.7-0.3)	10.1 (-0.4-20.5)	89.3 (-1.1-179.6)	0.2 (0-0.4)	10.1 (-3.6-23.8)
	Model 4	3.3 (-2-8.6)	5.5 (1.9-9.2)	8.4 (1.2-15.7)	0 (-0.2-0.3)	-0.3 (-0.8-0.2)	14.2 (4.2-24.2)	118.9 (31.9-205.8)	0.2 (0.1-0.4)	12.4 (1.2-23.7)
PBR _{feed vessel}	Model 1	3.8 (-1.2-8.9)	6.3 (0.6-12.1)	5.8 (-2.5-14)	0 (-0.3-0.3)	-0.3 (-0.8-0.3)	12 (-0.6-24.7)	99.5 (-5.8-204.7)	0.2 (0-0.4)	13 (-2-27.9)
	Model 2	3.5 (-1.7-8.7)	5 (-0.6-10.6)	3.4 (-4.5-11.3)	0 (-0.3-0.3)	-0.2 (-0.8-0.4)	10.8 (-2.2-23.7)	97.4 (-10.9-205.7)	0.2 (-0.1-0.4)	10.3 (-4.7-25.3)
	Model 3	3.4 (-1.7-8.5)	4.6 (0.2-9)	4.7 (-3.2-12.5)	0 (-0.3-0.3)	-0.2 (-0.7-0.3)	10 (-0.3-20.4)	80.4 (-9.5-170.4)	0.2 (0-0.3)	8.2 (-5.5-21.9)
	Model 4	4 (-1.2-9.1)	5.7 (2.2-9.3)	7 (-0.2-14.1)	0.1 (-0.2-0.3)	-0.2 (-0.7-0.3)	12 (2.1-21.9)	94.5 (7.9-181.1)	0.2 (0-0.4)	8.5 (-2.8-19.7)
PBR _{capillary}	Model 1	0.8 (-4.3-6)	-2.1 (-8-3.8)	0.8 (-7.5-9.2)	0 (-0.3-0.3)	0.2 (-0.4-0.7)	-11.3 (-24-1.4)	-115.6 (-219.9--11.4)	-0.2 (-0.4-0)	4.6 (-10.7-19.8)
	Model 2	0.6 (-4.5-5.8)	-2.7 (-8.3-3)	-0.1 (-8-7.7)	0 (-0.3-0.3)	0.2 (-0.4-0.8)	-12 (-24.7-0.6)	-118.6 (-223.6--13.7)	-0.2 (-0.4-0)	3.4 (-11.6-18.4)
	Model 3	1.7 (-3.3-6.8)	-0.4 (-4.9-4.1)	-1 (-8.8-6.8)	0 (-0.3-0.3)	0.1 (-0.4-0.6)	-8.8 (-19.1-1.4)	-94 (-181.4--6.5)	-0.1 (-0.3-0)	7 (-6.4-20.5)
	Model 4	2.4 (-2.7-7.6)	1 (-2.8-4.8)	1.9 (-5.5-9.2)	0.1 (-0.2-0.4)	0.1 (-0.4-0.6)	-7.1 (-17.3-3)	-82.8 (-169.7-4.1)	-0.1 (-0.3-0.1)	8.1 (-3.1-19.2)

Results are based on linear regression analyses of the Dutch premenopausal women population. The beta coefficient (95% CI) can be interpreted as differences in coagulation parameter levels per SD change in PBR.

Model 1 = crude model.

Model 2 = model 1 + age.

Model 3 = model 2 + BMI, current smoking status, current use of the oral contraceptive pill, and current use of hormone replacement therapy.

Model 4 = model 3 + serum CRP, serum leptin concentration, and serum GlycA concentration.

Abbreviation: PBR_{Total}: PBR of total vessels from 4-25µm; PBR_{feed vessel}: PBR of feed vessels from 10-19µm; PBR_{capillary}: PBR of capillaries from 4-9µm.

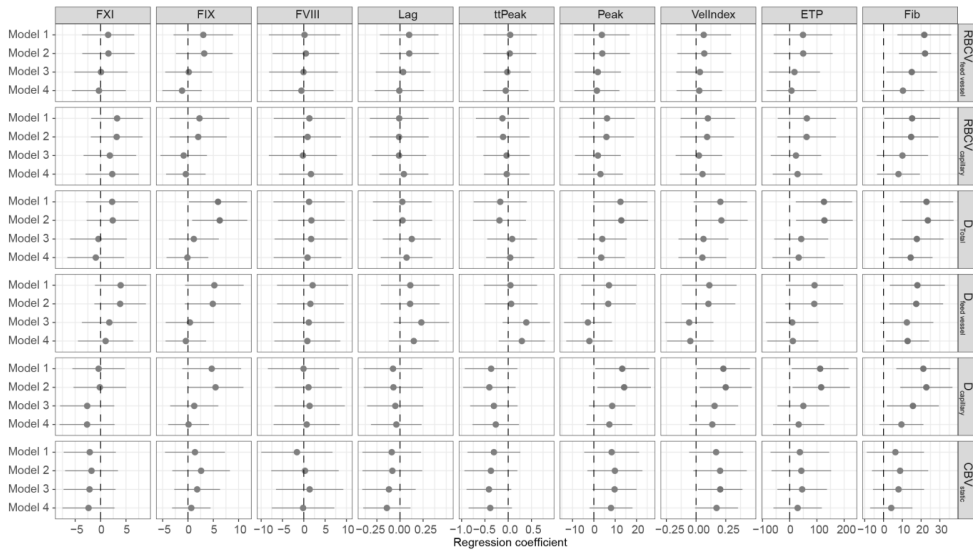


Figure S6. Association between microcirculatory-perfusion-related SDF imaging parameters and levels of coagulation parameters in premenopausal women. After stratification for menopausal status, differences in premenopausal women between the microcirculatory-perfusion-related parameters and coagulation factor levels can be observed. Model 1: crude model; Model 2: model 1 + age; Model 3: model 2 + BMI, current smoking status, current use of the oral contraceptive pill, and current use of hormone replacement therapy; Model 4: model 3 + serum CRP, serum leptin concentration, and serum GlycA concentration. The effect size and 95% confidence interval were depicted by a horizontal line with a dot. A non-significant association was represented by the color grey, and a substantial positive association was represented by the color red. Abbreviations: RBCV_{feed vessel}: feed vessel RBC velocity; RBCV_{capillary}: capillary RBC velocity; D_{Total}: total valid vessel density with measurable RBC velocity; D_{feed vessel}: perfused feed vessel density; D_{capillary}: perfused capillary density; CBV_{static}: capillary blood volume.

Table S8. Association between microcirculatory-perfusion-related SDF imaging parameters and levels of coagulation parameters in premenopausal women.

		FXI activity	FIX activity	FVIII activity	Lag time	ttPeak	Peak	ETP	VelIndex	Fibrinogen
RBCV _{feed vessel}	Model 1	1.5 (-3.7-6.6)	3 (-2.9-8.9)	0.2 (-8.2-8.5)	0.1 (-0.2-0.4)	0 (-0.5-0.6)	3.7 (-9.3-16.7)	48.9 (-58.5-156.3)	0.1 (-0.2-0.3)	21.7 (7.4-36)
	Model 2	1.5 (-3.6-6.7)	3.2 (-2.4-8.8)	0.5 (-7.3-8.3)	0.1 (-0.2-0.4)	0 (-0.5-0.6)	3.9 (-9-16.9)	49.7 (-58.4-157.7)	0.1 (-0.2-0.3)	22.1 (8.2-36)
	Model 3	0.1 (-5.2-5.3)	0.2 (-4.5-4.8)	-0.1 (-8.1-8)	0 (-0.3-0.3)	0 (-0.5-0.5)	1.9 (-9-12.7)	17.6 (-76.1-111.2)	0 (-0.2-0.2)	15 (1.6-28.5)
	Model 4	-0.3 (-5.6-5)	-1.2 (-5.1-2.7)	-0.6 (-8.1-7)	0 (-0.3-0.3)	-0.1 (-0.5-0.4)	1.4 (-9.1-12)	6.6 (-84.9-98.1)	0 (-0.2-0.2)	10.3 (-0.9-21.6)
RBCV _{capillary}	Model 1	3.3 (-1.8-8.3)	2.3 (-3.6-8.2)	1.3 (-7.9-7)	0 (-0.3-0.3)	-0.1 (-0.7-0.4)	6.2 (-6.8-19.1)	63.2 (-43.8-170.2)	0.1 (-0.1-0.3)	15.2 (0.4-30)
	Model 2	3.2 (-1.9-8.3)	2 (-3.6-7.7)	0.9 (-6.9-8.7)	0 (-0.3-0.3)	-0.1 (-0.7-0.5)	5.9 (-7-18.8)	62.2 (-45.5-169.9)	0.1 (-0.1-0.3)	14.7 (0.2-29.2)
	Model 3	1.8 (-3.4-7)	-0.8 (-5.4-3.7)	-0.2 (-8.2-7.8)	0 (-0.3-0.3)	0 (-0.5-0.5)	1.9 (-8.8-12.6)	23.1 (-69.6-115.8)	0 (-0.2-0.2)	10.1 (-3.6-23.7)
	Model 4	2.3 (-3-7.5)	-0.4 (-4.3-3.5)	1.7 (-5.8-9.2)	0 (-0.2-0.3)	0 (-0.5-0.5)	3.1 (-7.4-13.6)	28.9 (-62.2-120)	0.1 (-0.1-0.2)	8 (-3.4-19.4)
D _{Total}	Model 1	2.3 (-2.9-7.4)	5.9 (0.2-11.7)	1.2 (-7.1-9.6)	0 (-0.3-0.3)	-0.2 (-0.7-0.4)	12.5 (-0.2-25.1)	126 (22.6-229.5)	0.2 (0-0.4)	22.9 (8.7-37.1)
	Model 2	2.4 (-2.7-7.5)	6.3 (0.8-11.7)	1.8 (-6-9.6)	0 (-0.3-0.3)	-0.2 (-0.8-0.4)	12.9 (0.3-25.4)	127.5 (23.5-231.6)	0.2 (0-0.4)	23.6 (9.8-37.3)
	Model 3	-0.4 (-6.5-2)	1.2 (-3.8-6.1)	1.7 (-6.8-10.3)	0.1 (-0.2-0.4)	0.1 (-0.4-0.6)	3.9 (-7.5-15.4)	42.5 (-56.6-141.7)	0.1 (-0.1-0.3)	17.7 (3.5-31.9)
	Model 4	-1 (-6.5-4.6)	-0.1 (-4.2-4)	0.9 (-7.1-8.8)	0.1 (-0.2-0.4)	0 (-0.5-0.6)	3.5 (-7.6-14.6)	33.2 (-63.1-129.4)	0.1 (-0.1-0.3)	14.5 (2.8-26.1)
D _{feed vessel}	Model 1	3.9 (-1.1-9)	5.2 (-0.6-11)	2.1 (-6.3-10.4)	0.1 (-0.2-0.4)	0 (-0.5-0.6)	7.1 (-5.8-20)	91.4 (-14.4-197.1)	0.1 (-0.1-0.3)	18 (3.4-32.7)
	Model 2	3.8 (-1.2-8.9)	4.9 (-0.6-10.4)	1.5 (-6.3-9.4)	0.1 (-0.2-0.4)	0.1 (-0.5-0.6)	6.8 (-6.1-19.6)	90.3 (-16.2-196.7)	0.1 (-0.1-0.3)	17.4 (3.1-31.7)
	Model 3	1.7 (-3.7-7.1)	0.4 (-4.4-5.2)	1.2 (-7.1-9.5)	0.2 (-0.1-0.5)	0.4 (-0.1-0.9)	-2.8 (-14-8.3)	9.4 (-87.4-106.1)	-0.1 (-0.3-0.1)	12.4 (-1.7-26.6)
	Model 4	1 (-4.5-6.4)	-0.4 (-4.4-3.6)	0.8 (-6.9-8.6)	0.1 (-0.1-0.4)	0.3 (-0.2-0.8)	-2.1 (-12.9-8.7)	11.6 (-82.4-105.7)	0 (-0.2-0.1)	12.8 (1.4-24.2)
D _{capillary}	Model 1	-0.4 (-5.5-4.8)	4.7 (-1.1-10.5)	-0.1 (-8.4-8.3)	-0.1 (-0.4-0.2)	-0.4 (-0.9-0.2)	13.3 (0.7-25.9)	112 (7.6-216.5)	0.2 (0-0.5)	21.2 (6.8-35.6)
	Model 2	-0.2 (-5.3-5)	5.4 (-0.1-11)	1.1 (-6.7-8.9)	-0.1 (-0.4-0.3)	-0.4 (-1-0.2)	14.2 (1.7-26.7)	115.8 (10.5-221.1)	0.2 (0-0.5)	22.8 (8.9-36.7)
	Model 3	-2.6 (-8-2.7)	1.2 (-3.5-6)	1.4 (-6.9-9.6)	-0.1 (-0.4-0.3)	-0.3 (-0.8-0.2)	8.6 (-2.3-19.4)	50.2 (-45.1-145.4)	0.2 (0-0.4)	15.7 (1.9-29.5)
	Model 4	-2.7 (-8.1-2.8)	0.1 (-3.9-4.1)	0.7 (-7.1-8.4)	0 (-0.3-0.2)	-0.3 (-0.8-0.2)	7.3 (-3.4-18)	33.1 (-60.9-127.1)	0.1 (-0.1-0.3)	9.6 (-2.1-21.2)
CBV _{static}	Model 1	-2.1 (-7.3-3)	1.4 (-4.5-7.3)	-1.6 (-10-6.7)	-0.1 (-0.4-0.2)	-0.3 (-0.9-0.3)	8.3 (-4.5-21.2)	37.4 (-70.3-145.2)	0.2 (-0.1-0.4)	6.3 (-8.9-21.6)
	Model 2	-1.8 (-7-3.4)	2.6 (-3.1-8.3)	0.3 (-7.6-8.2)	-0.1 (-0.4-0.2)	-0.4 (-0.9-0.2)	9.9 (-3-22.7)	42.9 (-66.6-152.4)	0.2 (0-0.4)	8.8 (-6.1-23.8)
	Model 3	-2.2 (-7.3-2.9)	1.8 (-2.7-6.3)	1.4 (-6.5-9.3)	-0.1 (-0.4-0.2)	-0.4 (-0.9-0.1)	9.7 (-0.6-20)	45.8 (-45.4-136.9)	0.2 (0-0.4)	8 (-5.6-21.6)
	Model 4	-2.4 (-7.5-2.7)	0.7 (-3.1-4.4)	-0.2 (-7.5-7.2)	-0.1 (-0.4-0.1)	-0.4 (-0.9-0.1)	8 (-2-18.1)	29.2 (-59.6-118)	0.2 (0-0.4)	4.1 (-7.1-15.4)

Results are based on linear regression analyses of the Dutch premenopausal women population. The beta coefficient (95% CI) can be interpreted as differences in coagulation parameter levels per SD change in PBR.

Model 1 = crude model.

Model 2 = model 1 + age.

Model 3 = model 2 + BMI, current smoking status, current use of the oral contraceptive pill, and current use of hormone replacement therapy.

Model 4 = model 3 + serum CRP, serum leptin concentration, and serum GlycA concentration.

Abbreviation: RBCV_{feed vessel}: feed vessel RBC velocity; RBCV_{capillary}: capillary RBC velocity; D_{Total}: total valid vessel density with measurable RBC velocity; D_{feed vessel}: perfused feed vessel density; D_{capillary}: perfused capillary density; CBV_{static}: capillary blood volume.

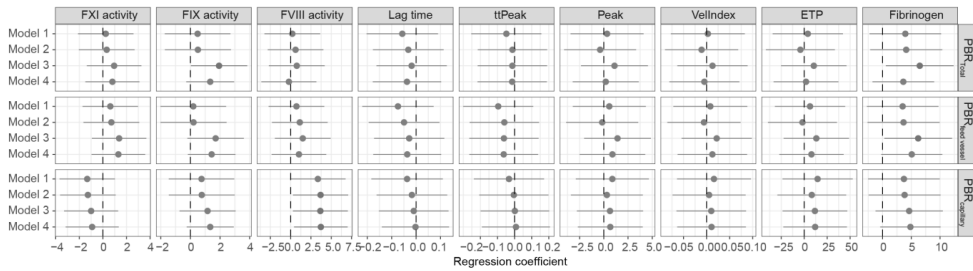


Figure S7. Association between glycoalyx-related SDF imaging parameters and levels of coagulation parameters in postmenopausal women. After stratification for menopausal status, differences in postmenopausal women between the glycoalyx-related parameters and coagulation factor levels can be observed. Model 1: crude model; Model 2: model 1 + age; Model 3: model 2 + BMI, current smoking status, current use of the oral contraceptive pill, and current use of hormone replacement therapy; Model 4: model 3 + serum CRP, serum leptin concentration, and serum GlycA concentration. The effect size and 95% confidence interval were depicted by a horizontal line with a dot. A non-significant association was represented by the color grey, and a substantial positive association was represented by the color red. Abbreviations: PBR_{Total}: PBR of total vessels from 4-25 μ m; PBR_{feed vessel}: PBR of feed vessels from 10-19 μ m; PBR_{capillary}: PBR of capillaries from 4-9 μ m.

Table S9. Association between glyocalyx-related SDF imaging parameters and levels of coagulation parameters in postmenopausal women.

		FXI activity	FIX activity	FVIII activity	Lag time	ttPeak	Peak	ETP	VelIndex	Fibrinogen
PBR _{Total}	Model 1	0.2 (-2.1-2.6)	0.5 (-1.7-2.7)	0.2 (-3.2-3.6)	-0.1 (-0.2-0.1)	0 (-0.3-0.2)	0.3 (-3.4-4.1)	3.9 (-34.4-42.2)	0 (-0.1-0.1)	4 (-2.3-10.2)
	Model 2	0.3 (-2-2.7)	0.5 (-1.7-2.7)	0.6 (-2.8-4)	0 (-0.2-0.1)	0 (-0.2-0.2)	-0.4 (-4.1-3.3)	-4.1 (-41.7-33.4)	0 (-0.1-0.1)	4.1 (-2.2-10.4)
	Model 3	1 (-1.4-3.3)	1.9 (0-3.8)	0.8 (-2.7-4.2)	0 (-0.2-0.1)	0 (-0.2-0.2)	1.1 (-2.4-4.6)	10.5 (-25.1-46.1)	0 (-0.1-0.1)	6.5 (0.6-12.4)
	Model 4	0.8 (-1.5-3.1)	1.3 (-0.3-3)	-0.2 (-3.6-3.2)	0 (-0.2-0.1)	0 (-0.2-0.2)	0.2 (-3.2-3.6)	2 (-33.3-37.3)	0 (-0.1-0.1)	3.6 (-1.8-9)
PBR _{feed vessel}	Model 1	0.6 (-1.7-3)	0.2 (-2-2.4)	0.7 (-2.7-4.1)	-0.1 (-0.2-0.1)	-0.1 (-0.3-0.1)	0.6 (-3.2-4.3)	6.3 (-31.9-44.6)	0 (-0.1-0.1)	3.5 (-2.8-9.7)
	Model 2	0.7 (-1.6-3.1)	0.2 (-2-2.4)	1.1 (-2.3-4.6)	0 (-0.2-0.1)	-0.1 (-0.3-0.1)	-0.2 (-3.9-3.6)	-1.9 (-39.5-35.7)	0 (-0.1-0.1)	3.6 (-2.6-9.9)
	Model 3	1.4 (-0.9-3.7)	1.7 (-0.2-3.6)	1.5 (-1.9-4.9)	0 (-0.2-0.1)	-0.1 (-0.3-0.1)	1.4 (-2-4.9)	13.2 (-22.3-48.8)	0 (-0.1-0.1)	6.2 (0.3-12.1)
	Model 4	1.3 (-1-3.6)	1.4 (-0.2-3)	1 (-2.3-4.4)	0 (-0.2-0.1)	-0.1 (-0.3-0.1)	0.9 (-2.5-4.3)	7.9 (-27.1-43)	0 (-0.1-0.1)	5.1 (-0.2-10.4)
PBR _{capillary}	Model 1	-1.3 (-3.7-1)	0.8 (-1.5-3)	3.4 (-0.1-6.8)	0 (-0.2-0.1)	0 (-0.2-0.2)	0.9 (-2.9-4.7)	14.6 (-23.7-52.8)	0 (-0.1-0.1)	3.7 (-2.5-10)
	Model 2	-1.3 (-3.6-1.1)	0.8 (-1.5-3)	3.7 (0.3-7.1)	0 (-0.2-0.1)	0 (-0.2-0.2)	0.3 (-3.4-4)	8.3 (-29.2-45.7)	0 (-0.1-0.1)	3.8 (-2.4-10.1)
	Model 3	-1 (-3.3-1.3)	1.2 (-0.7-3.1)	3.7 (0.3-7)	0 (-0.2-0.1)	0 (-0.2-0.2)	0.6 (-2.8-4.1)	11.6 (-23.6-46.9)	0 (-0.1-0.1)	4.6 (-1.2-10.5)
	Model 4	-0.9 (-3.2-1.3)	1.3 (-0.3-2.9)	3.7 (0.4-7)	0 (-0.1-0.1)	0 (-0.2-0.2)	0.7 (-2.7-4)	11.9 (-22.7-46.5)	0 (-0.1-0.1)	4.8 (-0.4-10.1)

Results are based on linear regression analyses of the Dutch postmenopausal women population. The beta coefficient (95% CI) can be interpreted as differences in coagulation parameter levels per SD change in PBR.

Model 1 = crude model.

Model 2 = model 1 + age.

Model 3 = model 2 + BMI, current smoking status, current use of the oral contraceptive pill, and current use of hormone replacement therapy.

Model 4 = model 3 + serum CRP, serum leptin concentration, and serum GlycA concentration.

Abbreviation: PBR_{Total}: PBR of total vessels from 4-25µm; PBR_{feed vessel}: PBR of feed vessels from 10-19µm; PBR_{capillary}: PBR of capillaries from 4-9µm.

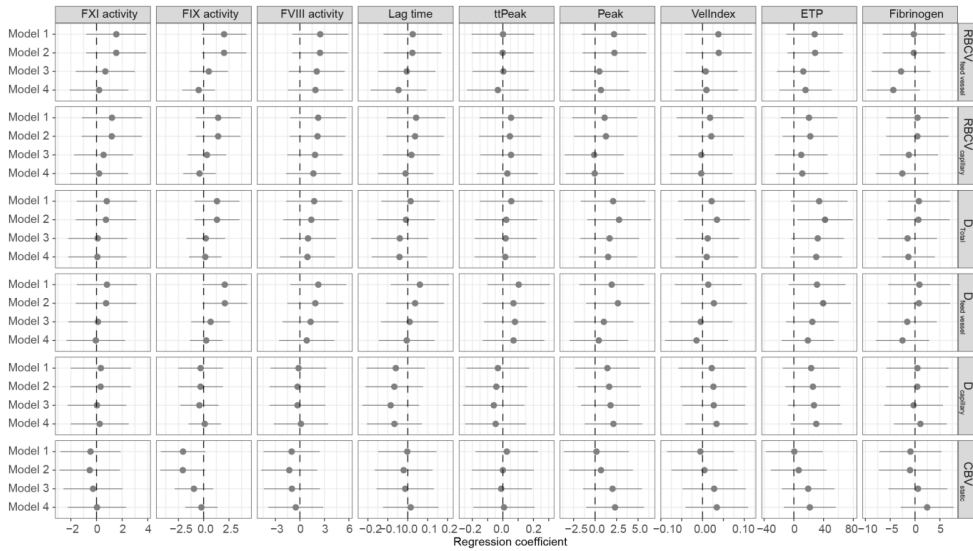


Figure S8. Association between microcirculatory-perfusion-related SDF imaging parameters and levels of coagulation parameters in postmenopausal women. After stratification for menopausal status, differences in postmenopausal women between the microcirculatory-perfusion-related parameters and coagulation factor levels can be observed. Model 1: crude model; Model 2: model 1 + age; Model 3: model 2 + BMI, current smoking status, current use of the oral contraceptive pill, and current use of hormone replacement therapy; Model 4: model 3 + serum CRP, serum leptin concentration, and serum GlycA concentration. The effect size and 95% confidence interval were depicted by a horizontal line with a dot. A non-significant association was represented by the color grey, and a substantial positive association was represented by the color red. Abbreviations: RBCV_{feed vessel}: feed vessel RBC velocity; RBCV_{capillary}: capillary RBC velocity; D_{Total}: total valid vessel density with measurable RBC velocity; D_{feed vessel}: perfused feed vessel density; D_{capillary}: perfused capillary density; CBV_{static}: capillary blood volume.

Table S10. Association between microcirculatory-perfusion-related SDF imaging parameters and levels of coagulation parameters in postmenopausal women.

		FXI activity	FIX activity	FVIII activity	Lag time	ttPeak	Peak	ETP	VelIndex	Fibrinogen
RBCV _{feed vessel}	Model 1	1.5 (-0.8-3.9)	2 (-0.2-4.2)	2.5 (-0.9-5.9)	0 (-0.1-0.2)	0 (-0.2-0.2)	2.2 (-1.6-6)	28.1 (-10.1-66.2)	0 (0-0.1)	-0.2 (-6.5-6)
	Model 2	1.5 (-0.8-3.9)	2 (-0.2-4.2)	2.5 (-0.9-5.9)	0 (-0.1-0.2)	0 (-0.2-0.2)	2.3 (-1.4-5.9)	28.6 (-8.6-65.8)	0 (0-0.1)	-0.3 (-6.5-6)
	Model 3	0.7 (-1.6-3)	0.5 (-1.4-2.4)	2.1 (-1.4-5.5)	0 (-0.1-0.1)	0 (-0.2-0.2)	0.5 (-2.9-3.9)	12.7 (-22.8-48.2)	0 (-0.1-0.1)	-2.8 (-8.7-3.1)
	Model 4	0.2 (-2.1-2.5)	-0.5 (-2.1-1.1)	1.9 (-1.5-5.3)	0 (-0.2-0.1)	0 (-0.2-0.2)	0.7 (-2.7-4.1)	15.8 (-19.4-50.9)	0 (-0.1-0.1)	-4.4 (-9.7-1)
RBCV _{capillary}	Model 1	1.2 (-1.1-3.6)	1.4 (-0.8-3.6)	2.2 (-1.2-5.7)	0 (-0.1-0.2)	0.1 (-0.2-0.3)	1.1 (-2.7-4.9)	20.4 (-17.8-58.6)	0 (-0.1-0.1)	0.5 (-5.8-6.7)
	Model 2	1.2 (-1.2-3.5)	1.4 (-0.8-3.6)	2.2 (-1.2-5.6)	0 (-0.1-0.2)	0 (-0.2-0.2)	1.3 (-2.4-5)	22.2 (-15.1-59.4)	0 (-0.1-0.1)	0.5 (-5.8-6.7)
	Model 3	0.6 (-1.7-2.8)	0.3 (-1.6-2.2)	1.9 (-1.6-5.3)	0 (-0.1-0.2)	0.1 (-0.1-0.3)	-0.1 (-3.5-3.3)	10 (-25.3-45.3)	0 (-0.1-0.1)	-1.2 (-7.1-4.6)
	Model 4	0.2 (-2.1-2.5)	-0.4 (-2-1.2)	1.7 (-1.7-5)	0 (-0.1-0.1)	0 (-0.2-0.2)	0 (-3.4-3.3)	11.3 (-23.5-46.2)	0 (-0.1-0.1)	-2.6 (-7.9-2.7)
D _{Total}	Model 1	0.8 (-1.5-3.1)	1.3 (-0.9-3.5)	1.8 (-1.7-5.2)	0 (-0.1-0.2)	0.1 (-0.2-0.3)	2.1 (-1.7-5.9)	34.1 (-4-72.2)	0 (-0.1-0.1)	0.8 (-5.5-7)
	Model 2	0.7 (-1.6-3.1)	1.3 (-0.9-3.5)	1.4 (-2-4.8)	0 (-0.2-0.1)	0 (-0.2-0.2)	2.8 (-0.9-6.5)	42 (4.7-79.3)	0 (0-0.1)	0.7 (-5.6-7)
	Model 3	0.1 (-2.2-2.4)	0.2 (-1.7-2.1)	1 (-2.4-4.4)	0 (-0.2-0.1)	0 (-0.2-0.2)	1.7 (-1.8-5.1)	32.2 (-3.2-67.5)	0 (-0.1-0.1)	-1.5 (-7.4-4.4)
	Model 4	0.1 (-2.2-2.3)	0.2 (-1.5-1.8)	0.9 (-2.4-4.3)	0 (-0.2-0.1)	0 (-0.2-0.2)	1.5 (-1.9-4.9)	30.1 (-4.7-64.9)	0 (-0.1-0.1)	-1.3 (-6.7-4)
D _{feed vessel}	Model 1	0.8 (-1.5-3.2)	2.1 (-0.1-4.3)	2.3 (-1.2-5.7)	0.1 (-0.1-0.2)	0.1 (-0.1-0.3)	1.9 (-1.8-7.5)	31.2 (-6.9-69.3)	0 (-0.1-0.1)	0.9 (-5.4-7.1)
	Model 2	0.7 (-1.6-3.1)	2.1 (-0.1-4.3)	1.9 (-1.5-5.3)	0 (-0.1-0.2)	0.1 (-0.1-0.3)	2.7 (-1.1-6.4)	39.5 (2.2-76.8)	0 (-0.1-0.1)	0.8 (-5.5-7.1)
	Model 3	0.1 (-2.2-2.4)	0.7 (-1.2-2.6)	1.3 (-2.1-4.8)	0 (-0.1-0.2)	0.1 (-0.1-0.3)	1 (-2.4-4.5)	24.9 (-10.6-60.5)	0 (-0.1-0.1)	-1.6 (-7.5-4.4)
	Model 4	-0.1 (-2.3-2.2)	0.2 (-1.4-1.9)	0.8 (-2.5-4.2)	0 (-0.1-0.1)	0.1 (-0.1-0.3)	0.4 (-3-3.8)	18.9 (-16.2-54)	0 (-0.1-0.1)	-2.5 (-7.9-2.8)
D _{capillary}	Model 1	0.3 (-2-2.7)	-0.3 (-2.5-1.9)	-0.2 (-3.6-3.3)	-0.1 (-0.2-0.1)	0 (-0.2-0.2)	1.4 (-2-3-5.2)	23.3 (-14.9-61.5)	0 (-0.1-0.1)	0.5 (-5.8-6.7)
	Model 2	0.3 (-2-2.7)	-0.3 (-2.5-1.9)	-0.3 (-3.7-3.1)	-0.1 (-0.2-0.1)	0 (-0.2-0.2)	1.6 (-2-1-5.3)	25.7 (-11.6-63)	0 (-0.1-0.1)	0.4 (-5.8-6.7)
	Model 3	0 (-2.3-2.3)	-0.4 (-2.3-1.5)	-0.3 (-3.7-3.1)	-0.1 (-0.2-0.1)	-0.1 (-0.3-0.1)	1.8 (-1.6-5.2)	27.1 (-8.1-62.3)	0 (0-0.1)	-0.3 (-6.2-5.6)
	Model 4	0.2 (-2-2.5)	0.1 (-1.5-1.7)	0.1 (-3.2-3.5)	-0.1 (-0.2-0.1)	0 (-0.2-0.2)	2.1 (-1.2-5.5)	30.2 (-4.4-64.7)	0 (0-0.1)	1.1 (-4.2-6.4)
CBV _{static}	Model 1	-0.5 (-2.8-1.9)	-2 (-4.3-0.2)	-1 (-4.4-2.4)	0 (-0.1-0.1)	0 (-0.2-0.2)	0.2 (-3.6-3.9)	0.6 (-37.6-38.9)	0 (-0.1-0.1)	-0.9 (-7.2-5.3)
	Model 2	-0.5 (-2.9-1.8)	-2.1 (-4.3-0.1)	-1.3 (-4.7-2.1)	0 (-0.2-0.1)	0 (-0.2-0.2)	0.7 (-3-4)	6.5 (-31-44)	0 (-0.1-0.1)	-1 (-7.3-5.3)
	Model 3	-0.3 (-2.6-2)	-1 (-2.9-0.9)	-1 (-4.4-2.4)	0 (-0.2-0.1)	0 (-0.2-0.2)	2 (-1.4-5.5)	19.3 (-16.1-54.7)	0 (0-0.1)	0.6 (-5.3-6.5)
	Model 4	0 (-2.2-2.3)	-0.2 (-1.8-1.4)	-0.5 (-3.9-2.9)	0 (-0.1-0.2)	0 (-0.2-0.2)	2.3 (-1-5.7)	21.5 (-13.4-56.4)	0 (0-0.1)	2.4 (-2.9-7.8)

Results are based on linear regression analyses of the Dutch postmenopausal women population. The beta coefficient (95% CI) can be interpreted as differences in coagulation parameter levels per SD change in PBR.

Model 1 = crude model.

Model 2 = model 1 + age.

Model 3 = model 2 + BMI, current smoking status, current use of the oral contraceptive pill, and current use of hormone replacement therapy.

Model 4 = model 3 + serum CRP, serum leptin concentration, and serum GlycA concentration.

Abbreviation: RBCV_{feed vessel}: feed vessel RBC velocity; RBCV_{capillary}: capillary RBC velocity; D_{Total}: total valid vessel density with measurable RBC velocity; D_{feed vessel}: perfused feed vessel density; D_{capillary}: perfused capillary density; CBV_{static}: capillary blood volume.

CHAPTER

3

Altered HDL composition is associated with risk for complications in type 2 diabetes mellitus in South Asian descendants: a cross-sectional, case-control study on lipoprotein subclass profiling

Lushun Yuan^{1,2}, Ruifang Li-Gao³, Aswin Verhoeven⁴, Huub J. van Eyk^{1,5}, Maurice B. Bizino⁶, Patrick C.N. Rensen^{1,5}, Martin Giera⁴, Ingrid M. Jazet^{1,5}, Hildo J. Lamb⁶, Ton J. Rabelink^{1,2}, Bernard M. van den Berg^{1,2}

¹ *Eindhoven Laboratory for Vascular and Regenerative Medicine, Leiden University Medical Center, Leiden, the Netherlands.*

² *Department of Internal Medicine, Division of Nephrology, Leiden University Medical Center, Leiden, the Netherlands.*

³ *Department of Clinical Epidemiology, Leiden University Medical Center, Leiden, the Netherlands.*

⁴ *Center for Proteomics and Metabolomics, Leiden University Medical Center, Leiden, the Netherlands.*

⁵ *Department of Internal Medicine, Division of Endocrinology, Leiden University Medical Center, Leiden, the Netherlands.*

⁶ *Department of Radiology, Leiden University Medical Center, Leiden, the Netherlands.*

Abstract

Background: Composition of high-density lipoproteins (HDL) is emerging as an important determinant in the development of microvascular complications in type 2 diabetes mellitus (T2DM). Dutch South Asian (DSA) individuals with T2DM display an increased risk of microvascular complications compared to Dutch white Caucasian (DwC) individuals with T2DM. In this study, we aimed to investigate whether changes in HDL composition associate with increased microvascular risk in this ethnic group and lead to new lipoprotein biomarkers.

Methods: Using ¹H nuclear magnetic resonance (NMR) spectroscopy and Bruker IVDr Lipoprotein Subclass Analysis (B.I.LISA™) software, plasma lipoprotein changes were determined in 51 healthy individuals (30 DwC, 21 DSA) and 92 individuals with T2DM (45 DwC, 47 DSA) in a cross-sectional, case-control study. Differential HDL subfractions were investigated using multinomial logistic regression analyses, adjusting for possible confounders including BMI and diabetes duration.

Results: We identified HDL compositional differences between healthy and diabetic individuals in both ethnic groups. Specifically, levels of ApoA2 and HDL-4 subfractions were lower in DSA compared to DwC with T2DM. ApoA2 and HDL-4 subfractions also negatively correlated with waist circumference, waist-to-hip ratio, HbA1c, glucose levels, and disease duration in DSA with T2DM, and associated with increased incidence of microvascular complications.

Conclusion: While HDL composition differed between controls and T2DM in both ethnic groups, the lower levels of lipid content in the smallest HDL subclass (HDL-4) in DSA with T2DM appeared to be more clinically relevant, with higher odds of having diabetes-related pan-microvascular complications such as retinopathy and neuropathy. These typical differences in HDL could be used as ethnicity-specific T2DM biomarkers.

Keywords: High-density lipoprotein composition, NMR, Dutch South Asians, type 2 diabetes mellitus, microvascular complications

Introduction

The worldwide rising prevalence of type 2 diabetes mellitus (T2DM) is one of the major challenges to public health in the 21st century ¹. Being overweight and obese are the most prominent risk factors for T2DM. However, South Asians (SA) have a significantly higher risk of developing T2DM compared to white Caucasians (wC) even with a body mass index (BMI) of around 23, which strongly suggests that different pathophysiological pathways in this particular ethnic group may lead to T2DM progression ². Additionally, compared to other ethnic groups, SAs tend to develop T2DM 5 to 10 years earlier ², and SA patients with T2DM are more prone to develop microvascular complications such as diabetic retinopathy, with a faster progression and greater disease severity compared to West European patients with T2DM ³⁻⁵.

Previous studies showed that since the reduction of in particular low-density lipoproteins (LDL) by statins was associated with insulin resistance and increased risk of hyperglycaemic complications in T2DM, high-density lipoproteins (HDL) may be a better biomarker in diabetes progression ⁶⁻⁸. HDL is composed of various lipids and proteins including apolipoproteins, enzymes, and lipid transfer factors, and exhibit large heterogeneity in size, density, and composition. The various HDL fractions have different functionalities with respect to mediating cholesterol efflux, anti-oxidation, anti-inflammation, and anti-thrombotic processes ^{9,10}. Low plasma HDL cholesterol (HDL-C) levels, for instance, were found associated with an increased risk of T2DM and cardiovascular disease ¹¹⁻¹³, while also the importance of HDL functionality to cardiovascular disease incidence and prognosis of heart failure was observed ¹⁴⁻¹⁶, one of the main complications among T2DM patients. Emerging evidence further indicated that HDL particle quality has a causative impact on diabetes ¹⁷⁻²⁰.

The majority of these studies were performed in Western populations, however, very little is known about HDL functional changes in individuals with T2DM from other ethnic groups. Given that SA represent a unique high-risk population with different pathophysiological

pathways to T2DM progression, dysfunction of HDL might be an important aspect overlooked in this population. Therefore, we hypothesized that specific differences in HDL composition in Dutch SA (DSA) with T2DM relate to their increased vulnerability to diabetes-related microvascular complications. In the present study, we aimed to investigate whether differences in plasma HDL composition in DSA with T2DM in relation to Dutch wC (DwC) with T2DM and their respective non-diabetic controls are associated with diabetes-related microvascular complications to provide possible new biomarkers. For this, we used ¹H nuclear magnetic resonance (NMR) spectroscopy and the validated Bruker IVDr Lipoprotein Subclass Analysis (B.I.LISA™) software ²¹⁻²⁶ to measure plasma HDL subclass and lipid concentrations for HDL composition determination in DSA individuals with and without T2DM, compared with DwC without or with T2DM.

Material and methods

Study population. For the present cross-sectional study, baseline samples were used from the MAGNetic resonance Assessment of VICTOza efficacy in the Regression of cardiovascular dysfunction in type 2 diAbetes mellitus (MAGNA VICTORIA) study from two previous randomized controlled trials (RCT, ClinicalTrials.gov NCT01761318 ²⁷ and NCT02660047 ²⁸, respectively), together with age and gender matched healthy controls from both ethnic groups ²⁹. In the first trial, 50 DwC with T2DM were recruited while 51 DSA with T2DM were recruited in the second trial. T1DM patients were excluded in both trials. One DwC-T2DM and four DSA-T2DM patients withdrew from the RCTs. Healthy controls were recruited by advertisement in Leiden University Medical Center (Leiden, The Netherlands) and local newspapers, as mentioned elsewhere ²⁹. Additionally, 51 healthy non-diabetic control participants (30 DwC-C and 21 DSA-C) were prospectively enrolled with a similar age and sex distribution to the corresponding T2DM patients. Ethnicity was based on the self-identified and self-reported biological parents' and ancestors' origins. Participants with complete informed consent were included. The study conformed to the

revised Declaration of Helsinki and ethical approval was obtained from the Institutional Review Board (Leiden University Medical Center, Leiden, the Netherlands).

For the present study, we excluded participants of whom plasma samples were not available.

Sample preparation for ^1H nuclear magnetic resonance (NMR) spectroscopy. Sample preparation was performed consistently with the requirements of the Bruker B.I.LISA lipoprotein analysis protocol. The EDTA plasma samples were thawed at room temperature and immediately homogenized by inverting the tubes 10 times. Next, 200 μL of plasma was manually transferred to a Ritter 96 deep-well plate. A Gilson 215 liquid handler robot was used to mix 120 μL of plasma with 120 μL , 75 mM disodium phosphate buffer in $\text{H}_2\text{O}/\text{D}_2\text{O}$ (80/20) with a pH of 7.4 containing 6.15 mM NaN_3 and 4.64 mM sodium 3-[trimethylsilyl] d4-propionate (Cambridge Isotope Laboratories). Using a modified second Gilson 215 liquid handler, 190 μL of each sample was transferred into 3 mm Bruker SampleJet NMR tubes. Subsequently, the tubes were sealed by POM ball insertion and transferred to the SampleJet autosampler where they were kept at 6°C while queued for acquisition.

NMR spectroscopy measurement and processing. All proton nuclear magnetic resonance (^1H -NMR) experiments were acquired on a 600 MHz Bruker Avance Neo spectrometer (Bruker Corporation, Billerica, USA) equipped with a 5-mm triple resonance inverse (TCI) cryogenic probe head with a Z-gradient system and automatic tuning and matching.

The NMR spectra were acquired following the Bruker B.I.Methods protocol. Before the measurements, a standard 3 mm sample of 99.8% methanol-d4 (Bruker) was used for temperature calibration³⁰. A standard 3 mm QuantRefC sample (Bruker) was measured as the quantification reference and for quality control. All experiments were recorded at 310 K. The duration of the $\pi/2$ pulses was automatically calibrated for each sample using a

homonuclear-gated nutation experiment on the locked and shimmed samples after automatic tuning and matching of the probe head³¹. For water suppression, presaturation of the water resonance with an effective field of $\gamma B_1 = 25$ Hz was applied during the relaxation delay and the mixing time of the NOESY1D experiment³².

The NOESY1D experiment was recorded using the first increment of a NOESY pulse sequence with a relaxation delay of 4 s and a mixing time of 10 ms³³. After applying 4 dummy scans, 32 scans of 98,304 points covering a sweep width of 17,857 Hz were recorded.

The lipoprotein values were extracted from the NOESY1D plasma spectra by submitting the data to the commercial Bruker IVDr Lipoprotein Subclass Analysis (B.I.LISA) platform²¹⁻²⁶. This approach extracts information about lipoproteins and lipoprotein subfractions in plasma. In the current study, we focused on the HDL particles; dissected into four subclasses (sorted according to increasing density and decreasing size; i.e., HDL-1, HDL-2, HDL-3, and HDL-4), component concentration and composition. Lipid content including total cholesterol, free cholesterol, phospholipids, and triglycerides within total HDL and HDL subclasses represents the composition of HDL, called HDL main fractions and subfractions. The calculated esterified cholesterol was not included in the present study.

Isolation of primary human umbilical vein endothelial cells (HUVEC). Primary HUVECs were isolated from human umbilical cords obtained at the Leiden University Medical Center after written informed consent was obtained and the umbilical cord was collected and processed anonymously. The umbilical cord was rinsed with PBS to remove any remaining blood. To detach the endothelial cells from the umbilical cord, trypsin/EDTA (BE17-161E, Lonza, B-4800 Verviers, Belgium) was used. After 20 minutes of incubation at 37°C, the trypsin was inactivated with 20% FCS in PBS, and the entire solution in the umbilical cord was collected. The umbilical vein was flushed with PBS one more time to ensure that all detached cells were collected before centrifugation at 1200 rpm for 7 minutes. Cells were

then cultured in 1% gelatin pre-coated flasks in endothelial growth medium (EGM2 medium, C-22011 supplemented with SupplementMix, Promocell, Heidelberg, Germany) with 1% antibiotics (penicillin/streptomycin, 15070063, Gibco, Paisley, UK). We cultured HUVECs from two different donors (one boy and one girl). We pooled them together and froze them in several vials for future experiments once they were confluent.

HDL isolation. Leftover plasma samples from ¹H NMR measurements were used to isolate HDL based on the protocol from a previous study by Mulder *et al.* ³⁴. First, a 1:2 mixture of 36% polyethylene glycol (PEG 6000, 442714K, VWR International, Lutterworth, UK) in 10 mM HEPES (pH 8, H3375, Sigma Aldrich, the Netherlands) and plasma was prepared. Following that, samples were incubated for 30 min on ice to precipitate ApoB-containing lipoproteins, and centrifuged for 30 minutes at 2200 g. The HDL-containing supernatants were collected, kept at 4°C, and used the following day for HDL functionality tests.

HDL anti-thrombotic capacity. Primary HUVECs were used to test HDL's anti-thrombotic properties. In the 96-well plate, HUVECs (passage 3) were seeded at a density of 4×10⁵ cells/well. The following day, HUVECs were pre-incubated for 30 min with 2% ApoB-depleted plasma or an equal volume of precipitation reagent in HEPES as a control. Tumor necrosis factor α (TNF-α, H8916, Sigma Aldrich, the Netherlands) was then added at a concentration of 10 ng/mL. After another 5 h of incubation, the cell surface was washed once with HBSS, no calcium, and no magnesium (14170120, Gibco™, Paisley, UK). Each well received 50 μL of normal pooled plasma before being placed in the Fluorometer for a 10-min incubation at 37°C. The formation of thrombin was started by mixing 10 μL of the fluorogenic substrate with calcium (TS50.00 FluCa-kit; Thrombinoscope BV, Maastricht, the Netherlands). The final reaction volume was 60 μL. Thrombin formation was measured every 20 sec for 60 min and calibrated using Thrombinoscope software (Supplemental

Figure S4a). To assess HDL anti-thrombotic capacity, endogenous thrombin potential (ETP) was measured. To limit potential variation due to different plate conditions, HDL anti-thrombotic capacity measurements were performed at the same time using the same batch of pooled HUVECs and reagents. For each individual, measurements were taken in three technical replicates. To avoid batch effects, each plate contains samples from four groups.

Statistical analyses. Differences in baseline characteristics were tested between 4 groups, namely DwC healthy controls (DwC-C), DwC-T2DM, DSA healthy controls (DSA-C), and DSA-T2DM. Categorical variables were expressed as total number (percentage, %) and differences between groups were tested with the Chi-square test or Fisher's exact test. Normally distributed continuous variables were expressed as mean (standard deviation, SD), and differences were evaluated by post hoc tests of unpaired One-way ANOVA test; skewed continuous variables were presented as median (25-75 percentile) and differences were assessed using the Kruskal-Wallis test.

Based on ¹H NMR spectroscopy, a total of 112 lipoprotein main fractions and subfractions were extracted. To confirm the reliability of the NMR measurements, correlation analyses were performed between clinical routine measurements and corresponding parameters from NMR. We first extracted concentrations of all lipoprotein subclasses and performed a Pearson's correlation between clinical routine measurements (total triglycerides, total cholesterol, LDL-cholesterol [LDL-C], and HDL-C) and corresponding parameters from NMR.

Four groups (DSA-T2DM, DSA-C, DwC-T2DM, and DwC-C) were considered as four outcomes, and concentrations of HDL main fractions and subfractions were scaled (z-normalization, i.e., with mean=0 and SD=1) to identify lipoproteins with different concentrations, and multinomial logistic regression analysis (MLR) was used. We set a specific reference for each comparison: between DSA-T2DM and DSA-C, DSA-C was the reference; between DwC-T2DM and DwC-C, DwC-C was the reference; between DSA-T2DM and DwC-T2DM, DwC-

T2DM was the reference; between DSA-C and DwC-C, DwC-C was the reference. The analyses were adjusted for several potential confounding factors. First, age (continuous variable), sex (dichotomous variable), and current smoking status (dichotomous variable) were adjusted for model 1. Second, model 1 was further adjusted for BMI (continuous variable) (model 2). Third, when comparing T2DM individuals from two ethnic groups, we set the disease duration of healthy individuals as zero and adjusted the diabetes duration (continuous variable) (model 3). We considered a p-value < 0.05 as significant. The results were expressed as regression coefficient (β), and odds ratios (ORs) with a 95% confidence interval (CI) to evaluate the differences between concentrations of HDL main fractions and subfractions and different groups. We followed the STROBE guidelines to report our findings.

Next, based on HDL main fractions and subfractions, supervised dimension reduction analysis called sparse partial least squares discriminant analysis (sPLS-DA) was performed by using the “mixOmics” package in R ³⁵. sPLS-DA enables the selection of the most predictive or discriminative features in the data to classify the samples. Thus, by using this analysis, we aimed to rank and validate the features according to their contribution between DSA-T2DM and DSA-C, DwC-T2DM and DwC-C, DSA-T2DM and DwC-T2DM, and DSA-C and DwC-C. We then compared the rank of features determined by sPLS-DA and those generated from multinomial logistic regression by using Spearman’s correlation to further validate the findings. The contribution of loading features was calculated based on two components for each sPLS-DA model.

Pearson’s correlation analyses were performed to reveal associations between differential HDL subfractions and laboratory markers including fasting levels of gamma-glutamyl transferase (GGT), haemoglobin A1c (HbA1c), and glucose and anthropometrics markers including visceral adipose tissue (VAT), waist circumference, and waist-to-hip ratio.

We then investigated the correlation between disease duration and differential HDL subfractions, and further examined the associations between HDL subfractions and pan-microvascular-related complications, which were defined as composite diabetes-related

complications including diabetic nephropathy, diabetic neuropathy, and diabetic retinopathy. A T2DM participant with one or more of these complications was considered as having a pan-microvascular-related complication. This analysis was performed separately for DSA and DwC populations, and the Mann-Whitney-Wilcoxon test was used to assess the statistical differences between the cases (e.g., with pan-microvascular-related complications) and controls (e.g., without pan-microvascular-related complications) for each ethnic group. Statistical analyses were performed in R (version 4.1.0) and GraphPad Prism version 8 (Graphpad Inc., La Jolla, CA, USA).

Results

Clinical characteristics. After consecutive exclusion of one T1DM individual from the MAGNA VICTORIA study, 5 individuals who withdrew from the RCT, and 3 individuals with missing plasma samples, 92 individuals with T2DM were included. None of the healthy controls were excluded (Figure 1). In total, 143 individuals were included in the present study: 47 DSA-T2DM subjects (19 men/28 women), 21 DSA-C (9 men/15 women), 45 DwC-T2DM subjects (25 men/20 women), and 30 DwC-C (16 men/14 women), (Table 1).

Compared to DSA-C, systolic blood pressure, body surface area (BSA), BMI, waist circumference, waist-to-hip ratio, fasting glucose, HbA1c, triglyceride levels, and VAT were higher in DSA-T2DM; while total cholesterol, HDL-C, and LDL-C were lower (Table 1). In the DwC-T2DM group, BSA, BMI, waist circumference, waist-to-hip ratio, total cholesterol, LDL-C, total body fat, and SAT were higher compared to DwC-C, together with a higher proportion of current smokers. Comparing individuals with T2DM between the ethnic groups, DSA subjects had a longer diabetes duration, a higher incidence of vascular-related complications (e.g., retinopathy and macrovascular problems), and a higher albumin/creatinine ratio compared to DwC subjects.

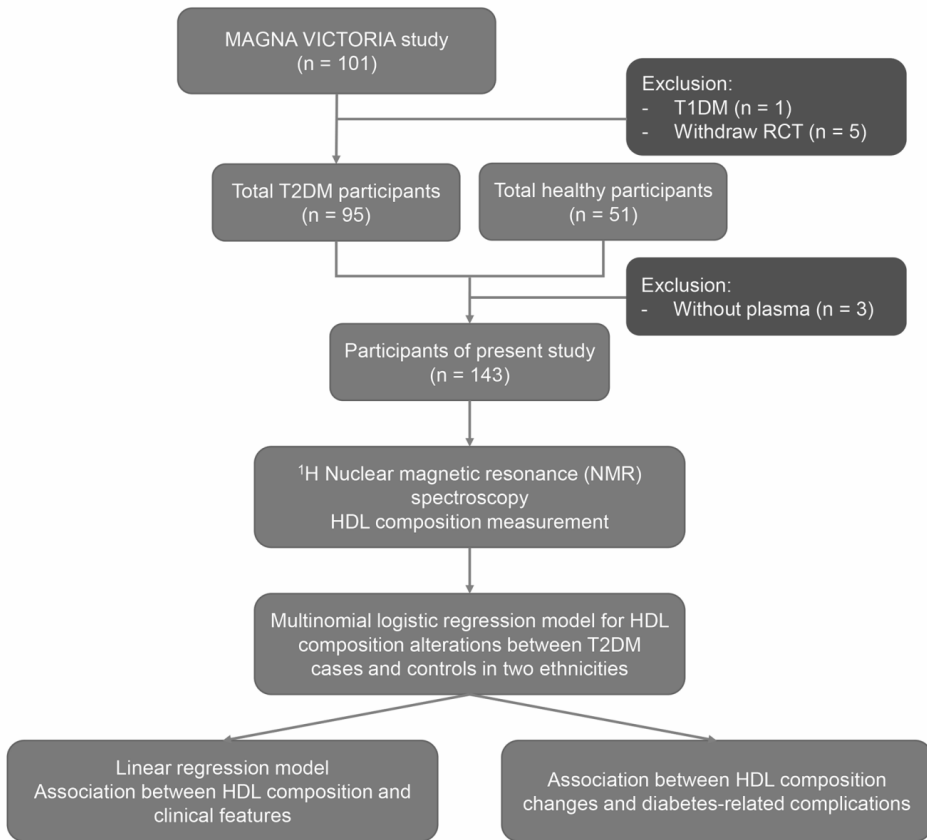


Figure 1. Flow chart of the study

Table 1. Clinical Characteristics of study participants.

	Dutch South Asian			Dutch white Caucasian			Dutch South Asian T2DM vs Dutch white Caucasian T2DM
	Control (n=21)	T2DM (n=47)	p-value ¹	Control (n=30)	T2DM (n=45)	p-value ¹	p-value ²
Demographics							
Age (years)	48.3 (8.1)	54.9 (10.1)	0.0367	57.9 (7.9)	59.0 (6.5)	ns	ns
Women (no, %)	15 (71.4%)	28 (59.6%)	ns	14 (46.7%)	20 (44.4%)	ns	ns
Current smoker (no, %)	3 (14.3%)	7 (14.9%)	ns	1 (3.3%)	9 (20.0%)	0.0437	ns
Medical history diabetes							
Duration diabetes mellitus (years)	-	17.9 (10)	-	-	10.3 (6.0)	-	<0.0001
Nephropathy (n, %)	-	10 (21.3%)	-	-	11 (23.4%)	-	ns
Neuropathy (n, %)	-	14 (29.8%)	-	-	15 (31.9%)	-	ns
Retinopathy (n, %)	-	24 (51.1%)	-	-	5 (10.6%)	-	<0.0001
Macrovascular (n, %)	-	13 (27.7%)	-	-	2 (4.3%)	-	0.0037
Medication use							
Metformin (n, %)	-	45 (95.7%)	-	-	45 (100%)	-	ns
Sulfonylurea derivatives (n, %)	-	8 (17.0%)	-	-	13 (28.9%)	-	ns
Insulin (n, %)	-	36 (76.6%)	-	-	29 (64.4%)	-	ns
Anti-hypertensive medication (n, %)	-	34 (72.3%)	-	-	34 (75.6%)	-	ns
ACE-inhibitors (n, %)	-	13 (27.7%)	-	-	17 (37.8%)	-	ns
Statins (n, %)	-	36 (76.6%)	-	-	36 (80.0%)	-	ns
Blood pressure							
Systolic blood pressure (mmHg)	123.5 (13.7)	144.6 (21.5)	0.0003	126.2 (12.1)	141.3 (15.0)	0.0007	ns
Diastolic blood pressure (mmHg)	80.2 (11.8)	85.3 (10.0)	ns	80 (77-83)	86.9 (8.8)	0.0158	ns
Anthropometrics							
BSA, m ²	1.7 (0.2)	1.9 (0.2)	<0.0001	1.9 (0.2)	2.2 (0.2)	<0.0001	<0.0001
BMI (kg/m ²)	23.5 (3.0)	29.5 (4.0)	<0.0001	24.3 (3.3)	32.3 (3.9)	<0.0001	0.0018
Waist circumference, cm	82.0 (7.4)	101.0 (9.5)	<0.0001	86.6 (9.1)	110.4 (8.9)	<0.0001	<0.0001
Waist-to-hip ratio	0.9 (0.1)	1 (0.1)	<0.0001	0.9 (0.1)	1 (0.1)	<0.0001	0.0039
Laboratory markers							
Fasting glucose (mmol/L)	5.0 (0.3)	8.1 (3.0)	<0.0001	5.2 (0.5)	7.8 (2.1)	<0.0001	ns
HbA1c (mmol/mol)	35.5 (2.4)	67.8 (11.3)	<0.0001	35.5 (2.7)	64.9 (10.7)	<0.0001	ns
GGT (IU/L)	-	28 (18-37.5)	-	-	32 (21-45)	-	ns
Total cholesterol (mmol/L)	5.4 (0.8)	4.2 (0.9)	<0.0001	5.7 (1.1)	4.8 (1.0)	0.0018	0.0226
HDL-cholesterol (mmol/L)	1.6 (0.3)	1.2 (0.3)	0.0028	1.9 (0.5)	1.3 (0.3)	<0.0001	ns
LDL-cholesterol (mmol/L)	3.4 (0.7)	2.1 (0.8)	<0.0001	3.3 (1.0)	2.6 (0.8)	0.0017	0.0416
Triglycerides (mmol/L)	0.9 (0.3)	1.8 (1.4)	0.0031	0.9 (0.7-1.2)	2.1 (1.3)	<0.0001	ns
Serum creatinine (μmol/mL)	68.0 (60.0-79.0)	67.0 (59.0-83.5)	ns	73.0 (68.0-85.0)	68.0 (57.0-80.0)	ns	ns
Urinary markers							
Albumin/creatinine ratio (mg/mmol)	-	2.7 (0.55-8.45)	-	-	0.7 (0-2.5)	-	0.0037
Micro-albuminuria (n, %) ^a	-	15 (31.9%)	-	-	7 (15.6%)	-	-
Macro-albuminuria (n, %) ^b	-	7 (14.9%)	-	-	1 (2.2%)	-	-
Radiology based markers							
Total body fat (%)	32.4 (7.1)	37.1 (9.1)	ns	32.5 (7.1)	37.2 (9.3)	<0.0001	ns
VAT, cm ²	73.2 (29.8)	166.4 (55.8)	<0.0001	74.7 (34.1)	205.6 (75.6)	<0.0001	ns
SAT, cm ²	233.2 (195.9-258.8)	300.1 (228.3-371.4)	0.0561	189.7 (148.8-238.6)	335.7 (262.4-419.5)	<0.0001	ns

Data are presented as mean (SD), median (25-75 percentile), or percentage.

Abbreviations: *ACE* Angiotensin-converting enzyme, *BMI* body mass index, *BSA* body surface area, *HDL* high-density lipoprotein, *LDL* low-density lipoprotein, *ns* not-significant, *SAT* subcutaneous adipose tissue, *VAT* visceral adipose tissue.

¹Post hoc tests of unpaired One-way ANOVA, Kruskal-Wallis test or Chi-square test, p<0.05

²Post hoc tests of unpaired One-way ANOVA or Kruskal-Wallis test, Chi-square test or Fisher's exact test, p<0.05

^aAlbumin-creatinine ratio between 3.0 – 30 mg/mmol. ^bAlbumin-creatinine ratio > 30 mg/mmol

Most of these data have been published before ²⁷⁻²⁹.

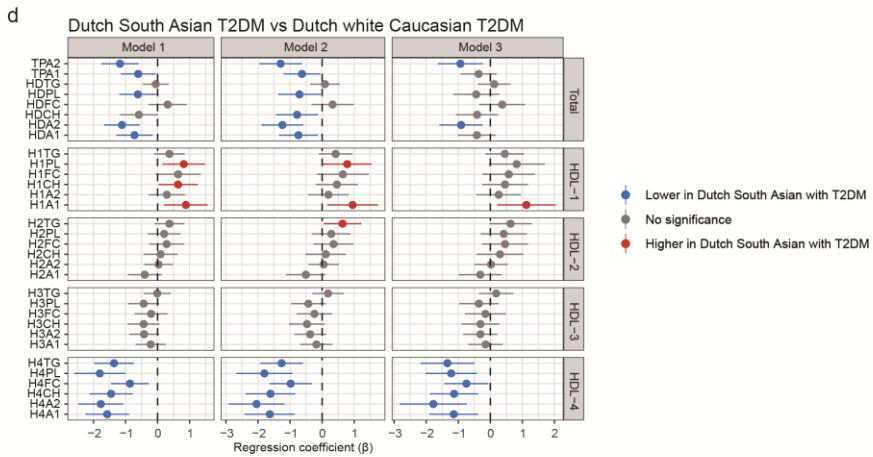
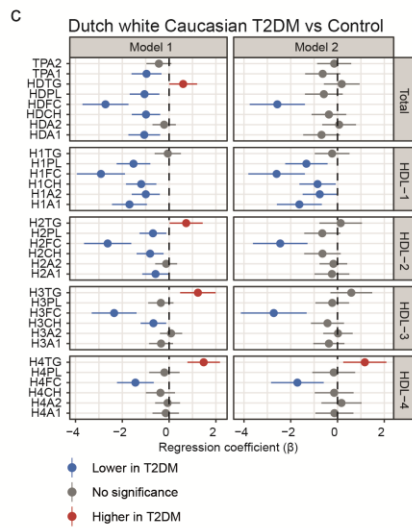
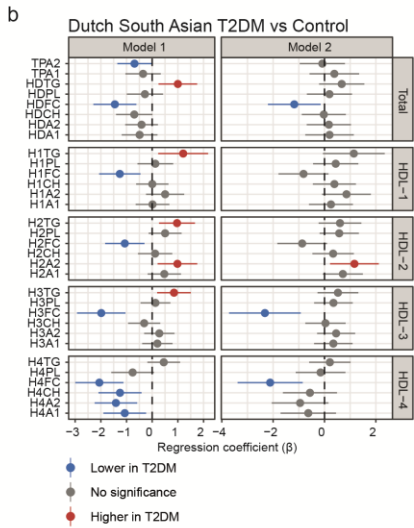
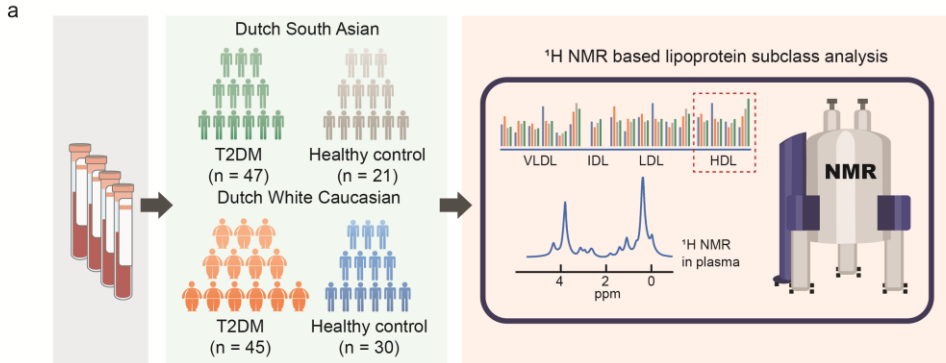
Comparison between NMR-based results vs clinical chemistry approach. NMR-based lipoprotein subclass measurements are shown in Figure 2a. To verify the quality of the NMR measurements we compared: total triglycerides, total cholesterol, HDL-C, and LDL-C to the clinical chemistry measurements revealing a high correlation in the total cohort ($R = 0.81-0.99$, $p\text{-value} < 2e-16$) as well as any single group (Supplemental Figure S1).

Different HDL compositions between healthy and diabetic individuals in two ethnic groups. To identify differences in HDL composition between the various groups, 32 HDL main fractions and subfractions were tested (Supplemental Table S1) using multinomial logistic regression analyses. Comparing healthy and diabetic individuals in Dutch South Asians, we found that 14 HDL subfractions were different (5 higher and 9 lower) in DSA-T2DM compared to DSA-C (Figure 2b and Supplemental Table S2, model 1); 21 HDL subfractions were different (4 higher and 17 lower) in DwC-T2DM compared to DwC-C (Figure 2c and Supplemental Table S3, model 1). After the adjustment of BMI (model 2), only 4 HDL subfractions remained significant (ApoA2 content in HDL-2 was higher and free cholesterol content in total HDL, HDL-3, and HDL-4 were lower) in DSA-T2DM (Figure 2b and Supplemental Table S2, model 2); 10 HDL subfractions persisted (triglyceride content in HDL-4 was higher and HDL-1 subfractions except H1TG and free cholesterol content in HDL were lower) in DwC-T2DM (Figure 2c and Supplemental Table S3, model 2). As multinomial logistic regression analysis was used to evaluate the association between HDL composition and the odds of having T2DM, the common trend in both ethnic groups showed that higher free cholesterol content in most HDL subclasses was associated with lower odds of having T2DM (Supplemental Table S2 and S3). Specifically, higher ApoA2 content in HDL-2 was associated with higher odds of having T2DM in DSA. In DwC, higher HDL-1 subfractions were associated with lower odds of having T2DM and higher triglyceride content in the smallest and dense HDL (i.e., HDL-4) was associated with higher odds of having T2DM (Supplemental Table S2 and S3).

Furthermore, sPLS-DA, a supervised machine learning method combining variable selection and classification in a one-step procedure was performed by using HDL-related features. A clear separation between T2DM and healthy controls was observed in both ethnicities, and the top 5 ranked features in DSA-T2DM were free cholesterol content in total HDL and subclasses (HDL-2, HDL-3, and HDL-4) and ApoA2 in HDL-4 (HDFC, H2FC, H3FC, H4FC, and H4A2). Those in DwC-T2DM were free cholesterol content in total HDL and subclasses (HDL-1, HDL-2, and HDL-4) and ApoA1 in HDL1 (HDFC, H1FC, H2FC, H3FC, and H1A1), (Supplemental Figure S2c-d). The ranks generated from MLR and sPLS-DA tightly correlated in both ethnic groups (Supplemental Figure S2e-f). Our findings revealed ethnic differences in HDL composition between healthy and diabetic individuals that were not detectable by routine lipid or laboratory assessments.

Figure 2. The ethnicity-specific distinction of HDL composition between Dutch South Asians and Dutch white Caucasians based on ¹H NMR. (a) Scheme of ¹H nuclear magnetic resonance in the present study. (b) Forest plot of differential lipoprotein subfractions between DSA-C and DSA-T2DM. (c) Forest plot of differential lipoprotein subfractions between DwC-C and DwC-T2DM. (d) Forest plot of differential lipoprotein subfractions between DSA-T2DM and DwC-T2DM. The regression coefficient and 95% confidence interval were depicted by a horizontal line with a dot. A non-significant association was represented by the color grey, a positive association was represented by the color red, and a substantial negative association was represented by the color blue. Model 1: adjusted age, gender, and current smoking status; Model 2 = model 1 + BMI; Model 3: model 2 + diabetes duration.

Abbreviations: A1: apolipoprotein A1; A2: apolipoprotein A2; CH: cholesterol; FC: free cholesterol; PL: phospholipid; TG: triglyceride. Abbreviations of lipoprotein main fractions and subfractions are shown in Supplemental Table S1.



HDL composition in plasma revealed ethnicity specificity in individuals with and without T2DM in two ethnic groups. When we compared T2DM subjects between DSA and DwC, notable differences were observed in HDL-4 subclass composition. Total ApoA1 and ApoA2, and phospholipid content in total HDL (HDPL) were lower in DSA-T2DM when compared to DwC-T2DM; whereas large HDL subclass composition such as ApoA1, cholesterol, and phospholipid content in HDL-1 (H1A1, H1CH, and H1PL) were higher in DSA-T2DM compared to DwC-T2DM (Supplemental Table S4 and Figure 2d, Model 1). After further adjustment for BMI and diabetes duration, the regression coefficient of differential HDL subfractions, albeit attenuated, remained different (Supplemental Table S4 and Figure 2d, Model 2 and Model 3), particularly the HDL-4 subclass composition and ApoA2 presence. Moreover, a significant difference in T2DM was observed between the two ethnic groups when using sPLS-DA (Figure 3a). Ranking HDL-related feature measurements by discriminating capability, we found that HDL-4 subclass composition and ApoA2 presence had the greatest contribution (Figure 3b). Notably, the rank generated from MLR and sPLS-DA highly correlated ($\rho = 0.97$, p -value $< 2.2e-16$, Figure 3c), which further validated our previous findings.

Considering the higher prevalence of T2DM in DSA, we also compared HDL composition among healthy individuals of both ethnicities and found that the majority of the HDL compounds were lower in DSAs, with only the triglyceride content in the HDL subclasses showing comparable distributions (Supplemental Table S5 and Supplemental Figure S3a). Meanwhile, similar but less profound findings generated from sPLS-DA were found in healthy individuals between the two ethnic groups (Supplemental Figure S2b-d). These results suggested that ApoA2 and the HDL-4 subclass composition were different in T2DM and had ethnic specificity.

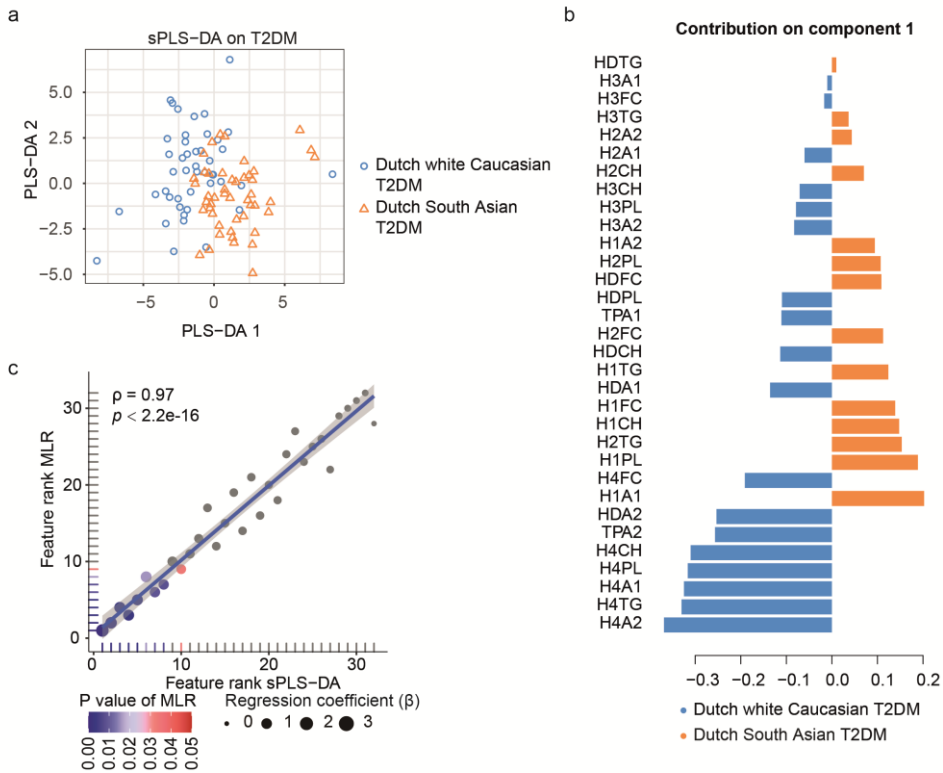


Figure 3. Sparse partial least squares discriminant analysis (sPLS-DA) differentiates DSA-T2DM from DwC-T2DM. (a) sPLS-DA performed on HDL main fractions and subfractions separates DSA-T2DM from DwC-T2DM. (b) Loading values of features with the contribution to differentiating DSA-T2DM from DwC-T2DM in the sPLS-DA. (c) Spearman's correlation between the rank generated from MLR and sPLS-DA. Dot color represents the p-value of MLR, and dot size represents the absolute value of regression coefficient.

Abbreviations of lipoprotein main fractions and subfractions are shown in Supplemental Table S1.

HDL anti-thrombotic capacity reduction in T2DM in both ethnicities. Anti-thrombotic capacity was measured in 142 subjects to evaluate HDL functionality (47 DSA-T2DM, 21 DSA-C, 45 DwC-T2DM, and 29 DwC-C). Based on the thrombin generation curve, diabetic plasma generated more thrombin than non-diabetic plasma samples in both ethnic groups

(Supplemental Figure S4b and d). Furthermore, the endogenous thrombin potential (ETP) was significantly higher in T2DM patients versus healthy controls in both ethnicities (Supplemental Figure S4c and e), revealing that HDL functionality in anti-thrombin formation was impaired both in DSA and DwC with T2DM.

Associations between differential HDL subfractions and clinical outcomes. We further investigated the associations between differential HDL subfractions (ApoA2 and HDL-4 subclass composition) and clinical outcomes (laboratory and anthropometric markers). In DSA-T2DM, except H4TG, the other lipid content in HDL-4 subclass negatively correlated with waist-to-hip ratio and waist circumference; ApoA1 and ApoA2, cholesterol and phospholipid content in HDL-4 (H4A1, H4A2, H4CH, and H4PL) revealed a negative correlation with VAT; H4CH, H4FC, and H4PL negatively correlated with HbA1c and H4FC and H4PL negatively correlated with fasting glucose. Interestingly, H4A1 and H4A2 positively correlated with GGT (Supplemental Figure S5a).

In DwC-T2DM, TPA2 and HDA2 negatively correlated with waist-to-hip ratio; HDA2 and H4A2 correlated negatively with waist circumference while H4FC showed a negative correlation with fasting glucose levels (Supplemental Figure S5b). These results suggested that changes in HDL composition were clinically relevant, especially in DSA-T2DM which could partly reflect long-term dysregulated blood-glucose control.

Associations between differential HDL subfractions and pan-microvascular-related complications. As a longer disease duration may lead to a higher incidence of complications (Figure 4a and b), we examined the correlation between HDL subfractions and diabetes duration in cases of both ethnicities. Notably, we discovered that ApoA2 and all HDL-4 subfractions except H4TG negatively associated with diabetes duration in DSA-T2DM while we did not find these associations in DwC-T2DM (Figure 4c and d).

Given glycaemic control is associated with multiple diabetes-related complications, especially microvascular problems; we then investigated the associations between differential HDL subfractions (ApoA2 and HDL-4 subclass composition) and microvascular complications. Interestingly, there was no association between HDL subfractions and pan-microvascular-related complications in white Caucasian subjects with T2DM; while, in DSA-T2DM, we observed that total ApoA2, HDA2, H4A1, H4FC, and H4PL were lower in patients with pan-microvascular-related complications. When we compared single complications, TPA2, HDA2, H4A1, H4A2, and H4FC were significantly lower in DSA-T2DM with retinopathy, while H4FC was higher in DwC-T2DM with retinopathy (Figure 4b). In DSA-T2DM, TPA2, H4A1, H4A2, H4CH, H4FC, and H4PL were significantly lower in diabetic neuropathy while none of these HDL subfractions were associated with diabetic neuropathy in DwC-T2DM (Figure 4e and f). None of the differential HDL subfractions changed between groups with and without diabetic nephropathy. These data suggest that changes in HDL composition, especially TPA2 and HDL-4 subclass composition (except H4TG in DSA), were associated with diabetes-related microvascular complications such as neuropathy and retinopathy.

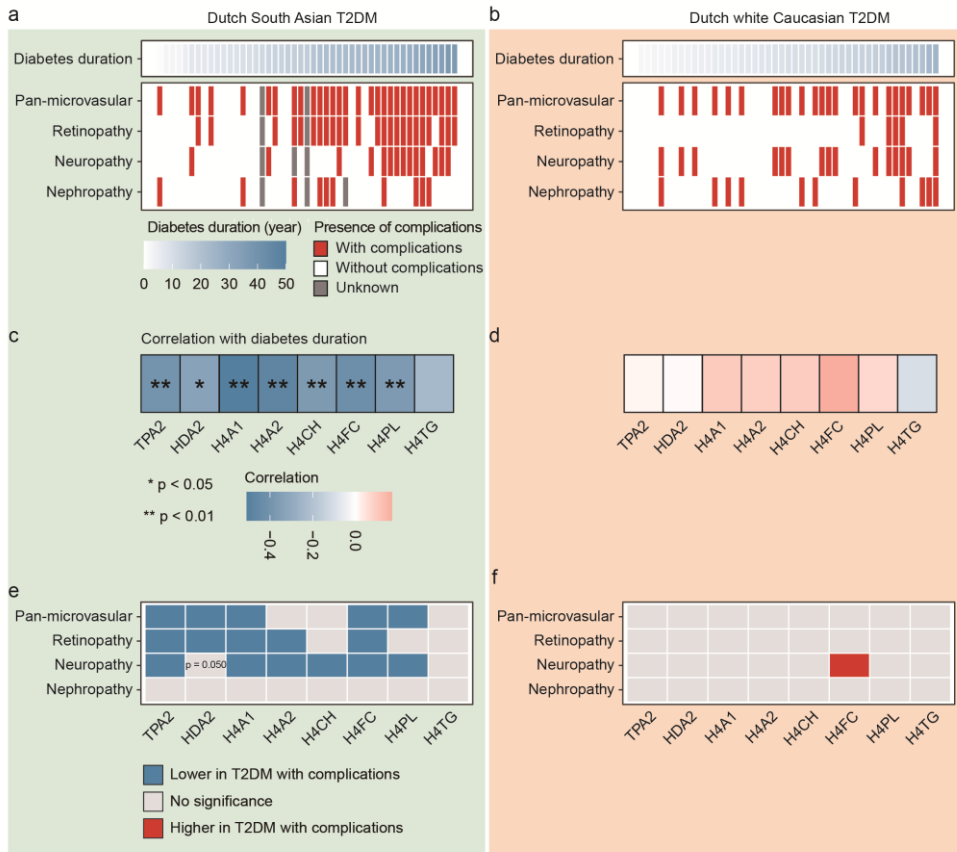


Figure 4. Associations between differential HDL subfractions and diabetes-related microvascular complications. (a) Association between disease duration and presence of diabetes-related microvascular complications in DSA-T2DM. (b) Association between disease duration and presence of diabetes-related microvascular complications in DwC-T2DM. (c) Pearson's correlation between diabetes duration and differential HDL subfractions in DSA-T2DM. (d) Correlation between diabetes duration and differential HDL subfractions in DwC-T2DM. Pearson's correlation analysis was performed. The color of scale bar represented Pearson's correlation R. * $p < 0.05$; ** $p < 0.01$. (e) Summary heatmap showing the associations between differential HDL subfractions and diabetes-related microvascular complications in DSA-T2DM. (f) Summary heatmap showing the associations between differential HDL subfractions and diabetes-related microvascular complications in DSA-T2DM.

Abbreviations of lipoprotein main fractions and subfractions are shown in Supplemental Table S1.

Discussion

In the present study, we observed HDL compositional differences between healthy and diabetic individuals in both ethnic groups. Specifically, we discovered that lower ApoA2 presence and HDL-4 subclass compositional changes in DSA individuals with T2DM were associated with a higher incidence of diabetes-related pan-microvascular complications such as retinopathy and neuropathy compared to DwC individuals with T2DM. These results indicated that differences in HDL composition might be used as an ethnicity-specific biomarker for DSA with T2DM and may provide a mechanism underlying the increased risk of microvascular complications in DSA.

Previous studies investigating HDL particle subspecies did not account for the HDL composition, particularly the lipid content, and the majority of these studies were conducted on white ethnic groups^{36,37}. Only a single study showed HDL-2 and HDL-3 were associated with insulin resistance and beta cell function in South Asians at risk of T2DM³⁸. In our study, we included both DSA and DwC populations and generated HDL main fractions and subfractions including 32 features, providing a higher resolution of HDL lipoprotein fraction than HDL-C alone. Sparse partial least squares discriminant analysis (sPLS-DA) based on HDL composition could not only distinguish healthy controls from T2DM in both ethnic groups but also show the distinction between T2DM in these two ethnic groups. This suggested that this technique may be clinically meaningful beyond the measurement of HDL-C, especially in different ethnicities.

We observed ethnicity-specific associations between HDL composition and T2DM and found a loss of large HDL subclass and higher triglycerides in the smallest HDL subclass in DwC with T2DM, consistent with the finding of the PREVEND study that HDL size is inversely associated with T2DM risk³⁶. Interestingly, in DSA with T2DM, we observed an opposite trend that the lipid content in the smallest HDL subclass was specifically lower and triglycerides were higher in the largest HDL subclass when adjusting for age, gender, and current smoking status. After BMI adjustment, only free cholesterol content in HDL

persisted, suggesting that BMI plays a vital role in affecting HDL composition in DSA-T2DM and highlighting the importance of ethnic-specific guidelines for BMI. Furthermore, a randomised trial proved that a structured weight management programme incorporating a total diet replacement weight loss phase was acceptable to individuals of SA ethnicity and could achieve T2DM remissions similarly to other populations, indicating the favourable aspects of dietary weight-management in this high-risk population ³⁹.

In our study, with individuals with T2DM of both ethnicities receiving similar medical care, we still discovered that total ApoA1 and ApoA2, as well as HDL-4 subclass composition, were significantly lower in DSA with T2DM than DwC with T2DM. Specifically small HDL particles played a role in cellular cholesterol efflux, and had antioxidative, antithrombotic, anti-inflammatory, and antiapoptotic capacities ^{40,41}. These observations support our findings in DSA and we hypothesize that in DSA with T2DM, impaired HDL function might be explained by the loss of functional small HDL subfractions; while in DwC with T2DM, increased triglyceride content in small HDL subclass might lead to HDL dysfunction. Our in-house HDL functional assay revealed that individuals with T2DM in both ethnic groups had significantly reduced anti-thrombotic capacity due to impaired HDL function, which is also consistent with earlier findings showing that individuals with T2DM had impaired HDL function in terms of its capacity to suppress TNF-induced vascular cell adhesion molecule-1 (VCAM-1) expression in endothelial cells *in vitro* ¹⁹. A previous study by Bakker *et al.* reported that in obese DSA, without T2DM, only the ability of HDL to prevent LDL oxidation was reduced in overweight DSA when compared to obese DwC (without T2DM) ²⁵. Following these findings, we discovered that obese DSA with T2DM had a specific change in HDL composition, implying that T2DM could be an additional ethnicity-specific risk factor for cardiovascular disease.

HDL-4 subfractions in DSA with T2DM had the most clinical relevance, but not in DwC with T2DM. There were notable associations between HDL-4 subfractions with both waist circumference and waist-to-hip ratio, which were reported in the HELIUS study as critical predictors for T2DM regardless of ethnic background ⁴². Additionally, lipid content of HDL-

4 was discovered to have associations with glycemic control parameters, which were risk factors for diabetes progression ⁴³⁻⁴⁵. In the current study, we also observed that HDL-4 subfractions negatively correlated with diabetes duration in DSA, and exhibited remarkable differences between patients with and without pan-microvascular complications, particularly neuropathy and retinopathy. In contrast, there was no link between HDL compositional differences and diabetes-related complications in DwC subjects with T2DM. This could indicate that changes in HDL composition occur as a consequence of hyperglycemia and disease duration rather than as a driving factor associated with diabetes-related complications. HDL-related pharmacological strategies that have been tested involving HDL-mimetic peptides, showed remarkable effects on reducing inflammation, preventing oxidation, and promoting cholesterol efflux ⁴⁶⁻⁴⁸. We found that HDL-4 subfractions were associated with disease duration in DSA with T2DM, suggesting the necessity of future studies to test the HDL-mimetic peptide effects on T2DM in individuals of SA descent.

The strength of our study is that we measured the HDL composition in detail in two ethnic groups of diabetic and non-diabetic individuals. Our findings further indicated impaired HDL function in T2DM, linking it with diabetes-related complications. Meanwhile, we revealed ethnic differences in HDL composition. Of note, there are still several limitations to our study. First, our study is a cross-sectional study, which precludes statements on causality. Second, sample sizes are relatively small, which might limit generalization potential and preclude stratification analyses. Third, Dutch South Asians with T2DM have longer disease duration than Dutch white Caucasians with T2DM in our study, which may affect incidence of complications. However, DSA-T2DM showed much faster disease progression than DwC-T2DM, which is a typical ethnic hallmark; future studies with larger sample size and multiple ethnicities are needed to verify our observations. Fourth, statin use could also affect HDL concentration, composition, and function ^{49,50}, suggesting that differences in HDL composition between healthy controls and T2DM may not be solely due to diabetes status. Fifth, due to limited plasma availability, we were only able to perform an in-house HDL anti-

thrombotic capacity assay, without performing cholesterol efflux capacity, anti-oxidation capacity, or anti-inflammatory capacity measurements. Besides, we could not perform experiments to evaluate the anti-thrombotic capacity between large/buoyant HDL and small dense HDL. Sixth, the biological response of HUVECs is variable; therefore, our in-house assay is not comparable to clinical chemistry determinations.

Conclusions

In conclusion, Dutch T2DM patients of both white Caucasian and South Asian descent exhibited altered HDL composition when compared to healthy individuals, but revealed a distinct phenotype. In Dutch South Asian subjects, lower ApoA2 and HDL-4 were associated with higher incidence of diabetes-related complications such as retinopathy and neuropathy, suggesting that they could be used as ethnicity-specific biomarkers for T2DM patients.

Abbreviations

ApoA1: apolipoprotein A1; ApoA2: apolipoprotein A2; ACE: angiotensin-converting enzyme; B.I.LISA: Bruker IVDr Lipoprotein Subclass Analysis; BMI: body mass index; BSA: body surface area; CI: confidence interval; DSA: Dutch South Asian; DwC: Dutch white Caucasian; ETP: endogenous thrombin potential; GGT: gamma-glutamyl transferase; HbA1c: hemoglobin A1c; HDL: high-density lipoprotein; HDL-C: high-density lipoprotein cholesterol; HUVEC: human umbilical vein endothelial cell; LDL: low-density lipoprotein; MAGNA VICTORIA: MAGNetic resonance Assessment of VICTOza efficacy in the Regression of cardiovascular dysfunction In type 2 diAbetes mellitus; MLR: multinomial logistic regression analysis; NMR: Nuclear magnetic resonance; OR: odds ratio; RCT: randomized controlled trial; SA: South Asian; SAT: subcutaneous adipose tissue; SD: standard deviation; T1DM: type 1 diabetes mellitus; T2DM: type 2 diabetes mellitus; TBF: total body fat percentage; TNF- α : tumor necrosis factor α ; VAT: visceral adipose tissue; WC: white Caucasian.

Acknowledgments

We thank all the patients who participated in the MAGNA VICTORIA study and healthy volunteers. We express our gratitude to the researchers, nurses, and physicians that helped organize this study. We would also like to thank Wendy M.P.J. Sol for helping with HDL isolation.

Authors' contributions

LY, MAG, and BMvdB contributed to the study concept, design, and analysis; LY analysed and interpreted data, and critically revised the manuscript; RL-G interpreted data and revised the manuscript; AV performed NMR measurements; HJvE and MBB collected data for the MAGNA VICTORIA studies, IMJ supervised the MAGNA VICTORIA studies, with HJL serving as study director; PCNR and MAG interpreted NMR data; and LY, TJR, and BMvdB drafted the manuscript. The final manuscript was read, commented on, and approved by all authors.

Funding

The work was supported by ZonMW (The Enabling Technologies Hotels program, grant: 435005003, 2019) and by the China Scholarship Council grant to Lushun Yuan (CSC no. 201806270262).

Availability of data and materials

All data and methods supporting the findings of this study are available from the corresponding author upon reasonable request.

Ethics approval and consent to participate

The T2DM participants were from baseline samples of two previous randomized controlled trials (ClinicalTrials.gov NCT01761318 and NCT02660047). The study protocol was approved by the Institutional Review Board (Leiden University Medical Center, Leiden, The Netherlands), and all participants provided written informed consent.

Consent for publication

The manuscript was approved by all authors for publication.

Competing interests

The authors declare that they have no competing interests.

References

1. Unnikrishnan R, Pradeepa R, Joshi SR, Mohan V. Type 2 Diabetes: Demystifying the Global Epidemic. *Diabetes*. 2017;66(6):1432-1442.
2. Sattar N, Gill JM. Type 2 diabetes in migrant south Asians: mechanisms, mitigation, and management. *Lancet Diabetes Endocrinol*. 2015;3(12):1004-1016.
3. van Niel J, Geelhoed-Duijvestijn P, Numans ME, Kharagjitsing AV, Vos RC. Type 2 diabetes in South Asians compared to Europeans: Higher risk and earlier development of major cardiovascular events irrespective of the presence and degree of retinopathy. Results from The HinDu The Hague Diabetes Study. *Endocrinol Diabetes Metab*. 2021;4(3):e00242.

4. Pardhan S, Gilchrist J, Mahomed I. Impact of age and duration on sight-threatening retinopathy in South Asians and Caucasians attending a diabetic clinic. *Eye (Lond)*. 2004;18(3):233-240.
5. Raymond NT, Varadhan L, Reynold DR, et al. Higher prevalence of retinopathy in diabetic patients of South Asian ethnicity compared with white Europeans in the community: a cross-sectional study. *Diabetes Care*. 2009;32(3):410-415.
6. Mansi IA, Chansard M, Lingvay I, Zhang S, Halm EA, Alvarez CA. Association of Statin Therapy Initiation With Diabetes Progression: A Retrospective Matched-Cohort Study. *JAMA Intern Med*. 2021;181(12):1562-1574.
7. Liew SM, Lee PY, Hanafi NS, et al. Statins use is associated with poorer glycaemic control in a cohort of hypertensive patients with diabetes and without diabetes. *Diabetol Metab Syndr*. 2014;6:53.
8. Sukhija R, Prayaga S, Marashdeh M, et al. Effect of statins on fasting plasma glucose in diabetic and nondiabetic patients. *J Investig Med*. 2009;57(3):495-499.
9. Mineo C, Shaul PW. Novel biological functions of high-density lipoprotein cholesterol. *Circ Res*. 2012;111(8):1079-1090.
10. Jialal I, Jialal G, Adams-Huet B. The platelet to high density lipoprotein -cholesterol ratio is a valid biomarker of nascent metabolic syndrome. *Diabetes Metab Res Rev*. 2021;37(6):e3403.
11. Schmidt MI, Duncan BB, Bang H, et al. Identifying individuals at high risk for diabetes: The Atherosclerosis Risk in Communities study. *Diabetes Care*. 2005;28(8):2013-2018.
12. Wilson PW, Meigs JB, Sullivan L, Fox CS, Nathan DM, D'Agostino RB, Sr. Prediction of incident diabetes mellitus in middle-aged adults: the Framingham Offspring Study. *Arch Intern Med*. 2007;167(10):1068-1074.
13. Sacks FM, Hermans MP, Fioretto P, et al. Association between plasma triglycerides and high-density lipoprotein cholesterol and microvascular kidney disease and retinopathy in type 2 diabetes mellitus: a global case-control study in 13 countries. *Circulation*. 2014;129(9):999-1008.
14. Jia C, Anderson JLC, Gruppen EG, et al. High-Density Lipoprotein Anti-Inflammatory Capacity and Incident Cardiovascular Events. *Circulation*. 2021;143(20):1935-1945.
15. Ajala ON, Demler OV, Liu Y, et al. Anti-Inflammatory HDL Function, Incident Cardiovascular Events, and Mortality: A Secondary Analysis of the JUPITER Randomized Clinical Trial. *J Am Heart Assoc*. 2020;9(17):e016507.
16. Emmens JE, Jia C, Ng LL, et al. Impaired High-Density Lipoprotein Function in Patients With Heart Failure. *J Am Heart Assoc*. 2021;10(9):e019123.

17. Constantinou C, Karavia EA, Xepapadaki E, et al. Advances in high-density lipoprotein physiology: surprises, overturns, and promises. *Am J Physiol Endocrinol Metab*. 2016;310(1):E1-E14.
18. Xepapadaki E, Nikdima I, Sagiadinou EC, Zvintzou E, Kypreos KE. HDL and type 2 diabetes: the chicken or the egg? *Diabetologia*. 2021;64(9):1917-1926.
19. Ebtehaj S, Gruppen EG, Parvizi M, Tietge UJF, Dullaart RPF. The anti-inflammatory function of HDL is impaired in type 2 diabetes: role of hyperglycemia, paraoxonase-1 and low grade inflammation. *Cardiovasc Diabetol*. 2017;16(1):132.
20. Heier M, Borja MS, Brunborg C, et al. Reduced HDL function in children and young adults with type 1 diabetes. *Cardiovasc Diabetol*. 2017;16(1):85.
21. Lounila J, Ala-Korpela M, Jokisaari J, Savolainen MJ, Kesaniemi YA. Effects of orientational order and particle size on the NMR line positions of lipoproteins. *Phys Rev Lett*. 1994;72(25):4049-4052.
22. Jeyarajah EJ, Cromwell WC, Otvos JD. Lipoprotein particle analysis by nuclear magnetic resonance spectroscopy. *Clin Lab Med*. 2006;26(4):847-870.
23. Jiang H, Peng J, Zhou ZY, et al. Establishing (1)H nuclear magnetic resonance based metabonomics fingerprinting profile for spinal cord injury: a pilot study. *Chin Med J (Engl)*. 2010;123(17):2315-2319.
24. Straat ME, Martinez-Tellez B, Nahon KJ, et al. Comprehensive (apo)lipoprotein profiling in patients with genetic hypertriglyceridemia using LC-MS and NMR spectroscopy. *J Clin Lipidol*. 2022;16(4):472-482.
25. Bakker LE, Boon MR, Annema W, et al. HDL functionality in South Asians as compared to white Caucasians. *Nutr Metab Cardiovasc Dis*. 2016;26(8):697-705.
26. Nodeland M, Klevjer M, Saether J, et al. Atherogenic lipidomics profile in healthy individuals with low cardiorespiratory fitness: The HUNT3 fitness study. *Atherosclerosis*. 2022;343:51-57.
27. Bizino MB, Jazet IM, Westenberg JJM, et al. Effect of liraglutide on cardiac function in patients with type 2 diabetes mellitus: randomized placebo-controlled trial. *Cardiovasc Diabetol*. 2019;18(1):55.
28. van Eyk HJ, Paiman EHM, Bizino MB, et al. A double-blind, placebo-controlled, randomised trial to assess the effect of liraglutide on ectopic fat accumulation in South Asian type 2 diabetes patients. *Cardiovasc Diabetol*. 2019;18(1):87.
29. Paiman EHM, van Eyk HJ, Bizino MB, et al. Phenotyping diabetic cardiomyopathy in Europeans and South Asians. *Cardiovascular diabetology*. 2019;18(1):133.
30. Findeisen M, Brand T, Berger S. A 1H-NMR thermometer suitable for cryoprobes. *Magn Reson Chem*. 2007;45(2):175-178.

31. Wu PS, Otting G. Rapid pulse length determination in high-resolution NMR. *J Magn Reson*. 2005;176(1):115-119.
32. Price WS. Water signal suppression in NMR spectroscopy. *Annu Rep Nmr Spectro*. 1999;38:289-354.
33. Kumar A, Ernst RR, Wuthrich K. A two-dimensional nuclear Overhauser enhancement (2D NOE) experiment for the elucidation of complete proton-proton cross-relaxation networks in biological macromolecules. *Biochem Biophys Res Commun*. 1980;95(1):1-6.
34. Mulder DJ, de Boer JF, Graaff R, et al. Skin autofluorescence is inversely related to HDL anti-oxidative capacity in type 2 diabetes mellitus. *Atherosclerosis*. 2011;218(1):102-106.
35. Rohart F, Gautier B, Singh A, Le Cao KA. mixOmics: An R package for 'omics feature selection and multiple data integration. *PLoS Comput Biol*. 2017;13(11):e1005752.
36. Sokooti S, Flores-Guerrero JL, Heerspink HJL, et al. Lipoprotein particle sizes and incident type 2 diabetes: the PREVEND cohort study. *Diabetologia*. 2022;65(2):402-405.
37. Sokooti S, Flores-Guerrero JL, Kieneker LM, et al. HDL Particle Subspecies and Their Association With Incident Type 2 Diabetes: The PREVEND Study. *J Clin Endocrinol Metab*. 2021;106(6):1761-1772.
38. Yahya R, Jainandunsing S, Rashid M, et al. HDL associates with insulin resistance and beta-cell dysfunction in South Asian families at risk of type 2 diabetes. *J Diabetes Complications*. 2021;35(10):107993.
39. Sattar N, Welsh P, Leslie WS, et al. Dietary weight-management for type 2 diabetes remissions in South Asians: the South Asian diabetes remission randomised trial for proof-of-concept and feasibility (STANDBY). *Lancet Reg Health Southeast Asia*. 2023;9:100111.
40. Camont L, Lhomme M, Rached F, et al. Small, dense high-density lipoprotein-3 particles are enriched in negatively charged phospholipids: relevance to cellular cholesterol efflux, antioxidative, antithrombotic, anti-inflammatory, and antiapoptotic functionalities. *Arterioscler Thromb Vasc Biol*. 2013;33(12):2715-2723.
41. He Y, Ronsein GE, Tang C, et al. Diabetes Impairs Cellular Cholesterol Efflux From ABCA1 to Small HDL Particles. *Circ Res*. 2020;127(9):1198-1210.
42. Zethof M, Mosterd CM, Collard D, et al. Differences in Body Composition Convey a Similar Risk of Type 2 Diabetes Among Different Ethnic Groups With Disparate Cardiometabolic Risk-The HELIUS Study. *Diabetes care*. 2021;44(7):1692-1698.
43. Stuhldreher WL, Becker DJ, Drash AL, et al. The association of waist/hip ratio with diabetes complications in an adult IDDM population. *J Clin Epidemiol*. 1994;47(5):447-456.
44. Li W, Gong X, Wang W, et al. Association of different kinds of obesity with diabetic retinopathy in patients with type 2 diabetes. *BMJ Open*. 2022;12(5):e056332.

45. Marcovecchio ML, Lucantoni M, Chiarelli F. Role of chronic and acute hyperglycemia in the development of diabetes complications. *Diabetes Technol Ther.* 2011;13(3):389-394.
46. D'Souza W, Stonik JA, Murphy A, et al. Structure/function relationships of apolipoprotein a-I mimetic peptides: implications for antiatherogenic activities of high-density lipoprotein. *Circ Res.* 2010;107(2):217-227.
47. Van Lenten BJ, Wagner AC, Jung CL, et al. Anti-inflammatory apoA-I-mimetic peptides bind oxidized lipids with much higher affinity than human apoA-I. *J Lipid Res.* 2008;49(11):2302-2311.
48. Dunbar RL, Movva R, Bloedon LT, et al. Oral Apolipoprotein A-I Mimetic D-4F Lowers HDL-Inflammatory Index in High-Risk Patients: A First-in-Human Multiple-Dose, Randomized Controlled Trial. *Clin Transl Sci.* 2017;10(6):455-469.
49. Orsoni A, Therond P, Tan R, et al. Statin action enriches HDL3 in polyunsaturated phospholipids and plasmalogens and reduces LDL-derived phospholipid hydroperoxides in atherogenic mixed dyslipidemia. *J Lipid Res.* 2016;57(11):2073-2087.
50. Pirillo A, Catapano AL. Pitavastatin and HDL: Effects on plasma levels and function(s). *Atheroscler Suppl.* 2017;27:e1-e9.

Supporting information

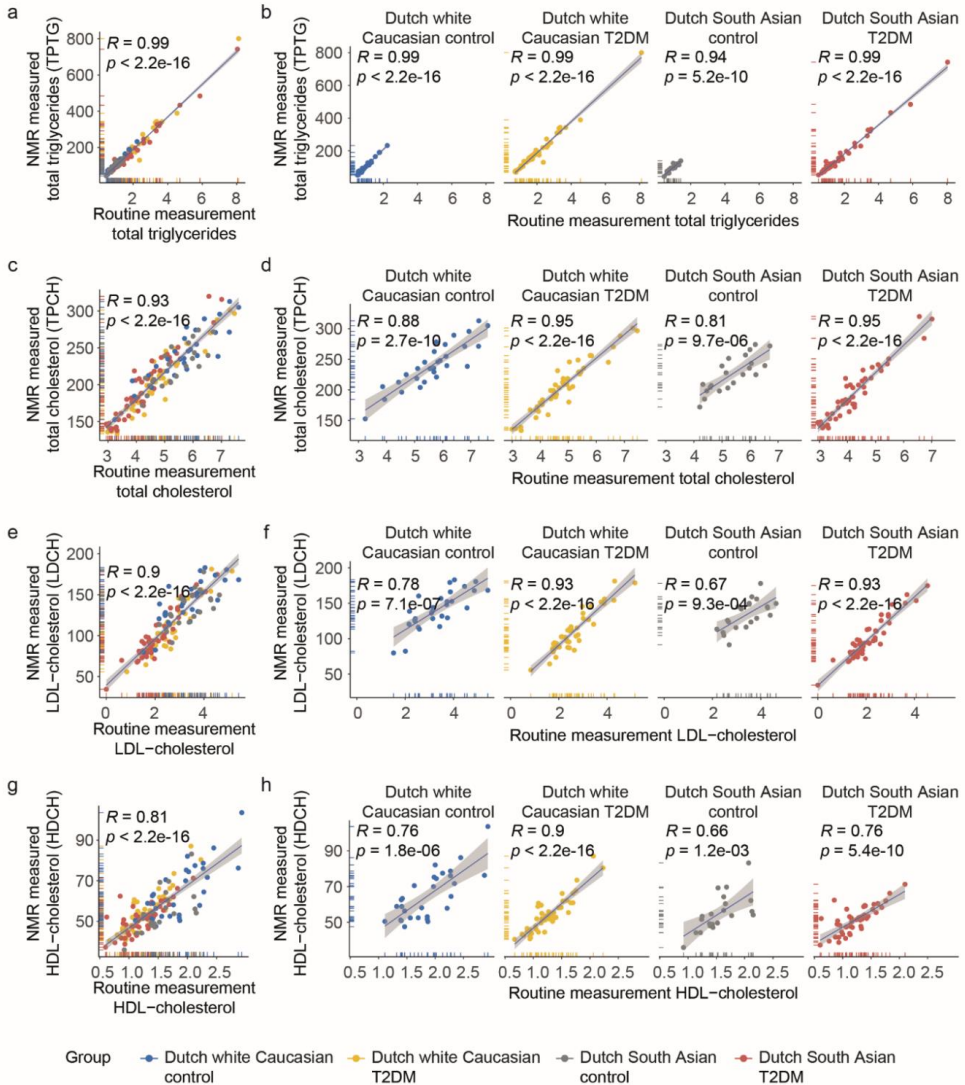
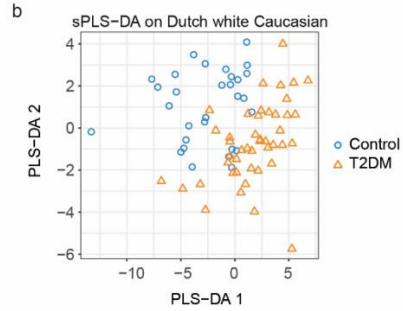
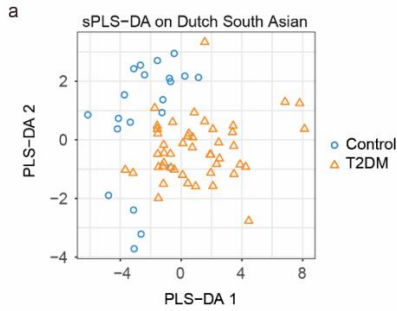


Figure S1. Association between lipids and apolipoproteins measured by NMR

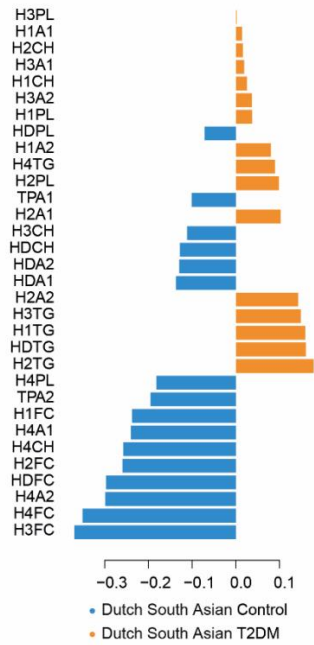
spectroscopy vs clinical chemistry approach. Pearson's correlation between routine total triglyceride levels (mmol/L) and NMR extracted total triglyceride concentrations (TPTG, mg/dL) in (a) the total cohort and (b) the individual groups. Pearson's correlation between routine total cholesterol (mmol/L) levels and NMR extracted total cholesterol (TPCH, mg/dL) concentrations in (c) the total cohort and (d) the individual groups. Pearson's

correlation between routine LDL-cholesterol (mmol/L) levels and NMR extracted LDL-cholesterol (LDCH, mg/dL) concentrations in (e) the total cohort and (f) the individual groups. Pearson's correlation between routine HDL-cholesterol levels (mmol/L) and NMR extracted HDL-cholesterol concentrations (mg/dL) in (g) the total cohort and (h) the individual groups.

Abbreviations of lipoprotein main fractions and subfractions are shown in Supplemental Table S1.



c Contribution on component 1



d Contribution on component 1

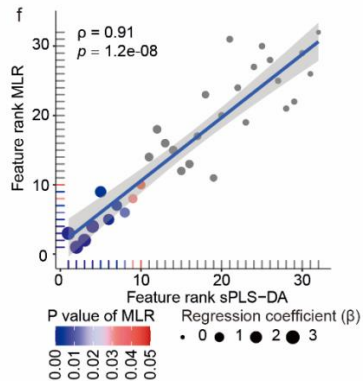
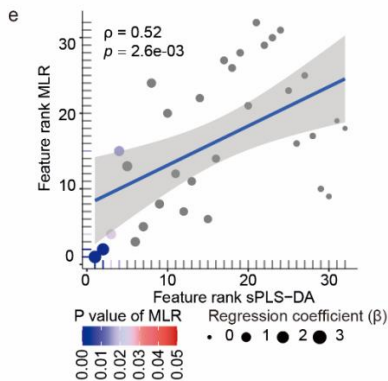
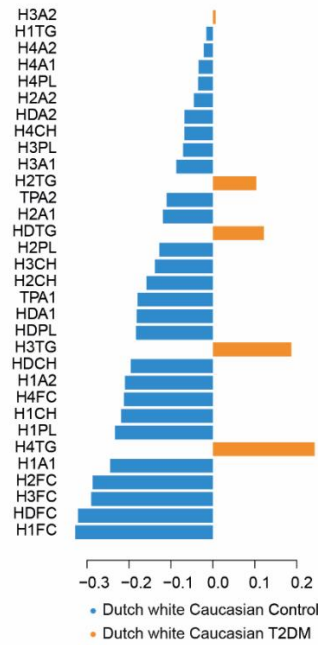


Figure S2. Sparse partial least squares discriminant analysis (sPLS-DA) differentiates patients with T2DM from healthy controls and T2DM in two ethnicities. sPLS-DA performed on HDL-related features separates patients with T2DM from healthy controls in (a) Dutch South Asians and (b) Dutch white Caucasians. Loading values of features in (c) Dutch South Asians and (d) Dutch white Caucasians with the contribution to differentiating T2DM from healthy control using sPLS-DA. Spearman's correlation between the rank generated from multinomial logistic regression (MLR) and sPLS-DA in (e) Dutch South Asians and (f) Dutch white Caucasians. Dot color represents the p-value of MLR, and dot size represents the absolute value of regression coefficient.

Abbreviations of lipoprotein main fractions and subfractions are shown in Supplemental Table S1.

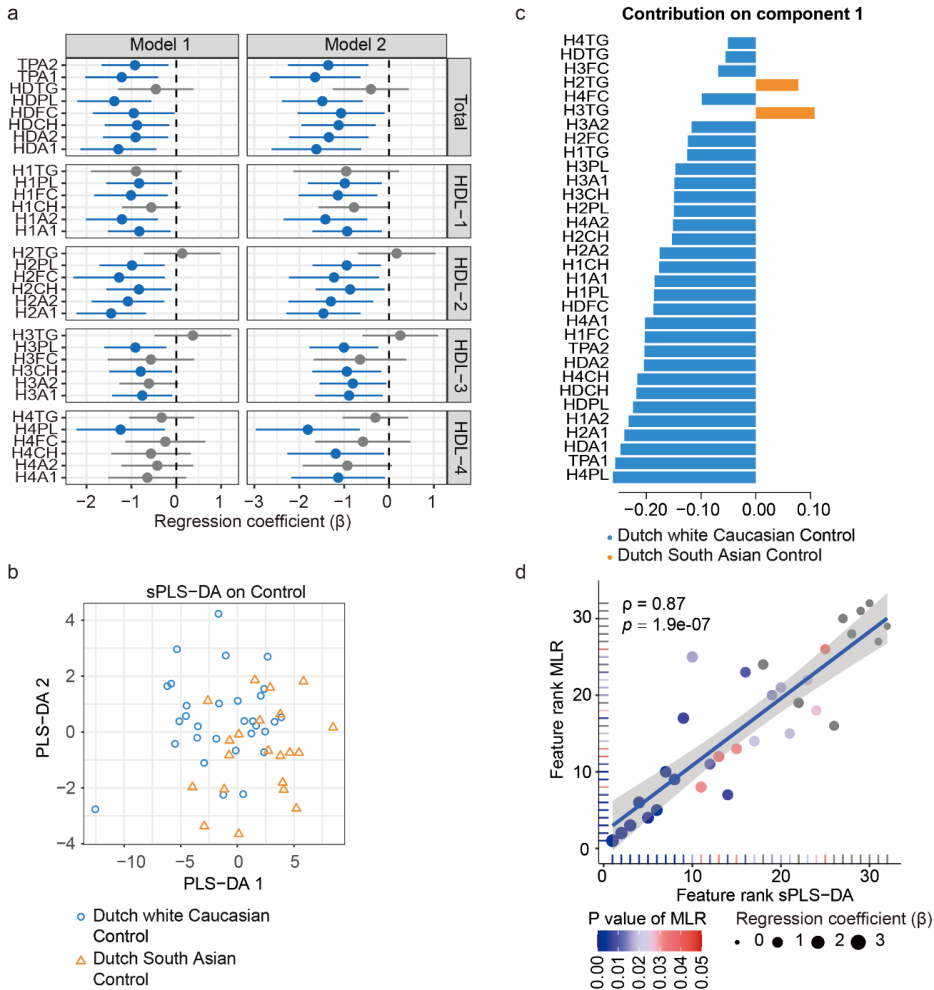


Figure S3. Different HDL composition between health individuals of Dutch South Asian and Dutch white Caucasian. (a) Forest plot of differential lipoprotein subfractions between health individuals of Dutch South Asian and Dutch white Caucasian. Regression coefficients and 95% confidence intervals are depicted by horizontal lines with dots. Non-significant associations are represented in grey, and substantial negative associations are represented in blue. (b) sPLS-DA performed on HDL-related features separates healthy individuals of Dutch South Asians from those of Dutch white Caucasians. (c) Loading values of features with the contribution to differentiating healthy individuals of Dutch South Asians from those of Dutch white Caucasians using sPLS-DA. (d) Spearman's correlation between the rank generated from multinomial logistic regression (MLR) and sPLS-DA. Dot colors represent p-values of MLR, and dot sizes represent the absolute values of regression coefficients.

Abbreviations: *A1*: apolipoprotein A1; *A2*: apolipoprotein A2; *CH*: cholesterol; *FC*: free cholesterol; *PL*: phospholipid; *TG*: triglyceride. Abbreviations of lipoprotein main fractions and subfractions are shown in Supplemental Table S1.

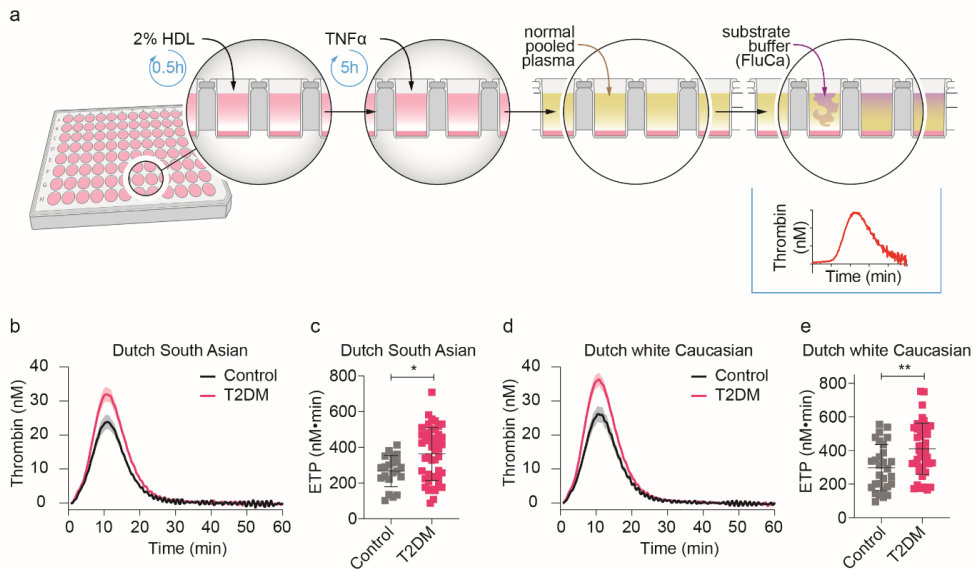


Figure S4. Impaired HDL anti-thrombotic capacity in T2DM in both ethnicities. (a) Scheme of HDL anti-thrombotic capacity assay. (b) Anti-thrombotic capacity between healthy and diabetic individuals in Dutch South Asian visualized by thrombin generation curve. (c) Difference of endogenous thrombin potential (ETP) between T2DM and control in Dutch South Asians. (d) Anti-thrombotic capacity measurement between healthy and diabetic individuals in Dutch white Caucasian visualized by thrombin generation curve. (e) Difference of ETP between T2DM and control in Dutch white Caucasians. Graphs represent means \pm SEM for the thrombin generation curve and means \pm SD for the dot plots. Non-paired two-tailed Mann-Whitney-Wilcoxon tests were performed; * $p < 0.05$, ** $p < 0.01$.

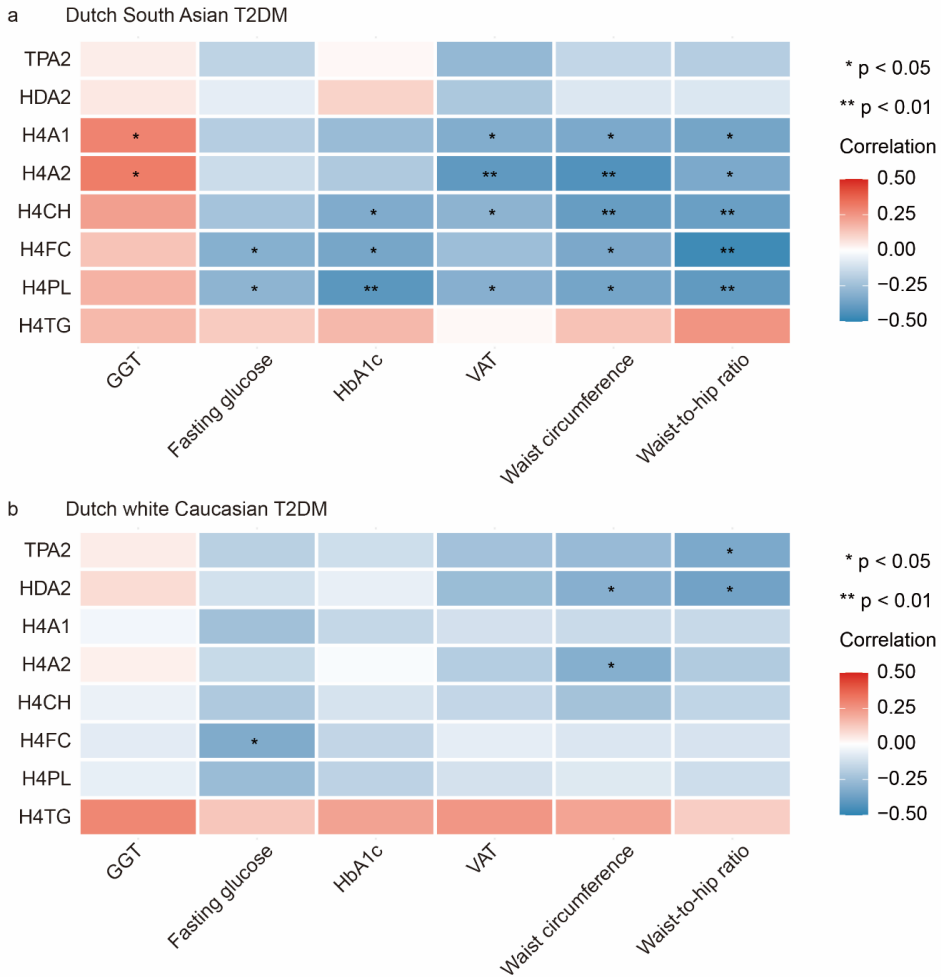


Figure S5. Correlation between differential HDL composition and clinical outcomes. Pearson’s Correlation between the levels of VAT, waist circumference, waist-to-hip ratio, glucose, HbA1c, and GGT with differential HDL composition in (a) Dutch South Asians and (b) Dutch white Caucasians. Pearson’s correlation analysis was performed. The color of scale bar represented Pearson’s correlation R. *p<0.05; **p<0.01.

Abbreviations: *GGT*: gamma-glutamyl transferase; *HbA1c*: hemoglobin A1c; *VAT*: visceral adipose tissue. Abbreviations of lipoprotein main fractions and subfractions are shown in Supplemental Table S1.

Table S1: Quantified HDL lipoprotein main fractions and subfractions.

Abbreviation	Lipoprotein subfraction
TPA1	Total apolipoprotein A1 (ApoA1)
TPA2	Total apolipoprotein A2 (ApoA2)
HDA1	ApoA1 content in total HDL
HDA2	ApoA2 content in total HDL
HDCH	Cholesterol content in total HDL
HDFC	Free Cholesterol content in total HDL
HDPL	Phospholipid content in total HDL
HDTG	Triglyceride content in total HDL
H1A1	ApoA1 content in HDL-1 subclass
H1A2	ApoA2 content in HDL-1 subclass
H1CH	Cholesterol content in HDL-1 subclass
H1FC	Free Cholesterol content HDL-1 subclass
H1PL	Phospholipid content in HDL-1 subclass
H1TG	Triglyceride content in HDL-1 subclass
H2A1	ApoA1 content in HDL-2 subclass
H2A2	ApoA2 content in HDL-2 subclass
H2CH	Cholesterol content in HDL-2 subclass
H2FC	Free Cholesterol content HDL-2 subclass
H2PL	Phospholipid content in HDL-2 subclass
H2TG	Triglyceride content in HDL-2 subclass
H3A1	ApoA1 content in HDL-3 subclass
H3A2	ApoA2 content in HDL-3 subclass
H3CH	Cholesterol content in HDL-3 subclass
H3FC	Free Cholesterol content HDL-3 subclass
H3PL	Phospholipid content in HDL-3 subclass
H3TG	Triglyceride content in HDL-3 subclass

H4A1	ApoA1 content in HDL-4 subclass
H4A2	ApoA2 content in HDL-4 subclass
H4CH	Cholesterol content in HDL-4 subclass
H4FC	Free Cholesterol content HDL-4 subclass
H4PL	Phospholipid content in HDL-4 subclass
H4TG	Triglyceride content in HDL-4 subclass

Table S2. Differential HDL composition between DSA-T2DM and DSA-C based on multinomial logistic regression analysis. (Reference: healthy controls DSA-C)

Model 1: adjusted for age, gender, current smoking status							Model 2: Model 1 + BMI								
HDL composition	Regression coefficient (β)			Odds ratio (OR)			P-value	HDL composition	Regression coefficient (β)			Odds ratio (OR)			P-value
	β	CI2.5	CI97.5	OR	CI2.5	CI97.5			β	CI2.5	CI97.5	OR	CI2.5	CI97.5	
HDCH	-0.70	-1.41	0.01	0.50	0.25	1.01	5.35E-02	HDCH	-0.03	-0.88	0.83	0.97	0.41	2.29	9.52E-01
TPA1	-0.36	-1.04	0.33	0.70	0.35	1.40	3.11E-01	TPA1	0.38	-0.58	1.35	1.47	0.56	3.85	4.36E-01
TPA2	-0.69	-1.36	-0.02	0.50	0.26	0.98	4.33E-02	TPA2	-0.08	-0.96	0.80	0.92	0.38	2.22	8.52E-01
HDTG	1.00	0.25	1.75	2.72	1.28	5.76	9.19E-03	HDTG	0.67	-0.21	1.55	1.96	0.81	4.72	1.36E-01
HDFC	-1.45	-2.29	-0.62	0.23	0.10	0.54	6.63E-04	HDFC	-1.18	-2.20	-0.15	0.31	0.11	0.86	2.44E-02
HDPL	-0.28	-0.99	0.42	0.75	0.37	1.53	4.32E-01	HDPL	0.19	-0.69	1.07	1.21	0.50	2.92	6.66E-01
HDA1	-0.49	-1.19	0.21	0.61	0.31	1.23	1.67E-01	HDA1	0.20	-0.75	1.14	1.22	0.47	3.13	6.84E-01
HDA2	-0.41	-1.05	0.22	0.66	0.35	1.25	2.02E-01	HDA2	0.17	-0.69	1.03	1.19	0.50	2.81	6.99E-01
H1TG	1.21	0.23	2.18	3.34	1.26	8.83	1.49E-02	H1TG	1.14	-0.06	2.35	3.14	0.94	10.44	6.25E-02
H2TG	0.97	0.27	1.67	2.63	1.31	5.29	6.72E-03	H2TG	0.60	-0.23	1.44	1.83	0.80	4.20	1.55E-01
H3TG	0.85	0.19	1.51	2.34	1.21	4.51	1.12E-02	H3TG	0.52	-0.27	1.32	1.69	0.76	3.74	1.97E-01
H4TG	0.45	-0.19	1.09	1.57	0.83	2.97	1.66E-01	H4TG	0.21	-0.60	1.02	1.23	0.55	2.76	6.11E-01
H1CH	0.00	-0.62	0.63	1.00	0.54	1.88	9.92E-01	H1CH	0.39	-0.45	1.22	1.47	0.64	3.40	3.67E-01
H2CH	0.11	-0.55	0.78	1.12	0.57	2.18	7.39E-01	H2CH	0.34	-0.47	1.14	1.40	0.62	3.14	4.14E-01
H3CH	-0.31	-0.94	0.31	0.73	0.39	1.37	3.28E-01	H3CH	0.04	-0.75	0.82	1.04	0.47	2.27	9.25E-01
H4CH	-1.25	-2.09	-0.42	0.29	0.12	0.66	3.39E-03	H4CH	-0.57	-1.62	0.49	0.57	0.20	1.63	2.92E-01
H1FC	-1.26	-2.07	-0.46	0.28	0.13	0.63	2.14E-03	H1FC	-0.82	-1.79	0.16	0.44	0.17	1.17	1.00E-01
H2FC	-1.07	-1.83	-0.30	0.34	0.16	0.74	6.30E-03	H2FC	-0.87	-1.84	0.10	0.42	0.16	1.10	7.84E-02
H3FC	-1.98	-2.93	-1.04	0.14	0.05	0.35	3.76E-05	H3FC	-2.32	-3.72	-0.92	0.10	0.02	0.40	1.13E-03
H4FC	-2.06	-3.00	-1.12	0.13	0.05	0.33	1.69E-05	H4FC	-2.12	-3.38	-0.85	0.12	0.03	0.43	1.08E-03
H1PL	0.12	-0.57	0.82	1.13	0.56	2.26	7.31E-01	H1PL	0.44	-0.44	1.32	1.55	0.64	3.73	3.31E-01
H2PL	0.50	-0.14	1.14	1.65	0.87	3.14	1.24E-01	H2PL	0.57	-0.19	1.34	1.78	0.83	3.81	1.41E-01
H3PL	0.13	-0.45	0.71	1.14	0.64	2.03	6.69E-01	H3PL	0.35	-0.40	1.10	1.42	0.67	3.01	3.63E-01
H4PL	-0.76	-1.59	0.07	0.47	0.20	1.07	7.20E-02	H4PL	-0.15	-1.12	0.81	0.86	0.33	2.26	7.57E-01
H1A1	0.01	-0.64	0.67	1.01	0.53	1.95	9.70E-01	H1A1	0.25	-0.60	1.11	1.29	0.55	3.03	5.64E-01
H2A1	0.47	-0.18	1.12	1.60	0.84	3.06	1.54E-01	H2A1	0.72	-0.06	1.49	2.05	0.94	4.45	7.13E-02
H3A1	0.20	-0.39	0.79	1.22	0.68	2.21	5.04E-01	H3A1	0.34	-0.40	1.09	1.41	0.67	2.98	3.66E-01
H4A1	-1.07	-1.90	-0.24	0.34	0.15	0.79	1.17E-02	H4A1	-0.63	-1.71	0.45	0.53	0.18	1.57	2.52E-01
H1A2	0.50	-0.24	1.25	1.66	0.79	3.48	1.84E-01	H1A2	0.86	-0.09	1.81	2.35	0.91	6.08	7.70E-02
H2A2	0.98	0.21	1.76	2.67	1.23	5.79	1.26E-02	H2A2	1.17	0.22	2.11	3.21	1.24	8.28	1.59E-02
H3A2	0.28	-0.31	0.87	1.32	0.73	2.38	3.58E-01	H3A2	0.45	-0.29	1.19	1.57	0.75	3.30	2.30E-01
H4A2	-1.41	-2.24	-0.59	0.24	0.11	0.56	8.18E-04	H4A2	-0.95	-2.05	0.16	0.39	0.13	1.17	9.25E-02

Table S3. Differential HDL composition between DwC-T2DM and DwC-C based on multinomial logistic regression analysis. (Reference: DwC-C)

Model 1: adjusted for age, gender, current smoking status							Model 2: Model 1 + BMI								
HDL composition	Regression coefficient (β)			Odds ratio (OR)			P-value	HDL composition	Regression coefficient (β)			Odds ratio (OR)			P-value
	β	CI2.5	CI97.5	OR	CI2.5	CI97.5			β	CI2.5	CI97.5	OR	CI2.5	CI97.5	
HDCH	-0.99	-1.59	-0.38	0.37	0.20	0.68	1.40E-03	HDCH	-0.37	-1.11	0.37	0.69	0.33	1.45	3.29E-01
TPA1	-0.97	-1.60	-0.33	0.38	0.20	0.72	3.03E-03	TPA1	-0.63	-1.38	0.12	0.53	0.25	1.12	9.76E-02
TPA2	-0.44	-0.97	0.09	0.65	0.38	1.10	1.07E-01	TPA2	-0.14	-0.87	0.58	0.87	0.42	1.79	7.01E-01
HDTG	0.60	0.00	1.20	1.82	1.00	3.31	4.90E-02	HDTG	0.18	-0.58	0.94	1.20	0.56	2.57	6.43E-01
HDFC	-2.72	-3.70	-1.74	0.07	0.02	0.18	5.86E-08	HDFC	-2.57	-3.75	-1.39	0.08	0.02	0.25	1.91E-05
HDPL	-1.05	-1.68	-0.42	0.35	0.19	0.66	1.14E-03	HDPL	-0.58	-1.39	0.22	0.56	0.25	1.25	1.56E-01
HDA1	-1.06	-1.74	-0.38	0.35	0.18	0.68	2.12E-03	HDA1	-0.68	-1.47	0.10	0.50	0.23	1.10	8.72E-02
HDA2	-0.21	-0.71	0.29	0.81	0.49	1.33	4.06E-01	HDA2	0.07	-0.65	0.79	1.07	0.52	2.20	8.52E-01
H1TG	-0.06	-0.62	0.50	0.95	0.54	1.66	8.44E-01	H1TG	-0.23	-0.97	0.51	0.79	0.38	1.67	5.42E-01
H2TG	0.73	0.02	1.44	2.07	1.02	4.20	4.29E-02	H2TG	0.14	-0.77	1.04	1.15	0.46	2.84	7.70E-01
H3TG	1.23	0.47	1.99	3.42	1.60	7.31	1.47E-03	H3TG	0.59	-0.30	1.48	1.80	0.74	4.41	1.95E-01
H4TG	1.48	0.78	2.17	4.39	2.19	8.79	3.11E-05	H4TG	1.17	0.25	2.09	3.21	1.28	8.08	1.31E-02
H1CH	-1.19	-1.84	-0.54	0.30	0.16	0.58	3.10E-04	H1CH	-0.85	-1.63	-0.08	0.43	0.20	0.92	3.09E-02
H2CH	-0.81	-1.39	-0.24	0.44	0.25	0.79	5.70E-03	H2CH	-0.64	-1.42	0.14	0.53	0.24	1.15	1.06E-01
H3CH	-0.67	-1.22	-0.13	0.51	0.30	0.88	1.59E-02	H3CH	-0.43	-1.13	0.28	0.65	0.32	1.32	2.33E-01
H4CH	-0.37	-0.99	0.25	0.69	0.37	1.28	2.42E-01	H4CH	-0.14	-0.97	0.69	0.87	0.38	1.99	7.35E-01
H1FC	-2.91	-3.94	-1.89	0.05	0.02	0.15	2.70E-08	H1FC	-2.60	-3.81	-1.40	0.07	0.02	0.25	2.38E-05
H2FC	-2.63	-3.64	-1.62	0.07	0.03	0.20	3.31E-07	H2FC	-2.45	-3.61	-1.28	0.09	0.03	0.28	3.81E-05
H3FC	-2.35	-3.31	-1.39	0.10	0.04	0.25	1.56E-06	H3FC	-2.73	-4.13	-1.32	0.07	0.02	0.27	1.45E-04
H4FC	-1.44	-2.23	-0.66	0.24	0.11	0.52	3.21E-04	H4FC	-1.72	-2.84	-0.59	0.18	0.06	0.55	2.81E-03
H1PL	-1.52	-2.24	-0.80	0.22	0.11	0.45	3.34E-05	H1PL	-1.33	-2.24	-0.43	0.26	0.11	0.65	3.95E-03
H2PL	-0.69	-1.26	-0.12	0.50	0.28	0.89	1.82E-02	H2PL	-0.65	-1.42	0.12	0.52	0.24	1.12	9.67E-02
H3PL	-0.35	-0.89	0.19	0.70	0.41	1.21	2.01E-01	H3PL	-0.23	-0.95	0.49	0.80	0.39	1.64	5.38E-01
H4PL	-0.20	-0.85	0.45	0.82	0.43	1.56	5.42E-01	H4PL	-0.16	-1.08	0.75	0.85	0.34	2.13	7.30E-01
H1A1	-1.69	-2.44	-0.95	0.18	0.09	0.39	8.99E-06	H1A1	-1.63	-2.59	-0.67	0.20	0.07	0.51	8.73E-04
H2A1	-0.58	-1.15	-0.01	0.56	0.32	0.99	4.43E-02	H2A1	-0.24	-0.98	0.51	0.79	0.37	1.66	5.29E-01
H3A1	-0.34	-0.86	0.17	0.71	0.43	1.18	1.89E-01	H3A1	-0.37	-1.03	0.30	0.69	0.36	1.34	2.76E-01
H4A1	-0.14	-0.71	0.42	0.87	0.49	1.52	6.16E-01	H4A1	-0.13	-0.94	0.68	0.88	0.39	1.97	7.49E-01
H1A2	-1.00	-1.60	-0.40	0.37	0.20	0.67	1.09E-03	H1A2	-0.76	-1.49	-0.03	0.47	0.23	0.97	4.13E-02
H2A2	-0.13	-0.59	0.34	0.88	0.55	1.41	6.00E-01	H2A2	-0.18	-0.77	0.42	0.84	0.46	1.51	5.60E-01
H3A2	0.08	-0.39	0.56	1.09	0.68	1.75	7.30E-01	H3A2	0.02	-0.61	0.65	1.02	0.54	1.91	9.52E-01
H4A2	-0.07	-0.60	0.47	0.94	0.55	1.59	8.09E-01	H4A2	0.17	-0.69	1.03	1.19	0.50	2.79	6.98E-01

Table S4. Differential HDL composition between DSA-T2DM and DwC-T2DM based on multinomial logistic regression analysis. (Reference: DwC-T2DM)

Model 1: adjusted for age, gender, current smoking status					Model 2: Model 1 + BMI					Model 3: Model 2 + Diabetes duration				
HDL composition	Regression coefficient (β)			P-value	HDL composition	Regression coefficient (β)			P-value	HDL composition	Regression coefficient (β)			P-value
	β	CI2.5	CI97.5			β	CI2.5	CI97.5			β	CI2.5	CI97.5	
HDCH	-0.58	-1.18	0.01	5.37E-02	HDCH	-0.78	-1.44	-0.12	1.99E-02	HDCH	-0.41	-1.07	0.24	2.18E-01
TPA1	-0.61	-1.15	-0.06	2.88E-02	TPA1	-0.63	-1.20	-0.05	3.18E-02	TPA1	-0.36	-0.92	0.20	2.05E-01
TPA2	-1.17	-1.75	-0.60	6.77E-05	TPA2	-1.30	-1.96	-0.63	1.46E-04	TPA2	-0.93	-1.63	-0.23	9.07E-03
HDTG	-0.06	-0.46	0.35	7.84E-01	HDTG	0.09	-0.37	0.54	7.12E-01	HDTG	0.12	-0.38	0.63	6.35E-01
HDFC	0.32	-0.27	0.91	2.93E-01	HDFC	0.33	-0.33	0.98	3.29E-01	HDFC	0.37	-0.35	1.09	3.12E-01
HDPL	-0.61	-1.19	-0.03	3.80E-02	HDPL	-0.71	-1.37	-0.04	3.64E-02	HDPL	-0.44	-1.16	0.28	2.32E-01
HDA1	-0.72	-1.29	-0.15	1.31E-02	HDA1	-0.74	-1.34	-0.13	1.67E-02	HDA1	-0.42	-1.01	0.17	1.64E-01
HDA2	-1.11	-1.66	-0.56	8.19E-05	HDA2	-1.24	-1.89	-0.59	1.77E-04	HDA2	-0.91	-1.59	-0.23	8.36E-03
H1TG	0.37	-0.11	0.85	1.32E-01	H1TG	0.42	-0.10	0.94	1.13E-01	H1TG	0.45	-0.15	1.06	1.41E-01
H2TG	0.37	-0.10	0.83	1.19E-01	H2TG	0.64	0.06	1.22	3.17E-02	H2TG	0.63	-0.03	1.29	5.98E-02
H3TG	-0.01	-0.43	0.41	9.57E-01	H3TG	0.19	-0.30	0.67	4.59E-01	H3TG	0.18	-0.35	0.71	5.02E-01
H4TG	-1.36	-1.98	-0.73	2.03E-05	H4TG	-1.26	-1.93	-0.59	2.26E-04	H4TG	-1.34	-2.18	-0.50	1.76E-03
H1CH	0.64	0.03	1.25	4.06E-02	H1CH	0.46	-0.20	1.11	1.69E-01	H1CH	0.46	-0.26	1.17	2.09E-01
H2CH	0.09	-0.44	0.62	7.31E-01	H2CH	0.11	-0.52	0.74	7.24E-01	H2CH	0.30	-0.42	1.03	4.14E-01
H3CH	-0.44	-0.94	0.06	8.79E-02	H3CH	-0.47	-1.03	0.09	9.76E-02	H3CH	-0.31	-0.90	0.29	3.13E-01
H4CH	-1.45	-2.12	-0.77	2.59E-05	H4CH	-1.61	-2.38	-0.84	4.58E-05	H4CH	-1.13	-1.88	-0.38	3.13E-03
H1FC	0.64	-0.06	1.35	7.37E-02	H1FC	0.65	-0.16	1.46	1.15E-01	H1FC	0.58	-0.25	1.40	1.71E-01
H2FC	0.28	-0.26	0.83	3.09E-01	H2FC	0.35	-0.27	0.98	2.65E-01	H2FC	0.46	-0.26	1.18	2.10E-01
H3FC	-0.20	-0.72	0.32	4.46E-01	H3FC	-0.24	-0.79	0.31	3.96E-01	H3FC	-0.15	-0.79	0.48	6.38E-01
H4FC	-0.86	-1.45	-0.27	4.22E-03	H4FC	-0.98	-1.64	-0.32	3.83E-03	H4FC	-0.75	-1.43	-0.06	3.36E-02
H1PL	0.82	0.16	1.48	1.55E-02	H1PL	0.78	0.02	1.54	4.38E-02	H1PL	0.82	-0.05	1.70	6.48E-02
H2PL	0.21	-0.31	0.72	4.32E-01	H2PL	0.28	-0.32	0.89	3.57E-01	H2PL	0.42	-0.30	1.14	2.54E-01
H3PL	-0.43	-0.92	0.05	7.91E-02	H3PL	-0.43	-0.97	0.11	1.19E-01	H3PL	-0.36	-0.97	0.26	2.56E-01
H4PL	-1.80	-2.60	-1.00	9.58E-06	H4PL	-1.80	-2.68	-0.93	5.52E-05	H4PL	-1.22	-2.02	-0.42	2.92E-03
H1A1	0.88	0.20	1.56	1.09E-02	H1A1	0.95	0.16	1.74	1.78E-02	H1A1	1.12	0.21	2.04	1.60E-02
H2A1	-0.40	-0.93	0.13	1.37E-01	H2A1	-0.51	-1.12	0.10	1.04E-01	H2A1	-0.31	-0.98	0.36	3.60E-01
H3A1	-0.21	-0.69	0.26	3.75E-01	H3A1	-0.18	-0.68	0.33	4.93E-01	H3A1	-0.14	-0.68	0.39	5.99E-01
H4A1	-1.57	-2.25	-0.89	6.14E-06	H4A1	-1.63	-2.41	-0.85	4.10E-05	H4A1	-1.14	-1.90	-0.38	3.25E-03
H1A2	0.29	-0.28	0.86	3.19E-01	H1A2	0.20	-0.44	0.83	5.41E-01	H1A2	0.26	-0.43	0.95	4.61E-01
H2A2	0.03	-0.42	0.48	8.95E-01	H2A2	0.05	-0.43	0.52	8.45E-01	H2A2	0.02	-0.50	0.54	9.33E-01
H3A2	-0.42	-0.88	0.05	7.78E-02	H3A2	-0.37	-0.86	0.12	1.38E-01	H3A2	-0.31	-0.84	0.22	2.54E-01
H4A2	-1.77	-2.47	-1.07	8.22E-07	H4A2	-2.05	-2.93	-1.17	4.92E-06	H4A2	-1.78	-2.83	-0.73	9.27E-04

Table S5. Differential HDL composition between DSA-C and DwC-C based on multinomial logistic regression analysis. (Reference: DwC-C)

Model 1: adjusted for age, gender, current smoking status					Model 2: Model 1 + BMI				
HDL composition	Regression coefficient (β)			P-value	HDL composition	Regression coefficient (β)			P-value
	β	CI2.5	CI97.5			β	CI2.5	CI97.5	
HDCH	-0.87	-1.60	-0.15	1.77E-02	HDCH	-1.12	-1.95	-0.30	7.84E-03
TPA1	-1.22	-2.03	-0.40	3.42E-03	TPA1	-1.65	-2.66	-0.63	1.43E-03
TPA2	-0.92	-1.67	-0.17	1.57E-02	TPA2	-1.35	-2.25	-0.45	3.18E-03
HDTG	-0.45	-1.29	0.38	2.88E-01	HDTG	-0.40	-1.25	0.44	3.49E-01
HDFC	-0.95	-1.86	-0.03	4.19E-02	HDFC	-1.07	-2.04	-0.10	3.07E-02
HDPL	-1.38	-2.20	-0.56	9.91E-04	HDPL	-1.48	-2.39	-0.58	1.23E-03
HDA1	-1.29	-2.14	-0.44	2.90E-03	HDA1	-1.62	-2.62	-0.62	1.52E-03
HDA2	-0.91	-1.63	-0.18	1.44E-02	HDA2	-1.34	-2.23	-0.45	3.06E-03
H1TG	-0.90	-1.91	0.12	8.40E-02	H1TG	-0.95	-2.13	0.23	1.13E-01
H2TG	0.13	-0.72	0.98	7.62E-01	H2TG	0.17	-0.69	1.03	6.98E-01
H3TG	0.37	-0.48	1.22	3.95E-01	H3TG	0.25	-0.59	1.09	5.58E-01
H4TG	-0.33	-1.05	0.40	3.76E-01	H4TG	-0.30	-1.04	0.43	4.15E-01
H1CH	-0.56	-1.21	0.09	9.32E-02	H1CH	-0.78	-1.57	0.01	5.29E-02
H2CH	-0.83	-1.56	-0.10	2.53E-02	H2CH	-0.87	-1.63	-0.10	2.70E-02
H3CH	-0.79	-1.50	-0.09	2.67E-02	H3CH	-0.94	-1.71	-0.17	1.69E-02
H4CH	-0.57	-1.45	0.32	2.11E-01	H4CH	-1.19	-2.27	-0.11	3.08E-02
H1FC	-1.01	-1.83	-0.19	1.59E-02	H1FC	-1.14	-2.02	-0.26	1.10E-02
H2FC	-1.28	-2.29	-0.26	1.41E-02	H2FC	-1.23	-2.23	-0.22	1.65E-02
H3FC	-0.57	-1.53	0.40	2.50E-01	H3FC	-0.65	-1.68	0.39	2.21E-01
H4FC	-0.24	-1.14	0.65	5.91E-01	H4FC	-0.58	-1.64	0.48	2.84E-01
H1PL	-0.83	-1.56	-0.10	2.65E-02	H1PL	-0.98	-1.81	-0.16	1.92E-02
H2PL	-0.99	-1.71	-0.26	7.76E-03	H2PL	-0.94	-1.70	-0.18	1.52E-02
H3PL	-0.91	-1.60	-0.22	9.55E-03	H3PL	-1.00	-1.77	-0.24	1.03E-02
H4PL	-1.24	-2.23	-0.26	1.35E-02	H4PL	-1.81	-2.97	-0.65	2.23E-03
H1A1	-0.82	-1.52	-0.13	2.08E-02	H1A1	-0.93	-1.71	-0.16	1.85E-02
H2A1	-1.45	-2.23	-0.67	2.54E-04	H2A1	-1.46	-2.29	-0.63	5.63E-04
H3A1	-0.76	-1.43	-0.09	2.72E-02	H3A1	-0.89	-1.64	-0.14	2.07E-02
H4A1	-0.65	-1.52	0.22	1.46E-01	H4A1	-1.13	-2.18	-0.09	3.38E-02
H1A2	-1.21	-2.01	-0.41	3.12E-03	H1A2	-1.42	-2.35	-0.48	2.94E-03
H2A2	-1.08	-1.89	-0.27	9.32E-03	H2A2	-1.30	-2.24	-0.35	7.31E-03
H3A2	-0.61	-1.27	0.04	6.78E-02	H3A2	-0.81	-1.55	-0.06	3.34E-02
H4A2	-0.42	-1.22	0.38	3.01E-01	H4A2	-0.93	-1.92	0.07	6.78E-02

CHAPTER

4

Diacylglycerol abnormalities in diabetic nephropathy in Dutch South Asians and Dutch white Caucasians with type 2 diabetes mellitus: lipidomic phenotyping of plasma in a cross-sectional study

Lushun Yuan^{1,2}, Niek Blomberg³, Aswin Verhoeven³, Huub J. van Eyk⁴, Maurice B. Bizino⁵, Patrick C.N. Rensen^{1,4}, Ingrid M. Jazet⁴, Hildo J. Lamb⁵, Ton. J Rabelink^{1,2}, Martin Giera³, Bernard M. van den Berg^{1,2}

¹ Eindhoven Laboratory for Vascular and Regenerative Medicine, Leiden University Medical Center, Leiden, the Netherlands.

² Department of Internal Medicine, Division of Nephrology, Leiden University Medical Center, Leiden, the Netherlands.

³ Center for Proteomics and Metabolomics, Leiden University Medical Center, Leiden, the Netherlands.

⁴ Department of Internal Medicine, Division of Endocrinology, Leiden University Medical Center, Leiden, the Netherlands.

⁵ Department of Radiology, Leiden University Medical Center, Leiden, the Netherlands.

Abstract

Objective: Type 2 diabetes mellitus (T2DM) confers a higher risk for complications in South Asian individuals as compared to other ethnic groups. It has been hypothesized that altered lipid metabolism may at least partly mediate this risk. Here we investigate lipidomic changes between Dutch South Asians (DSA) and Dutch white Caucasians (DwC) with and without T2DM and their association with clinical features.

Methods: Plasma samples were measured using the targeted quantitative LC/MS-based Shotgun Lipidomics Assistant (SLA) platform in a cross-sectional study, including 51 healthy participants (21 DSA, 30 DwC) and 92 participants with T2DM (47 DSA, 45 DwC), resulting in a comprehensive mapping of the circulating lipidome. Unbiased weighted correlation network analysis was used to identify clinically relevant lipid modules (lipid clusters associated with disease) and key mediatory lipids.

Results: In both the DSA and DwC populations, differences in lipidomic profiles (lipid classes and lipid species) between T2DM patients and healthy controls were found. DSA-T2DM lipid changes correlated to clinical features, particularly diacylglycerols (DGs), and associated with glycemic control and renal function. Furthermore, when compared to DwC controls, DSA controls already had a diabetes-prone lipid profile in their circulation at baseline.

Conclusions: This study demonstrates ethnic disparities in the circulating lipidomic profiles of T2DM patients and healthy controls. Our results revealed an ethnic distinction of lipid modules in relation to clinical outcomes. Additionally, we have identified specific diacylglycerols, particularly DG 18:1_18:2, as potential biomarkers for glycemic control and renal function in DSA-T2DM.

Keywords: Lipidomics, Dutch South Asian, Dutch white Caucasian, type 2 diabetes mellitus, diabetic nephropathy

Introduction

One of the major challenges to public health in the twenty-first century is the worldwide rise in type 2 diabetes mellitus (T2DM) prevalence. T2DM is characterized by insulin resistance and insufficient compensatory insulin secretion, the mechanism of which varies by ethnicity¹. South Asians (SAs), as one of the high-risk populations, have a higher T2DM incidence than other ethnic groups². As a result the South Asian (SA) population with T2DM tend to develop the disease at an earlier age, around 5-10 years ahead, and often with a lower body mass index (BMI), compared to white Caucasians (wC), thus revealing a distinct disease phenotype². SAs possess a distinct body composition characterized by a higher prevalence of abdominal obesity and a larger proportion of visceral fat³. This unique phenotype contributes to the production and secretion of specific inflammatory cytokines, which can result in an elevated chronic low-grade inflammatory state and increasing the risk of developing T2DM among this population^{4,5}. Furthermore, SA patients with T2DM were found to be more prone to develop microvascular complications such as diabetic nephropathy (DN), as well as progressing to end-stage renal disease at a faster rate than Caucasian European patients with T2DM^{6,7}.

While emerging lipidomic approaches generally revealed specific molecular lipid changes leading to T2DM (6-8), most of these studies were only performed in single ethnicity lacking differential information on T2DM development between different ethnic groups. Of note, a number of epidemiological studies highlighted the role of dyslipidemia in relation to the incidence of T2DM^{8,9}, hinting that development of dyslipidemia may be a sign of future T2DM. Additionally, several studies found that dyslipidemia was associated with an increased risk of diabetes-related microvascular complications such as nephropathy, neuropathy, and retinopathy¹⁰⁻¹². Given that dyslipidemia patterns differ by race/ethnicity¹³ and may influence disease outcome¹⁴, it suggests that lipid metabolism may play a vital role in ethnic differences in risk and progression of T2DM. In the present study, we measured lipidomic phenotypes in Dutch South Asian (DSA) and Dutch white Caucasian (DwC) participants, with or without T2DM, using the differential mobility mass

spectrometry (DMS/MS)-based Shotgun Lipidomics Assistant (SLA) platform¹⁵. Based on this platform, we sought to investigate differences in lipid class and lipid species correlating with disease risk and progression between these two ethnic groups.

Material and methods

Study population

For the present cross-sectional study, baseline samples were used from the MAGNetic resonance Assessment of VICTOza efficacy in the Regression of cardiovascular dysfunction in type 2 dIAbetes mellitus (MAGNA VICTORIA) study from two previous randomized controlled trials (RCT, ClinicalTrials.gov [NCT01761318]¹⁶ and [NCT02660047]¹⁷, respectively), together with age and gender matched healthy controls from both ethnic groups¹⁸. The details of both trials can be found elsewhere^{16, 17}. Both trials had the following inclusion criteria: BMI \geq 23, age between 18 and 74 years, and HbA1c levels between 6.5% and 11.0% (\geq 47.5 and \leq 96.4 mmol/mol). Patients were allowed to take specific glucose-lowering medication (metformin, sulfonylurea derivatives, or insulin) at a stable dosage for at least 3 months prior to participating in the study. They could also use antihypertensives and statins. Exclusion criteria included the use of glucose-lowering medication other than those specified, renal disease, congestive heart failure (NYHA class III-IV), uncontrolled hypertension (systolic blood pressure $>$ 180 mm Hg and/or diastolic blood pressure $>$ 110 mm Hg), or recent acute coronary or cerebrovascular events within 30 days before study enrolment. We excluded samples with missing plasma, diagnosed with T1DM, and individuals who withdraw from the randomized clinical trial. In total, 47 DSA with T2DM (DSA-T2DM, age 54.9 [SD: 10.1] years, 59.6% women, BMI: 29.5 [4.0] kg/m²), 21 DSA healthy individuals (DSA-C, age 48.3 [SD: 8.1] years, 71.4% women, BMI: 23.5 [3.0] kg/m²), 45 DwC with T2DM (DwC-T2DM, age 59.0 [SD: 6.5] years, 44.4% women, BMI: 32.3 [3.9] kg/m²), and 30 DwC healthy individuals (DwC-C, age 57.9 [SD: 7.9] years, 46.7% women,

BMI: 24.3 [3.3] kg/m²) were included. Ethnicity was based on the self-identified and self-reported biological parents' and ancestors' origins. Participants with complete informed consent were included. The study was conducted in accordance with the revised Helsinki Declaration, and the Institutional Review Board granted ethical approval (Leiden University Medical Center, Leiden, the Netherlands).

Lipidomics profiling using the SLA platform

Plasma samples were prepared according to Ghorasaini *et al*¹⁹, and analyzed on the SLA platform (Figure 1). The SLA consists of a SCIEX QTRAP 5500 mass spectrometer with a SelexION differential mobility spectroscopy (DMS) interface and a Nexera X2 ultrahigh-performance liquid chromatography system that is controlled by the SLA software. Detailed protocols on its operation can be found elsewhere^{15, 19}.

Statistical analyses

For the SLA data pre-processing we first calculated the missing values per lipid class for all individuals per group (DSA-T2DM, DSA-C, DwC-T2DM, and DwC-C). Per lipid class, specific lipids with more than 30% missing values in each group were excluded. Missing values were imputed with half of the minimum concentration per lipid class (Figure S1 and Table S2).

Next, to determine the relative abundance of each lipid class, we performed a calculation by normalizing the concentration of each lipid class. This involved summing up the concentrations of all lipid species within each class and dividing it by the total concentration across all lipid classes. By applying this normalization process, a more accurate understanding of how each lipid class contributes to the overall lipid composition is obtained and allows to clearly assess the proportional representation of different lipid classes. Subsequently, principle component analysis (PCA) and hierarchical cluster analysis

(HCA) were performed in all participants in both ethnicities based on relative lipid class abundance. Differences in relative lipid class abundance between healthy controls and T2DM, as well as between healthy individuals and T2DM from two ethnic groups were examined.

Multinomial logistic regression analysis (MLR) was used to differentiate the various specific lipids. The four groups were considered as outcomes (DSA-T2DM, DSA-C, DwC-T2DM, and DwC-C). The lipid concentrations were scaled (z-score normalization). When comparing DSA-T2DM to DSA-C, we used DSA-C as reference, and when comparing DwC-T2DM to DwC-C, we used DwC-C as reference. Age (continuous variable), sex (dichotomous variable), and current smoking status (dichotomous variable) were adjusted for the complete model. Multiple testing corrections were used, with a false discovery rate (FDR) of 0.05 considered significant. To assess the relationship between lipid concentrations and T2DM, the results were expressed as a regression coefficient (β) with a 95% confidence interval (CI).

For weighted correlation network analysis, the "WGCNA" R package was used to investigate the role of lipid species in association with observed clinical features²⁰. Using this algorithm, a proper soft threshold was first chosen and lipids with similar concentration patterns could be grouped into multiple modules, each of which was linked to a concomitant clinical feature. These modules were tagged with colour codes. This makes it possible to identify some clinically relevant lipids within potential lipid modules in relation to respective clinical features. Diabetes-related complications-associated lipid modules were considered key modules in this study. Key mediatory lipids that correspond to the clinical parameters were derived from key lipid modules and the differentiated lipids (between the various groups, Figure S4). Pearson's correlation analysis was used to determine the relationship between those key mediatory lipids and clinical parameters related to dyslipidaemia, kidney function, and glycemic control.

To validate our observations, we used a published external dataset of Chinese IgA nephropathy patients to investigate the relation between commonly changed lipids and

renal function ²¹. To this end, we first examined the changes in these lipids between healthy controls and IgA nephropathy patients. Next, the relationship between these lipids and kidney function parameters was determined using Pearson's correlation analysis.

For each ethnic group, the Wilcoxon signed-rank test was used to assess the statistical differences between cases (i.e., those with diabetes-related complications) and controls (i.e., those without diabetes-related complications). R (version 4.1.0) and GraphPad Prism version 8 (Graphpad Inc., La Jolla, CA, USA) were used for statistical analysis.

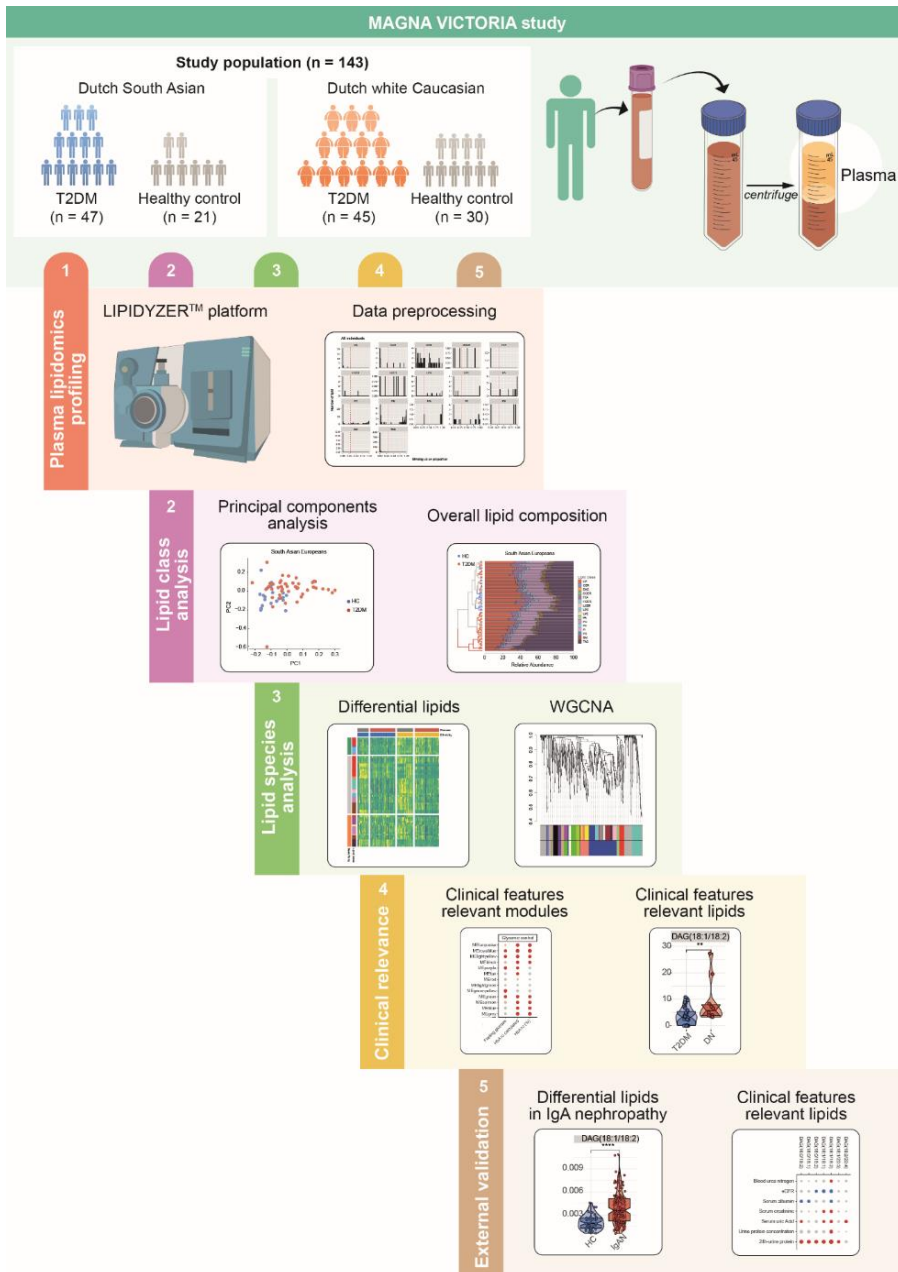


Fig. 1. Study workflow and design.

Abbreviations: *T2DM* type 2 diabetes mellitus; *WGCNA* Weighted Correlation Network Analysis

Results

Pre-processing of plasma lipidome profiles of individuals with T2DM vs. healthy participants

Targeted lipidomic analysis quantified lipids from 17 different lipid classes (Figure 1). After exclusion of lipids with 30% missing values, we distinguished 689, 686, 679, 699, and 668 lipids in DSA-T2DM, DSA-C, DwC-T2DM, and DwC-C, respectively (Figure S1), of which 654 common lipid species across lipid classes (CE, cholesteryl ester; CER [Cer d18:1/FA], ceramide; DG, diacylglyceride; DCER [Cer d18:0/FA], dihydroceramide; FA, fatty acid; HexCER, hydroxyceramide; LacCER, lactosylceramide; LPC, lysophosphatidylcholine; LPE, lysophosphatidylethanolamine; PA, phosphatidic acid; PC, phosphatidylcholine; PE, phosphatidylethanolamine; PI, phosphatidylinositol; PS, phosphatidylserine; SM, sphingomyelin; TG, triglyceride) were chosen for further analysis (Figure S1 and Table S2).

Healthy individuals of Dutch South Asian ethnicity reveal a pre-diabetes lipid class profile

We first applied PCA analysis to identify clusters of subjects based upon similarities in their relative abundance of lipid classes in both ethnic groups, regardless of their prespecified group. Although the distinction was not perfect, we observed that relative lipid class abundance had better power to distinguish patients with T2DM from healthy controls in DwC than in DSA (Figure S2A, B). Hierarchical cluster analysis revealed that in DSA, all subjects were clustered into two main subclusters, one with patients with T2DM only and the other with patients with T2DM and healthy individuals; whereas in DwC, most of the healthy subjects were clustered together and separated from patients with T2DM (Figure 2). Between DSA-T2DM and DSA-C, 10 lipid classes (9 lower and 1 higher), and between DwC-T2DM and DwC-C, 11 lipid classes (10 lower and 1 higher) were changed significantly (Figure S2C, D). When DSA-T2DM and DwC-T2DM were compared, the DG lipid class was found to be more abundant, with the greatest relative difference, in DSA with T2DM than

in DwC with T2DM (Figure S2E). Similarly, we also found that the abundance of DG lipid class was higher in DSA than DwC among healthy individuals (Figure S2F). These findings indicated that based on lipid class abundance, DSA-C already had a phenotype more closely related to DSA-T2DM; there were marginal differences in lipid class abundance between T2DM in the two ethnic groups.

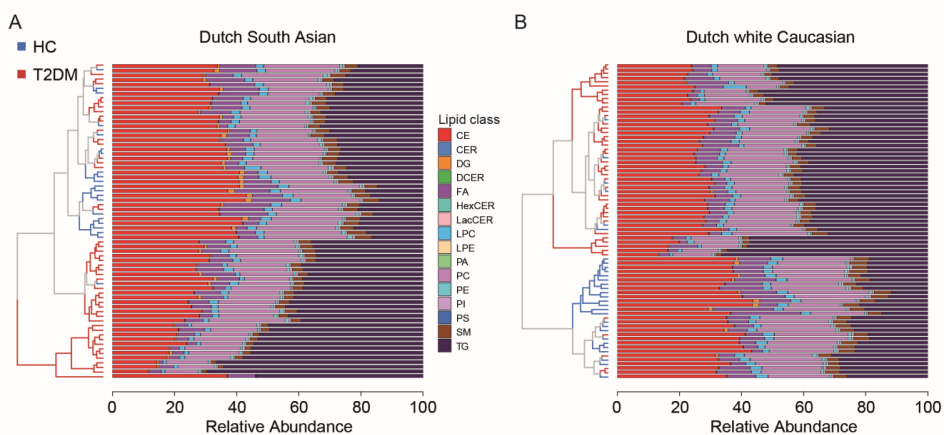


Fig. 2. Lipid class abundance between patients with T2DM and healthy controls. (A) Stack plot with the hierarchical cluster in Dutch South Asian. (B) Stack plot with the hierarchical cluster in Dutch white Caucasian.

Abbreviations: *CE* cholesteryl ester; *CER* ceramide; *DCER* dihydroceramide; *DG* diacylglyceride; *FA* fatty acid; *HC* healthy control; *HexCER* hydroxyceramide; *LacCER* lactosylceramide; *LPC* lysophosphatidylcholine; *LPE* lysophosphatidylethanolamine; *PA* phosphatidic acid; *PC* phosphatidylcholine; *PE* phosphatidylethanolamine; *PI* phosphatidylinositol; *PS* phosphatidylserine; *SM* sphingomyelin; *T2DM* type 2 diabetes mellitus; *TG* triglyceride.

Comparison of differential lipids between patients with T2DM and healthy controls in two ethnicities

After multinomial logistic regression analyses and multiple testing corrections, we found 436 differential lipids (396 higher and 40 lower) in DSA-T2DM compared to DSA-C (Figure 3A and Table S3); 519 differential lipids (471 higher and 48 lower) in DwC-T2DM compared to DwC-C (Figure 3A and Table S4). To further investigate the significance of each lipid change between two ethnicities, we compared the regression coefficients (T2DM vs healthy controls) and discovered that lipids from the DGs and TGs classes in DSA showed higher regression coefficients than those in DwC, while the CEs in DwC showed lower regression coefficients; the remaining lipids behaved similarly (Figure 3A).

We found 9 lipids that were specifically lower in DSA-T2DM (mostly from the CEs and LPCs) and 17 lipids that were specifically lower in DwC-T2DM (including lipids from the FAs, PCs, SMs, and TGs) (Figure 3B, D, and Table S5). Furthermore, 13 lipids were specifically higher in DSA-T2DM (primarily from the DGs, PEs, and TGs), while 88 lipids were specifically higher in DwC-T2DM (primarily from the CEs, DGs, PCs, PEs, and TGs) (Figure 3C, E and Table S5). These findings indicate that different lipid metabolism phenotypes were found in both ethnicities, and differential lipids, particularly DGs and TGs, contributed more to the risk of T2DM in DSA.

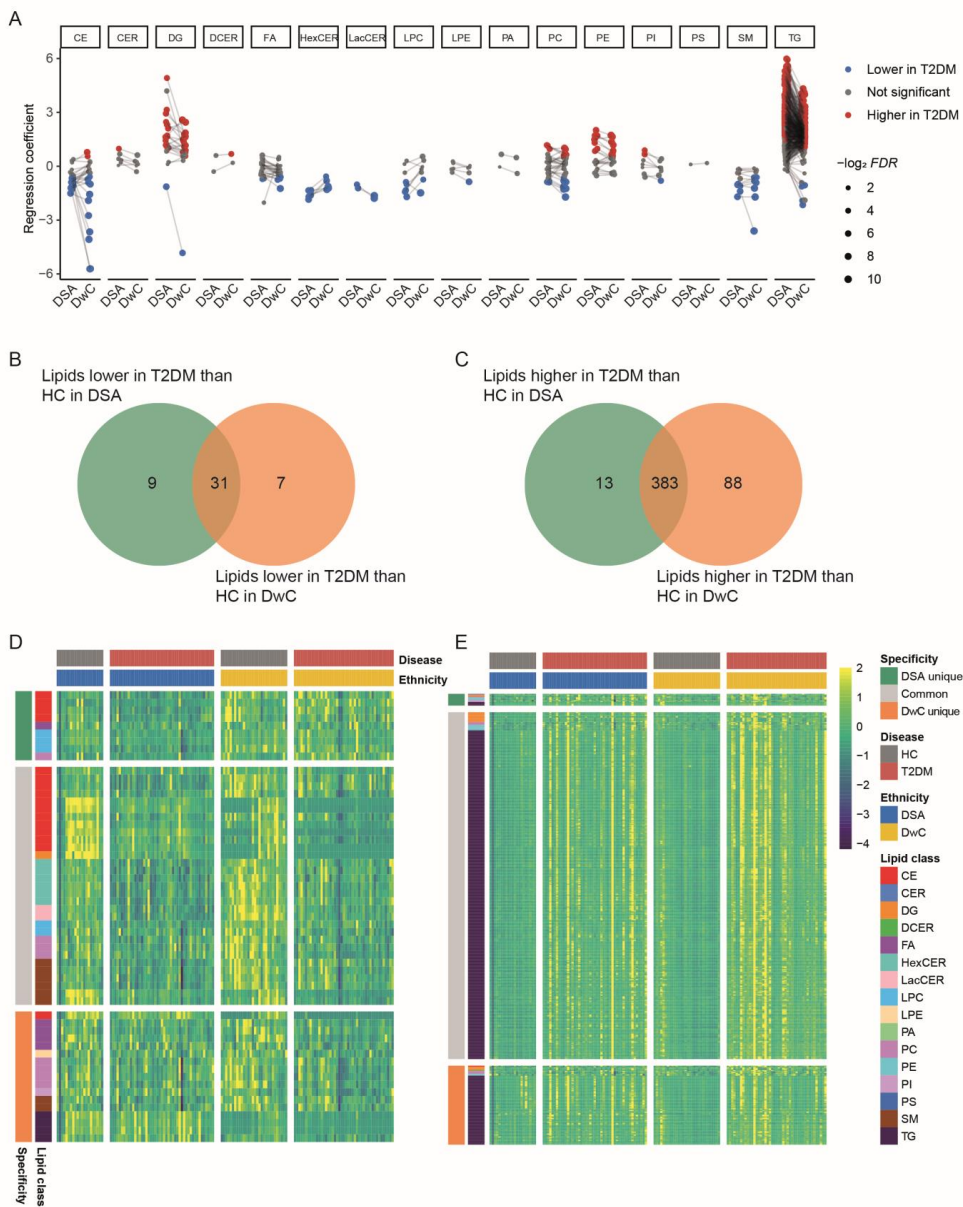


Fig. 3. Comparison of differential lipids between patients with T2DM and healthy controls in two ethnicities. (A) Differential lipids per lipid class between patients with T2DM and healthy controls, as well as a comparison across two ethnicities. The color grey represents

lipids with no significance ($FDR > 0.05$), the color blue represents lipids lower in T2DM, and the color red represents lipids higher in T2DM. The dot size represents $-\log_2 FDR$. Venn diagram of (B) lipids lower in T2DM and (C) higher in T2DM than healthy controls (HC) in DSA and DwC. Heatmap of lipids that are commonly/uncommonly (D) lower and (E) higher in DSA and DwC with T2DM.

Abbreviations: *CE* cholesteryl ester; *CER* ceramide; *DCER* dihydroceramide; *DG* diacylglyceride; *DwC* Dutch white Caucasian; *DSA* Dutch South Asian; *FA* fatty acid; *FDR* false discovery rate; *HexCER* hydroxyceramide; *LacCER* lactosylceramide; *LPC* lysophosphatidylcholine; *LPE* lysophosphatidylethanolamine; *PA* phosphatidic acid; *PC* phosphatidylcholine; *PE* phosphatidylethanolamine; *PI* phosphatidylinositol; *PS* phosphatidylserine; *SM* sphingomyelin; *TG* triglyceride.

Ethnic distinction in associations of lipid correlation network modules with clinical features

To identify highly connected lipid modules and the relevance between baseline clinical traits and each lipid module, we performed a weighted correlation network analysis (WGCNA, Figure S3). Except for the grey module, which corresponded to the set of lipids that were not clustered in any module, the other lipids in both ethnicities were clustered into 12 modules.

Total TG concentration measured on the SLA platform matched the clinical routine measurements. In both ethnic groups, we did observe lipid modules consisting of TG species that had a positive correlation with total TG concentration (Figure 4). Surprisingly, there were noticeable differences between the two ethnic groups. In DSA-T2DM, the lipid modules were positively correlated with glycemic control parameters, and negatively correlated with HDL-cholesterol (Figure 4A). While in DwC-T2DM, the lipid modules showed positive correlations with anthropometric parameters, total cholesterol, and LDL-cholesterol and negative correlations with blood pressure and kidney function (Figure 4B). We also found several modules associated with diabetes-related complications. In DSA-T2DM, the 'royal blue' module, as only module, was correlated with diabetic nephropathy

(DN); whereas in DwC-T2DM, the 'light green', 'black', and 'grey60' modules were associated with diabetic retinopathy (DR) and DN, respectively (Figure 4).

By combining lipids in diabetes-related-complications modules with differential lipids, we identified 7 lipids from the DG class (two lipids showed ethnicity-specific difference) in DSA and 5 lipids from the CEs, TGs, and DG classes in DwC (Figure S4), which we considered as key mediatory lipids. Our findings revealed ethnic differences in the associations between lipid modules and clinical features, particularly in DSA-T2DM, where lipid modules were correlated with high TGs, low HDL-cholesterol, and poor glycemic control.

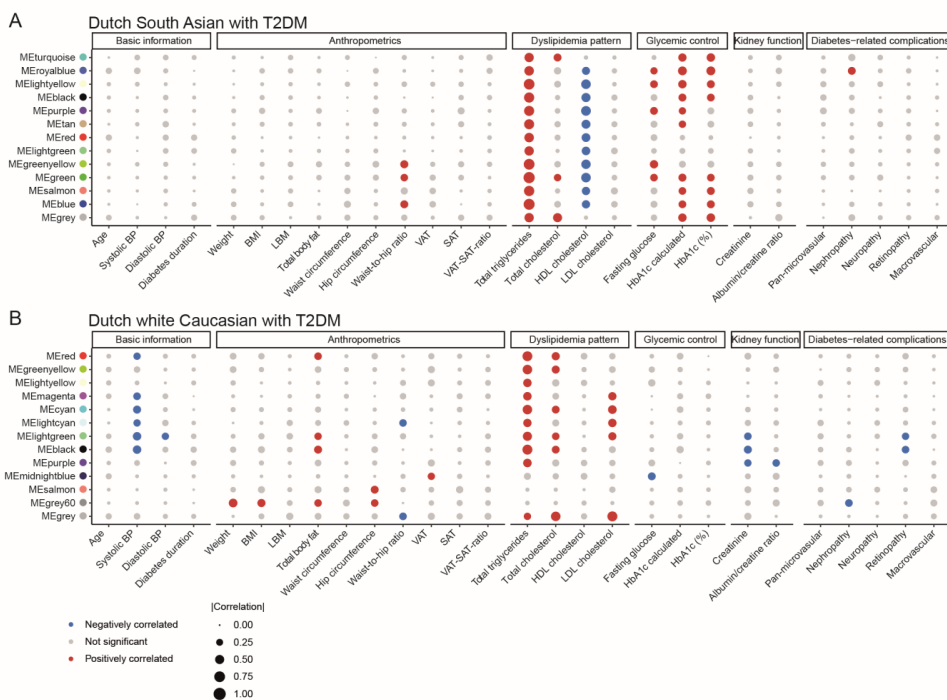


Fig. 4. Association of lipid correlation network modules with clinical features in (A) Dutch South Asians with T2DM and (B) Dutch white Caucasians with T2DM. The color grey denotes a lipid cluster with no significant associations with clinical features, the color blue denotes a lipid cluster with a negative association with clinical features, and the color red

denotes a lipid cluster with a positive association with clinical features. The correlation coefficients are represented by the size of the dots (Spearman's rank correlation test).

Abbreviations: *BP* blood pressure; *BMI* body mass index; *HbA1c* hemoglobin A1c; *HDL* high-density lipoprotein; *LBM* lean body mass; *LDL* low-density lipoprotein; *SAT* subcutaneous adipose tissue; *VAT* visceral adipose tissue.

Clinical relevance screening for key mediatory lipids from two ethnicities

The key mediatory lipids of DSA were first investigated in relation to clinical features such as dyslipidaemia, kidney function, and glycemic control parameters in both ethnicities. These lipids correlated positively with total TGs, total cholesterol, albumin/creatinine ratio, and HbA1c in DSA-T2DM, but negatively with HDL-cholesterol and LDL-cholesterol (Figure 5A). Since these lipids were derived from a DN-related module, we next compared the lipid concentrations in patients with and without DN. All the lipids, except DG 18:2_20:4, were higher in DN than T2DM in DSA (Figure 5B). However, we found only a few correlations between these lipids and LDL-cholesterol in DwC-T2DM (Figure 5C). In DwC, between T2DM and DN, those lipids exhibited the opposite behaviour (Figure 5D).

Key mediatory lipids derived from modules in DwC were then examined. Only limited correlations with clinical parameters could be observed in both ethnic groups (Figure S4A, C). None of them showed associations with DR or DN in either ethnicity (Figure S4B, D). These findings suggested that DGs were more strongly associated with DSA-T2DM than DwC-T2DM and with DN and kidney function.

We finally investigated key mediatory lipids of DSA in an external Chinese cohort of patients with IgA nephropathy and found that they were all higher in patients with IgA nephropathy than in healthy controls, with DG 18:1_18:2 showing the strongest correlation with renal function parameters (Figure S5).

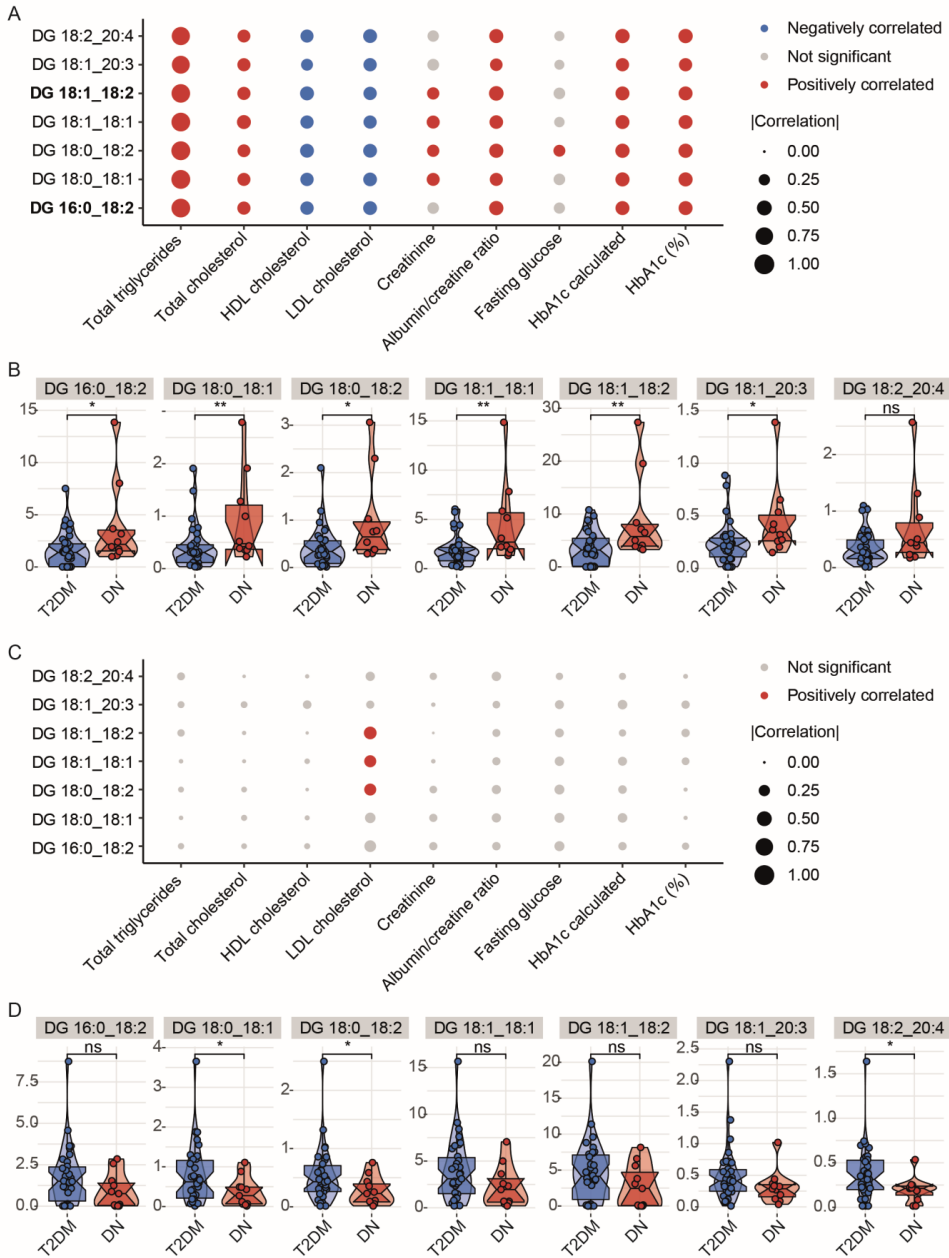


Fig. 5. Correlations between key mediatory lipids in diabetic nephropathy-associated module of Dutch South Asians and lipoproteins, kidney function, and glycemic control. (A)

Bubble plot depicting the correlations of lipids with lipoproteins, kidney function, and glycemic control in Dutch South Asians with T2DM. (B) Violin plots of lipids between T2DM with and without diabetic nephropathy in Dutch South Asians. (C) Bubble plot depicting the correlations of lipids with lipoproteins, kidney function, and glycemic control in Dutch white Caucasians with T2DM. (D) Violin plots of lipids between T2DM with and without DN in Dutch white Caucasians. Lipids in bold indicated that they were specifically different in Dutch South Asians. The color grey indicates no significant correlations with clinical features; the color blue indicates a negative correlation with clinical features, and the color red indicates a positive correlation with clinical features. The size of the dots represents the correlation coefficients (Pearson's correlation). The Wilcoxon signed-rank test was performed; * $p < 0.05$, ** $p < 0.01$.

Abbreviations: *DG* diacylglyceride; *DN* diabetic nephropathy; *HbA1c* hemoglobin A1c; *HDL* high-density lipoprotein; *LDL* low-density lipoprotein; *T2DM* type 2 diabetes mellitus.

Discussion

In the current lipidomic phenotyping study, we discovered differences in lipid classes and lipid species between patients with T2DM and healthy individuals in both the Dutch South Asian (DSA) and Dutch white Caucasian (DwC) populations. Specifically, lipid changes in individuals with T2DM of DSA were found to be more strongly associated with clinical parameters than DwC, with diacylglycerols (DGs) showing strong associations to diabetic nephropathy and renal function. Furthermore, we observed that healthy DSA individuals already had a diabetes-prone lipid distribution. These findings imply that impaired DG metabolism in DSA could be a potential hallmark and that lipidomic phenotyping could provide detailed insights into lipid metabolic complexity and interindividual variations among T2DM patients of various ethnic groups.

Previous studies suggested that SAs may have a lower ability to secrete insulin, lower muscle mass and a higher ectopic fat deposition which contributed to the higher T2DM prevalence^{3,22}. In the current study, it is worth noting that healthy DSA individuals already revealed a diabetic lipid distribution, which partly could predict the higher risk in developing T2DM in this population. Additionally, our study revealed remarkable differences in lipidomic profiles between both ethnic groups, lending credence to previously established

associations between T2DM and dysregulated lipoprotein composition using ^1H NMR lipoprotein profiling ²³. Our results demonstrate distinct differences in the lipidome between patients with T2DM and healthy controls, mainly related to CE, DG, PE, SM, and TG metabolism. This was consistent with previous findings observed in the case-cohort study nested within the PREDIMED trial ²⁴ and the longitudinal METSIM study ²⁵. However, conflicting results were reported in two studies based on Chinese populations ^{26, 27}; for instance, compared to healthy controls, FFA, SM and LPC lipid species were higher in Chinese patients with T2DM, whereas we found opposite results in Dutch patients with T2DM, further highlighting the variability in lipidomics profile between ethnicities.

The comprehensive analysis for lipidomics profiling performed in the current study allows for testing clinically relevance. As a hallmark of T2DM, insulin resistance affects regulation of lipid and lipoprotein metabolism ^{28, 29}. In line with previous studies, we found that lipid modules in DSA-T2DM positively correlated with TG, total cholesterol and negatively correlated with HDL-C; whereas lipid modules in DwC-T2DM correlated with total TG, cholesterol, and LDL-C, suggesting an ethnic preference in correlation with dyslipidemia patterns. Insulin resistance also impairs glucose metabolism and TG metabolism ³⁰⁻³². Interestingly, we discovered ethnicity differences in lipid modules (mainly consisting of TGs and DGs) demonstrating a correlation with both short- and long-term glycemic control exclusively in DSA-T2DM, rather than in the DwC-T2DM population. Also, our observation that certain lipid modules correlated with DN in both ethnic groups was in line with the reported dyslipidemia as a hallmark of chronic kidney disease (CKD) ³³. Moreover, a previous study revealed that patients with CKD had abnormalities in glycerolipid metabolism such as monoradylglycerolipids (MG), DGs, and TGs ³⁴, which is also consistent with our findings in DSA-T2DM. However, we did not observe these associations in DwC-T2DM; one possible hypothesis might be a shorter duration in diabetes, which resulted in the more excessive changes in lipid metabolism.

By combining lipid abundance and lipid species analysis, we have identified a specific lipid class, DG, which contributes to the increased risk in development and progression of T2DM

among SAs. DG is derived from lipoprotein lipase (LPL)-mediated hydrolysis of TGs, and our observations reveal low DG abundance alongside high TG levels in T2DM in both ethnicities. However, DG lipid class abundance was much higher in DSA than DwC in both healthy and diabetic individuals, hinting to possible lipolysis dysregulation in SAs. Insulin resistance, a crucial factor in T2DM development, has been found to be higher in SAs than in wCs^{35, 36}. LPL has been associated with insulin resistance^{37, 38}, and this could potentially explain the higher proportion of DG observed in our study, as higher insulin resistance in SAs impairs the ability of insulin to suppress lipolysis, leading to an increased release of fatty acids that are subsequently converted to DGs. Previous research has reported the impact of DGs on hepatic insulin resistance. Increased levels of DGs are commonly observed in animal models of lipid-induced hepatic insulin resistance^{39, 40}. Furthermore, several human studies have demonstrated significant associations between total hepatic DG content or specific DG species and insulin resistance markers, such as homeostasis model assessment-estimated insulin resistance (HOMA-IR)⁴¹⁻⁴⁴. These associations were found to be stronger than those observed with variables like body mass index, ceramide content, and markers of endoplasmic reticulum stress⁴¹. Interestingly, DGs and their targets protein kinase C (PKC) and protein kinase D (PKD) have been shown to regulate multiple critical cellular responses⁴⁵, which might be a plausible mechanism for inhibition of insulin signalling leading to hepatic insulin resistance. Once DG accumulates, it could lead to hyperactivation of PKC/PKD and play an important role in development of diabetic nephropathy^{46, 47}. Our observation that DG metabolism in the circulation was disturbed, with a higher correlation to clinical outcomes, may argue that a dysregulated DG-PKC/PKD signalling network could disrupt the redox balance and lead to more oxidative stress⁴⁷, and in part could explain why DSA-T2DM patients are more vulnerable to diabetic nephropathy progression.

The strength of our study is that we measured detailed lipidomic profiles in two ethnic groups of diabetic and healthy individuals. Our findings confirmed lipidomic perturbations in patients with T2DM in both ethnic groups; meanwhile, we revealed an ethnic distinction of lipid modules in relation to clinical outcomes (e.g., glycemic control). Notably, there are

still several limitations to our study. First, our study is a cross-sectional study; therefore, we cannot address issues of causality in the association of T2DM. Second, the relatively small sample size limits the power of generalization and precludes stratification analyses. Third, as waist-to-hip ratio was found to be the most reliable predictor of T2DM in the HELIUS study, regardless of ethnicity ⁴⁸, lack of a WHR matching design might be a shortcoming in our study. Fourth, oxidized lipids induced by oxidative stress play a critical role in the development and progression of T2DM ^{49, 50}, however, we were not able to detect high-throughput oxidized lipids by using this platform. Fifth, for renal function validation we only used an external cohort of patients with IgA nephropathy instead of diabetic nephropathy, and in a singular ethnic group. Therefore, further longitudinal studies with multiple ethnic groups and larger sample sizes are needed to verify our findings.

Conclusions

In conclusion, Dutch patients with T2DM of both white Caucasian and South Asian descent exhibited altered circulating lipidomes when compared to healthy individuals of the same ethnicity. In DSA the lipid changes of especially DGs, were clinically more relevant than in DwC. These DGs, particularly DG 18:1_18:2, were associated with glycemic control and renal function in DSA patients with T2DM and Chinese patients with IgA nephropathy (validation cohort). These observations suggest that they could be used as ethnicity-specific biomarkers for diabetic nephropathy patients. In addition, lipidomics phenotyping provides detailed insight into lipid metabolic complexity and interindividual variations among patients with T2DM from various ethnic groups.

Abbreviations

ACE: Angiotensin-converting enzyme; BMI: body mass index; BP: blood pressure; CE: cholesteryl ester; CER: ceramide; CI: confidence interval; CKD: chronic kidney disease; DCER: dihydroceramide; DG: diacylglyceride; DMS: differential mobility mass spectrometry; DN: diabetic nephropathy; DR: diabetic retinopathy; DSA: Dutch South Asian; DwC: Dutch white Caucasian; eGFR: estimated glomerular filtration rate; FA: fatty acid; FDR: false discovery rate; HbA1c hemoglobin A1c; HC: healthy control; HCA: hierarchical cluster analysis; HDL: high-density lipoprotein; HDL-C: high-density lipoprotein-cholesterol; HexCER: hydroxyceramide; IgAN: IgA nephropathy; LacCER: lactosylceramide; LBM: lean body mass; LC/MS: liquid chromatography/mass spectrometry; LDL: low-density lipoprotein; LDL-C: low-density lipoprotein-cholesterol; LPC: lysophosphatidylcholine; LPE: lysophosphatidylethanolamine; LPL: lipoprotein lipase; MG: monoradylglycerolipid; MLR: multinomial logistic regression analysis ns: not significant; PA: phosphatidic acid; PC: phosphatidylcholine; PCA: principle component analysis; PE: phosphatidylethanolamine; PI: phosphatidylinositol; PKC: protein kinase C; PS: phosphatidylserine; SAT: subcutaneous adipose tissue; SD: standard deviation; SLA: shotgun lipidomics assistant; SM: sphingomyelin; T2DM: type 2 diabetes mellitus; TG: triglyceride; VAT: visceral adipose tissue; WGCNA: weighted correlation network analysis.

Acknowledgments

We would like to express our gratitude to all of the patients and healthy volunteers who took part in the MAGNA VICTORIA study. We would like to thank the researchers, nurses, and physicians who helped organize this study.

Authors' contributions

LY, MG, and BMvdB contributed to the study concept, design and analysis; LY analyzed and interpreted data, and critically revised the manuscript; AV and NB carried out the SLA

experiments and first data analysis; HvE and MB collected data for the MAGNA VICTORIA study, IMJ supervised the study, with HJL as study director; PCNR interpreted lipidomics data; LY, TJR, and BMvdB drafted the manuscript. All authors read, commented on, and approved the final manuscript.

Funding

The work was supported by ZonMW (The Enabling Technologies Hotels program, grant: 435005003, 2019) and by China Scholarship Council grant to Lushun Yuan (CSC no. 201806270262).

Availability of data and materials

All data and methods supporting the findings of this study are available from the corresponding author upon reasonable request.

Competing interests

The authors declare that they have no relevant financial interests or personal relationships.

Ethics approval and consent to participate

Participants were drawn from two prior randomized controlled trials (ClinicalTrials.gov NCT01761318 and NCT02660047). The study protocol was approved by the Institutional Review Board (Leiden University Medical Center, Leiden, The Netherlands), and all participants gave written informed consent.

Consent for publication

The manuscript was approved by all authors for publication.

References

1. Unnikrishnan R, Pradeepa R, Joshi SR & Mohan V. Type 2 Diabetes: Demystifying the Global Epidemic. *Diabetes* 2017 **66** 1432-1442.
2. Sattar N & Gill JM. Type 2 diabetes in migrant south Asians: mechanisms, mitigation, and management. *Lancet Diabetes Endocrinol* 2015 **3** 1004-1016.
3. Bakker LE, Sleddering MA, Schoones JW, Meinders AE & Jazet IM. Pathogenesis of type 2 diabetes in South Asians. *Eur J Endocrinol* 2013 **169** R99-R114.
4. Kawai T, Autieri MV & Scalia R. Adipose tissue inflammation and metabolic dysfunction in obesity. *Am J Physiol Cell Physiol* 2021 **320** C375-C391.
5. Chait A & den Hartigh LJ. Adipose Tissue Distribution, Inflammation and Its Metabolic Consequences, Including Diabetes and Cardiovascular Disease. *Front Cardiovasc Med* 2020 **7** 22.
6. Chandie Shaw PK, Vandenbroucke JP, Tjandra YI, Rosendaal FR, Rosman JB, Geerlings W, de Charro FT & van Es LA. Increased end-stage diabetic nephropathy in Indo-Asian immigrants living in the Netherlands. *Diabetologia* 2002 **45** 337-341.
7. Chandie Shaw PK, Baboe F, van Es LA, van der Vijver JC, van de Ree MA, de Jonge N & Rabelink TJ. South-Asian type 2 diabetic patients have higher incidence and faster progression of renal disease compared with Dutch-European diabetic patients. *Diabetes Care* 2006 **29** 1383-1385.
8. Wang YL, Koh WP, Talaei M, Yuan JM & Pan A. Association between the ratio of triglyceride to high-density lipoprotein cholesterol and incident type 2 diabetes in Singapore Chinese men and women. *J Diabetes* 2017 **9** 689-698.
9. Peng J, Zhao F, Yang X, Pan X, Xin J, Wu M & Peng YG. Association between dyslipidemia and risk of type 2 diabetes mellitus in middle-aged and older Chinese adults: a secondary analysis of a nationwide cohort. *BMJ Open* 2021 **11** e042821.
10. Rao H, Jalali JA, Johnston TP & Koulen P. Emerging Roles of Dyslipidemia and Hyperglycemia in Diabetic Retinopathy: Molecular Mechanisms and Clinical Perspectives. *Front Endocrinol (Lausanne)* 2021 **12** 620045.
11. Hukportie DN, Li FR, Zhou R, Zheng JZ, Wu XX, Zou MC & Wu XB. Lipid variability and risk of microvascular complications in Action to Control Cardiovascular Risk in Diabetes (ACCORD) trial: A post hoc analysis. *J Diabetes* 2022 **14** 365-376.
12. Narindrarangkura P, Bosl W, Rangsin R & Hatthachote P. Prevalence of dyslipidemia associated with complications in diabetic patients: a nationwide study in Thailand. *Lipids Health Dis* 2019 **18** 90.
13. Frank AT, Zhao B, Jose PO, Azar KM, Fortmann SP & Palaniappan LP. Racial/ethnic differences in dyslipidemia patterns. *Circulation* 2014 **129** 570-579.

14. Zakai NA, Minnier J, Safford MM, Koh I, Irvin MR, Fazio S, Cushman M, Howard VJ & Pamir N. Race-Dependent Association of High-Density Lipoprotein Cholesterol Levels With Incident Coronary Artery Disease. *J Am Coll Cardiol* 2022 **80** 2104-2115.
15. Su B, Bettcher LF, Hsieh WY, Hornburg D, Pearson MJ, Blomberg N, Giera M, Snyder MP, Raftery D, Bensinger SJ & Williams KJ. A DMS Shotgun Lipidomics Workflow Application to Facilitate High-Throughput, Comprehensive Lipidomics. *J Am Soc Mass Spectrom* 2021 **32** 2655-2663.
16. Bizino MB, Jazet IM, Westenberg JJM, van Eyk HJ, Paiman EHM, Smit JWA & Lamb HJ. Effect of liraglutide on cardiac function in patients with type 2 diabetes mellitus: randomized placebo-controlled trial. *Cardiovasc Diabetol* 2019 **18** 55.
17. van Eyk HJ, Paiman EHM, Bizino MB, de Heer P, Geelhoed-Duijvestijn PH, Kharagitsingh AV, Smit JWA, Lamb HJ, Rensen PCN & Jazet IM. A double-blind, placebo-controlled, randomised trial to assess the effect of liraglutide on ectopic fat accumulation in South Asian type 2 diabetes patients. *Cardiovasc Diabetol* 2019 **18** 87.
18. Paiman EHM, van Eyk HJ, Bizino MB, Dekkers IA, de Heer P, Smit JWA, Jazet IM & Lamb HJ. Phenotyping diabetic cardiomyopathy in Europeans and South Asians. *Cardiovasc Diabetol* 2019 **18** 133.
19. Ghorasaini M, Mohammed Y, Adamski J, Bettcher L, Bowden JA, Cabruja M, Contrepolis K, Ellenberger M, Gajera B, Haid M, Hornburg D, Hunter C, Jones CM, Klein T, Mayboroda O, Mirzaian M, Moaddel R, Ferrucci L, Lovett J, Nazir K, Pearson M, Ubhi BK, Raftery D, Riols F, Sayers R, Sijbrands EJG, Snyder MP, Su B, Velagapudi V, Williams KJ, de Rijke YB & Giera M. Cross-Laboratory Standardization of Preclinical Lipidomics Using Differential Mobility Spectrometry and Multiple Reaction Monitoring. *Anal Chem* 2021 **93** 16369-16378.
20. Langfelder P & Horvath S. WGCNA: an R package for weighted correlation network analysis. *BMC Bioinformatics* 2008 **9** 559.
21. Deng Y, Wu Q, Chen W, Zhu L, Liu W, Xia F, Sun L, Lin X & Zeng R. Lipidomics reveals association of circulating lipids with body mass index and outcomes in IgA nephropathy patients. *J Mol Cell Biol* 2021.
22. Narayan KMV & Kanaya AM. Why are South Asians prone to type 2 diabetes? A hypothesis based on underexplored pathways. *Diabetologia* 2020 **63** 1103-1109.
23. Yuan L, Li-Gao R, Verhoeven A, van Eyk HJ, Bizino MB, Rensen PCN, Giera M, Jazet IM, Lamb HJ, Rabelink TJ & van den Berg BM. Altered high-density lipoprotein composition is associated with risk for complications in type 2 diabetes mellitus in South Asian descendants: A cross-sectional, case-control study on lipoprotein subclass profiling. *Diabetes Obes Metab* 2023.
24. Razquin C, Toledo E, Clish CB, Ruiz-Canela M, Dennis C, Corella D, Papandreou C, Ros E, Estruch R, Guasch-Ferre M, Gomez-Gracia E, Fito M, Yu E, Lapetra J, Wang D, Romaguera D, Liang L, Alonso-Gomez A, Deik A, Bullo M, Serra-Majem L, Salas-Salvado J, Hu FB & Martinez-Gonzalez MA. Plasma Lipidomic Profiling and Risk of Type 2 Diabetes in the PREDIMED Trial. *Diabetes Care* 2018 **41** 2617-2624.

25. Suvitaival T, Bondia-Pons I, Yetukuri L, Poho P, Nolan JJ, Hyotylainen T, Kuusisto J & Oresic M. Lipidome as a predictive tool in progression to type 2 diabetes in Finnish men. *Metabolism* 2018 **78** 1-12.
26. Xuan Q, Hu C, Zhang Y, Wang Q, Zhao X, Liu X, Wang C, Jia W & Xu G. Serum lipidomics profiles reveal potential lipid markers for prediabetes and type 2 diabetes in patients from multiple communities. *Front Endocrinol (Lausanne)* 2022 **13** 966823.
27. Zhang L, Hu Y, An Y, Wang Q, Liu J & Wang G. The Changes of Lipidomic Profiles Reveal Therapeutic Effects of Exenatide in Patients With Type 2 Diabetes. *Front Endocrinol (Lausanne)* 2022 **13** 677202.
28. Taskinen MR. Insulin resistance and lipoprotein metabolism. *Curr Opin Lipidol* 1995 **6** 153-160.
29. Choi SH & Ginsberg HN. Increased very low density lipoprotein (VLDL) secretion, hepatic steatosis, and insulin resistance. *Trends Endocrinol Metab* 2011 **22** 353-363.
30. Norton L, Shannon C, Gastaldelli A & DeFronzo RA. Insulin: The master regulator of glucose metabolism. *Metabolism* 2022 **129** 155142.
31. Ma M, Liu H, Yu J, He S, Li P, Ma C, Zhang H, Xu L, Ping F, Li W, Sun Q & Li Y. Triglyceride is independently correlated with insulin resistance and islet beta cell function: a study in population with different glucose and lipid metabolism states. *Lipids Health Dis* 2020 **19** 121.
32. Yan YZ, Ma RL, Zhang JY, He J, Ma JL, Pang HR, Mu LT, Ding YS, Guo H, Zhang M, Liu JM, Rui DS, Wang K & Guo SX. Association of Insulin Resistance with Glucose and Lipid Metabolism: Ethnic Heterogeneity in Far Western China. *Mediators Inflamm* 2016 **2016** 3825037.
33. Baek J, He C, Afshinnia F, Michailidis G & Pennathur S. Lipidomic approaches to dissect dysregulated lipid metabolism in kidney disease. *Nat Rev Nephrol* 2022 **18** 38-55.
34. Chen H, Chen L, Liu D, Chen DQ, Vaziri ND, Yu XY, Zhang L, Su W, Bai X & Zhao YY. Combined Clinical Phenotype and Lipidomic Analysis Reveals the Impact of Chronic Kidney Disease on Lipid Metabolism. *J Proteome Res* 2017 **16** 1566-1578.
35. Ehtisham S, Crabtree N, Clark P, Shaw N & Barrett T. Ethnic differences in insulin resistance and body composition in United Kingdom adolescents. *J Clin Endocrinol Metab* 2005 **90** 3963-3969.
36. Gujral UP, Pradeepa R, Weber MB, Narayan KM & Mohan V. Type 2 diabetes in South Asians: similarities and differences with white Caucasian and other populations. *Ann N Y Acad Sci* 2013 **1281** 51-63.
37. Miyashita Y & Shirai K. Clinical determination of the severity of metabolic syndrome: preheparin lipoprotein lipase mass as a new marker of metabolic syndrome. *Curr Med Chem Cardiovasc Hematol Agents* 2005 **3** 377-381.
38. Huang Y, Li X, Wang M, Ning H, A L, Li Y & Sun C. Lipoprotein lipase links vitamin D, insulin resistance, and type 2 diabetes: a cross-sectional epidemiological study. *Cardiovasc Diabetol* 2013 **12** 17.
39. Camporez JP, Jornayvaz FR, Petersen MC, Pesta D, Guigni BA, Serr J, Zhang D, Kahn M, Samuel VT, Jurczak MJ & Shulman GI. Cellular mechanisms by which FGF21 improves insulin sensitivity in male mice. *Endocrinology* 2013 **154** 3099-3109.

40. Camporez JPG, Kanda S, Petersen MC, Jornayvaz FR, Samuel VT, Bhanot S, Petersen KF, Jurczak MJ & Shulman GI. ApoA5 knockdown improves whole-body insulin sensitivity in high-fat-fed mice by reducing ectopic lipid content. *J Lipid Res* 2015 **56** 526-536.
41. Kumashiro N, Erion DM, Zhang D, Kahn M, Beddow SA, Chu X, Still CD, Gerhard GS, Han X, Dziura J, Petersen KF, Samuel VT & Shulman GI. Cellular mechanism of insulin resistance in nonalcoholic fatty liver disease. *Proc Natl Acad Sci U S A* 2011 **108** 16381-16385.
42. Jornayvaz FR & Shulman GI. Diacylglycerol activation of protein kinase Cepsilon and hepatic insulin resistance. *Cell Metab* 2012 **15** 574-584.
43. Luukkonen PK, Zhou Y, Sadevirta S, Leivonen M, Arola J, Oresic M, Hyotylainen T & Yki-Jarvinen H. Hepatic ceramides dissociate steatosis and insulin resistance in patients with non-alcoholic fatty liver disease. *J Hepatol* 2016 **64** 1167-1175.
44. Ter Horst KW, Gilijamse PW, Versteeg RI, Ackermans MT, Nederveen AJ, la Fleur SE, Romijn JA, Nieuwdorp M, Zhang D, Samuel VT, Vatner DF, Petersen KF, Shulman GI & Serlie MJ. Hepatic Diacylglycerol-Associated Protein Kinase Cepsilon Translocation Links Hepatic Steatosis to Hepatic Insulin Resistance in Humans. *Cell Rep* 2017 **19** 1997-2004.
45. Wang QJ. PKD at the crossroads of DAG and PKC signaling. *Trends Pharmacol Sci* 2006 **27** 317-323.
46. Noh H & King GL. The role of protein kinase C activation in diabetic nephropathy. *Kidney Int Suppl* 2007 S49-53.
47. Pan D, Xu L & Guo M. The role of protein kinase C in diabetic microvascular complications. *Front Endocrinol (Lausanne)* 2022 **13** 973058.
48. Zethof M, Mosterd CM, Collard D, Galenkamp H, Agyemang C, Nieuwdorp M, van Raalte DH & van den Born BH. Differences in Body Composition Convey a Similar Risk of Type 2 Diabetes Among Different Ethnic Groups With Disparate Cardiometabolic Risk-The HELIUS Study. *Diabetes Care* 2021 **44** 1692-1698.
49. Augustine J, Troendle EP, Barabas P, McAleese CA, Friedel T, Stitt AW & Curtis TM. The Role of Lipoxidation in the Pathogenesis of Diabetic Retinopathy. *Front Endocrinol (Lausanne)* 2020 **11** 621938.
50. Reis A, Rocha S, Dias IH, Costa R, Soares R, Sanchez-Quesada JL, Perez A & de Freitas V. Type 2 Diabetes mellitus alters the cargo of (poly)phenol metabolome and the oxidative status in circulating lipoproteins. *Redox Biol* 2023 **59** 102572.

Supporting information

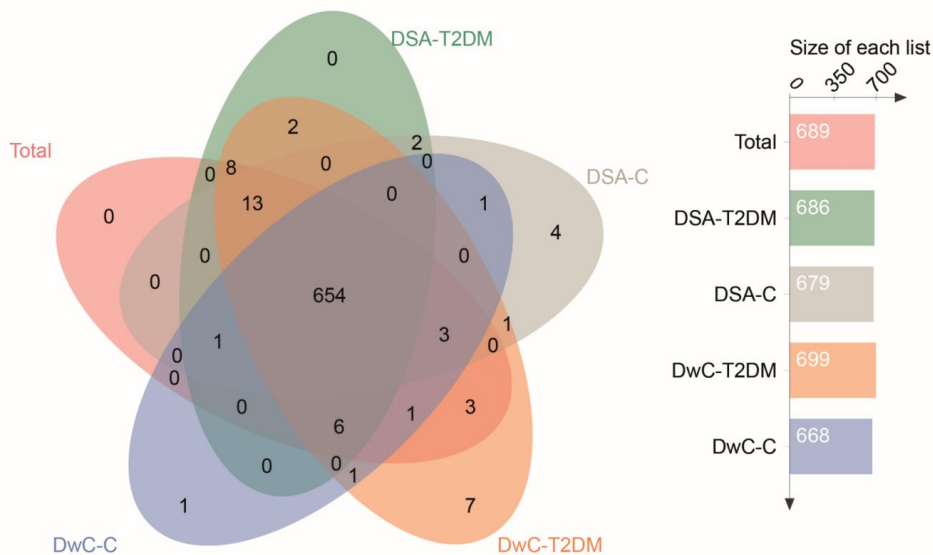


Fig. S1. Lipid species selected for analysis. Missing value percentage quantification per lipid class in total individuals, Dutch South Asians with T2DM (DSA-T2DM), Healthy Dutch South Asians (DSA-C), Dutch white Caucasians with T2DM (DwC-T2DM), and healthy Dutch white Caucasians (DwC-C). Details of missing values are shown in Additional file 2: Table S2. Common lipids with a missing value percentage of less than 30%.

Abbreviations: *DSA* Dutch South Asian; *DwC* Dutch white Caucasian; *T2DM* type 2 diabetes mellitus; *TG* triglyceride.

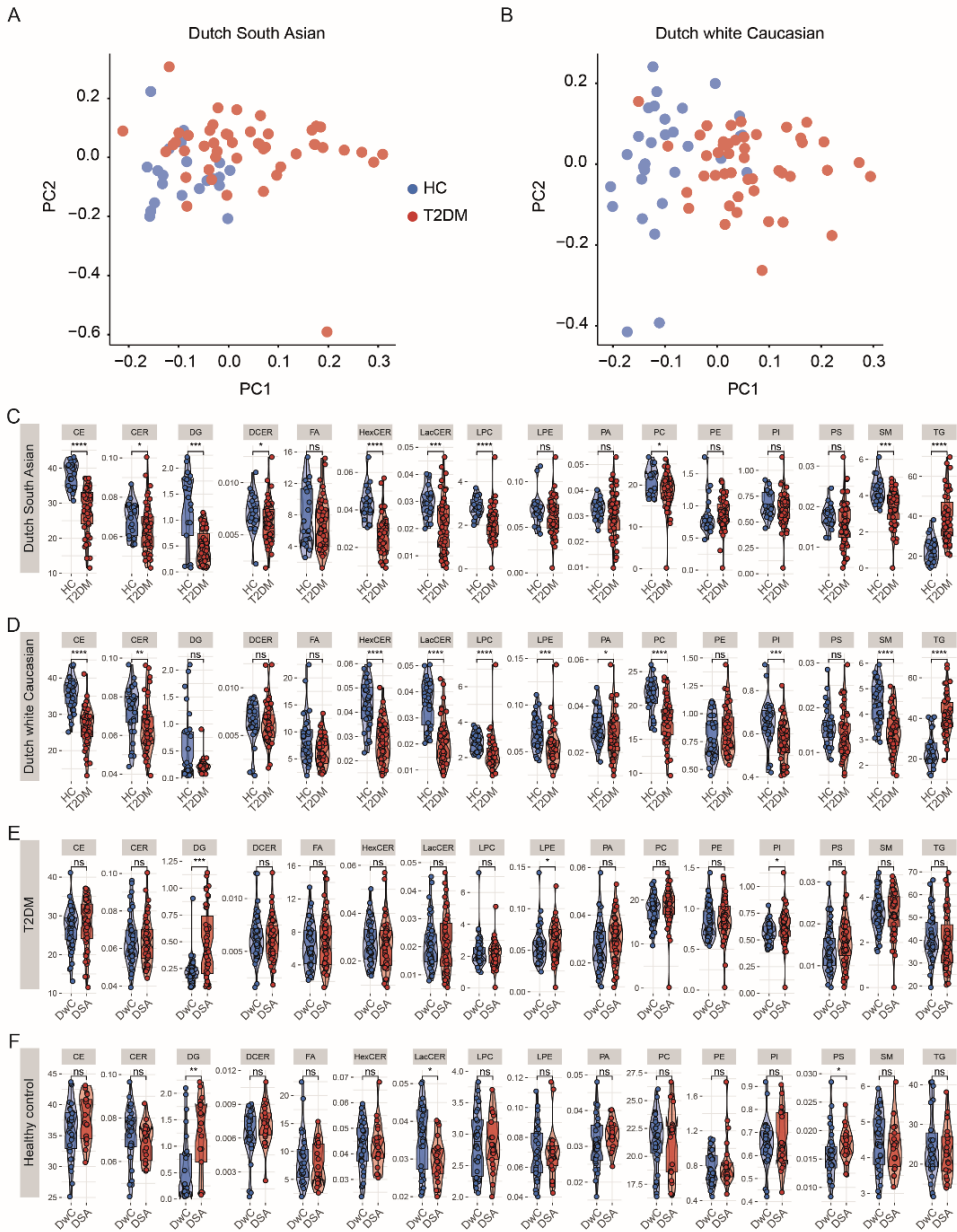


Fig. S2. Lipid abundance comparison between individuals from two ethnic groups. Principle component analysis using lipid class abundance in (A) Dutch South Asians and (B) Dutch white Caucasians. (C) Violin plot of lipid class abundance between patients with

T2DM and healthy controls in Dutch South Asians. (D) Violin plot of lipid class abundance between patients with T2DM and healthy controls in Dutch white Caucasians. (E) Violin plot of lipid class abundance between Dutch South Asians with T2DM and Dutch white Caucasians with T2DM. (F) Violin plot of lipid class abundance in healthy individuals between Dutch South Asians and Dutch white Caucasians. Wilcoxon signed-rank test was performed; * $p < 0.05$, ** $p < 0.01$, *** $p < 0.001$, **** $p < 0.0001$.

Abbreviations: *CE* cholesteryl ester; *CER* ceramide; *DCER* dihydroceramide; *DG* diacylglyceride; *DSA* Dutch South Asian; *DwC* Dutch white Caucasian; *FA* fatty acid; *HC* healthy control; *HexCER* hydroxyceramide; *LacCER* lactosylceramide; *LPC* lysophosphatidylcholine; *LPE* lysophosphatidylethanolamine; *PA* phosphatidic acid; *PC* phosphatidylcholine; *PE* phosphatidylethanolamine; *PI* phosphatidylinositol; *PS* phosphatidylserine; *SM* sphingomyelin; *T2DM* type 2 diabetes mellitus; *TG* triglyceride.

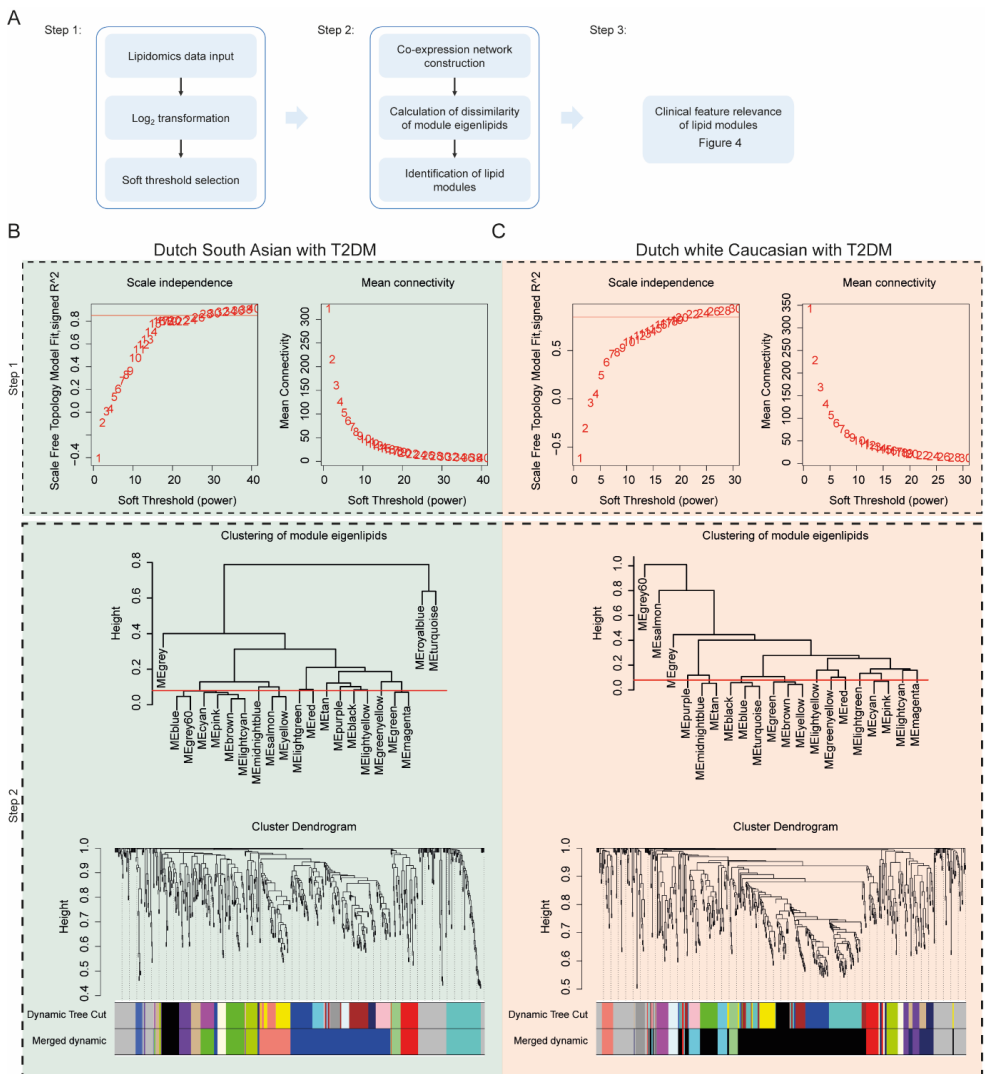


Fig. S3. Step-by-step WGCNA analysis. (A) Workflow of WGCNA analysis using the lipidomics profiles. Step 1 and Step 2 of WGCNA analysis in (B) Dutch South Asian and (C) Dutch white Caucasian.

Abbreviations: *ME* module eigenlipids

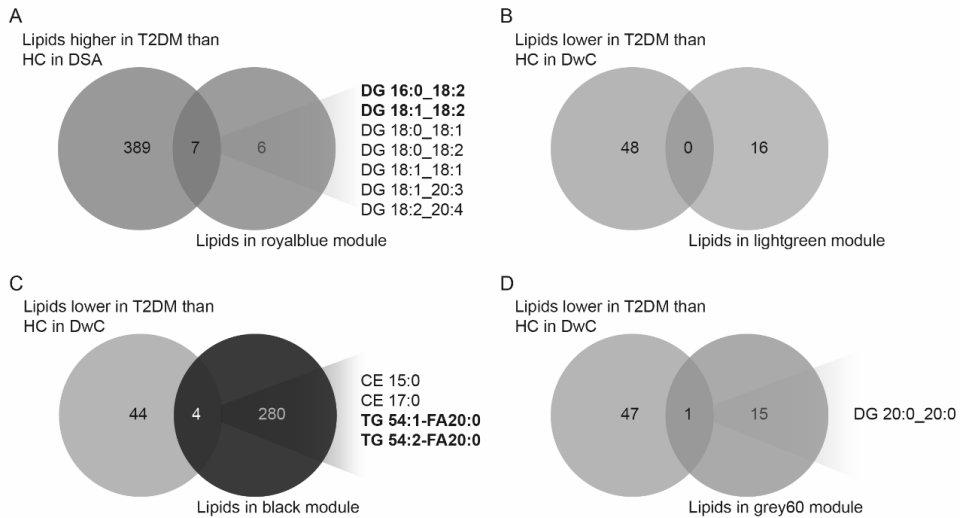


Fig. S4. Identification of key mediatory lipids. (A) Key mediatory lipid species (from diabetic nephropathy [DN] and glycemic control associated module, ‘royal blue’ module) in Dutch South Asians. (B) Key mediatory lipid species (from DR-associated module, ‘light green’ module) in Dutch white Caucasians. (C) Key mediatory lipid species (from diabetic retinopathy [DR]-associated module, ‘black’ module) in Dutch white Caucasians. (D) Key mediatory lipid species (diabetic nephropathy [DN]-associated module, ‘grey60’ module) in DwC. Bold lipids indicated that they were specifically different in DSA/DwC.

Abbreviations: *CE* cholesteryl ester; *DG* diacylglyceride; *DN* diabetic nephropathy; *DR* diabetic retinopathy; *DSA* Dutch South Asian; *DwC* Dutch white Caucasian; *HC* healthy control; *T2DM* type 2 diabetes mellitus; *TG* triglyceride.

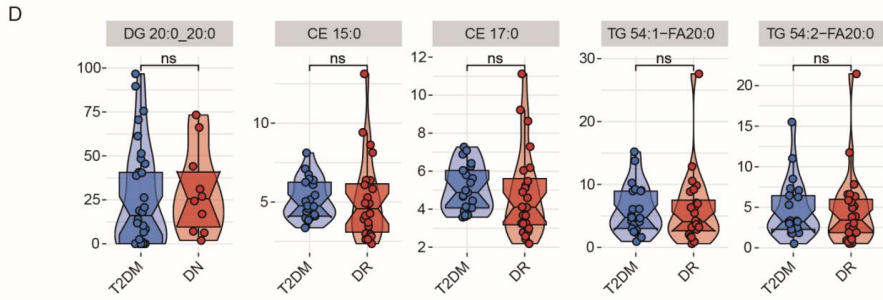
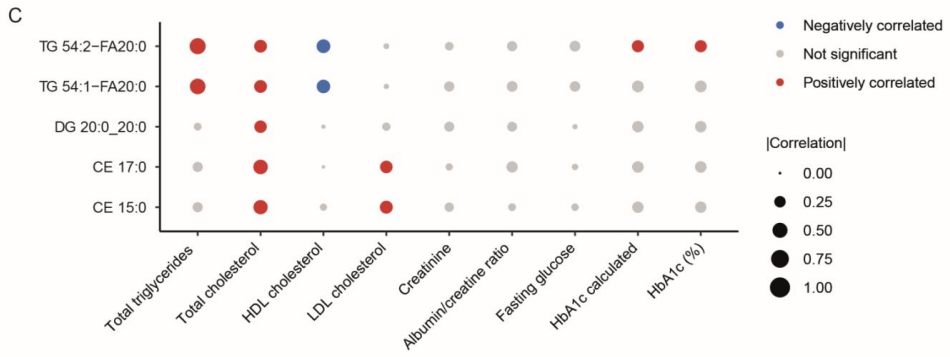
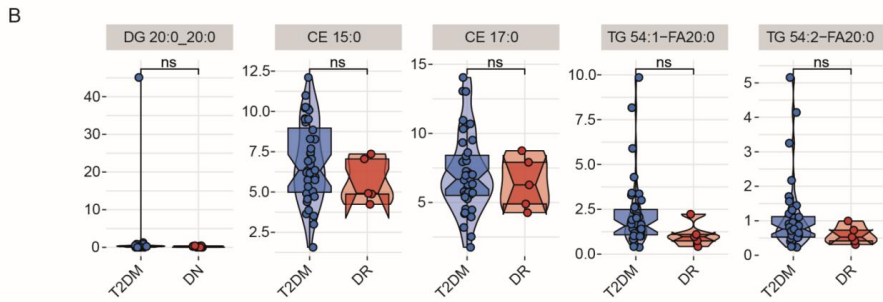
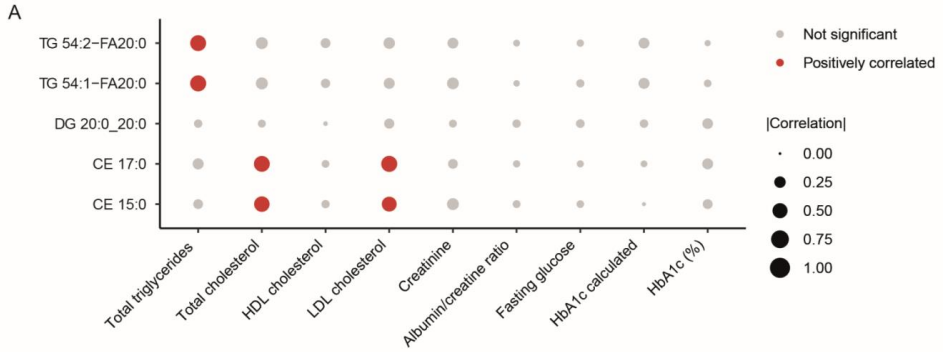


Fig. S5. Correlations between key mediatory lipids in Dutch white Caucasians and dyslipidemia, kidney function, and glycemic control. (A) A bubble plot depicting the correlations of lipids with lipoproteins, kidney function, and glycemic control in Dutch South Asians with T2DM. (B) Violin plot of lipids between T2DM with and without DN/DR in Dutch South Asians. (C) A bubble plot depicting the correlations of lipids with lipoproteins, kidney function, and glycemic control in Dutch South Asians with T2DM. (D) Violin plot of lipids between T2DM with and without DN/DR in Dutch South Asians. The color grey indicates no significant correlations with clinical features, the color blue indicates a negative correlation with clinical features, and the color red indicates a positive correlation with clinical features. The size of the dots represents the correlation coefficients (Pearson's correlation). The Wilcoxon signed-rank test was performed.

Abbreviations: *CE* cholesteryl ester; *DG* diacylglyceride; *DN* diabetic nephropathy; *DR* diabetic retinopathy; *HbA1c* hemoglobin A1c; *HDL* high-density lipoprotein; *LDL* low-density lipoprotein; *ns* not significant; *T2DM* type 2 diabetes mellitus; *TG* triglyceride.

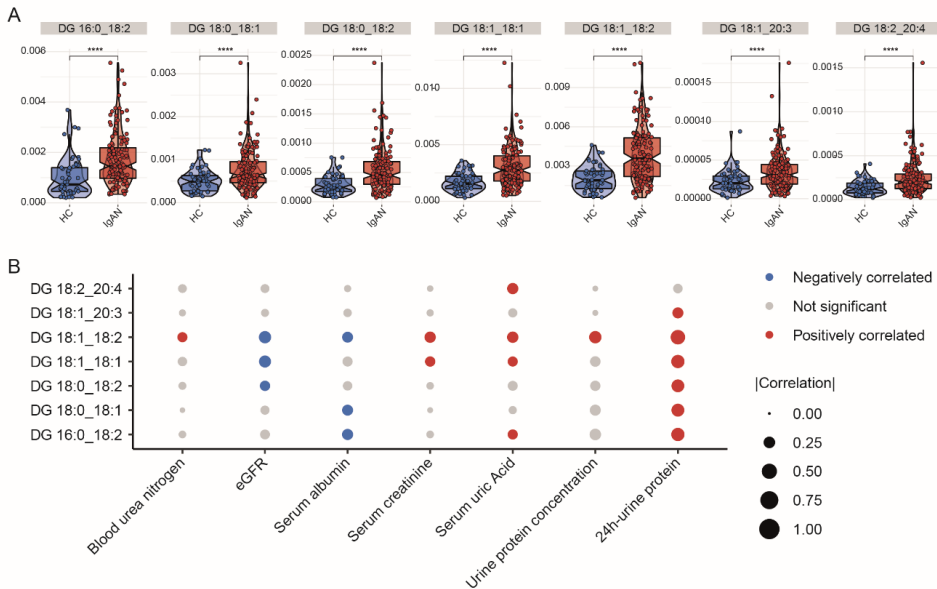


Fig. S6. The role of key mediatory lipids in DN-associated module of DSA in IgA nephropathy and their relationships with kidney function. (A) Violin plot of lipid differences between healthy controls and IgA nephropathy. (B) A bubble plot illustrating the relationships between the key mediatory lipids of Dutch South Asians and kidney function parameters in IgA nephropathy. The color grey denotes no significant correlations with clinical features, the color blue denotes a negative correlation with clinical features, and the color red denotes a positive correlation with clinical features. The correlation coefficients (Pearson's correlation) are represented by the size of the dots. The Wilcoxon signed-rank test was performed; **** $p < 0.0001$.

Abbreviations: *CE* cholesteryl ester; *DG* diacylglyceride; *eGFR* estimated glomerular filtration rate; *HC* healthy control; *IgAN* IgA nephropathy.

Table S1. Clinical characteristics of study participants

	Dutch South Asian			Dutch white Caucasian			DSA-T2DM vs Dwc-T2DM
	Control (n=21)	T2DM (n=47)	p-value ¹	Control (n=30)	T2DM (n=45)	p-value ¹	p-value ²
Demographics							
Age (years)	48.3 (8.1)	54.9 (10.1)	0.0367	57.9 (7.9)	59.0 (6.5)	>0.9999	0.1606
Women (no, %)	15 (71.4%)	28 (59.6%)	0.3489	14 (46.7%)	20 (44.4%)	0.8498	0.1464
Current smoker (no, %)	3 (14.3%)	7 (14.9%)	1.0000	1 (3.3%)	9 (20.0%)	0.0437	0.7108
Medical history diabetes							
Duration diabetes mellitus (years)	-	17.9 (10)	-	-	10.3 (6.0)	-	<0.0001
Pan-microvascular (n, %)	-	30 (63.8%)	-	-	24 (51.1%)	-	0.3067
Nephropathy (n, %)	-	10 (21.3%)	-	-	11 (23.4%)	-	0.7174
Neuropathy (n, %)	-	14 (29.8%)	-	-	15 (31.9%)	-	0.7144
Retinopathy (n, %)	-	24 (51.1%)	-	-	5 (10.6%)	-	<0.0001
Macrovascular (n, %)	-	13 (27.7%)	-	-	2 (4.3%)	-	0.0037
Medication use							
Metformin (n, %)	-	45 (95.7%)	-	-	45 (100%)	-	0.4947
Sulfonylurea derivatives (n, %)	-	8 (17.0%)	-	-	13 (28.9%)	-	0.2682
Insulin (n, %)	-	36 (76.6%)	-	-	29 (64.4%)	-	0.2935
Anti-hypertensive medication (n, %)	-	34 (72.3%)	-	-	34 (75.6%)	-	0.7255
ACE-inhibitors (n, %)	-	13 (27.7%)	-	-	17 (37.8%)	-	0.4165
Statins (n, %)	-	36 (76.6%)	-	-	36 (80.0%)	-	0.8864
Blood pressure							
Systolic blood pressure (mmHg)	123.5 (13.7)	144.6 (21.5)	0.0003	126.2 (12.1)	141.3 (15.0)	0.0007	>0.9999
Diastolic blood pressure (mmHg)	80.2 (11.8)	85.3 (10.0)	0.1746	80 (77-83)	86.9 (8.8)	0.0158	0.8458
Anthropometrics							
Weight	63.6 (9.9)	79.7 (11.7)	<0.0001	73.3 (10.5)	96.4 (13.6)	<0.0001	<0.0001
BMI (kg/m ²)	23.5 (3.0)	29.5 (4.0)	<0.0001	24.3 (3.3)	32.3 (3.9)	<0.0001	0.0018
Total body fat (%)	32.4 (7.1)	37.1 (9.1)	0.1576	32.5 (7.1)	37.2 (9.3)	<0.0001	0.9998
Waist circumference, cm	82.0 (7.4)	101.0 (9.5)	<0.0001	86.6 (9.1)	110.4 (8.9)	<0.0001	<0.0001
Hip circumference, cm	95.2 (7.3)	104.1 (8.0)	<0.0001	98.2 (6.1)	107.6 (7.5)	<0.0001	0.1264
Waist-to-hip ratio	0.9 (0.1)	1 (0.1)	<0.0001	0.9 (0.1)	1 (0.1)	<0.0001	0.0039
VAT, cm ²	73.2 (29.8)	166.4 (55.8)	<0.0001	74.7 (34.1)	205.6 (75.6)	<0.0001	0.4342
SAT, cm ²	233.2 (195.9-258.8)	300.1 (228.3-371.4)	0.0561	189.7 (148.8-238.6)	335.7 (262.4-419.5)	<0.0001	>0.9999
VAT-SAT ratio	0.3 (0.2-0.4)	0.5 (0.4-0.7)	0.0017	0.4 (0.3-0.6)	0.6 (0.4-0.9)	0.0064	>0.9999
Glycemic control							
Fasting glucose (mmol/L)	5.0 (0.3)	8.1 (3.0)	<0.0001	5.2 (0.5)	7.8 (2.1)	<0.0001	>0.9999
HbA1c (mmol/mol)	35.5 (2.4)	67.8 (11.3)	<0.0001	35.5 (2.7)	64.9 (10.7)	<0.0001	>0.9999
Lipid panels							
Total cholesterol (mmol/L)	5.4 (0.8)	4.2 (0.9)	<0.0001	5.7 (1.1)	4.8 (1.0)	0.0018	0.0226
HDL-cholesterol (mmol/L)	1.6 (0.3)	1.2 (0.3)	0.0028	1.9 (0.5)	1.3 (0.3)	<0.0001	0.9008
LDL-cholesterol (mmol/L)	3.4 (0.7)	2.1 (0.8)	<0.0001	3.3 (1.0)	2.6 (0.8)	0.0017	0.0416
Total Triglycerides (mmol/L)	0.9 (0.3)	1.8 (1.4)	0.0031	0.9 (0.7-1.2)	2.1 (1.3)	<0.0001	0.2758
Kidney function panels							
Serum creatinine (μmol/mL)	68.0 (60.0-79.0)	67.0 (59.0-83.5)	0.4096	73.0 (68.0-85.0)	68.0 (57.0-80.0)	0.9582	0.9823
Albumin/creatinine ratio (mg/mmol)	-	2.7 (0.55-8.45)	-	-	0.7 (0-2.5)	-	0.0037
Micro-albuminuria (n, %) ^a	-	15 (31.9%)	-	-	7 (15.6%)	-	-
Macro-albuminuria (n, %) ^b	-	7 (14.9%)	-	-	1 (2.2%)	-	-

Data are presented as mean (SD), median (25-75 percentile), or percentage.

Abbreviations: *ACE* Angiotensin-converting enzyme, *BMI* body mass index, *HbA1c* Hemoglobin A1c, *HDL* high-density lipoprotein, *LDL* low-density lipoprotein, *SAT* subcutaneous adipose tissue, *VAT* visceral adipose tissue.

¹Post hoc tests of unpaired One-way ANOVA, Kruskal-Wallis test, or Chi-square test, p<0.05

²Post hoc tests of unpaired One-way ANOVA or Kruskal-Wallis test, Chi-square test, or Fisher's exact test, p<0.05

^aAlbumin-creatinine ratio between 3.0 – 30 mg/mmol. ^bAlbumin-creatinine ratio > 30 mg/mmol

Most of these data have been published before ^{14, 15}.

CHAPTER

5

Heparan sulfate mimetic fucoidan restores the endothelial glycocalyx and protects against dysfunction induced by serum of COVID-19 patients in the intensive care unit

Lushun Yuan¹, Shuzhen Cheng², Wendy M.P.J. Sol¹, Anouk I.M. van der Velden¹, Hans Vink^{3,4}, Ton J. Rabelink¹, Bernard M. van den Berg¹, in collaboration with the BEAT-COVID study group⁵

The Einthoven Laboratory for Vascular and Regenerative Medicine, department of Internal Medicine, Nephrology¹ and Thrombosis and Hemostasis², Leiden University Medical Center, Leiden, the Netherlands.

³Department of Physiology, Cardiovascular Research Institute Maastricht, Maastricht, the Netherlands

⁴MicroVascular Health Solutions LLC, Alpine, Utah, USA

⁵BEAT-COVID study group

Abstract

Accumulating evidence proves that endothelial dysfunction is involved in COVID-19 progression. We previously demonstrated that the endothelial surface glycocalyx has a critical role in maintenance of vascular integrity. Here we hypothesized that serum factors of severe COVID-19 patients affect the glycocalyx and result into endothelial dysfunction.

We included blood samples of 32 COVID-19 hospitalized patients at the Leiden University Medical Center: of which 26 from intensive care unit (ICU), 6 non-ICU, 18 convalescent samples 6 weeks after hospital discharge, and of 12 age-matched healthy donors (control) during the first period of the outbreak. First, we determined endothelial (angiopoietin 2, ANG2) and glycocalyx degradation (soluble thrombomodulin, sTM and syndecan-1, sSDC1) markers in plasma.

In plasma of COVID-19 patients, circulating ANG2 and sTM were elevated in patients on the ICU. Primary lung microvascular endothelial cells (HPMEC) and human glomerular microvascular ECs (GEnCs) cultures in the presence of these sera led to EC glycocalyx degradation, barrier disruption, inflammation and increased coagulation on the endothelial surface, significantly different compared to healthy control and non-ICU patient sera. These changes all could be restored in the presence of fucoidan.

In conclusion, our data highlight the link between endothelial glycocalyx degradation, barrier failure and induction of a procoagulant surface in COVID-19 patients on ICU which could be targeted earlier in disease by the presence of heparan sulfate (HS) mimetics.

Keywords: SARS-CoV-2 disease, COVID-19, endothelial dysfunction, glycocalyx, endothelial barrier, coagulation, fucoidan

Introduction

The coronavirus disease 2019 (COVID-19) caused by severe acute respiratory syndrome coronavirus-2 (SARS-CoV-2) has rapidly spread worldwide that lead to an unprecedented global pandemic since late 2019 [1]. Most of the COVID-19 cases are asymptomatic or cause only mild illness [2]. However, in a considerable proportion of patients, respiratory illness that require hospitalization occurred, which might develop into progressive disease and lead to hypoxemic respiratory failure, requiring long-term ventilatory support [3, 4]. Besides severe respiratory symptoms during hospitalization at the intensive care unit (ICU), a high incidence of thromboembolism events was observed [5]. Acute respiratory distress syndrome and coagulopathy are leading causes of COVID-19 patient mortality [6], while endothelial dysfunction is reported to be involved in both acute respiratory distress syndrome (ARDS) and coagulopathy [7, 8]. Consistent with autopsy findings that severe lung endothelial injury was observed in patients who succumbed to COVID-19 [9], COVID-19 could be considered as a vascular disease and vascular dysfunction might play a critical role in the pathogenesis of ARDS and coagulopathy.

The glycocalyx is a key regulator of endothelial cell integrity and homeostasis, it regulates vascular barrier permeability, prevents inflammation and ensures vessel patency [10-13]. It's a gel-like layer composed of the glycosaminoglycans heparan sulfate, hyaluronan (HA), chondroitin sulfate, and associated proteins, that covers the luminal surface of vascular endothelial cells [14]. Inflammation-induced glycocalyx degradation can lead to hyperpermeability of blood vessels, vasodilation disorders, microvascular thrombosis and increased leukocyte adhesion [15]. In previous studies, glycocalyx destruction and dysfunction was observed in sepsis, acute kidney injury and ARDS, and was associated with worse patient outcome [15, 16]. Recently, it was reported that the endothelial glycocalyx-degrading enzyme heparanase contributed to vascular leakage and inflammation, and its activity was associated with disease severity in COVID-19 patients [11, 17]. Meanwhile, the MYSTIC study also provided evidence that glycocalyx health, as measured by changes in the perfused boundary region (PBR), was a predictive prognostic

marker for COVID-19 septic patients [18].

Here we test whether preservation of the endothelial glycocalyx might be an effective intervention to improve vascular health. For this, we examined the possible beneficial effects of the heparan sulfate mimetic fucoidan [19], in restoring the endothelial functionality.

Material and methods

For detailed information see supplemental information

BEAT-COVID cohort study population and study design

A prospective observational cohort study was set up, in which patients with PCR-confirmed SARS-CoV-2 infection after hospital admission were recruited from April 2020 until August 2020, before the use of medication such as dexamethasone and vaccines were implemented (supplementary figure S1). Plasma and serum samples were collected from 32 patients, of which 26 were hospitalized in the ICU and 6 in a non-ICU medical floor. In 18 of the 32 included patients, follow-up data was obtained 6 weeks after discharge from the hospital. In addition, samples of 12 age-matched controls were obtained. Patient characteristics are shown in supplementary Table 1. Due to the limited amount of material per sample that could be obtained pooled sera were used in some experiments as indicated. The trial was registered in the Dutch Trial Registry (NL8589). 12 Age-matched healthy donors with a male: female ratio of 2:1, were included after confirmed negative SARS-CoV-2 IgG. Ethical approval was obtained from the Medical Ethical Committee Leiden-Den Haag-Delft (NL73740.058.20).

Circulating markers of endothelial dysfunction and glycocalyx shedding

Plasma samples were used to measure angiotensin 2 (Ang-2, DANG20, R&D Systems, Abingdon, UK), soluble thrombomodulin (sTM, M850720096, Diaclone, Besançon, France) and soluble syndecan-1 (sSDC1, DY2780, R&D Systems) according to manufacturer's respective protocols.

Endothelial barrier function assay

Endothelial barrier function analysis was performed with impedance-based cell monitoring using the electric cell-substrate impedance sensing system (ECIS Z θ , Applied Biophysics, New York, USA). ECIS plates (96W20idf PET, Applied Biophysics) were pre-treated with 10 mM L-cysteine and coated with 1% gelatine for primary human glomerular microvascular ECs (GEnCs; ACBRI-128, Cell Systems, Kirkland, WA, USA) or without 1% gelatine for primary pulmonary microvascular endothelial cells (HPMECs; PromoCell, Heidelberg, Germany). HPMECs (p5) were seeded at a concentration of 4.5×10^5 cells/well and for GEnCs (p5), the concentration was 3×10^5 cells/well in EGM medium (basal medium MV, C-22220, PromoCell) supplemented with C-39220 (PromoCell) and 1% antibiotics (penicillin/streptomycin, 15070063, Gibco, Paisley, UK) at 37°C and 5% CO₂.

Initial baseline resistance was measured for 2 hours before endothelial cells were seeded into the plate. Multiple frequency/time mode was used for the real-time assessment of the barrier function. Once the stable monolayer was formed, endothelial cells were incubated with 10% serum (healthy (n=12), COVID-19 non-ICU (n=8) and ICU (n=26)) and measured for 20 hours. Afterwards, modelling data R_b which represents barrier function could be generated.

In additional experiments, HPMECs were exposed to 10% healthy serum (n=12), COVID-19 ICU serum (n=26) with or without fucoidan (10 μ g/mL, gift from MicroVascular Health

Solutions LLC, Alpine, UT, USA). The natural fucoidan provided (Iso 9000 and GMP certified from Omnipharm, S.A.S, Chambéry, France) was extracted from *Laminaria japonica* as a powder of 91.20% purity and further tested, for instance, on the presence of heavy metals (arsenic, lead, cadmium, mercury) or microbiology parameters (European Pharmacopoeia VIII, Ed 2,6,12: total plate count, yeast, mold, *E. coli*, *Salmonella spp.*). A 50x times stock solution was prepared by dissolving the appropriate amount of powder in milliQ water and passed through a 0.22µm filter before use.

RNA isolation and RT-PCR

RNA of cultured cells is isolated using RNeasy Mini Kit (74106, Qiagen, Venlo, The Netherlands) according to manufacturer's protocol RT-PCR analysis was conducted using SYBR Select Master Mix (4472908, Applied Biosystems, Landsmeer, The Netherlands) and specific primers as indicated in supplementary table s2. Gene expression was normalized to GAPDH of 5 separate experiments.

Immunoblotting analysis

Western blots were performed from protein extracts of HPMECs [12]. 10% Mini-PROTEAN® TGX™ Protein Gels (4561031, Bio-Rad Laboratories, Veenendaal, The Netherlands) were used for protein size separation and proteins were transferred to PVDF membranes (1704156, Bio-Rad). Membranes were blocked in 5% milk in PBST at room temperature for 1 hour and further incubated with primary antibody rabbit anti-human ICAM1 (4915, Cell Signalling Technology), rabbit anti-human total NF-κB p65 (8242, Cell Signalling Technology), rabbit anti-human phosphor-NF-κB p65 (Ser536) (3033, Cell Signalling Technology) or mouse anti-human GAPDH (MA5-15738, ThermoFisher) overnight at 4°C. Protein was detected using HRP-conjugated antibody (P0447 and P0448,

Dako, Amstelveen, The Netherlands) and Western Lightning Plus-ECL, Enhanced Chemiluminescence Substrate (NEL103001EA, PerkinElmer, Groningen, The Netherlands). Intensity of the bands were analysed using ImageJ software. Relative intensity was determined by levels of GAPDH.

Immunofluorescence of cultured cells

HPMECs (p5) were cultured in 8-well chamber slides (ibiTreat, μ -Slide 8 Well). Confluent monolayers were incubated with 10% pooled serum (healthy control (pooled n = 12), non-ICU (pooled n = 8) and ICU (pooled n = 26) in no FCS medium for 24 hours. Next, cells were fixed with 4% PFA and 0.2% Triton-X100 in HBSS or 4% PFA in HBSS (for HS and LEA staining) for 10 minutes at room temperature, blocked with 3% goat serum in HBSS and incubated with FITC labelled *Lycopersicon esculentum* (LEA-FITC, L0401, Sigma, Houten, The Netherlands), Mouse Anti-Human VE cadherin (55-7H1; BD Biosciences), Mouse Anti-heparan sulfate (10E4, 370255-1, AMSBIO, Abingdon, UK) or Mouse Anti-TM (MA5-11454, ThermoFisher) at 4°C overnight, followed by an appropriate secondary antibody and phalloidin-TRITC (VE-cadherin samples) for 1 hour. Finally, Hoechst 33528 (1/1,000) was added and cells using a LEICA SP8 WLL confocal microscope (Leica, Rijswijk, the Netherlands). Fluorescent images were analysed using Image J software. Quantification is described in Supplementary info.

FX activation by extrinsic tenase complex (TF-FVIIa)

Confluent HPMECs were incubated with 10% control (n=12), COVID-19 non-ICU (n=8) and ICU serum (n=26, with or without presence of fucoidan) in no FCS medium for 24 hours. Cell culture supernatants were collected and centrifuged for ELISA assays. Factor VIIa (80 μ L, 10 nM, HCVIIA-0031, Haematologic Technologies, Huissen, The Netherlands) was

added and incubated for 15 minutes at 37°C and 5%CO₂. The reaction was initiated by adding factor X (80 µL, 400 nM, HCX-0050, Haematologic Technologies) to detect the production of active factor X. Aliquots were quenched in HBS supplemented with 50mM EDTA to stop the reaction and determined by SpecXa conversion (250 µM), at 405 nm.

Thrombin generation Assay

Confluent HPMECs were incubated with 10% healthy (n=12), COVID-19 non-ICU (n=8) and ICU serum (n=26, with or without presence of fucoidan) in no FCS medium for 24 hours. Thrombin generation curves were obtained by supplementing normal pooled plasma. Thrombin formation was initiated by adding substrate buffer (FluCa-kit, 86197, Thrombinoscope BV, Leiden, The Netherlands) to the plasma. Thrombin formation was determined using Thrombinoscope software.

Markers of endothelial dysfunction and glycocalyx shedding in cell cultured supernatant

Supernatants collected were used to measure Ang-2, sTM, IL-6 (M9316, Sanquin, Amsterdam, The Netherlands) and VWF (A0082, Dako).

Statistics

Data are presented as mean ± SD, unless indicated otherwise. For all experiments, 3 to 5 independent experiments were performed. Shapiro-Wilk test and Levene test were performed to evaluate the normality and variances first. Then non-paired/paired 2-tailed t test were used to assess the differences between two groups. One-way ANOVA followed by Tukey's multiple comparisons test and Kruskal-Wallis test followed by Dunn's multiple comparisons test were assessed for multiple groups. Statistical analysis were performed

using SPSS statistical software version 25 (SPSS Inc., Chicago, IL) and GraphPad Prism version 8 (Graphpad Inc., La Jolla, CA, USA). A significance level of 0.05 was considered statistically significant.

Results

COVID-19 leads to endothelial dysfunction and glycocalyx degradation

Overall endothelial health in COVID-19 patients was assessed by measuring plasma ANG2 concentrations which were found to be significantly increased in COVID-19 patients on the ICU (figure 1a). ANG2 levels of non-ICU patients were not distinguishable from control levels or recovered patients 6 weeks after discharge. Circulating fragments of thrombomodulin (sTM), one of the glycocalyx components, were also markedly increased in COVID-19 ICU patients compared to healthy controls, non-ICU patients, and after recovery (figure 1b). Shedding of the glycocalyx core protein, syndecan-1 (sSDC1), was found not to be significantly raised in COVID-19 ICU patients in comparison to healthy controls or non-ICU patients (figure 1c). Pearson's correlation between each of 2 markers was analysed and showed that ANG2 moderately correlated with sTM and sSDC1 ($R=0.49$, $p<0.0001$ and $R=0.33$, $p=0.015$ respectively), and sTM positively correlated with sSDC1 ($R=0.50$, $p=0.0002$) indicating that endothelial dysfunction could lead to glycocalyx shedding (figure 1d-f).

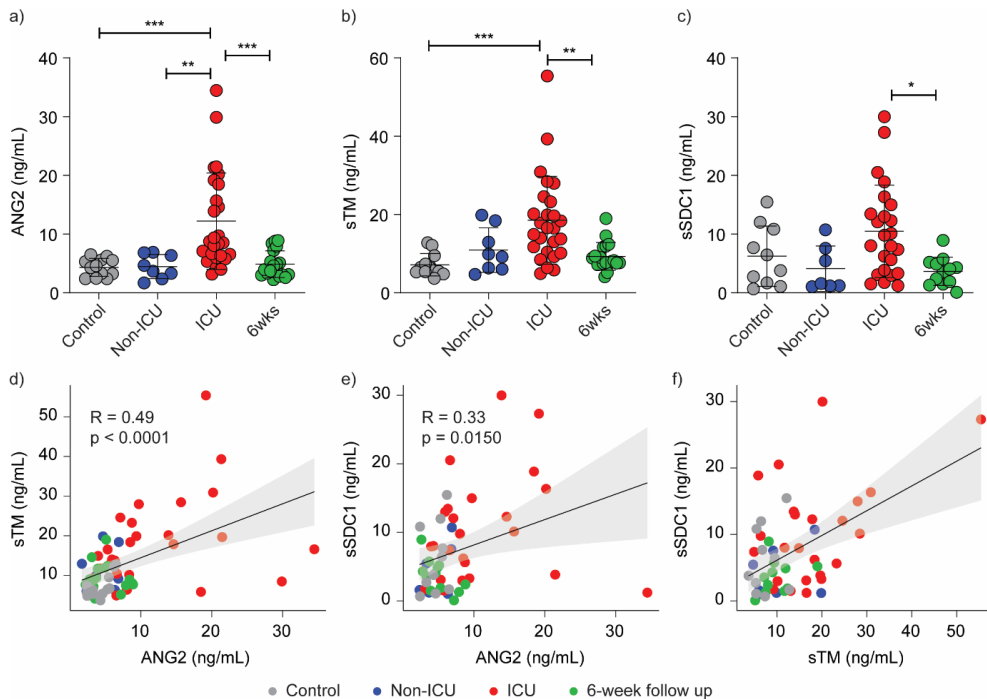


Figure 1 Comparison and association of endothelial dysfunction and glycocalyx shedding related markers in COVID-19 patients and healthy controls. Levels of a) angiotensin 2 (ANG2), b) soluble thrombomodulin (sTM) and c) soluble syndecan-1 (sSDC1) between healthy controls (grey, n = 12), COVID-19 non-ICU patients (blue, n = 8), COVID-19 ICU patients (red, n = 26) and recovered patients (green, n = 18). Pearson's correlation between d) ANG2 and sTM, e) ANG2 and sSDC1, f) sTM and sSDC1. Graphs represent the mean \pm SD. One-way ANOVA followed by Tukey's multiple comparisons test and Pearson's correlation analysis were performed; * $p < 0.05$, ** $p < 0.01$, *** $p < 0.001$.

Endothelial glycocalyx degradation in presence of COVID-19 ICU serum

To determine the effect of systemic blood factors during COVID-19 disease on endothelial surface glycocalyx expression, HPMECs were cultured in the presence of 10% pooled serum of either healthy controls, COVID-19 non-ICU and COVID-19 ICU patients for 24 hours and stained for overall glycocalyx presence (LEA-FITC), for heparan sulfates (HS) and thrombomodulin (TM). The COVID-19 ICU group showed a marked reduced surface

expression of LEA-FITC (figure 2a,b), TM (figure 2a,c) and HS (figure S2a,b), compared to healthy control- and COVID-19 non-ICU groups.

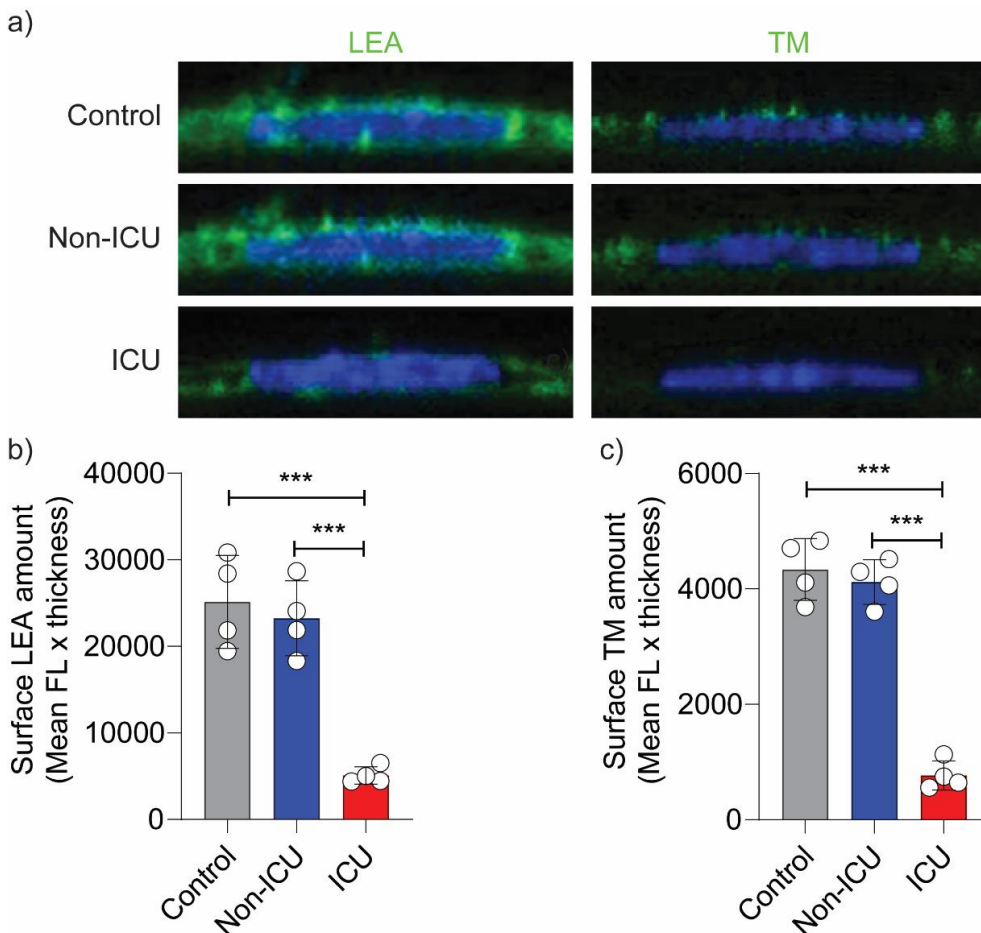


Figure 2 Loss of glycofocalyx in primary human pulmonary microvascular endothelial cells in presence of serum of COVID-19 patients on ICU. a) Representative fluorescence confocal images of *Lycopersicon esculentum*-FITC (LEA) or anti-thrombomodulin (TM) staining on the surface of primary human pulmonary microvascular endothelial cells (HPMECs) in the presence of 10% serum of pooled- healthy controls (n = 12), COVID-19 non-ICU (n = 8) and COVID-19 ICU (n = 26) samples for 24hrs. HPMEC surface expression quantification of b) LEA-FITC and c) TM in the presence of 10% pooled- healthy control , COVID-19 non-ICU and COVID-19 ICU serum for 24hrs All values are given as mean \pm SD of 4 independent experiments. One-way ANOVA followed by Tukey's multiple

comparisons test was performed; *** $p < 0.001$.

COVID-19 ICU serum induced loss of endothelial cell barrier function

Next, the ability of COVID-19 serum to disrupt the barrier integrity of primary human microvascular endothelial cells was tested. In contrast to healthy controls and COVID-19 non-ICU patients, serum from COVID-19 ICU patients induced a reduction in resistance of both HPMECs and GEnCs (figure 3a,c). The calculated areas under curve for the final 15 hours, showed that the COVID-19 ICU samples were significantly below healthy control samples, especially in HPMECs (figure 3b,d). The modelling value for barrier function, R_b , representing cell-cell-contacts, resulted in a similar reduction upon exposure to serum of COVID-19 ICU patients (figure 3e-h). Interestingly, we could find differences in vascular bed susceptibility in response to COVID-19 ICU patient sera, showing that the lung originating HPMECs were more sensitive than the kidney isolated GEnCs. While resistance and barrier function decreased in HPMECs during the entire incubation time, in GEnCs, both factors started to recover after 15 hours (figure 3a,c,e,g). Reduction of VE-cadherin, together with reduced cellular junction area, and increasing stress fibre formation in response to COVID-19 ICU patient serum in comparison to COVID-19 non-ICU and healthy control sera confirmed this EC barrier loss (figure 3i,j). This observed barrier function reduction correlated with the increased plasma levels of ANG2, sTM and sSDC1, linking EC activation and glycocalyx shedding to possible endothelial loss of barrier function in patients (figure 3k).

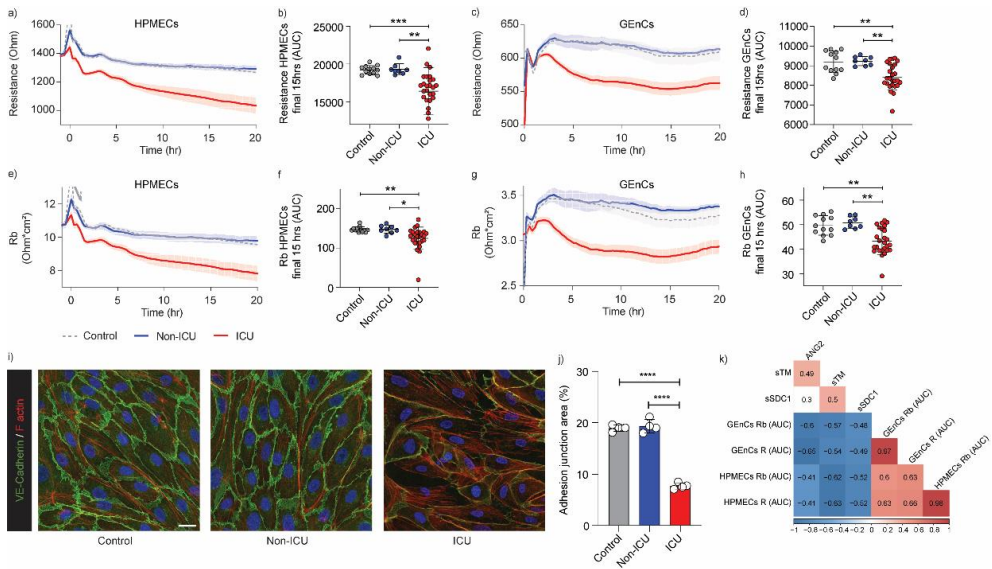


Figure 3 Serum mediators of COVID-19 patients on ICU induce microvascular barrier disruption. Barrier integrity parameter, resistance of a + b) primary human pulmonary microvascular endothelial cells (HPMECs) and c + d) primary human glomerular microvascular ECs (GENCs) assessed by electric cell-substrate impedance sensing system (ECIS Z0) in response to stimulation with 10% serum (at t=0hr) of healthy controls (n=12, grey dotted line), COVID-19 non-ICU (n=8, blue line) and COVID-19 ICU (n=26, red line). Cell-cell contact parameter, Rb of e + f) HPMECs and g + h) GENCs assessed by ECIS Z0 in response to stimulation with 10% serum (at t=0hr) of healthy controls (n=12, grey dotted line), COVID-19 non-ICU (n=8, blue line) and COVID-19 ICU (n=26, red line). In some cases, multiple samples (in ICU and out of ICU) from the same patient at different time points were obtained. Data of raw resistance and Rb values were shown and presented as mean \pm SEM. Quantification of barrier integrity was based on the measurements of area under curve over the final 15 hours of b) HPMECs and d) GENCs. Quantification of cell-cell contact was based on the measurements of area under curve over the final 15 hours of f) HPMECs and h) GENCs. i) Representative confocal images of VE-cadherin (green) and F-actin (red) staining on HPMECs in the presence of 10% pooled- healthy control (n = 12), COVID-19 non-ICU (n = 8) and COVID-19 ICU (n = 26) serum for 24hrs (scale bar = 20 μ m). j) Quantification of adhesion junction percentage of HPMECs in the presence of 10% pooled- healthy control, COVID-19 non-ICU and COVID-19 ICU serum for 24hrs of 4 independent experiments. Graphs represent the mean \pm SD. k) Pearson's correlation heatmap between endothelial dysfunction and glycocalyx shedding related markers (angiopoietin 2, soluble thrombomodulin and soluble syndecan-1) and barrier function related parameters (last 15hrs AUC of R and Rb in HPMECs and GENCs). Colours represent correlation, blue means negative correlation and red means positive correlation. Blank means no significance. One-way ANOVA followed by Tukey's multiple comparisons test

and Kruskal-Wallis test followed by Dunn's multiple comparisons test and were performed; * $p < 0.05$, ** $p < 0.01$, *** $p < 0.001$, **** $p < 0.0001$.

Fucoidan restores glycocalyx and ameliorates endothelial cell activation induced by COVID-19 serum

To test whether loss of surface glycocalyx could be restored, we cultured HPMECs in the presence of both ICU patient sera and the HS mimetic fucoidan (10 $\mu\text{g}/\text{mL}$).

Supplementation of fucoidan during culture in the presence of ICU serum dramatically restored the glycocalyx as was shown by LEA-FITC staining (figure 4a,b) and TM expression (figure 4a,c).

One of the mechanisms of glycocalyx loss is through enzymatic HS degradation by heparanase (HPSE-1), which is elevated in plasma of COVID-19 patients [17]. In our *in vitro* cultured HPMECs in the presence of 10% pooled patient or healthy control serum we observed significantly induced *HPSE-1* gene expression in cells from the ICU patient group without a change in the non-ICU group (supplementary figure S3a). Mechanistically, we observed that addition of fucoidan showed a trend of decreasing *HPSE-1* gene expression (supplementary figure S3a) in the ICU patient group, which coincided with reduced syndecan-1 gene expression (*SDC1*) and was significantly restored after fucoidan supplementation (supplementary figure S3b).

Further evaluation of endothelial cell dysfunction in the presence of patient sera showed that compared to healthy controls, gene expression of *ANGPT2*, *ICAM-1* and *IL-6* were significantly up regulated in the presence of COVID-19 ICU sera (figure S3c-e), while no effect was found with COVID-19 non-ICU samples. At protein level, ICAM-1 expression was also increased in presence of COVID-19 ICU serum (figure 4d,e). Since endothelial activation could induce NF κ B activation, we then detected the NF κ B phosphorylation levels and found a marked activation of these factors in ECs in the presence of COVID19 ICU sera, without significant changes between healthy control, COVID-19 non-ICU and

fucoïdan supplementation groups (figure 4d,f). This increased endothelial activation was further corroborated by the induced amount of released von Willebrand factor (VWF) and ANG2, from the Weibel-Palade bodies (WPBs) upon activation and secretion of IL-6 and shedding of sTM by these cells (supplementary figure S4). When comparing the response on individual patient serum level, fucoïdan reduced these markers significantly (figure 4g-j), in line with the observed normalization of ICAM-1 expression (figure 4d,e).

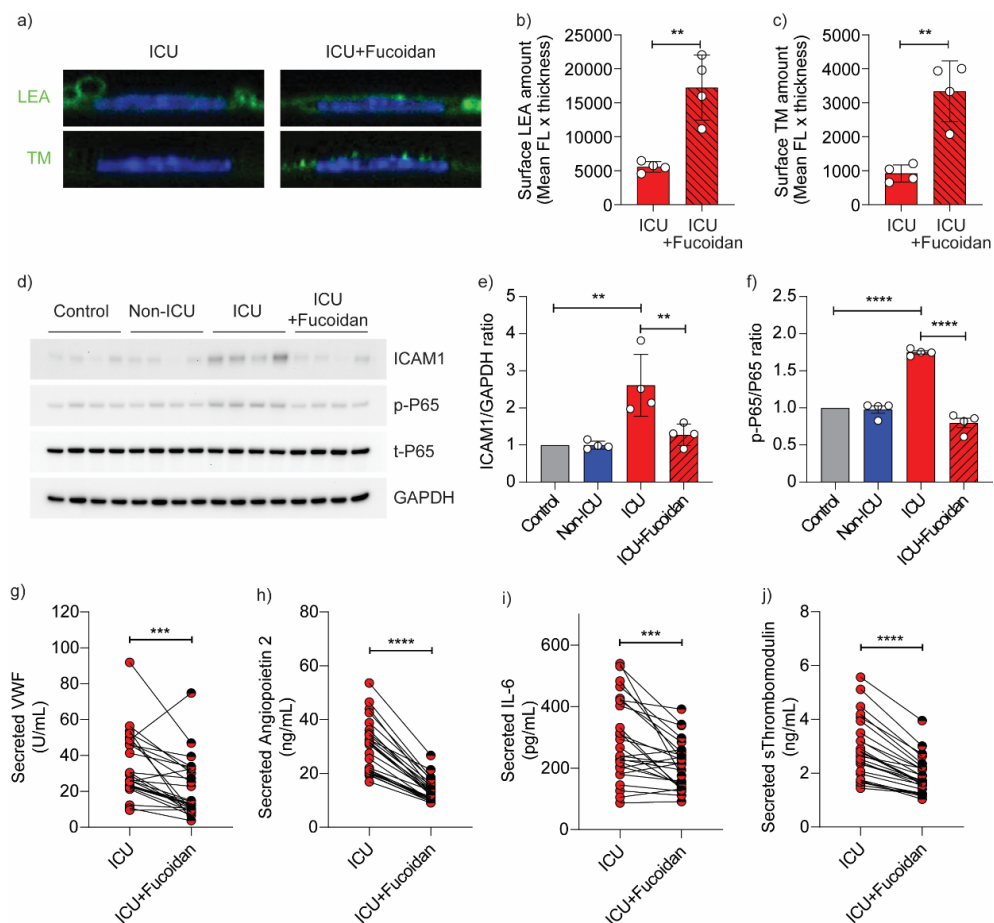


Figure 4 Fucoïdan restores glycocalyx thickness on HPMECs and reduces endothelial activation. a) Representative confocal images of *Lycopersicon esculentum*-FITC (LEA) or anti-thrombomodulin (TM) staining on the surface of primary human pulmonary microvascular endothelial cells (HPMECs) in the presence of 10% pooled COVID-19 ICU (n

= 26) serum with and without fucoidan (10 µg/mL) for 24hrs. Quantification of HPMECs surface b) LEA and c) TM expression in the presence of 10% pooled COVID-19 ICU serum with and without fucoidan (10 µg/mL) for 24hrs of 4 independent experiments. d) Western blot images of ICAM1, p-P65, t-P65 protein expression. Quantification of e) ICAM1/GAPDH ratio and f) p-P65/t-P65 ratio in HPMECs in response to 10% pooled-healthy control (n = 12), COVID-19 non-ICU (n = 8) and COVID-19 ICU (n = 26) serum with and without fucoidan (10 µg/mL) for 24hrs of 4 independent experiments, presented as fold change expression normalized to healthy control. Secreted g) VWF, h) angiotensin 2, i) IL6 and j) soluble thrombomodulin of HPMECs stimulated with 10% individual COVID-19 ICU sera (n = 26) with and without fucoidan (10 µg/mL) for 24hrs. One-way ANOVA followed by Tukey's multiple comparisons test, Kruskal-Wallis test followed by Dunn's multiple comparisons test and paired two-tailed Student t test were performed; *p<0.05, **p<0.01, ***p<0.001, ****p<0.0001.

Glycocalyx restoration could protect endothelial cell barrier function

As fucoidan supplementation could restore the glycocalyx and reduce inflammation we used ECIS to further investigate the effects of fucoidan on protection of the endothelial barrier function. After 24hrs of culturing the HPMECs with the various serum samples, addition of fucoidan had no effect during the first 7-8hrs. However, in the following time period, endothelial barrier integrity of HPMECs exposed to serum from COVID-19 ICU patients recovered significantly (figure 5a-d). Several samples even reached similar levels as control samples (figure 5b,d). Additionally, VE-cadherin and F-actin staining also showed a similar trend that fucoidan could strengthen the cell-cell contacts against COVID-19 ICU serum exposure (figure 5e,f).

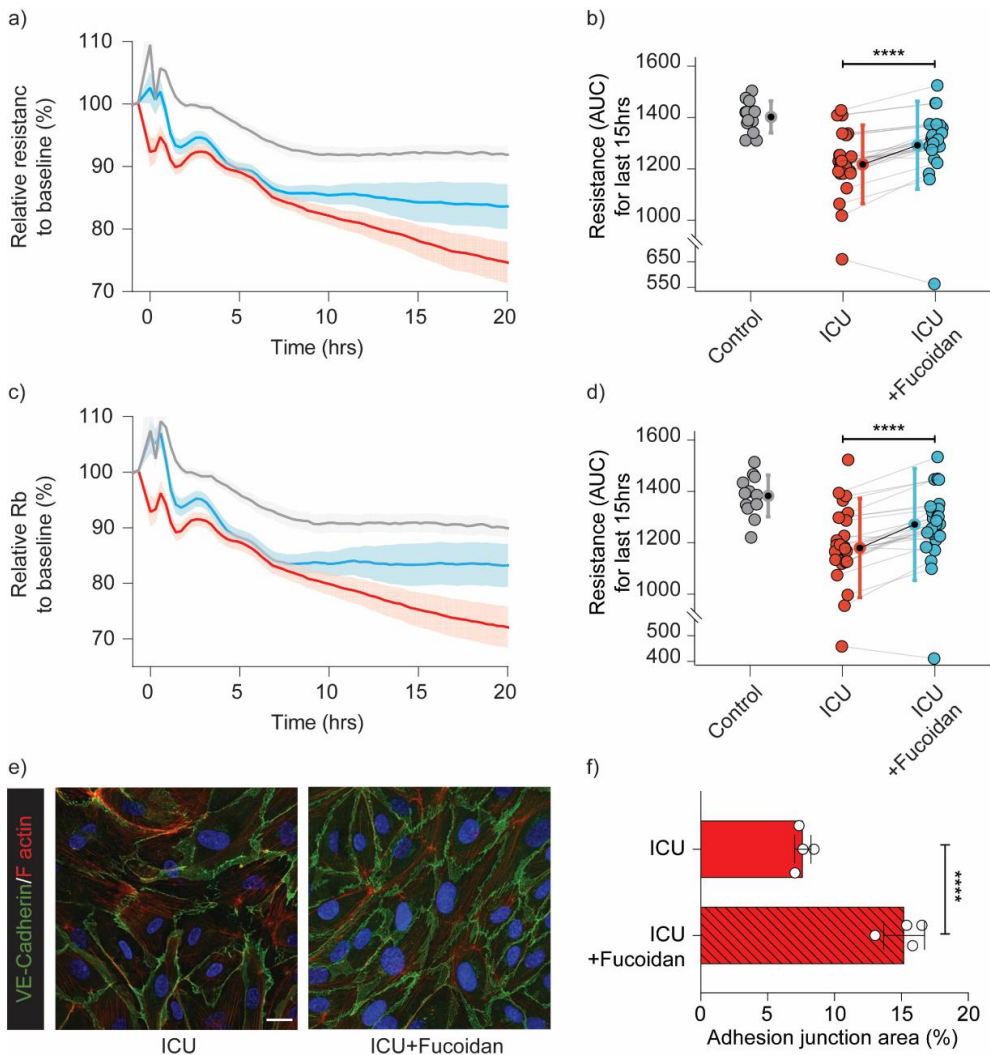


Figure 5 Fucoidan could ameliorate endothelial cell barrier function in presence of serum of COVID-19 ICU patients. a) Barrier integrity parameter, resistance of a) primary human pulmonary microvascular endothelial cells (HPMECs) assessed by ECIS in response to stimulation with 10% serum (at t=0hr) of healthy controls (n=12, grey line), COVID-19 ICU (n=26, red line) and COVID-19 ICU with fucoidan (n=26, blue line). Cell-cell contact parameter, Rb of c) primary human pulmonary microvascular endothelial cells (HPMECs) assessed by ECIS in response to stimulation with 10% serum (at t=0hr) of healthy controls (n=12, grey line), COVID-19 ICU (n=26, red line) and COVID-19 ICU with fucoidan (n=26, blue line). Data were normalized to the baseline resistance or Rb to calculate the relative resistance or Rb to baseline (%) and presented as mean \pm SEM. b) Quantification of barrier

integrity was based on the measurements of area under curve of final 15 hours. d) Quantification of cell-cell contact was based on the measurements of area under curve of final 15 hours. e) Representative confocal images of VE-cadherin (green) and F-actin (red) staining on HPMECs in the presence of 10% pooled COVID-19 ICU serum with and without fucoidan (10 µg/mL) for 24hr (scale bar = 20 µm). f) Quantification of adhesion junction percentage of HPMECs in the presence of 10% pooled COVID-19 ICU serum with and without fucoidan (10 µg/mL) for 24hr of 4 independent experiments. Graphs represent the mean ± SD. Nonpaired and paired two-tailed Student t test were performed; ****p<0.0001.

Fucoidan inhibits the formation of a procoagulant cell surface upon COVID-19 serum treatment

To test whether serum from COVID-19 ICU patient is capable of inducing a procoagulant cell surface, explaining the reported high incidence of (micro)thrombosis in COVID-19 ICU patients [20], we first examined tissue factor (TF) gene expression (*F3*) changes. Indeed, *F3* was significantly upregulated in COVID-19 ICU patient samples (supplementary figure S5a) and the presence of fucoidan normalized this expression again to control levels. Next, the production of factor Xa on endothelial cell surface was induced by 10% serum from healthy controls and COVID-19 patients (figure 6a) which resulted in a significant increase in factor Xa production in COVID-19 ICU samples compared to samples from healthy controls and COVID-19 non-ICU, indicating the formation of procoagulant cell surface (supplementary figure S5b,c). Consistent with the observed reduction in *F3* mRNA expression with fucoidan present, FX activation was considerably reduced within 1 hour and 2 hours (figure 6b,c).

Thrombin release (figure 6d), another product of the common coagulation pathway, was significantly increased in the COVID-19 ICU group, indicating serum from ICU patients could lead to EC hypercoagulable state (supplementary figure S5d). When comparing the COVID-19 ICU groups with and without fucoidan added, thrombin peak height, similar to the phenotype in Xa generation assay, showed a significant decrease in fucoidan treated COVID-19 ICU samples (figure 6f). Correlating FXa and thrombin generation with the

plasma levels of ANG2, sTM and sSDC1, we found there's a link between endothelial activation, glycocalyx degradation and EC surface coagulable state (figure 6g).

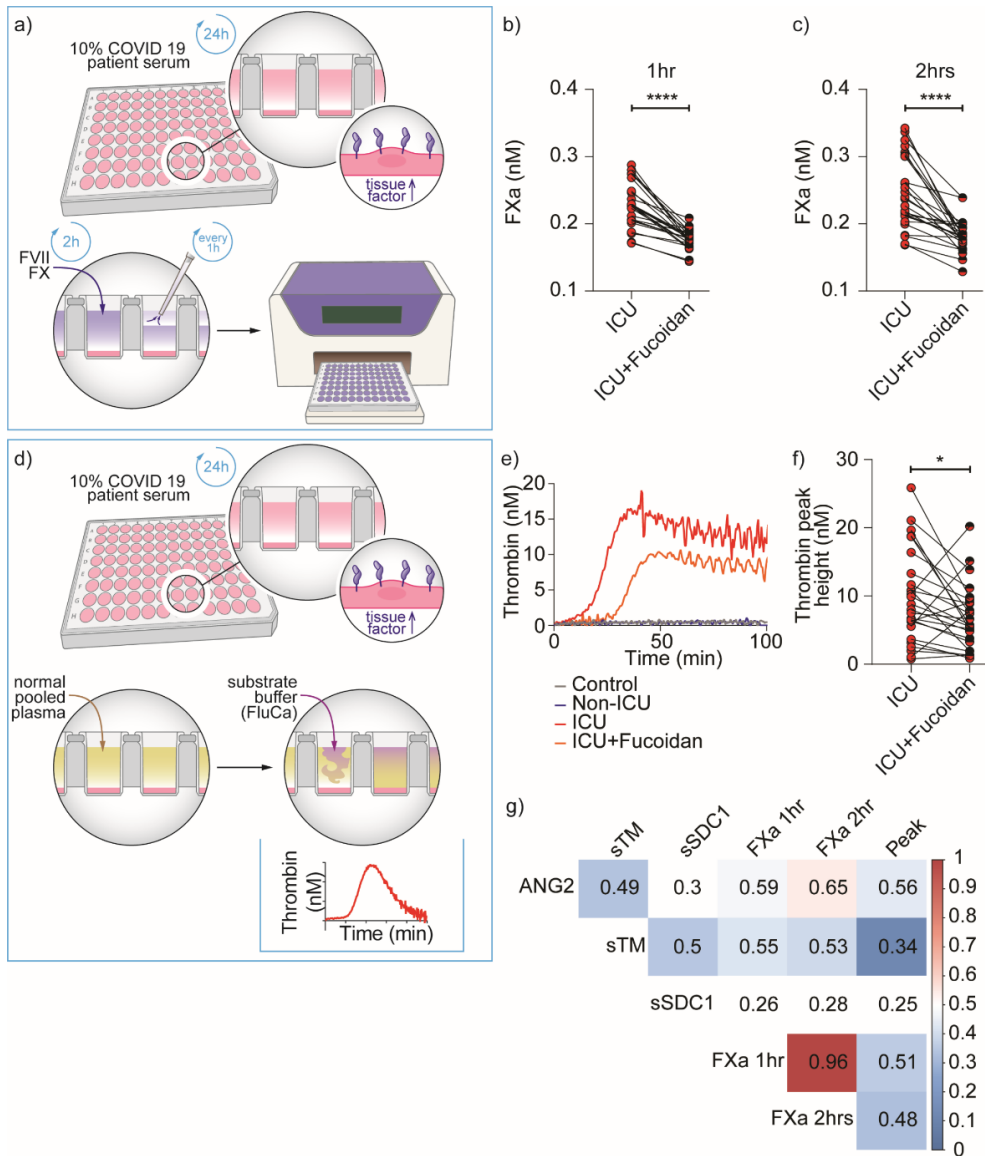


Figure 6 Fucoidan inhibits the formation of procoagulant cell surface in response to serum of COVID-19 ICU patients. a) Schematic overview showing how to detect FX activation on HPMEC cell surface in response to 10% healthy control or COVID-19 serum.

FXa production (nM) in b) first hour and c) second hour on HPMECs surface in the presence of 10% individual COVID-19 ICU sera (n = 26) with and without fucoidan (10 µg/mL) for 24hrs. d) Schematic overview showing how to detect thrombin generation on HPMECs cell surface in response to 10% healthy control or COVID-19 serum. e) Representative graph of thrombin generation assay in the presence of 10% healthy control, COVID-19 non-ICU, and COVID-19 ICU with and without fucoidan (same serum induced cell surface). f) Thrombin generation peak height (nM) measured on HPMECs surface in the presence of 10% individual COVID-19 ICU serum (n = 26) with and without fucoidan (10 µg/mL) for 24hrs. g) Pearson's correlation heatmap between endothelial dysfunction and glycocalyx shedding related markers (angiopoietin-2, soluble thrombomodulin and soluble syndecan-1) and coagulation assay parameters (FXa 1hr, FXa 2hr and thrombin peak height). Colours represent correlation, blue means negative correlated and red means positive correlated. Blank means no significance. Graphs represent the mean ± SD and paired two-tailed Student t test were performed; *p<0.05, ***p<0.0001.

Discussion

Our current study underpins the critical role for loss of the endothelial glycocalyx in severe COVID-19 infections. At a patient level, the endothelial activation marker ANG2 and glycocalyx shedding related markers sTM and sSDC1 were all increased in COVID-19 patients in ICU. At a cellular level, the loss of the endothelial glycocalyx induced by sera of these patients resulted in cellular activation, increased permeability and a hypercoagulable surface. Intervention with the HS-mimetic fucoidan restored not only the endothelial glycocalyx but subsequently reduced the endothelial activation state and restored the permeability barrier and anti-coagulant cell surface.

Increased circulating ANG2 levels have been associated with diminished respiratory function, increased coagulation activity, acute kidney injury and higher mortality in COVID-19 patients [18, 21-23]. Inhibition of the protective ANG1/TIE2 signalling cascade by ANG2 is a central regulator in protecting the vasculature against thrombus formation and vascular stabilization [24, 25]. Consistent with our findings, a decrease in plasma ANG2 levels upon recovery argues for ANG2 as a sensitive marker for acute endothelial dysfunction. The observed lower ANG2 levels in our study, together with the relative low

levels of sTM and sSDC1, in comparison to non-COVID-19 septic ICU patients, could argue that COVID-19 is a more locally presenting disease [26]. sTM has been reported to be associated with COVID-19 adverse outcome [27] and loss of endothelial surface TM was observed in COVID-19 lung autopsies [28]. We observed that once the microvascular lung endothelial cells were activated, the relatively highly expressed TM (supplementary figure S6) was shed, resulting in a procoagulant cell surface that indicates possible local vulnerability of lung microvessels.

We previously revealed that increased breakdown of HS by heparanase could lead to diminished glycocalyx coverage [29]. Further studies suggest that heparanase activity, the only mammalian enzyme which could degrade HS, was elevated in COVID-19 patients and associated with disease severity [17, 30]. Our observation of increased *HPSE-1* mRNA expression upon ICU COVID-19 serum treated ECs corresponded with reduced LEA-FITC, HS and TM surface expression [31], the induced upregulation of ANG2 and heparanase and loss of EC barrier function. These findings provide increasing evidence linking endothelial glycocalyx as an additional component of vascular barrier with the ANG/TIE2 signalling pathway to maintain EC homeostasis. Additionally, lung microvascular endothelial cells were more sensitive to COVID-19 ICU serum than glomerular microvascular endothelial cells, emphasizing that organs are differently affected by COVID-19 infection. Notably, the indirect effect by serum mediators, as was also suggested in recent papers [32, 33] in addition to possible direct viral infection, might contribute to patients' longer hospitalization or driving the disease progression to severe ARDS.

Coagulation disorder is often seen in COVID-19, especially in severe cases [34]. The endothelial glycocalyx is a crucial compartment for binding and regulating enzymes involved in the coagulation cascade [35]. Tissue factor is a primary trigger of extrinsic coagulation and plays an essential role in haemostasis, which is increased as a result of glycocalyx damage [36, 37]. Combining with our data, the increased endothelial *F3* expression corresponded with loss of the endothelial anticoagulant factors, such as TM, in

response to incubation with COVID-19 ICU patient serum. This may be a driver of COVID-19 related coagulopathy, which is corroborated by two different *ex vivo* assays (thrombin generation and Xa generation on endothelial cell surface).

Here we observed that restoration of glycocalyx components by fucoidan leads to reduction of endothelial activation through inactivation of NF κ B signalling pathway and downstream ICAM1 expression. Additionally, supplementary fucoidan induced endothelial barrier function recovery which might open a new therapeutic strategy to treat or prevent respiratory dysfunction. Moreover, fucoidan supplementation has beneficial effect for anticoagulation. First of all, fucoidan leads to EC surface TF reduction. Two preprint studies suggested that ANG2 has additional and direct effects on coagulation in COVID-19 [28, 38], and our data demonstrates that fucoidan has a strong effect on decreasing ANG2 expression, preventing TIE2 inactivation. These findings reveal that glycocalyx preservation has promising effects on controlling COVID-19 injury and our *in vitro* experiments show fucoidan as a novel HS mimetic could be a potential therapeutic substance.

Our study had some limitations due to the time of hospitalization of COVID-19 patients and official ethical approval. The present study only presents a limited group of patients who presented at the LUMC during the first wave before major changes in therapeutic interventions occurred, such as the inclusion of dexamethasone treatment. In addition, no non-COVID-19 ARDS ICU patients were included, limiting the attribution of our data as COVID-19 specific effects. However, similar lung mechanics and increased extravascular lung edema in COVID-19 related ARDS in comparison to non-COVID-19 ARDS have been found, indicating a similar contribution found in our study [39]. In addition, the Fucoidan we used in the present study, by itself was not intended to be for clinical use, but to exemplify possible glycocalyx restoring mechanisms and endothelial cell functionality.

In conclusion, our present study supports the concept that endothelial cell dysfunction and loss of endothelial glycocalyx might drive worse outcomes like ARDS or coagulopathy

in severe COVID-19 at later disease stage. Fucoidan restored the endothelial glycocalyx, ameliorated endothelial activation, which led to protection of endothelial barrier function and induced antithrombotic effects. Our findings support further validation whether glycocalyx preservation or restoration could prevent progression to severe COVID-19 and encourage more clinical trials to evaluate the efficacy of glycocalyx preservation for treatment of more severe forms of COVID-19.

Acknowledgements

We thank all patients and healthy volunteers for taking part in this study. The fucoidan, a main ingredient of the Endocalyx™ supplement (US patent # 9943572), is exclusively produced for MicroVascular Health Solutions LLC and was provided as a gift.

Author contributions

L. Yuan, T.J. Rabelink and B.M. van den Berg conceived and designed the study; L. Yuan, S. Chen, W.M.P.J. Sol and B.M. van den Berg performed experiments and original data collection; L. Yuan, T.J. Rabelink and B.M. van den Berg analysed and interpreted the data; L. Yuan, A.I.M. van der Velden, H. Vink, T.J. Rabelink and B.M. van den Berg edited and discussed the manuscript.

Support statement

This work was supported by the China Scholarship Council grant to L. Yuan (CSC number 201806270262) and BEAT-COVID funding by Leiden University Medical Center.

Availability of data and materials

All data and methods supporting the findings of this study are available from the corresponding author upon reasonable request.

Competing interests

The authors declare that they have no relevant financial interests or personal relationships.

Conflict of interest

L. Yuan reports support for the present manuscript received from the China Scholarship Council grant CSC number 201806270262. H. Vink is Chief Science Officer of MicroVascular Health Solutions LLC (Alpine, UT, USA) and reports the Endocalyx patent (number 9943572) granted to MicroVascular Health Solutions in 2018. The remaining authors have nothing to disclose.

Consent for publication

The manuscript was approved by all authors for publication.

Reference

1. Cascella M, Rajnik M, Aleem A, Dulebohn SC, Di Napoli R. Features, Evaluation, and Treatment of Coronavirus (COVID-19). StatPearls, Treasure Island (FL), 2021.
2. Huang C, Wang Y, Li X, Ren L, Zhao J, Hu Y, Zhang L, Fan G, Xu J, Gu X, Cheng Z, Yu T, Xia J, Wei Y, Wu W, Xie X, Yin W, Li H, Liu M, Xiao Y, Gao H, Guo L, Xie J, Wang G, Jiang R, Gao Z, Jin Q, Wang J, Cao B. Clinical features of patients infected with 2019 novel coronavirus in Wuhan, China. *Lancet* 2020; 395(10223): 497-506.
3. Ferrando C, Suarez-Sipmann F, Mellado-Artigas R, Hernandez M, Gea A, Arruti E, Aldecoa C, Martinez-Palli G, Martinez-Gonzalez MA, Slutsky AS, Villar J, Network C-SI. Clinical features, ventilatory management, and outcome of ARDS caused by COVID-19 are

similar to other causes of ARDS. *Intensive Care Med* 2020; 46(12): 2200-2211.

4. Grasselli G, Zangrillo A, Zanella A, Antonelli M, Cabrini L, Castelli A, Cereda D, Coluccello A, Foti G, Fumagalli R, Iotti G, Latronico N, Lorini L, Merler S, Natalini G, Piatti A, Ranieri MV, Scandroglio AM, Storti E, Cecconi M, Pesenti A, Network C-LI. Baseline Characteristics and Outcomes of 1591 Patients Infected With SARS-CoV-2 Admitted to ICUs of the Lombardy Region, Italy. *JAMA* 2020; 323(16): 1574-1581.
5. Cui S, Chen S, Li X, Liu S, Wang F. Prevalence of venous thromboembolism in patients with severe novel coronavirus pneumonia. *J Thromb Haemost* 2020; 18(6): 1421-1424.
6. Zhou F, Yu T, Du R, Fan G, Liu Y, Liu Z, Xiang J, Wang Y, Song B, Gu X, Guan L, Wei Y, Li H, Wu X, Xu J, Tu S, Zhang Y, Chen H, Cao B. Clinical course and risk factors for mortality of adult inpatients with COVID-19 in Wuhan, China: a retrospective cohort study. *Lancet* 2020; 395(10229): 1054-1062.
7. Vassiliou AG, Kotanidou A, Dimopoulou I, Orfanos SE. Endothelial Damage in Acute Respiratory Distress Syndrome. *Int J Mol Sci* 2020; 21(22).
8. Vallet B, Wiel E. Endothelial cell dysfunction and coagulation. *Crit Care Med* 2001; 29(7 Suppl): S36-41.
9. Ackermann M, Verleden SE, Kuehnel M, Haverich A, Welte T, Laenger F, Vanstapel A, Werlein C, Stark H, Tzankov A, Li WW, Li VW, Mentzer SJ, Jonigk D. Pulmonary Vascular Endothelialitis, Thrombosis, and Angiogenesis in Covid-19. *N Engl J Med* 2020; 383(2): 120-128.
10. van den Berg BM, Wang G, Boels MGS, Avramut MC, Jansen E, Sol W, Lebrin F, van Zonneveld AJ, de Koning EJP, Vink H, Grone HJ, Carmeliet P, van der Vlag J, Rabelink TJ. Glomerular Function and Structural Integrity Depend on Hyaluronan Synthesis by Glomerular Endothelium. *J Am Soc Nephrol* 2019; 30(10): 1886-1897.
11. Rabelink TJ, van den Berg BM, Garsen M, Wang G, Elkin M, van der Vlag J. Heparanase: roles in cell survival, extracellular matrix remodelling and the development of kidney disease. *Nature reviews Nephrology* 2017; 13(4): 201-212.
12. Wang G, Kostidis S, Tiemeier GL, Sol W, de Vries MR, Giera M, Carmeliet P, van den Berg BM, Rabelink TJ. Shear Stress Regulation of Endothelial Glycocalyx Structure Is Determined by Glucobiosynthesis. *Arteriosclerosis, thrombosis, and vascular biology* 2020; 40(2): 350-364.
13. Wang G, de Vries MR, Sol W, van Oeveren-Rietdijk AM, de Boer HC, van Zonneveld AJ, Quax PHA, Rabelink TJ, van den Berg BM. Loss of Endothelial Glycocalyx Hyaluronan Impairs Endothelial Stability and Adaptive Vascular Remodeling After Arterial Ischemia. *Cells* 2020; 9(4).
14. Boels MG, Lee DH, van den Berg BM, Dane MJ, van der Vlag J, Rabelink TJ. The endothelial glycocalyx as a potential modifier of the hemolytic uremic syndrome.

European journal of internal medicine 2013; 24(6): 503-509.

15. Uchimido R, Schmidt EP, Shapiro NI. The glycocalyx: a novel diagnostic and therapeutic target in sepsis. *Critical care* 2019; 23(1): 16.
16. Rovas A, Sackarnd J, Rossaint J, Kampmeier S, Pavenstadt H, Vink H, Kumpers P. Identification of novel sublingual parameters to analyze and diagnose microvascular dysfunction in sepsis: the NOSTRADAMUS study. *Critical care* 2021; 25(1): 112.
17. Buijsers B, Yanginlar C, de Nooijer A, Grondman I, Maciej-Hulme ML, Jonkman I, Janssen NAF, Rother N, de Graaf M, Pickkers P, Kox M, Joosten LAB, Nijenhuis T, Netea MG, Hilbrands L, van de Veerdonk FL, Duivenvoorden R, de Mast Q, van der Vlag J. Increased Plasma Heparanase Activity in COVID-19 Patients. *Frontiers in immunology* 2020; 11: 575047.
18. Rovas A, Osiaevi I, Buscher K, Sackarnd J, Tepassee PR, Fobker M, Kuhn J, Braune S, Gobel U, Tholking G, Groschel A, Pavenstadt H, Vink H, Kumpers P. Microvascular dysfunction in COVID-19: the MYSTIC study. *Angiogenesis* 2021; 24(1): 145-157.
19. Wang J, Zhang Q, Zhang Z, Zhang H, Niu X. Structural studies on a novel fucogalactan sulfate extracted from the brown seaweed *Laminaria japonica*. *International journal of biological macromolecules* 2010; 47(2): 126-131.
20. McFadyen JD, Stevens H, Peter K. The Emerging Threat of (Micro)Thrombosis in COVID-19 and Its Therapeutic Implications. *Circ Res* 2020; 127(4): 571-587.
21. Vassiliou AG, Keskinidou C, Jahaj E, Gallos P, Dimopoulou I, Kotanidou A, Orfanos SE. ICU Admission Levels of Endothelial Biomarkers as Predictors of Mortality in Critically Ill COVID-19 Patients. *Cells* 2021; 10(1).
22. Henry BM, de Oliveira MHS, Cheruiyot I, Benoit JL, Cooper DS, Lippi G, Le Cras TD, Benoit SW. Circulating level of Angiopoietin-2 is associated with acute kidney injury in coronavirus disease 2019 (COVID-19). *Angiogenesis* 2021.
23. Smadja DM, Guerin CL, Chocron R, Yatim N, Boussier J, Gendron N, Khider L, Hadjadj J, Goudot G, Debuc B, Juvin P, Hauw-Berlemont C, Augy JL, Peron N, Messas E, Planquette B, Sanchez O, Charbit B, Gaussem P, Duffy D, Terrier B, Mirault T, Diehl JL. Angiopoietin-2 as a marker of endothelial activation is a good predictor factor for intensive care unit admission of COVID-19 patients. *Angiogenesis* 2020; 23(4): 611-620.
24. Lovric S, Lukasz A, Hafer C, Kielstein JT, Haubitz M, Haller H, Kumpers P. Removal of elevated circulating angiopoietin-2 by plasma exchange--a pilot study in critically ill patients with thrombotic microangiopathy and anti-glomerular basement membrane disease. *Thromb Haemost* 2010; 104(5): 1038-1043.
25. Higgins SJ, De Ceunynck K, Kellum JA, Chen X, Gu X, Chaudhry SA, Schulman S, Libermann TA, Lu S, Shapiro NI, Christiani DC, Flaumenhaft R, Parikh SM. Tie2 protects the vasculature against thrombus formation in systemic inflammation. *J Clin Invest* 2018:

128(4): 1471-1484.

26. Bhatraju PK, Morrell ED, Zelnick L, Sathe NA, Chai XY, Sakr SS, Sahi SK, Sader A, Lum DM, Liu T, Koetje N, Garay A, Barnes E, Lawson J, Cromer G, Bray MK, Pipavath S, Kestenbaum BR, Liles WC, Fink SL, West TE, Evans L, Mikacenic C, Wurfel MM. Comparison of host endothelial, epithelial and inflammatory response in ICU patients with and without COVID-19: a prospective observational cohort study. *Crit Care* 2021; 25(1): 148.

27. Goshua G, Pine AB, Meizlish ML, Chang CH, Zhang H, Bahel P, Baluha A, Bar N, Bona RD, Burns AJ, Dela Cruz CS, Dumont A, Halene S, Hwa J, Koff J, Menninger H, Neparidze N, Price C, Siner JM, Tormey C, Rinder HM, Chun HJ, Lee AI. Endotheliopathy in COVID-19-associated coagulopathy: evidence from a single-centre, cross-sectional study. *Lancet Haematol* 2020; 7(8): e575-e582.

28. Schmaier AA, Hurtado GP, Manickas-Hill ZJ, Sack KD, Chen SM, Bhambhani V, Quadir J, Nath AK, Collier AY, Ngo D, Barouch DH, Gerszten RE, Yu XG, Collection MC-, Processing T, Peters K, Flaumenhaft R, Parikh SM. Tie2 activation protects against prothrombotic endothelial dysfunction in COVID-19. *medRxiv* 2021.

29. Boels MG, Avramut MC, Koudijs A, Dane MJ, Lee DH, van der Vlag J, Koster AJ, van Zonneveld AJ, van Faassen E, Grone HJ, van den Berg BM, Rabelink TJ. Atrasentan Reduces Albuminuria by Restoring the Glomerular Endothelial Glycocalyx Barrier in Diabetic Nephropathy. *Diabetes* 2016; 65(8): 2429-2439.

30. Potje SR, Costa TJ, Fraga-Silva TFC, Martins RB, Benatti MN, Almado CEL, de Sa KSG, Bonato VLD, Arruda E, Louzada-Junior P, Oliveira RDR, Zamboni DS, Becari C, Auxiliadora-Martins M, Tostes RC. Heparin prevents in vitro glycocalyx shedding induced by plasma from COVID-19 patients. *Life sciences* 2021; 276: 119376.

31. Stahl K, Gronski PA, Kiyani Y, Seeliger B, Bertram A, Pape T, Welte T, Hoepfer MM, Haller H, David S. Injury to the Endothelial Glycocalyx in Critically Ill Patients with COVID-19. *Am J Respir Crit Care Med* 2020; 202(8): 1178-1181.

32. Birnhuber A, Fliesser E, Gorkiewicz G, Zacharias M, Seeliger B, David S, Welte T, Schmidt J, Olschewski H, Wygrecka M, Kwapiszewska G. Between inflammation and thrombosis - endothelial cells in COVID-19. *The European respiratory journal : official journal of the European Society for Clinical Respiratory Physiology* 2021.

33. Michalick L, Weidenfeld S, Grimmer B, Fatykhova D, Solymosi PD, Behrens F, Dohmen M, Brack MC, Schulz S, Thomasch E, Simmons S, Muller-Redetzky H, Suttrop N, Kurth F, Neudecker J, Toennies M, Bauer TT, Eggeling S, Corman VM, Hocke AC, Witzenrath M, Hippenstiel S, Kuebler WM. Plasma mediators in patients with severe COVID-19 cause lung endothelial barrier failure. *The European respiratory journal : official journal of the European Society for Clinical Respiratory Physiology* 2021; 57(3).

34. Iba T, Levy JH, Levi M, Thachil J. Coagulopathy in COVID-19. *J Thromb Haemost* 2020; 18(9): 2103-2109.

35. Nieuwdorp M, van Haften TW, Gouverneur MC, Mooij HL, van Lieshout MH, Levi M, Meijers JC, Holleman F, Hoekstra JB, Vink H, Kastelein JJ, Stroes ES. Loss of endothelial glycocalyx during acute hyperglycemia coincides with endothelial dysfunction and coagulation activation in vivo. *Diabetes* 2006; 55(2): 480-486.
36. Grover SP, Mackman N. Tissue Factor: An Essential Mediator of Hemostasis and Trigger of Thrombosis. *Arterioscler Thromb Vasc Biol* 2018; 38(4): 709-725.
37. Ramnath R, Foster RR, Qiu Y, Cope G, Butler MJ, Salmon AH, Mathieson PW, Coward RJ, Welsh GI, Satchell SC. Matrix metalloproteinase 9-mediated shedding of syndecan 4 in response to tumor necrosis factor alpha: a contributor to endothelial cell glycocalyx dysfunction. *FASEB J* 2014; 28(11): 4686-4699.
38. Hultström M, Fromell K, Larsson A, Quaggin SE, Betsholtz C, Frithiof R, Lipcsey M, Jeansson M. Elevated Angiotensin-2 inhibits thrombomodulin-mediated anticoagulation in critically ill COVID-19 patients. *medRxiv* 2021: 2021.2001.2013.21249429.
39. Shi R, Lai C, Teboul JL, Dres M, Moretto F, De Vita N, Pham T, Bonny V, Mayaux J, Vaschetto R, Beurton A, Monnet X. COVID-19 ARDS is characterized by higher extravascular lung water than non-COVID-19 ARDS: the PiCCOVID study. *Critical Care* 2021; 25(1).

Supporting information

Supplementary Material and methods

Circulating markers of endothelial dysfunction and glycocalyx shedding

Plasma samples were thawed at room temperature. All plasma analytes were measured with immunoassays in duplicate according to manufacturer's recommendation. Samples were diluted in diluent reagent according to manufacturer's protocol. Analytes measured include angiopoietin 2 (Ang-2, DANG20, R&D Systems, Abingdon, UK), soluble thrombomodulin (sTM, M850720096, Diaclone, Besançon, France) and soluble syndecan-1 (sSDC1, DY2780, R&D Systems). For angiopoietin 2 and soluble thrombomodulin, commercial control samples were included in each plate to confirm the amount of protein level.

***In Vitro* Culture Experiments**

Primary human pulmonary microvascular endothelial cells (HPMECs) were purchased from PromoCell (Lot no. 455Z003, Heidelberg, Germany) and primary human glomerular microvascular ECs (GEnCs) were purchased from Cell Systems (ACBRI-128; Kirkland, WA, USA) and were both cultured in endothelial growth medium (basal medium MV, C-22220, PromoCell) supplemented with C-39220 (PromoCell) and 1% antibiotics (penicillin/streptomycin, 15070063, Gibco, Paisley, UK) at 37°C and 5% CO₂. For each cell line, passage 5 were used for experiments.

Endothelial barrier function assay

Endothelial barrier function analysis was performed with impedance-based cell monitoring using the electric cell-substrate impedance sensing system (ECIS Z θ , Applied

Biophysics, New York, USA). ECIS plates (96W20idf PET, Applied Biophysics) were pre-treated with 10 mM L-cysteine and coated with 1% gelatine (for GEnCs) or without 1% gelatine (for HPMECs). HPMECs (p5) were seeded at a concentration of 4.5×10^5 cells/well and for GEnCs (p5), the concentration was 3×10^5 cells/well. Medium was refreshed after 24 hours. Initial baseline resistance was measured for 2 hours before endothelial cells were seeded into the plate. Multiple frequency/time mode was used for the real-time assessment of the barrier function. Additionally, the real-time resistance was generated every 350 seconds. Once the stable monolayer was formed, endothelial cells were incubated with 10% serum (healthy (n=12), COVID-19 non-ICU (n=8) and ICU (n=26)) and measured for 20 hours. Afterwards, modelling data R_b which represents barrier function could be generated.

In additional experiments, HPMECs were exposed to 10% healthy serum (n=12), COVID-19 ICU serum (n=26) with or without fucoidan (10 $\mu\text{g}/\text{mL}$, gift from MicroVascular Health Solutions LLC, Alpine, UT, USA) and measured on the ECIS machine for 20 hours. The natural fucoidan provided (Iso 9000 and GMP certified from Omnipharm, S.A.S, Chambéry, France) was extracted from *Laminaria japonica* as a powder of 91.20% purity and further tested, for instance, on the presence of heavy metals (arsenic, lead, cadmium, mercury) or microbiology parameters (European Pharmacopoeia VIII, Ed 2,6,12: total plate count, yeast, mold, *E. coli*, *Salmonella spp.*). A 50x times stock solution was prepared by dissolving the appropriate amount of powder in milliQ water and passed through a 0.22 μm filter before use. Cell culturing supernatant and 10% serum in no FCS medium were collected and centrifuged for VWF ELISA assay.

RNA isolation and RT-PCR

Cells were harvested in TRIzol and total RNA was isolated using RNeasy Mini Kit (74106, Qiagen, Venlo, The Netherlands) according to its protocol. cDNA synthesis was transcribed

using GoScript™ Reverse Transcriptase kit (A5001, Promega, Leiden, The Netherlands). RT-PCR analysis was conducted using SYBR Select Master Mix (4472908, Applied Biosystems, Landsmeer, The Netherlands) and specific primers as indicated in supplementary table s2. Gene expression was normalized to GAPDH of 5 separate experiments.

Immunoblotting analysis

Western blots were performed from protein extracts of HPMECs. Cells were washed once with cold PBS and lysed in lysis buffer mentioned in our previous study[1]. After centrifugation of the samples at 12,000 rpm for 15 min at 4°C, supernatant was collected and protein concentration was measured using the Pierce BCA Protein Assay Kit (23255, ThermoFisher, Landsmeer, The Netherlands). Equal amounts of protein were denatured using DTT and incubated at 95°C for 10 minutes. 10% Mini-PROTEAN® TGX™ Protein Gels (4561031, Bio-Rad Laboratories, Veenendaal, The Netherlands) were used for protein size separation and proteins were transferred to PVDF membranes (1704156, Bio-Rad) using the Trans-Blot Turbo system. Afterwards, the membrane was blocked in 5% milk in PBST at room temperature for 1 hour. Primary antibody rabbit anti-human ICAM1 (4915, Cell Signalling Technology), rabbit anti-human total NF-κB p65 (8242, Cell Signalling Technology), rabbit anti-human phosphor-NF-κB p65 (Ser536) (3033, Cell Signalling Technology) and mouse anti-human GAPDH (MA5-15738, ThermoFisher) were incubated overnight at 4°C. Incubation with a secondary HRP-conjugated antibody (P0447 and P0448, Dako, Amstelveen, The Netherlands) and visualization using Western Lightning Plus-ECL, Enhanced Chemiluminescence Substrate (NEL103001EA, PerkinElmer, Groningen, The Netherlands). Intensity of the bands were analysed using ImageJ software. Relative intensity was determined by levels of GAPDH.

Immunofluorescence of cultured cells

HPMECs (p5) were cultured in 8-well chamber slides (ibiTreat, μ -Slide 8 Well). Medium was refreshed after 24 hours to remove non-attached cells. When HPMECs formed a confluent monolayer after 48 hours, they were incubated with 10% pooled serum (healthy control (pooled n = 12), non-ICU (pooled n = 8) and ICU (pooled n = 26) in no FCS medium for 24 hours. Next, cells were fixed with 4% PFA and 0.2% Triton-X100 in HBSS or 4% PFA in HBSS (for HS and LEA staining) for 10 minutes at room temperature, washed twice with 1% BSA in HBSS, and blocked with 3% goat serum in HBSS for 1 hour at room temperature. Then, cells were incubated with FITC labelled *Lycopersicon esculentum* (LEA-FITC, L0401, Sigma, Houten, The Netherlands), primary monoclonal Mouse Anti-Human VE cadherin (55-7H1; BD Biosciences), monoclonal Mouse Anti-heparan sulfate (10E4, 370255-1, AMSBIO, Abingdon, UK) and monoclonal Mouse Anti-TM (MA5-11454, ThermoFisher) at 4°C overnight, followed by an appropriate secondary antibody and phalloidin-TRITC (VE-cadherin samples) for 1 hour, all in blocking buffer. Cells were subsequently washed and incubated with Hoechst 33528 (1/1,000) for 10 minutes at room temperature.

Cells were imaged using a LEICA SP8 WLL confocal microscope (Leica, Rijswijk, the Netherlands) to create image stacks. Fluorescent images were analysed using Image J software. To quantify the total area of VE-cadherin staining, all VE-cadherin derived fluorescent signal below a threshold was included in a mask. The value for the threshold intensity was kept the same for each field and then the positive area of VE-cadherin is quantified as adhesion junction area. 10 fields per experiment were imaged for every condition for further analysis to quantify the glycocalyx coverage, endothelial nuclear region was selected and the thickness of the glycocalyx was quantified by calculating the distance from the half-maximum signal of the nuclear staining at the luminal side to the half-maximum signal at the luminal end of the staining in the z-direction. Fluorescence intensity was calculated based on the average fluorescence intensity from the half-maximum signal of the nuclear staining at the luminal side to the half-maximum signal at the luminal end of the staining in the z-direction. Surface amount of glycocalyx was presented as mean fluorescence intensity (Mean FL) times luminal thickness.

FX activation by extrinsic tenase complex (TF-FVIIa)

Primary human pulmonary microvascular endothelial cells at passage 5 were seeded into 96 wells plates at a concentration of 2.5×10^4 cells/well. Medium was refreshed after 24 hours and after 48 hours, HPMECs were incubated with 10% control (n=12), COVID-19 non-ICU (n=8) and ICU serum (n=26, with or without presence of fucoidan) in no FCS medium for 24 hours. Cell culture supernatants were collected and centrifuged for ELISA assays. Afterwards, cells were washed once with prewarmed HBSS with Ca^{2+} . Factor VIIa (80 μL , 10 nM, HCVIIA-0031, Haematologic Technologies, Huissen, The Netherlands) was added and incubated for 15 minutes at 37°C and 5% CO_2 . Then the reaction system was initiated by adding factor X (80 μL , 400 nM, HCVIIA-0050, Haematologic Technologies). The plate was kept in incubator to keep the reaction continuous and 2 time points were selected (1 hour and 2 hours) to detect the production of active factor X. Aliquots were taken and quenched in HBS supplemented with 50mM EDTA to stop the reaction. The amidolytic activity of each sample was determined by SpecXa conversion (250 μM), measuring the absorbance at 405 nm and the initial rates of chromogenic substrate hydrolysis were converted to nanomolar of product by reference to a corresponding FXa standard curve.

Thrombin generation Assay

Primary human pulmonary microvascular endothelial cells at passage 5 were seeded into 96 wells plates at a concentration of 2.5×10^4 cells/well. Medium was refreshed after 24 hours and after 48 hours, HPMECs were incubated with 10% healthy (n=12), COVID-19 non-ICU (n=8) and ICU serum (n=26, with or without presence of fucoidan) in no FCS medium for 24 hours. Warm HBSS without Ca^{2+} was used to wash the cells once. Thrombin generation curves were obtained by supplementing normal pooled plasma. Thrombin

formation was initiated by adding substrate buffer (FluCa-kit, 86197, Thrombinoscope BV, Leiden, The Netherlands) to the plasma. The final reaction volume was 120 μ L, of which 80 μ L was plasma, 20 μ L was HBSS/calibrator and 20 μ L was substrate. Thrombin formation was determined every 30 s for 120 min and corrected for the calibrator using Thrombinoscope software.

Markers of endothelial dysfunction and glycocalyx shedding in cell cultured supernatant

Supernatants collected from experiments mentioned above and stored at -80°C were measured with immunoassays in duplicate according to manufacturer's recommendation. Analytes measured include angiopoietin 2 (Ang-2, DANG20, R&D Systems), soluble thrombomodulin (TM, M850720096, Diaclone), IL-6 (M9316, Sanquin, Amsterdam, The Netherlands) and VWF (A0082, Dako). Samples were diluted 1:100, 1:5, 1:10 and 1:200 respectively in diluent reagent. For angiopoietin 2 and soluble thrombomodulin, commercial control samples were included in each plate to confirm the amount of protein level.

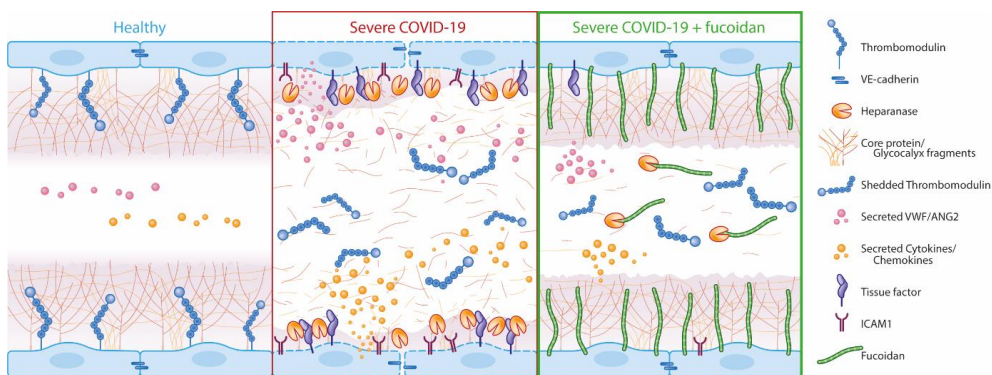
Public database mining

To further study the role of thrombomodulin in endothelial cells from different vascular beds, datasets from EC atlas (https://endotheliomics.shinyapps.io/ec_atlas/ [2]) and NCBI Gene expression Omnibus (<https://www.ncbi.nlm.nih.gov/geo/>) were downloaded. We then determined Thbd expression in mice ECs from 11 organs. For human ECs, 2 datasets (GSE43475 [3] and GSE21212 [4]) were downloaded and processed with RMA background correction, log₂ transformation and normalization in R. For annotation, we chose the gene with the highest expression as the gene symbol and annotated it via different annotation packages. Then THBD expression was detected in different EC lines.

References

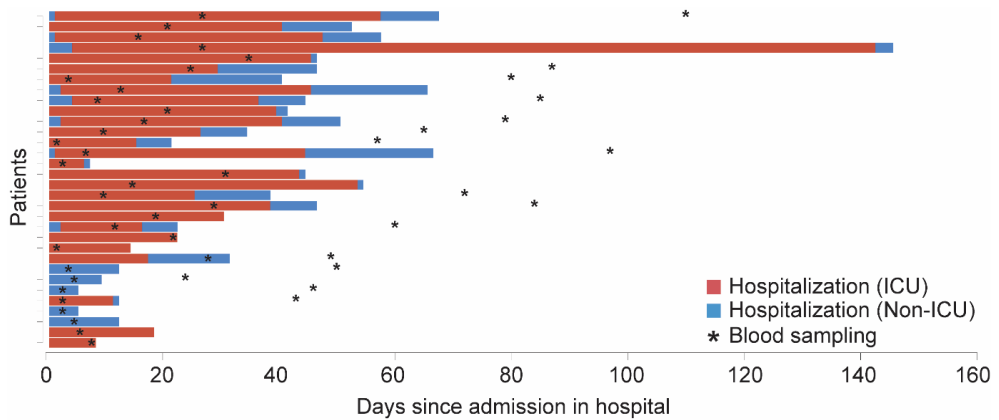
1. Wang G, Kostidis S, Tiemeier GL, Sol W, de Vries MR, Giera M, Carmeliet P, van den Berg BM, Rabelink TJ. Shear Stress Regulation of Endothelial Glycocalyx Structure Is Determined by Glucobiosynthesis. *Arteriosclerosis, thrombosis, and vascular biology* 2020; 40(2): 350-364.
2. Kalucka J, de Rooij L, Goveia J, Rohlenova K, Dumas SJ, Meta E, Conchinha NV, Taverna F, Teuwen LA, Veys K, Garcia-Caballero M, Khan S, Geldhof V, Sokol L, Chen R, Treppe L, Borri M, de Zeeuw P, Dubois C, Karakach TK, Falkenberg KD, Parys M, Yin X, Vinckier S, Du Y, Fenton RA, Schoonjans L, Dewerchin M, Eelen G, Thienpont B, Lin L, Bolund L, Li X, Luo Y, Carmeliet P. Single-Cell Transcriptome Atlas of Murine Endothelial Cells. *Cell* 2020; 180(4): 764-779 e720.
3. Aranguren XL, Agirre X, Beerens M, Coppiello G, Uriz M, Vandersmissen I, Benkheil M, Panadero J, Aguado N, Pascual-Montano A, Segura V, Prosper F, Luttun A. Unraveling a novel transcription factor code determining the human arterial-specific endothelial cell signature. *Blood* 2013; 122(24): 3982-3992.
4. Bhasin M, Yuan L, Keskin DB, Otu HH, Libermann TA, Oettgen P. Bioinformatic identification and characterization of human endothelial cell-restricted genes. *BMC Genomics* 2010; 11: 342.

Graphic abstract



Under homeostatic conditions (healthy), intact endothelial glycocalyx maintains a stable endothelial barrier. COVID-19 serum of patients on ICU induces endothelial activation (cytokine release, ANG2 and VWF and shedding of thrombomodulin), glycocalyx degradation, loss of endothelial barrier function and EC procoagulable state (increased tissue factor expression). Supplementation of the heparan sulfate mimetic fucoidan restores the endothelial glycocalyx and barrier function and reverses the endothelial procoagulable state.

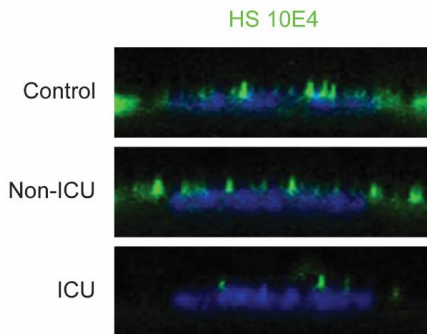
Supplementary figures



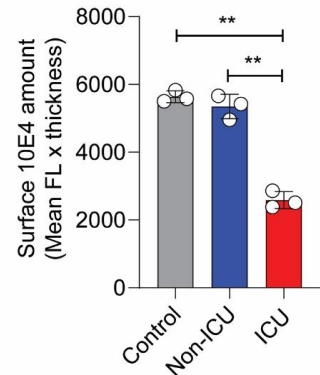
Supplementary figure S1 Patient's hospitalization timelines and blood sampling dates.

For each included patient, hospitalization on non-ICU (blue bar), and on ICU (red bar) are indicated, aligned to the day of admission. * represent blood sampling date. For some of the patients, blood samples were collected during the whole hospitalization (ICU and non-ICU) and recovery state (discharge after 6 weeks).

a)



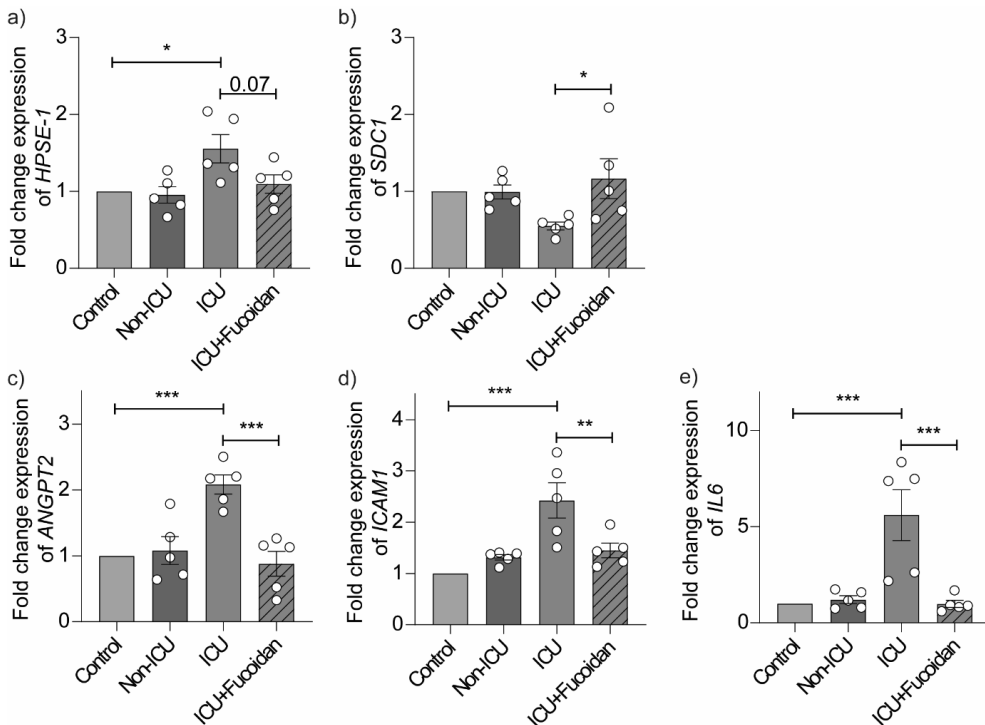
b)



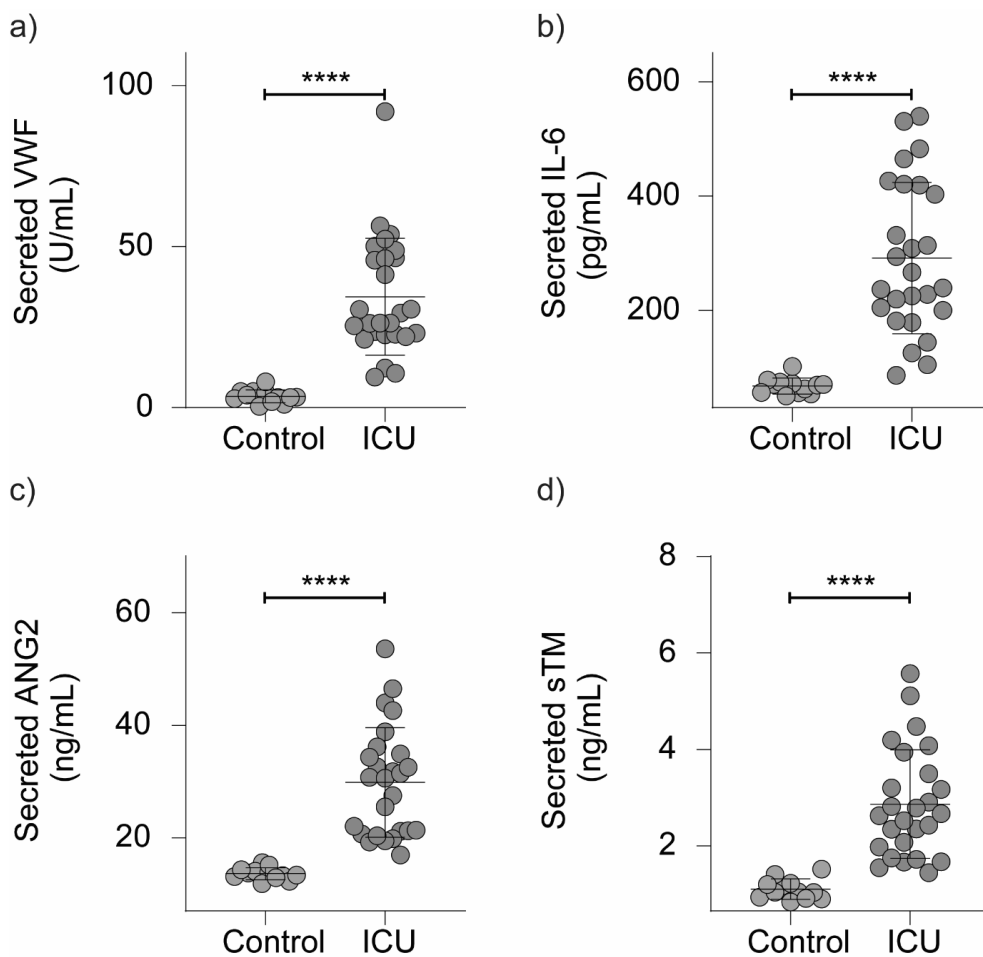
Supplementary figure S2 Loss of heparan sulfate in primary human pulmonary microvascular endothelial cells in presence of COVID-19 ICU serum

a) Representative confocal images of anti-heparan sulfate (HS, 10E4 clone) staining on the surface of primary human pulmonary microvascular endothelial cells (HPMECs) in the presence of 10% pooled- healthy control (n = 12), COVID-19 non-ICU (n = 8) and COVID-19 ICU (n = 26) serum for 24hrs. b) Quantification of HPMECs surface HS (10E4 clone) in the presence of

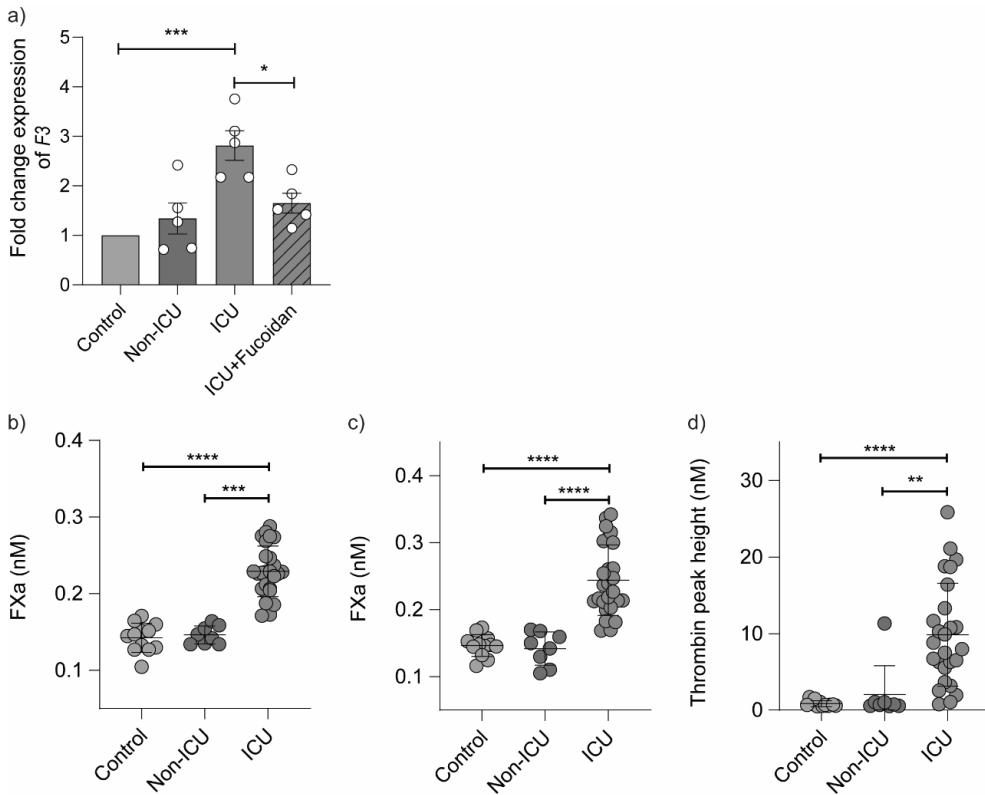
10% pooled- healthy control, COVID-19 non-ICU and COVID-19 ICU serum for 24hrs, presented as mean fluorescence times thickness of 3 independent experiments. Graphs represent the mean \pm SD. One-way ANOVA followed by Tukey's multiple comparisons test were performed; ** $p < 0.01$



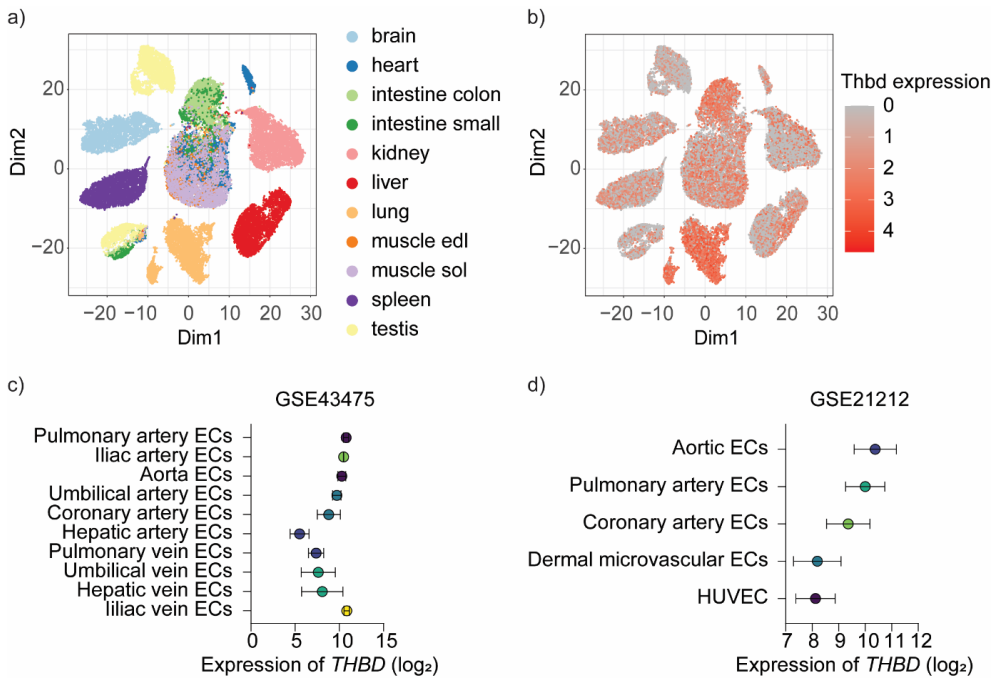
Supplementary figure S3 Fucoidan reduces mRNA expression of endothelial activation related markers. Gene expression data a) heparanase (*HPSE-1*), b) syndecan-1 (*SDC1*), c) *ICAM1*, d) angiopoietin 2 (*ANGPT2*) and e) *IL6* expression in response to 10% pooled-healthy control (n = 12), COVID-19 non-ICU (n = 8) and COVID-19 ICU (n = 26) serum with and without fucoidan (10 μ g/mL) for 24hrs, presented as fold change expression normalized to healthy control of 5 independent experiments. Graphs represent the mean \pm SEM. One-way ANOVA followed by Tukey's multiple comparisons test were performed; * $p < 0.05$, ** $p < 0.01$, *** $p < 0.001$



Supplementary figure S4 Comparison of endothelial dysfunction and glycocalyx shedding related markers in cell culture supernatants. Levels of a) secreted von Willebrand factor (VWF), b) secreted IL6, c) secreted angiotensin 2 (ANG2) and d) secreted soluble thrombomodulin (sTM) in cell culture supernatants of primary human pulmonary microvascular endothelial cells (HPMECS) in the presence of serum of healthy controls (grey, n = 12) and COVID-19 ICU patients (red, n = 26). Nonpaired two-tailed Student t test were performed; *p<0.05, **p<0.01, ***p<0.001, ****p<0.0001.



Supplementary figure S5 Serum mediators of COVID-19 patients on ICU promote activation of coagulation on endothelial cells. a) Gene expression of F3 (tissue factor) in response to 10% pooled healthy control (n = 12), COVID-19 non-ICU (n = 8) and COVID-19 ICU (n = 26) serum with and without fucoidan (10 $\mu\text{g}/\text{mL}$) for 24hrs, presented as fold change expression normalized to healthy control of 5 independent experiments. Factor X a (FXa) production (nM) in b) first hour and c) second hour on HPMECs surface in the presence of 10% individual healthy control (n=12), COVID-19 non-ICU (n=8) and COVID-19 ICU (n=26) serum for 24hrs . d) Thrombin generation peak height (nM) measured on HPMECs surface in the presence of 10% individual healthy control (n=12), COVID-19 non-ICU (n=8) and COVID-19 ICU (n=26) serum for 24hrs . One-way ANOVA followed by Tukey's multiple comparisons test were performed; * $p < 0.05$, ** $p < 0.01$, *** $p < 0.001$, **** $p < 0.0001$.



Supplementary figure S6 Thrombomodulin expression levels in different vascular beds.

a) tSNE plot revealing gene variation in 11 types of endothelial cells from mice based on EC atlas (https://endotheliomics.shinyapps.io/ec_atlas/). b) Thrombomodulin (*Thbd*) gene expression in 11 types of endothelial cells from mice. *THBD* expression from different human vascular beds based on databases c) GSE43475 and d) GSE21212.

Supplementary table S1. Demographic, clinical, and outcome data of patients in BEAT-COVID cohort

	Hospitalized (n = 32)	ICU (n =26)	Non-ICU (n = 6)	Healthy control (n = 12)
Age - years median (IQR)	61 (57-70)	62 (58-71)	56 (47-65)	60 (60-60)
Male sex - n (%)	26 (81)	21 (81)	5 (83)	8 (75)
BMI - kg/m2 median (IQR)	28 (24-30)	29 (26-30)	25 (20-32)	-
Admission Glasgow Coma Score - points median (IQR)	3 (3-15)	3 (3-15)	15 (15-15)	-
Days since hospital admission - median (IQR)	36 (14-47)	43 (22-52)	7 (5-11)	-
Days in ICU - median (IQR)	31 (19-43)	31 (19-43)	-	-
In-hospital mortality - n (%)	7 (21.9)	7 (26.9)	0 (0)	-
Glasgow Coma Score - points median (IQR)	3 (3-11.8)	3 (3-5.8)	15 (15-15)	-
SOFA score - median (IQR)	7 (7-11)	7 (7-11)	-	-
LUMC severity score - median (IQR)	12 (9.8-14)	13 (12-14)	3 (1.5-3.8)	-
Comorbidities				
Chronic cardiac disease - n (%)	7 (21.9)	6 (23.1)	1 (16.7)	-
Hypertension - n (%)	8 (25)	7 (26.9)	1 (16.7)	-
Chronic pulmonary disease - n (%)	3 (9.4)	3 (11.5)	0 (0)	-
Asthma - n (%)	6 (18.8)	6 (23.1)	0 (0)	-
Chronic kidney disease - n (%)	1 (3.1)	1 (3.9)	0 (0)	-
Chronic neurological disorder - n (%)	3 (9.4)	2 (7.7)	1 (16.7)	-
Diabetes	13 (40.6)	9 (34.6)	4 (66.7)	-
Smoking history - n (%)	10 (31.3)	10 (38.5)	0 (0)	-
Thromboembolic event - n (%)	4 (12.5)	4 (15.4)	0 (0)	-
Coagulopathy - n (%)	1 (3.1)	1 (3.9)	0 (0)	-
Respiratory function				
Respiratory rate - median (IQR)	26.5 (24-30)	28.5 (25-32)	20.5 (17-23)	-
SpO2 - % median (IQR)	90 (89-92)	89.5 (88-90)	94.5 (94-96)	-
FiO2 - % median (IQR)	60 (41-100)	60 (41-100)	-	-
PaO2/FiO2 ratio - median (IQR)	17 (12.7-20.8)	17 (12.7-20.8)	-	-
Non-invasive ventilation - n (%)	8 (25)	7 (27)	1 (17)*	-
Invasive ventilation - n (%)	17 (53)	16 (62)	1 (17)*	-
Coagulation				
Platelets - 10 ⁹ /L median (IQR)	230 (200-302)	2245 (194-309)	253 (223-274)	-
aPTT - seconds median (IQR)	37.5 (33.6-39.9)	37.8 (34.4-40.3)	33.5 (31.5-35.5)	-
PT - seconds median (IQR)	16.1 (14.8-16.8)	15.6 (14.7-16.7)	16.65 (16.6-16.7)	-
INR - median (IQR)	1.2 (1.1-1.2)	1.2 (1.1-1.2)	1.2 (1.2-1.2)	-
D-dimer - mg/L median (IQR)	2.24 (1.03-3.96)	2.24 (1.03-3.96)	-	-
Inflammation markers				
CRP - mg/L median (IQR)	164.4 (58.5-245.1)	185.5 (55.1-255.5)	128.8 (76.6-170.9)	-
Urea - mmol/L median (IQR)	13.4 (5.9-16.8)	15.2 (11.5-17.1)	5 (4.5-5.2)	-

* This patient was first in ICU when treated with non-invasive or invasive ventilation, and stopped ventilation when in non-ICU unit. Blood sampling for this patient was during non-ICU hospitalization.

BMI, body mass index; IQR, interquartile range.

Supplementary table S2. Primer sequences

Gene	Forward sequence	Reverse sequence
GAPDH	CCTGCACCACCAACTGCTTA	GGCCATCCACAGTCTTCTGAG
HPSE	TCCTGCGTACCTGAGGTTTG	CCATTCCAACCGTAACTTCTCCT
SDC1	CCACCATGAGACCTCAACCC	GCCACTACAGCCGTATTCTCC
ICAM1	GTATGAACTGAGCAATGTGCAAG	GTTCCACCCGTTCTGGAGTC
ANGPT2	CTCGAATACGATGACTCGGTG	TCATTAGCCACTGAGTGTTGTTT
IL6	GGTACATCCTCGACGGCATCT	GTGCCTCTTTGCTGCTTTCAC
F3 (TF)	CCCAAACCCGTCAATCAAGTC	CCAAGTACGTCTGCTTCACAT

CHAPTER

6

High-density lipoprotein composition related to endothelial dysfunction is associated with disease outcome in COVID-19 patients

Lushun Yuan^{1,2}, Aswin Verhoeven³, Shuzhen Cheng^{1,4}, Wendy M.P.J. Sol¹, Ton J. Rabelink^{1,2}, Martin Giera^{3,5}, Bernard M. van den Berg^{1,2,5}, in collaboration with the BEAT-COVID study group⁵

¹ Eindhoven Laboratory for Vascular and Regenerative Medicine, Leiden University Medical Center, Leiden, the Netherlands.

² Department of Internal Medicine, Division of Nephrology, Leiden University Medical Center, Leiden, the Netherlands.

³ Center for Proteomics and Metabolomics, Leiden University Medical Center, Leiden, the Netherlands.

⁴ Department of Internal Medicine, Division of Thrombosis and Hemostasis, Leiden University Medical Center, Leiden, the Netherlands.

⁵BEAT-COVID study group

Abstract

Background: Previous studies showed that endothelial dysfunction is involved in COVID-19 progression and high-density lipoproteins (HDL) have a variety of endothelial-protective properties. When considering that HDL composition is more representative of HDL function than HDL cholesterol (HDL-C) levels alone, we sought to investigate whether changes in HDL composition is associated with endothelial function and disease outcome in COVID-19 patients and lead to new risk stratification biomarkers.

Methods: Using ^1H nuclear magnetic resonance (NMR) spectroscopy and Bruker IVDr Lipoprotein Subclass Analysis (B.I.LISATM) software, an in-depth analysis of plasma lipoproteins was undertaken in a longitudinal study of COVID-19 patients with samples of healthy individuals as control.

Results: Higher triglyceride content in all HDL subclasses and lower HDL-4 plasma concentrations were found in COVID-19 patients compared to control, correlating with sequential organ failure assessment, circulating endothelial activation markers, and *in vitro* endothelial functional assay parameters.

Conclusion: The observed changes in HDL composition in COVID-19 patients which are associated with disease progression and possible survival suggest that these findings might be used as prognostic biomarkers in hospitalized COVID-19 patients.

Keywords: High-density lipoprotein composition, NMR, longitudinal, COVID-19, endothelial function

Introduction

The new coronavirus disease (COVID-19) caused by severe acute respiratory syndrome coronavirus-2 (SARS-CoV-2) led to a major worldwide pandemic characterized by acute lung injury and rapidly progressing to acute respiratory distress syndrome (ARDS) ¹. Previously, we showed that endothelial dysfunction, leading to endothelial glycocalyx degradation, barrier failure, and procoagulant surface formation was involved in COVID-19 progression ². In addition, early studies of lipid metabolism in patients revealed a role for high-density lipoproteins (HDL) protective factors in a variety of endothelial functions such as antioxidant, anti-inflammatory, anti-thrombotic, and even anti-infectious properties ^{3,4}. Recently, it was observed that the metabolic lipid profile in COVID-19 patients in the intensive care unit (ICU) was different when compared to healthy controls but also from patients with cardiogenic shock in ICU. ⁵

Increasing evidence suggested that low serum HDL-cholesterol (HDL-C) levels at hospital admission is associated with disease severity and mortality in COVID-19 ^{6,7}. However, other studies revealed that the HDL lipidome and proteome rather than quantitative HDL-C concentration played a more representative role in HDL function during disease ^{8,9}. In addition to HDL-C concentrations in COVID-19, several studies showed significant inflammatory remodeling of the HDL proteome, associated with COVID-19 disease severity in both adult and pediatric COVID-19 patients ⁹⁻¹¹.

However, limited studies are still available that show an association between COVID-19 related endothelial dysfunction and HDL composition and function. Furthermore, data is lacking whether the endothelial function related HDL composition is associated with disease outcome. Therefore, in the current study we used ¹H Nuclear magnetic resonance (NMR) spectroscopy and the validated Bruker IVDr Lipoprotein Subclass Analysis (B.I.LISA™) software ¹²⁻¹⁷ to measure blood HDL subclasses and lipid content concentrations in longitudinally collected serum samples from ICU and non-ICU, together with age-matched healthy controls. With the help of this in-depth analysis, we aimed to

identify changes in HDL composition in COVID-19 patients compared to healthy individuals and disease progression, screen for endothelial function related HDL composition, and investigate whether specific HDL compositional changes could lead to different outcomes in the course of the disease.

Material and methods

Study population.

A prospective observational cohort study was set up, in which patients with PCR-confirmed SARS-CoV-2 infection after hospital admission were recruited from April 2020 until August 2020, before the use of medication such as dexamethasone and vaccines were implemented. In the present study longitudinally collected plasma and serum samples from 37 patients with confirmed SARS-CoV-2 infection together with 12 age-matched controls were used (Figure 1A and supplemental figure S1). Patient characteristics are shown in supplemental table S1. Age-matched healthy donors with a male: female ratio of 2:1, were included after confirmed negative for SARS-CoV-2 IgG. The trial was registered in the Dutch Trial Registry (NL8589). Ethical approval was obtained from the Medical Ethical Committee Leiden-Den Haag-Delft (NL73740.058.20).

Sample preparation for ^1H nuclear magnetic resonance (NMR) spectroscopy.

Sample preparation was performed consistently with the requirements of the Bruker B.I.LISA lipoprotein analysis protocol. The EDTA plasma samples were thawed at room temperature and immediately homogenized by inverting the tubes 10 times. Next, 200 μL of plasma was manually transferred to a Ritter 96 deep-well plate. A Gilson 215 liquid handler robot was used to mix 120 μL of plasma with 120 μL , 75 mM disodium phosphate buffer in $\text{H}_2\text{O}/\text{D}_2\text{O}$ (80/20) with a pH of 7.4 containing 6.15 mM NaN_3 and 4.64 mM sodium

3-[trimethylsilyl] d4-propionate (Cambridge Isotope Laboratories). Using a modified second Gilson 215 liquid handler, 190 μ L of each sample was transferred into 3 mm Bruker SampleJet NMR tubes. Subsequently, the tubes were sealed by POM ball insertion and transferred to the SampleJet autosampler where they were kept at 6°C while queued for acquisition.

NMR spectroscopy measurement and processing.

All proton nuclear magnetic resonance ($^1\text{H-NMR}$) experiments were acquired on a 600 MHz Bruker Avance Neo spectrometer (Bruker Corporation, Billerica, USA) equipped with a 5-mm triple resonance inverse (TCI) cryogenic probe head with a Z-gradient system and automatic tuning and matching.

The NMR spectra were acquired following the Bruker B.I.Methods protocol. Before the measurements, a standard 3 mm sample of 99.8% methanol-d4 (Bruker) was used for temperature calibration¹⁸. A standard 3 mm QuantRefC sample (Bruker) was measured as the quantification reference and for quality control. All experiments were recorded at 310 K. The duration of the $\pi/2$ pulses was automatically calibrated for each sample using a homonuclear-gated nutation experiment on the locked and shimmed samples after automatic tuning and matching of the probe head¹⁹. For water suppression, presaturation of the water resonance with an effective field of $\gamma\text{B1} = 25$ Hz was applied during the relaxation delay and the mixing time of the NOESY1D experiment²⁰.

The NOESY1D experiment was recorded using the first increment of a NOESY pulse sequence with a relaxation delay of 4 s and a mixing time of 10 ms²¹. After applying 4 dummy scans, 32 scans of 98,304 points covering a sweep width of 17,857 Hz were recorded.

The lipoprotein values were extracted from the NOESY1D plasma spectra by submitting the data to the commercial Bruker IVDr Lipoprotein Subclass Analysis (B.I.LISA) platform¹²⁻¹⁷.

This approach extracts information about lipoproteins and lipoprotein subfractions in plasma. In the current study, we focused on the HDL particles; dissected into concentration, composition, and four subclasses (sorted according to increasing density and decreasing size), and accompanying lipids within the lipoprotein subclasses including total cholesterol, free cholesterol, phospholipids, and triglycerides. The calculated esterified cholesterol was not included in the present study. Details about the measured HDL subfractions were listed in supplemental table S2.

HDL functional assay.

Primary human umbilical vein endothelial cells were isolated according to the previous protocol and cultured in 1% gelatin pre-coated flasks in endothelial growth medium (EGM2 medium, C-22011 supplemented with SupplementMix, Promocell, Heidelberg, Germany) with 1% antibiotics (penicillin/streptomycin, 15070063, Gibco, Paisley, UK). HDL isolation was isolated from 7 COVID-19 ICU individuals, pooled healthy control serum (pooled serum from 12 samples), and pooled non-ICU COVID-19 serum (pooled serum from 8 samples) based on the protocol from a previous study by Mulder *et al.*²², stored on ice, and used the following day for HDL functionality tests. Primary human umbilical vein endothelial cells (HUVECs) were used to test HDL's anti-thrombotic properties. In the 96-well plate, HUVECs (passage 3) were seeded at a density of 4×10^5 cells/well. The following day, HUVECs were pre-incubated for 30 minutes with 2% apoB-depleted plasma or an equal volume of precipitation reagent in HEPES as a control. Tumor necrosis factor α (TNF- α , H8916, Sigma Aldrich, the Netherlands) was then added at a concentration of 10ng/mL. After another 5 hours of incubation, the cell surface was washed once with HBSS, no calcium, and no magnesium (14170120, Gibco™, Paisley, UK). Each well received 50 μ L of normal pooled plasma before being placed in the Fluorometer for a 10-minute incubation at 37°C. The formation of thrombin was started by mixing 10 μ L of the fluorogenic substrate with calcium (TS50.00 FluCa-kit; Thrombinoscope BV, Maastricht, the

Netherlands). The final reaction volume was 60 μ L. Thrombin formation was measured every 20 seconds for 60 minutes and calibrated using Thrombinoscope software (Additional file 1: Fig. S4a). To assess HDL anti-thrombotic capacity, we included all the parameters including thrombin peak height (Peak), endogenous thrombin potential (ETP), lag time, time to peak (ttPeak), and velocity of thrombin generation (VellIndex). To limit potential variation due to different plate conditions, HDL anti-thrombotic capacity measurements were performed at the same time using the same batch of pooled HUVECs and reagents. For each individual, measurements were taken in three technical replicates.

Statistical analyses.

Descriptive clinical and *in vitro* experimental characteristics of the study population were expressed as median with interquartile range (IQR) for non-normally distributed variables, mean with standard deviation (SD) for normally distributed variables, or percentages (%) for dichotomous variables. One-way ANOVA followed by Tukey's multiple comparisons test or Kruskal-Wallis followed by Dunn's multiple comparisons test were assessed for multiple groups. $P < 0.05$ were considered statistically significant.

Principle component analysis (PCA) was performed between healthy controls, non-ICU COVID-19 patients, and ICU COVID-19 patients based on HDL-related features.

Healthy control, non-ICU COVID-19, and ICU COVID-19 were considered as three outcomes, and concentrations of HDL-related features were scaled (z-normalization, i.e., with mean=0 and SD=1) to identify lipoproteins with different concentrations, and multinomial logistic regression analysis (MLR) was used. We set a specific reference for each comparison: between healthy control and non-ICU COVID-19, healthy control was the reference; between healthy control and ICU COVID-19, healthy control was the reference; between non-ICU COVID-19 and ICU COVID-19, non-ICU COVID-19 was the reference. We considered a p-value < 0.05 as significant. The results were expressed as a regression coefficient (β)

with a 95% confidence interval (CI) to evaluate the association between concentrations of HDL-related features and COVID-19.

Pearson's correlation analysis was performed between HDL-related features and clinical parameters, circulating markers (including soluble thrombomodulin, angiotensin 2, and soluble syndecan-1), and *in vitro* endothelial functional assay parameters (including factor X activation, thrombin generation, endothelial barrier function, and supernatant endothelial activation markers) from our previously published paper ².

We next stratified ICU COVID-19 patients into survivors and non-survivors and investigated HDL composition changes during disease development. The trend line for the longitudinal changes in HDL composition was performed according to loess regression. Additionally, we compared the changes in HDL subclasses between the first collected sample and the last sample during hospitalization. Statistical analyses were performed in R (version 4.1.0) and GraphPad Prism version 8 (Graphpad Inc., La Jolla, CA, USA).

Results

Clinical characteristics and experimental characteristics of the study population .

Supplemental table S1 shows the clinical and experimental characteristics of individuals in the present study. Of 37 included COVID-19 patients, 18.92% were women, with a median age of 61 years (interquartile range, 57–70 years). Among 37 COVID-19 patients, there were 5 non-ICU COVID-19 patients and 32 ICU COVID-19 patients (26 survivors and 6 non-survivors). Compared to non-ICU COVID-19 patients and healthy individuals, both ICU COVID-19 survivors and non-survivors had higher endothelial activation, higher disease severity, and higher *in vitro* serum induced endothelial activation. Notably, although not significant, ICU non-survivors revealed a more profound endothelial dysfunction phenotype than ICU survivors.

HDL anti-thrombotic capacity reduction in ICU COVID-19 patients.

The effect of purified HDL serum fractions of healthy individuals (n = 12, pooled), non-ICU COVID-19 patients (n = 5, pooled) and 7 survivor COVID-19 individuals in ICU was tested for its anti-thrombotic capacity on cultured endothelial cells. Based on the thrombin generation curve, the curves of most ICU COVID-19 patients were higher than the healthy control and non-ICU COVID-19 patient curves (supplemental Fig. S2A). Furthermore, the thrombin peak height, endogenous thrombin potential (ETP), and VelIndex were all higher in the ICU COVID-19 patients tested; whereas lag time and ttPeak were lower in ICU COVID-19 patients tested (supplemental Fig. S2B-F). These results that HDL functionality in anti-thrombin formation already could be impaired in COVID-19 patients when admitted to the ICU.

HDL composition in plasma can differentiate patients with COVID-19 from healthy controls.

PCA analysis on HDL-related features of all the samples (including controls, non-ICU and ICU patients), using the “ggfortify” R package revealed good separation of COVID-19 patients from healthy individuals (Fig. 1B). Further hierarchical clustering revealed that this division in HDL composition presented that triglyceride content in all HDL subclasses was standing out as a cluster with an increasing trend with disease severity (Fig. 1C).

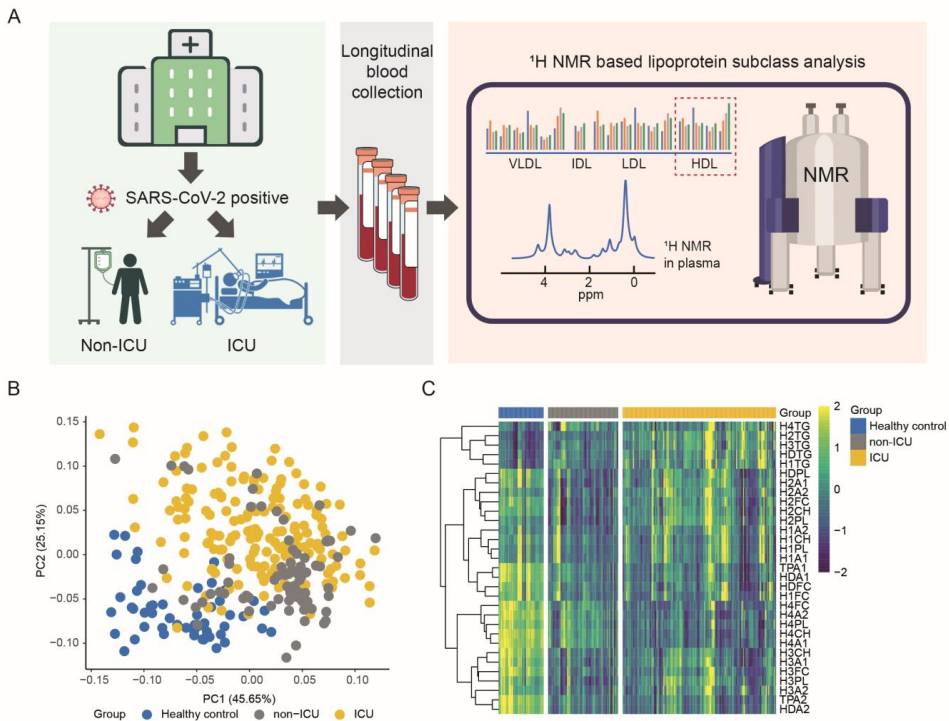


Figure 1. HDL composition between healthy individuals and COVID-19 patients based on ¹H NMR. (A) Scheme of study design and ¹H NMR in the present study. (B) Principal component analysis using HDL composition for longitudinally collected serum samples from ICU COVID-19 patients (yellow), non-ICU COVID-19 patients (grey), and samples from healthy controls (blue). (C) Heatmap showing overview of HDL composition in the present study indicating that triglyceride content in HDL subclasses increased with the disease progression whereas the rest of HDL composition such as HDL-4 subfractions decreased with the disease progression.

Distinct HDL composition between healthy controls, non-ICU COVID-19 patients, and ICU COVID-19 patients.

To identify further differences in HDL composition between the three groups multinomial logistic regression analysis was used. This analysis revealed that all HDL compositions (27

lower and 5 higher) were significantly different between healthy controls and non-ICU COVID-19 patients (Fig 2A, B and supplemental table S3) while 27 HDL subfractions (22 lower and 5 higher) differed significantly between healthy controls and ICU COVID-19 patients (Fig 2C, D and supplemental table S4). Comparing non-ICU and ICU COVID-19 patients showed notable changes in all the small and dense HDL subfractions which were lower in ICU COVID-19 patients and with a much higher triglyceride content in most HDL subclasses (Fig 2E, F and supplemental table S5). In addition, between COVID19 patients in ICU and not in ICU the HDL1-3 subfractions were significantly increased (Fig 2E, F and supplemental table S5).

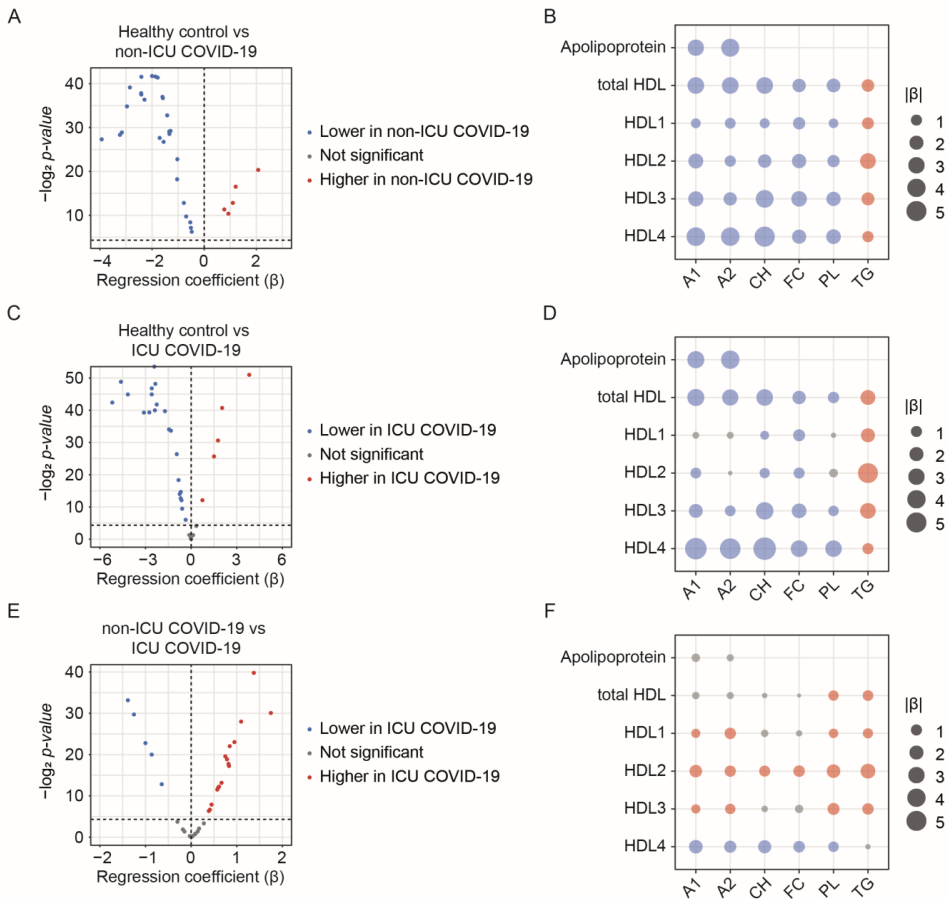


Figure 2. Differential HDL composition between ICU COVID-19, non-ICU COVID-19 patients, and healthy individuals. (A) Volcano plot and (B) Bubble plot of differential lipoprotein subfractions between non-ICU COVID-19 patients and healthy controls. (C) Volcano plot and (D) Bubble plot of differential lipoprotein subfractions between ICU COVID-19 patients and healthy controls. (E) Volcano plot and (F) Bubble plot of differential lipoprotein subfractions between ICU COVID-19 patients and non-ICU COVID-19 patients. Dot size of the bubble plot represented the absolute value of effect size based on MLR. The red color represented a higher concentration in the reference group, while the blue color represented a lower concentration in the reference group.

Associations between HDL composition and clinical and experimental parameters.

We next investigated the associations between HDL composition and clinical and experimental parameters (i.e, circulating markers, clinical assessment parameters, and *in vitro* endothelial functional assay parameters) using Pearson's correlation analysis. A positive correlation was observed between HDL-1-3 subclass triglyceride content and circulating endothelial activation markers angiopoietin 2, sequential organ failure assessment (SOFA) score, LUMC severity score, and respiratory failure assessment (Fig 3). These observations were also observed with the *in vitro* endothelial coagulation data from the Xa and thrombin generation measurements, endothelial activation markers in the supernatant, and endothelial barrier function loss. The HDL-4 subfraction only showed negative correlations with circulating and *in vitro* endothelial activation parameters. Furthermore, apolipoprotein A1 (ApoA1), total cholesterol, and free cholesterol content in each of the HDL subclasses were found to be negatively associated with endothelial activation and disease severity.

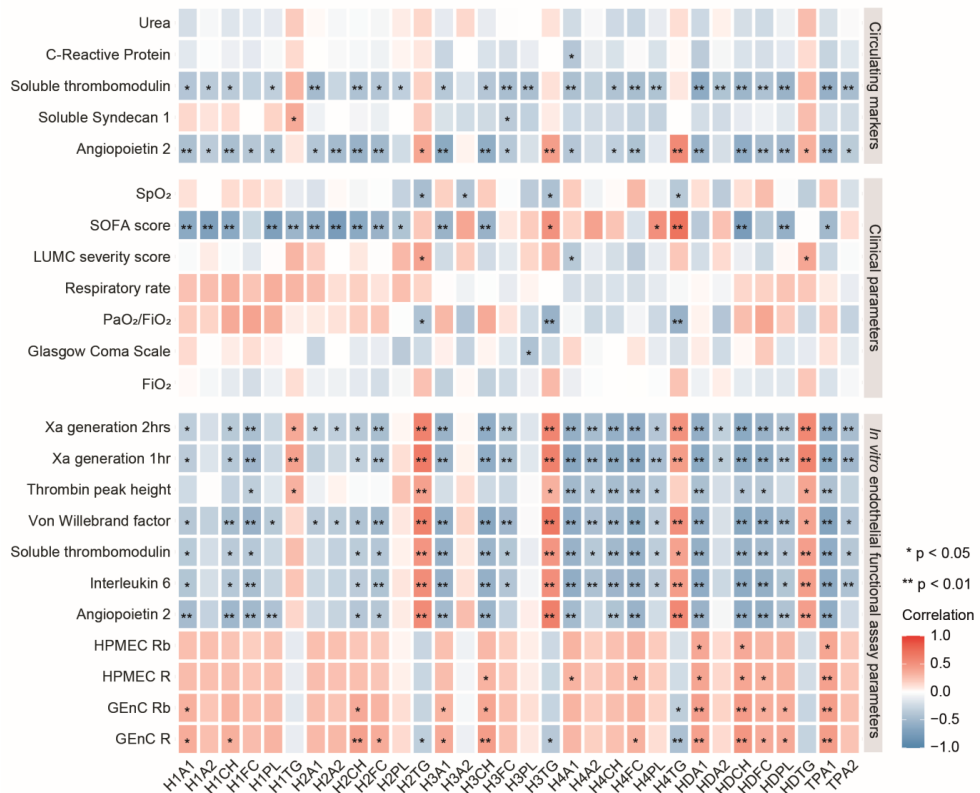


Figure 3. Correlation heatmap of circulating markers, clinical parameters, in vitro endothelial functional assay parameters, and HDL composition. The red indicated a positive correlation, while the blue indicated a negative correlation. Shading color and asterisks represented the value of corresponding correlation coefficients (* $p < 0.05$; ** $p < 0.01$).

Triglyceride content in HDL subclasses showed distinct longitudinal changes between non-ICU COVID-19 patients, ICU COVID-19 survivors, and ICU COVID-19 non-survivors.

Since triglyceride content in all the HDL subclasses was increased in COVID-19 patients compared to healthy individuals and associated with disease severity and clinical parameters, we then made the stratification analysis and evaluated the changes in disease

course. We found that most of the triglyceride content in HDL subclasses except in HDL-4, was initially higher in ICU non-survivors than in ICU survivors and non-ICU patients, and when it reached the peak (almost twice the levels of healthy individuals) and remained higher over time than in ICU survivors and non-ICU patients until the patients died (Fig 4A, C, E, G, I). Compared to the first collected sample in ICU with the last collected sample during hospitalization, only HDTG, H1TG, and H4TG were higher in the last collected samples than in the first collected samples in the ICU non-survivor group; H2TG and H3TG remained or decreased a bit. It is worth noting that all HDL subclass triglyceride was much higher in ICU non-survivors than in ICU survivors and non-ICU patients (Fig 4B, D, F, H, J).

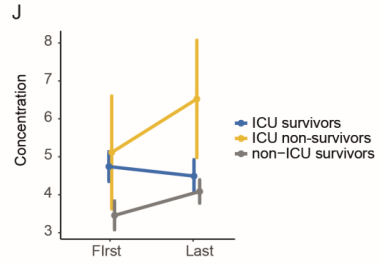
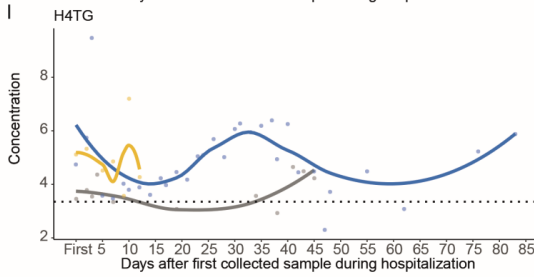
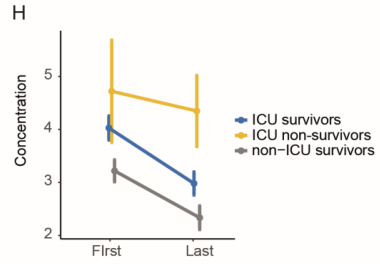
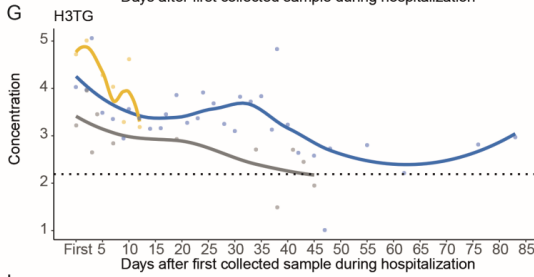
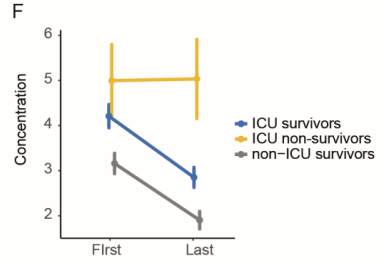
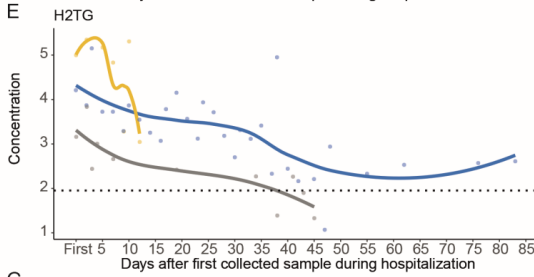
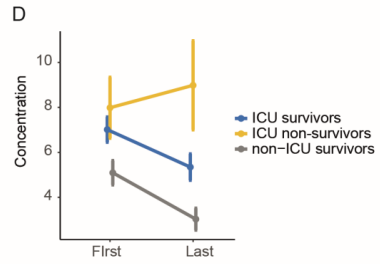
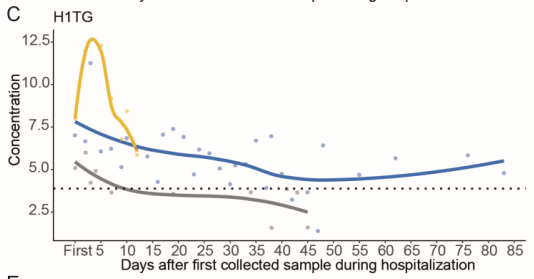
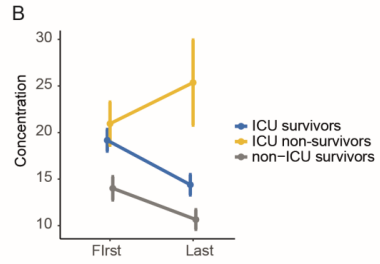
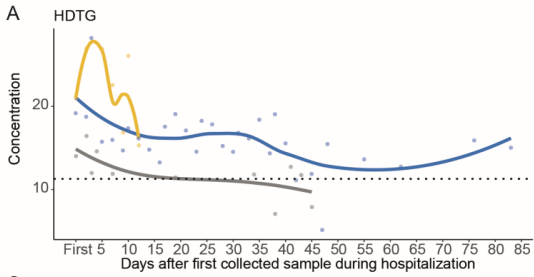


Figure 4. Changes of triglyceride content in HDL subclasses in the course of the disease of ICU survivors, non-survivors, and non-ICU patients. (A) HDTG changes during hospitalization. (B) HDTG changes between the first and last collected samples during hospitalization. (C) H1TG changes during hospitalization. (D) H1TG changes between the first and last collected samples during hospitalization. (E) H2TG changes during hospitalization. (F) H2TG changes between the first and last collected samples during hospitalization. (G) H3TG changes during hospitalization. (H) H3TG changes between the first and last collected samples during hospitalization. (I) H4TG changes during hospitalization. (J) H4TG changes between the first and last collected samples during hospitalization. The dashed line represented the average concentration of triglyceride content in HDL subclasses in healthy individuals.

HDL-4 subfraction showed distinct longitudinal changes between non-ICU COVID-19 patients, ICU COVID-19 survivors, and ICU COVID-19 non-survivors.

The HDL-4 subfraction was lower in ICU COVID-19 patients than in non-ICU COVID-19 patients. Investigating HDL-4 subfraction changes during the disease progression revealed that both concentrations continuously increased over time in non-ICU and ICU survivors (Fig 5). In ICU non-survivors, the levels first decreased then increased a little bit which were much lower than those in healthy individuals, especially H4A1. We also noticed that although the concentrations of HDL-4 subfractions increased in non-ICU and ICU survivors, they were still much lower than in healthy individuals (Fig 5A, C, E, G, I). We did not find any difference in HDL-4 subfractions at the initial time point, but we discovered that there were notable differences between the three groups in the last collected samples regarding the highest concentrations of HDL-4 subfractions in non-ICU and lowest concentrations of HDL-4 subfractions in ICU non-survivors (Fig 5B, D, F, H, J).

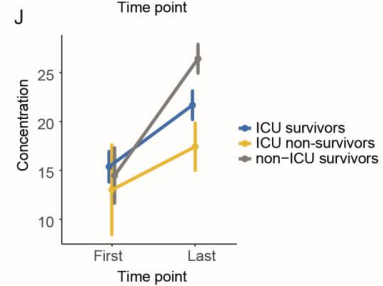
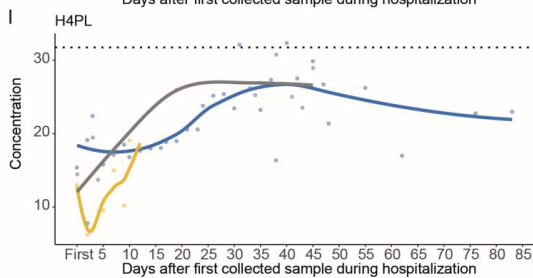
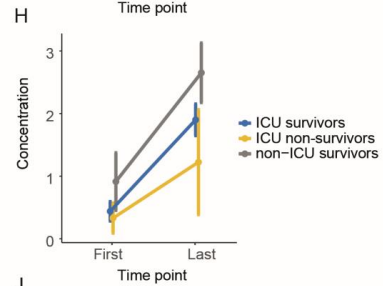
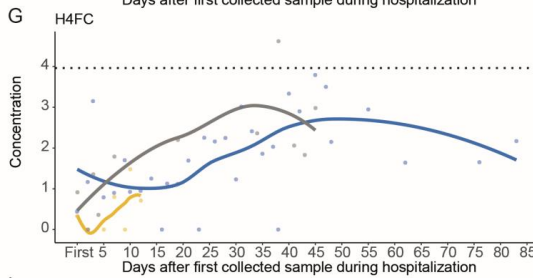
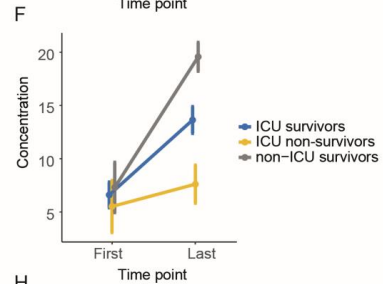
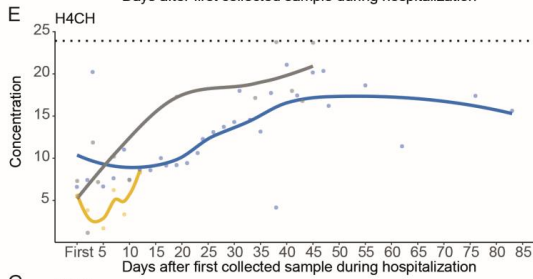
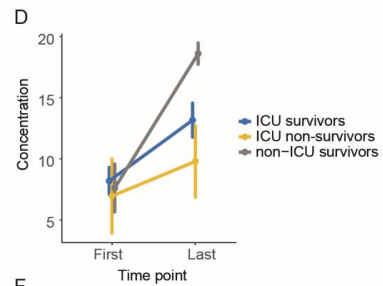
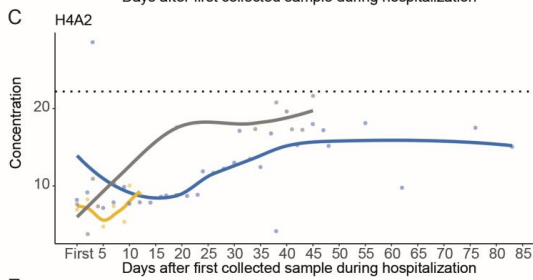
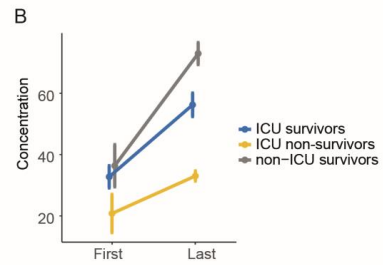
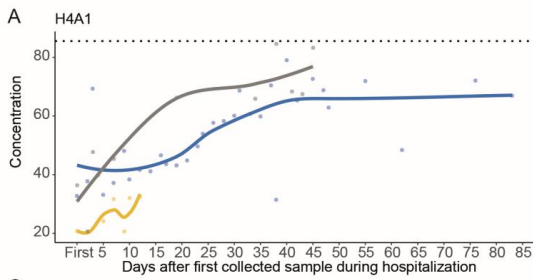


Figure 5 Changes of HDL-4 subfractions in the course of the disease of ICU survivors, non-survivors, and non-ICU patients. (A) H4A1 changes during hospitalization. (B) H4A1 changes between the first and last collected samples during hospitalization. (C) H4A2 changes during hospitalization. (D) H4A2 changes between the first and last collected samples during hospitalization. (E) H4CH changes during hospitalization. (F) H4CH changes between the first and last collected samples during hospitalization. (G) H4FC changes during hospitalization. (H) H4FC changes between the first and last collected samples during hospitalization. (I) H4PL changes during hospitalization. (J) H4PL changes between the first and last collected samples during hospitalization. The dashed line represented the average concentration of HDL-4 subfractions in healthy individuals.

Discussion

In the current study, we found that increased levels of triglycerides in all HDL subclasses and decreased levels of HDL-4 subfractions with disease progression. Altered HDL composition was correlated with SOFA score, circulating endothelial activation markers, and *in vitro* endothelial functional assay parameters, and was associated with distinct disease outcomes. Our findings indicate that changes in HDL composition might be used for risk stratification in disease progression in COVID-19 patients.

In general, higher triglyceride content in most of the HDL subclasses and HDL-4 subfractions were found in COVID-19 patients. These HDL compositional changes that we observed for COVID-19 compared with healthy individuals were in line with previous studies in Germany, Spain, and Australia^{5,23,24}. This finding further confirmed previous studies and proved that the NMR-based lipoprotein profiling technique was quite robust and may be clinically meaningful beyond the routine clinical chemistry measurement.

Our study, for the first time, linked the HDL composition with the *in vitro* endothelial functional assay parameters and identified the specific endothelial function related to HDL composition. Accumulating evidence suggested that hypertriglyceridemia was an independent risk factor for endothelial dysfunction²⁵. We observed that triglyceride content in HDL subclasses was positively correlated with circulating endothelial activation marker Angiotensin 2 which was relevant in respiratory and thrombotic related disorders in COVID-19 ICU patients, showing unfavorable prognostic value²⁶. Syndecan 1, one of the endothelial glycocalyx core proteins, was reported as a marker for disease progression and severity classification of COVID-19²⁷⁻²⁹. Also, we discovered that triglyceride content in HDL-1 showed a positive correlation with soluble Syndecan 1, implying that triglyceride content in large HDL may lead to more aggressive endothelial activation. Moreover, a comparison between non-ICU and ICU COVID-19 patients and the longitudinal changes concerning triglyceride content in HDL subclasses showed clear differences between non-ICU and ICU as well as ICU survivors and non-survivors, further supporting this concept.

Small and dense HDL particles are essential for cellular cholesterol efflux, antioxidative, antithrombotic, anti-inflammatory, and antiapoptotic functions ^{30,31}. Interestingly, our findings revealed that HDL-4 subfractions were lower in COVID-19 patients (both non-ICU and ICU) compared to healthy individuals. Moreover, COVID-19 patients in ICU even showed much lower concentrations of HDL-4 subfractions. Given that HDL-4 subfractions were negatively correlated with endothelial dysfunction, we hypothesized that a lack of specific vasoprotective HDL compositions would lead to disease progression, which was supported by the longitudinal changes in HDL-4 subfractions in COVID-19 patients with different outcomes.

Either higher triglyceride content in HDL subclasses or lower HDL-4 subfractions would cause dysfunction of HDL (data unpublished). The ICU non-survivors showed lower levels of HDL-4 subfractions and higher triglyceride content in HDL subclasses over time, which to some extent, implied that impaired HDL function with less vasoprotective functions might contribute to the worse outcome. Here, our in-house pilot HDL functional assay demonstrated that COVID-19 patients had impaired HDL function in terms of its capacity to suppress TNF α -induced procoagulant cell surface in endothelial cells which is also consistent with earlier findings that HDL from COVID-19 patients was less protective in endothelial cells stimulated by TNF α (permeability, VE-cadherin disorganization, and apoptosis) ³². Following these findings, we discovered that COVID-19 patients showed greater changes in HDL composition, particularly triglyceride content in HDL subclasses and HDL-4 subfractions, which contributed to risk stratification for COVID-19.

The strength of our study is that we measured detailed HDL compositions in a longitudinal population with different disease severity and our study was the first to link HDL compositional changes with serum-induced endothelial functional assay parameters. Our findings further confirmed altered HDL composition in COVID-19 patients with regard to reduced HDL anti-thrombotic capacity, linking it with disease severity assessment and endothelial activation markers; meanwhile, we revealed disease outcome related HDL compositional changes. However, the present study has some limitations mainly related to

the relatively small sample size of the cohort, which might limit generalizability and eliminate the possibility of stratification analyses. In addition, we did not include any ICU patients without COVID-19 to compare whether our findings were general changes for patients ending up in ICU or disease specific changes. Besides, medication use such as lipid lowering medications could affect HDL concentration, composition, and function^{33,34}, which indicated that the changes in HDL composition were not solely affected by the disease. Another limitation is that we only performed a pilot in-house HDL functional assay, which, while promising, was insufficiently conclusive, and more experiments with more time points and patients were required.

Conclusions

To conclude, compared to healthy individuals, non-ICU and ICU COVID-19 patients had altered HDL composition, and lower HDL-4 subfractions and higher triglyceride content in HDL subclasses were associated with endothelial function and disease progression, which might be useful for risk stratification for patients with COVID-19 in ICU.

Abbreviations

ARDS: acute respiratory distress syndrome; B.I.LISATM: Bruker IVDr Lipoprotein Subclass Analysis; CI: confidence interval; SARS-CoV-2: coronavirus causing severe acute respiratory syndrome; ETP: endogenous thrombin potential; HDL: High-density lipoprotein; HDL-C: HDL-cholesterol; HUVEC: Human umbilical vein endothelial cell; ICU: intensive care unit; IQR: interquartile range; NMR: nuclear magnetic resonance; PCA: Principle component analysis; SOFA: sequential organ failure assessment; SD: standard deviation; Peak: thrombin peak height; ttPeak: time to peak; TNF- α : Tumor necrosis factor α ; VelIndex: velocity of thrombin generation.

Acknowledgments

We thank all the patients and healthy volunteers who participated in this study. We express our gratitude to the researchers, nurses, and physicians who assisted in the organization of this study.

Authors' contributions

LY, MAG, and BMvdB contributed to the study concept, design, and analysis; LY analysed and interpreted data, and critically revised the manuscript; AV performed NMR measurements; LY, SZ, and WMPJS performed the *in vitro* endothelial functional assays; and LY, TJR, and BMvdB drafted the manuscript. The final manuscript was read, commented on, and approved by all authors.

Funding

This work was supported by the China Scholarship Council grant to Lushun Yuan (CSC no. 201806270262) and BEAT-COVID funding by Leiden University Medical Center.

Availability of data and materials

All data and methods supporting the findings of this study are available from the corresponding author upon reasonable request.

Ethics approval and consent to participate

The samples were from a trial registered in Dutch Trial Registry (NL8589). The study protocol was approved by the Institutional Review Board (Leiden University Medical Center, Leiden, The Netherlands), and ethical approval was obtained from the Medical Ethical Committee Leiden-Den Haag-Delft (NL73740.058.20).

Consent for publication

The manuscript was approved by all authors for publication.

Competing interests

The authors declare that they have no competing interests.

References

1. Chidambaram, V., Kumar, A., Majella, M.G., Seth, B., Sivakumar, R.K., Voruganti, D., Bavineni, M., Baghal, A., Gates, K., Kumari, A., et al. (2022). HDL cholesterol levels and susceptibility to COVID-19. *EBioMedicine* *82*, 104166. [10.1016/j.ebiom.2022.104166](https://doi.org/10.1016/j.ebiom.2022.104166).
2. Yuan, L., Cheng, S., Sol, W., van der Velden, A.I.M., Vink, H., Rabelink, T.J., and van den Berg, B.M. (2022). Heparan sulfate mimetic fucoidan restores the endothelial glycocalyx and protects against dysfunction induced by serum of COVID-19 patients in the intensive care unit. *ERJ Open Res* *8*. [10.1183/23120541.00652-2021](https://doi.org/10.1183/23120541.00652-2021).
3. Tanaka, S., Couret, D., Tran-Dinh, A., Duranteau, J., Montravers, P., Schwendeman, A., and Meilhac, O. (2020). High-density lipoproteins during sepsis: from bench to bedside. *Crit Care* *24*, 134. [10.1186/s13054-020-02860-3](https://doi.org/10.1186/s13054-020-02860-3).
4. Tran-Dinh, A., Diallo, D., Delbosc, S., Varela-Perez, L.M., Dang, Q.B., Lapergue, B., Burillo, E., Michel, J.B., Levoye, A., Martin-Ventura, J.L., and Meilhac, O. (2013). HDL and endothelial protection. *Br J Pharmacol* *169*, 493-511. [10.1111/bph.12174](https://doi.org/10.1111/bph.12174).
5. Schmelter, F., Foh, B., Mallagaray, A., Rahmoller, J., Ehlers, M., Lehrian, S., von Kopylow, V., Kunsting, I., Lixenfeld, A.S., Martin, E., et al. (2021). Metabolic and Lipidomic Markers Differentiate COVID-19 From Non-Hospitalized and Other Intensive Care Patients. *Front Mol Biosci* *8*, 737039. [10.3389/fmolb.2021.737039](https://doi.org/10.3389/fmolb.2021.737039).
6. Mahat, R.K., Rathore, V., Singh, N., Singh, N., Singh, S.K., Shah, R.K., and Garg, C. (2021). Lipid profile as an indicator of COVID-19 severity: A systematic review and meta-analysis. *Clin Nutr ESPEN* *45*, 91-101. [10.1016/j.clnesp.2021.07.023](https://doi.org/10.1016/j.clnesp.2021.07.023).
7. Chidambaram, V., Shanmugavel Geetha, H., Kumar, A., Majella, M.G., Sivakumar, R.K., Voruganti, D., Mehta, J.L., and Karakousis, P.C. (2022). Association of Lipid Levels With COVID-19 Infection, Disease Severity and Mortality: A Systematic

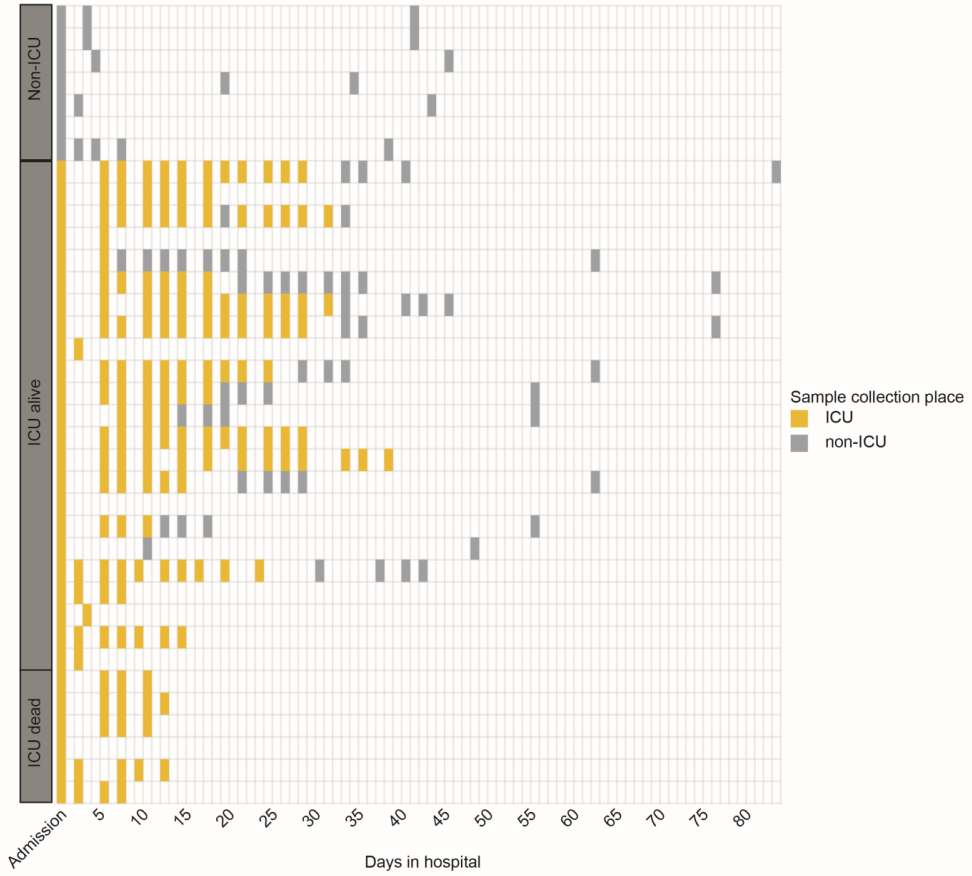
Review and Meta-Analysis. *Front Cardiovasc Med* 9, 862999.
10.3389/fcvm.2022.862999.

8. Jia, C., Anderson, J.L.C., Gruppen, E.G., Lei, Y., Bakker, S.J.L., Dullaart, R.P.F., and Tietge, U.J.F. (2021). High-Density Lipoprotein Anti-Inflammatory Capacity and Incident Cardiovascular Events. *Circulation* 143, 1935-1945.
10.1161/CIRCULATIONAHA.120.050808.
9. Souza Junior, D.R., Silva, A.R.M., Rosa-Fernandes, L., Reis, L.R., Alexandria, G., Bhosale, S.D., Ghilardi, F.R., Dalcoquio, T.F., Bertolin, A.J., Nicolau, J.C., et al. (2021). HDL proteome remodeling associates with COVID-19 severity. *J Clin Lipidol* 15, 796-804. 10.1016/j.jacl.2021.10.005.
10. Stadler, J.T., Mangge, H., Rani, A., Curcic, P., Herrmann, M., Pruller, F., and Marsche, G. (2022). Low HDL Cholesterol Efflux Capacity Indicates a Fatal Course of COVID-19. *Antioxidants (Basel)* 11. 10.3390/antiox11101858.
11. Mietus-Snyder, M., Suslovic, W., Delaney, M., Playford, M.P., Ballout, R.A., Barber, J.R., Otvos, J.D., DeBiasi, R.L., Mehta, N.N., and Remaley, A.T. (2022). Changes in HDL cholesterol, particles, and function associate with pediatric COVID-19 severity. *Front Cardiovasc Med* 9, 1033660.
10.3389/fcvm.2022.1033660.
12. Lounila, J., Ala-Korpela, M., Jokisaari, J., Savolainen, M.J., and Kesaniemi, Y.A. (1994). Effects of orientational order and particle size on the NMR line positions of lipoproteins. *Phys Rev Lett* 72, 4049-4052. 10.1103/PhysRevLett.72.4049.
13. Jeyarajah, E.J., Cromwell, W.C., and Otvos, J.D. (2006). Lipoprotein particle analysis by nuclear magnetic resonance spectroscopy. *Clin Lab Med* 26, 847-870.
10.1016/j.cll.2006.07.006.
14. Jiang, H., Peng, J., Zhou, Z.Y., Duan, Y., Chen, W., Cai, B., Yang, H., and Zhang, W. (2010). Establishing (1)H nuclear magnetic resonance based metabonomics fingerprinting profile for spinal cord injury: a pilot study. *Chin Med J (Engl)* 123, 2315-2319.
15. Straat, M.E., Martinez-Tellez, B., Nahon, K.J., Janssen, L.G.M., Verhoeven, A., van der Zee, L., Mulder, M.T., Kooijman, S., Boon, M.R., van Lennep, J.E.R., et al. (2022). Comprehensive (apo)lipoprotein profiling in patients with genetic hypertriglyceridemia using LC-MS and NMR spectroscopy. *J Clin Lipidol* 16, 472-482. 10.1016/j.jacl.2022.04.004.
16. Bakker, L.E., Boon, M.R., Annema, W., Dijkers, A., van Eyk, H.J., Verhoeven, A., Mayboroda, O.A., Jukema, J.W., Havekes, L.M., Meinders, A.E., et al. (2016). HDL functionality in South Asians as compared to white Caucasians. *Nutrition, metabolism, and cardiovascular diseases : NMCD* 26, 697-705.
10.1016/j.numecd.2016.02.010.

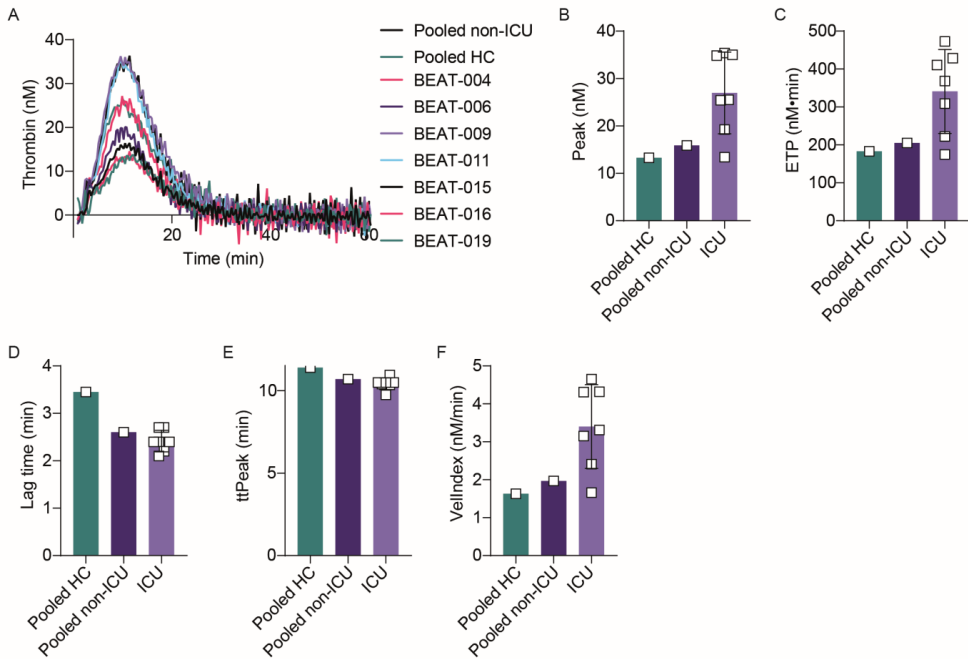
17. Nodeland, M., Klevjer, M., Saether, J., Giskeodegard, G., Bathen, T.F., Wisloff, U., and Bye, A. (2022). Atherogenic lipidomics profile in healthy individuals with low cardiorespiratory fitness: The HUNT3 fitness study. *Atherosclerosis* *343*, 51-57. 10.1016/j.atherosclerosis.2022.01.001.
18. Findeisen, M., Brand, T., and Berger, S. (2007). A ¹H-NMR thermometer suitable for cryoprobes. *Magn Reson Chem* *45*, 175-178. 10.1002/mrc.1941.
19. Wu, P.S., and Otting, G. (2005). Rapid pulse length determination in high-resolution NMR. *J Magn Reson* *176*, 115-119. 10.1016/j.jmr.2005.05.018.
20. Price, W.S. (1999). Water signal suppression in NMR spectroscopy. *Annu Rep Nmr Spectro* *38*, 289-354. Doi 10.1016/S0066-4103(08)60040-X.
21. Kumar, A., Ernst, R.R., and Wuthrich, K. (1980). A two-dimensional nuclear Overhauser enhancement (2D NOE) experiment for the elucidation of complete proton-proton cross-relaxation networks in biological macromolecules. *Biochem Biophys Res Commun* *95*, 1-6. 10.1016/0006-291x(80)90695-6.
22. Mulder, D.J., de Boer, J.F., Graaff, R., de Vries, R., Annema, W., Lefrandt, J.D., Smit, A.J., Tietge, U.J., and Dullaart, R.P. (2011). Skin autofluorescence is inversely related to HDL anti-oxidative capacity in type 2 diabetes mellitus. *Atherosclerosis* *218*, 102-106. 10.1016/j.atherosclerosis.2011.05.011.
23. Kimhofer, T., Lodge, S., Whiley, L., Gray, N., Loo, R.L., Lawler, N.G., Nitschke, P., Bong, S.H., Morrison, D.L., Begum, S., et al. (2020). Integrative Modeling of Quantitative Plasma Lipoprotein, Metabolic, and Amino Acid Data Reveals a Multiorgan Pathological Signature of SARS-CoV-2 Infection. *Journal of proteome research* *19*, 4442-4454. 10.1021/acs.jproteome.0c00519.
24. Bruzzone, C., Bizkarguenaga, M., Gil-Redondo, R., Diercks, T., Arana, E., Garcia de Vicuna, A., Seco, M., Bosch, A., Palazon, A., San Juan, I., et al. (2020). SARS-CoV-2 Infection Dysregulates the Metabolomic and Lipidomic Profiles of Serum. *iScience* *23*, 101645. 10.1016/j.isci.2020.101645.
25. Kajikawa, M., and Higashi, Y. (2019). Triglycerides and endothelial function: molecular biology to clinical perspective. *Curr Opin Lipidol* *30*, 364-369. 10.1097/MOL.0000000000000630.
26. Smadja, D.M., Guerin, C.L., Chocron, R., Yatim, N., Boussier, J., Gendron, N., Khider, L., Hadjadj, J., Goudot, G., Debuc, B., et al. (2020). Angiopoietin-2 as a marker of endothelial activation is a good predictor factor for intensive care unit admission of COVID-19 patients. *Angiogenesis* *23*, 611-620. 10.1007/s10456-020-09730-0.
27. Zhang, D., Li, L., Chen, Y., Ma, J., Yang, Y., Aodeng, S., Cui, Q., Wen, K., Xiao, M., Xie, J., et al. (2021). Syndecan-1, an indicator of endothelial glycocalyx

- degradation, predicts outcome of patients admitted to an ICU with COVID-19. *Mol Med* 27, 151. 10.1186/s10020-021-00412-1.
28. Suzuki, K., Okada, H., Tomita, H., Sumi, K., Kakino, Y., Yasuda, R., Kitagawa, Y., Fukuta, T., Miyake, T., Yoshida, S., et al. (2021). Possible involvement of Syndecan-1 in the state of COVID-19 related to endothelial injury. *Thromb J* 19, 5. 10.1186/s12959-021-00258-x.
 29. Ogawa, F., Oi, Y., Nakajima, K., Matsumura, R., Nakagawa, T., Miyagawa, T., Sakai, K., Saji, R., Taniguchi, H., Takahashi, K., et al. (2021). Temporal change in Syndecan-1 as a therapeutic target and a biomarker for the severity classification of COVID-19. *Thromb J* 19, 55. 10.1186/s12959-021-00308-4.
 30. Camont, L., Lhomme, M., Rached, F., Le Goff, W., Negre-Salvayre, A., Salvayre, R., Calzada, C., Lagarde, M., Chapman, M.J., and Kontush, A. (2013). Small, dense high-density lipoprotein-3 particles are enriched in negatively charged phospholipids: relevance to cellular cholesterol efflux, antioxidative, antithrombotic, anti-inflammatory, and antiapoptotic functionalities. *Arteriosclerosis, thrombosis, and vascular biology* 33, 2715-2723. 10.1161/ATVBAHA.113.301468.
 31. He, Y., Ronsein, G.E., Tang, C., Jarvik, G.P., Davidson, W.S., Kothari, V., Song, H.D., Segrest, J.P., Bornfeldt, K.E., and Heinecke, J.W. (2020). Diabetes Impairs Cellular Cholesterol Efflux From ABCA1 to Small HDL Particles. *Circ Res* 127, 1198-1210. 10.1161/CIRCRESAHA.120.317178.
 32. Begue, F., Tanaka, S., Mouktadi, Z., Rondeau, P., Veeren, B., Diotel, N., Tran-Dinh, A., Robert, T., Velia, E., Mavingui, P., et al. (2021). Altered high-density lipoprotein composition and functions during severe COVID-19. *Sci Rep* 11, 2291. 10.1038/s41598-021-81638-1.
 33. Orsoni, A., Therond, P., Tan, R., Giral, P., Robillard, P., Kontush, A., Meikle, P.J., and Chapman, M.J. (2016). Statin action enriches HDL3 in polyunsaturated phospholipids and plasmalogens and reduces LDL-derived phospholipid hydroperoxides in atherogenic mixed dyslipidemia. *J Lipid Res* 57, 2073-2087. 10.1194/jlr.P068585.
 34. Pirillo, A., and Catapano, A.L. (2017). Pitavastatin and HDL: Effects on plasma levels and function(s). *Atheroscler Suppl* 27, e1-e9. 10.1016/j.atherosclerosis.2017.05.001.

Supporting information



Supplemental figure S1. Timeline of the longitudinal sample collection in the present study.



Supplemental figure S2. Impaired HDL anti-thrombotic capacity in COVID-19 patients. (A) Thrombin generation curve of pooled healthy control (n = 1), pooled non-ICU COVID-19 (n = 1), and ICU COVID-19 patients (n = 7). (B) Difference of thrombin peak height between pooled healthy control, pooled non-ICU COVID-19, and ICU COVID-19 patients. (C) Difference of ETP between pooled healthy control, pooled non-ICU COVID-19, and ICU COVID-19 patients. (E) Difference of lag time between pooled healthy control, pooled non-ICU COVID-19, and ICU COVID-19 patients. (F) Difference of time to peak between pooled healthy control, pooled non-ICU COVID-19, and ICU COVID-19 patients. (G) Difference of thrombin generation velocity between pooled healthy control, pooled non-ICU COVID-19, and ICU COVID-19 patients.

Supplemental table S1. Clinical and experimental characteristics of the study population.

	COVID-19 patients (n = 37)	non-ICU (n = 5)	ICU survivors (n = 26)	ICU non-survivors (n = 6)	Healthy controls (n = 12)
Demographic					
Sex (% women)	18.92	20	19.23	16.67	25
Age, y	61 (57-70)	50 (46-61)	65 (59-71)	60 (58-64)	60 (60-60)
Respiratory function					
Respiratory rate	27.24 (7.53)	19.6 (4.56)	27.09 (6.49)	34.17 (7.25)	-
SpO ₂	90.36 (2.76)	94.8 (1.64)	90.05 (1.96)	87.83 (1.6)	-
FiO ₂	60 (41-100)	-	53 (40-85)	88 (64-100)	-
PaO ₂ /FiO ₂	16.7 (5.27)	-	17.85 (4.78)	13.08 (5.49)	-
Disease severity score					
GCS	3 (3-14)	15 (15-15)	4 (3-11)	3 (3-3)	-
LUMC severity score	12 (9-14)	3 (1-4)	12 (11-13)	16 (13-17)	-
SOFA score	7 (7-11)	-	8 (6-11)	7 (7-10)	-
Circulating markers					
Urea, mg/L	13 (5.15-16.8)	4.75 (4.32-5.05)	14.6 (7.35-17.78)	14.1 (12.85-15.5)	-
CRP, mmol/L	164.35 (61.77-243.7)	102.7 (70.05-139.33)	145 (48.05-239.08)	240.25 (181.45-259.75)	-
Circulating Angiopoietin 2, ng/mL	8.2 (6.21-16.4)	6.3 (4-6.55)	8.36 (5.86-17.09)*	11.2 (8.16-19.49)*	4.45 (2.4-5.53)
Circulating soluble thrombomodulin, ng/mL	14.46 (9.9-19.95)	9.2 (7.75-11.05)	16.51 (11.04-21.58)*	16.06 (9.77-19.69)	6.4 (5.38-8)
Circulating soluble Syndecan 1, ng/mL	9.8 (7.88)	4.3 (3.3)	9.32 (7.35)	14.85 (10.51)	6.26 (5.14)
In vitro endothelial functional assay parameters					
Supernatant Angiopoietin 2, ng/mL	27.39 (10.55)	14.63 (1.62)	29.06 (9.08)*#	32.44 (12.19)*#	13.63 (1.09)
Supernatant Interleukin 6, pg/mL	256.13 (146.4)	71.36 (16.84)	262.44 (121.31)*#	389.08 (130.15)*#	68.11 (13.95)
Supernatant soluble thrombomodulin, ng/mL	2.6 (1.21)	1.19 (0.46)	2.65 (0.88)*#	3.59 (1.59)*#	1.1 (0.21)
Supernatant Von Willebrand factor, U/ml	27.8 (22.9-46.46)	-	30.07 (14.14)*#	49.01 (23.67)*#	3.51 (2.04)
Xa generation 1hr, nM	0.22 (0.04)	0.15 (0.01)	0.22 (0.03)*#	0.25 (0.03)*#	0.14 (0.02)
Xa generation 2hrs, nM	0.23 (0.06)	0.15 (0.02)	0.23 (0.05)*#	0.27 (0.05)*#	0.15 (0.02)
Thrombin peak height, nM	7.51 (2.87-11.5)	0.74 (0.56-1.03)	8.39 (5.1-14.08)*	8.89 (6.76-10.64)*	0.7 (0.59-0.9)
ECIS HPMEC resistance, AUC	17160 (15802-18544)	19085 (19046-19727)	17160 (15589-18321)*	16193 (15366-16766)*#	19252 (18761-19558)
ECIS HPMEC Rb, AUC	131.1 (118-143)	145 (145-154)	134 (116-141)*	120 (115-127)*#	146 (144-149)
ECIS GEnC resistance, AUC	8577.52 (690.87)	9348.6 (197.52)	8497.9 (688.04)*	8200.33 (493.03)*#	9195.42 (547.29)
ECIS GEnC Rb, AUC	44.62 (5.89)	51.78 (2.31)	43.48 (5.87)*#	42.48 (3.33)#	49.65 (3.95)

Data are shown as mean (\pm SD), median (25th percentile–75th percentile), or percentage. One-way ANOVA followed by Tukey's multiple comparisons test or Kruskal-Wallis followed by Dunn's multiple comparisons test were performed; healthy control as reference: * $p < 0.05$; non-ICU as reference: # $p < 0.05$.

Abbreviations: *CRP* C-reaction protein; *ECIS* Electric cell-substrate impedance sensing system; *FiO₂* Fraction of inspired oxygen; *GCS* Glasgow Coma Scale; *PaO₂* Partial pressure of oxygen; *Rb* Resistance between cells; *SOFA score* Sequential organ failure assessment score; *SpO₂* Oxygen saturation.

Supplemental table S2. Quantified HDL-related lipoprotein subfractions.

Abbreviation	Lipoprotein subfraction
TPA1	Total apolipoprotein A1 (ApoA1)
TPA2	Total apolipoprotein A2 (ApoA2)
HDA1	ApoA1 content in total HDL
HDA2	ApoA2 content in total HDL
HDCH	Cholesterol content in total HDL
HDFC	Free Cholesterol content in total HDL
HDPL	Phospholipid content in total HDL
HDTG	Triglyceride content in total HDL
H1A1	ApoA1 content in HDL-1 subclass
H1A2	ApoA2 content in HDL-1 subclass
H1CH	Cholesterol content in HDL-1 subclass
H1FC	Free Cholesterol content HDL-1 subclass
H1PL	Phospholipid content in HDL-1 subclass
H1TG	Triglyceride content in HDL-1 subclass
H2A1	ApoA1 content in HDL-2 subclass
H2A2	ApoA2 content in HDL-2 subclass
H2CH	Cholesterol content in HDL-2 subclass
H2FC	Free Cholesterol content HDL-2 subclass
H2PL	Phospholipid content in HDL-2 subclass
H2TG	Triglyceride content in HDL-2 subclass
H3A1	ApoA1 content in HDL-3 subclass
H3A2	ApoA2 content in HDL-3 subclass
H3CH	Cholesterol content in HDL-3 subclass
H3FC	Free Cholesterol content HDL-3 subclass
H3PL	Phospholipid content in HDL-3 subclass
H3TG	Triglyceride content in HDL-3 subclass

H4A1	ApoA1 content in HDL-4 subclass
H4A2	ApoA2 content in HDL-4 subclass
H4CH	Cholesterol content in HDL-4 subclass
H4FC	Free Cholesterol content HDL-4 subclass
H4PL	Phospholipid content in HDL-4 subclass
H4TG	Triglyceride content in HDL-4 subclass

Supplemental table S3. Differential HDL composition between non-ICU COVID-19 patients and healthy controls based on multinomial logistic regression analysis. (Reference: healthy controls)

HDL composition	Regression coefficient (β)			P value
	β	CI2.5	CI97.5	
HDCH	-2.42	-3.10	-1.73	4.11E-12
TPA1	-2.29	-2.95	-1.63	1.14E-11
TPA2	-2.96	-3.84	-2.09	3.32E-11
HDTG	1.10	0.53	1.67	1.38E-04
HDFC	-1.33	-1.77	-0.89	2.57E-09
HDPL	-1.42	-1.85	-0.99	1.36E-10
HDA1	-2.41	-3.10	-1.73	5.08E-12
HDA2	-2.41	-3.06	-1.76	3.10E-13
H1TG	0.93	0.39	1.47	7.62E-04
H2TG	2.07	1.25	2.89	7.53E-07
H3TG	1.21	0.67	1.75	1.07E-05
H4TG	0.77	0.35	1.20	3.89E-04
H1CH	-0.53	-0.88	-0.18	2.96E-03
H2CH	-1.34	-1.78	-0.90	1.75E-09
H3CH	-2.85	-3.64	-2.06	1.66E-12
H4CH	-3.93	-5.25	-2.61	6.01E-09
H1FC	-1.03	-1.41	-0.65	1.40E-07
H2FC	-1.60	-2.06	-1.14	7.35E-12
H3FC	-2.00	-2.53	-1.46	2.74E-13
H4FC	-1.56	-2.09	-1.03	8.94E-09
H1PL	-0.48	-0.85	-0.10	1.32E-02
H2PL	-1.04	-1.47	-0.60	3.31E-06
H3PL	-1.58	-2.04	-1.13	8.96E-12
H4PL	-1.71	-2.28	-1.14	4.83E-09
H1A1	-0.51	-0.88	-0.14	7.03E-03
H2A1	-1.78	-2.26	-1.30	3.48E-13
H3A1	-1.87	-2.37	-1.37	2.98E-13
H4A1	-3.23	-4.30	-2.16	2.95E-09
H1A2	-0.69	-1.11	-0.27	1.18E-03
H2A2	-0.78	-1.18	-0.38	1.39E-04
H3A2	-1.29	-1.71	-0.87	1.59E-09
H4A2	-3.16	-4.19	-2.13	2.02E-09

Supplemental table S4. Differential HDL composition between ICU COVID-19 patients and healthy controls based on multinomial logistic regression analysis. (Reference: healthy controls)

HDL composition	Regression coefficient (β)			P value
	β	CI2.5	CI97.5	
HDCH	-2.38	-3.04	-1.73	9.19E-13
TPA1	-2.59	-3.24	-1.94	8.22E-15
TPA2	-3.11	-3.97	-2.25	1.50E-12
HDTG	1.77	1.21	2.33	6.06E-10
HDFC	-1.33	-1.73	-0.93	7.41E-11
HDPL	-0.83	-1.18	-0.48	3.02E-06
HDA1	-2.59	-3.26	-1.92	2.98E-14
HDA2	-2.26	-2.87	-1.66	2.63E-13
H1TG	1.50	0.98	2.03	1.88E-08
H2TG	3.82	2.90	4.74	4.44E-16
H3TG	2.04	1.48	2.59	5.53E-13
H4TG	0.74	0.35	1.14	2.32E-04
H1CH	-0.36	-0.65	-0.07	1.56E-02
H2CH	-0.59	-0.95	-0.23	1.44E-03
H3CH	-2.75	-3.51	-1.99	1.44E-12
H4CH	-5.18	-6.56	-3.81	1.72E-13
H1FC	-0.95	-1.27	-0.62	1.15E-08
H2FC	-0.75	-1.12	-0.39	6.11E-05
H3FC	-1.72	-2.19	-1.25	1.10E-12
H4FC	-2.42	-2.99	-1.85	0.00E+00
H1PL	-0.03	-0.33	0.27	8.46E-01
H2PL	0.34	-0.01	0.68	5.85E-02
H3PL	-0.63	-0.97	-0.30	2.32E-04
H4PL	-2.35	-2.94	-1.77	3.11E-15
H1A1	-0.12	-0.41	0.17	4.12E-01
H2A1	-0.69	-1.04	-0.33	1.52E-04
H3A1	-1.46	-1.89	-1.02	5.58E-11
H4A1	-4.62	-5.76	-3.48	2.00E-15
H1A2	0.13	-0.18	0.44	4.20E-01
H2A2	0.01	-0.31	0.33	9.67E-01
H3A2	-0.68	-1.00	-0.36	3.90E-05
H4A2	-4.16	-5.23	-3.09	3.02E-14

Supplemental table S5. Differential HDL composition between non-ICU COVID-19 patients and ICU COVID-19 patients based on multinomial logistic regression analysis. (Reference: non-ICU COVID-19 patients)

HDL composition	Regression coefficient (β)			P value
	β	CI2.5	CI97.5	
HDCH	0.03	-0.28	0.34	8.35E-01
TPA1	-0.30	-0.63	0.03	7.46E-02
TPA2	-0.15	-0.48	0.18	3.86E-01
HDTG	0.67	0.33	1.00	1.09E-04
HDFC	0.01	-0.29	0.30	9.73E-01
HDPL	0.59	0.27	0.91	2.49E-04
HDA1	-0.18	-0.50	0.14	2.73E-01
HDA2	0.15	-0.18	0.47	3.79E-01
H1TG	0.57	0.26	0.89	3.41E-04
H2TG	1.75	1.19	2.31	8.86E-10
H3TG	0.83	0.47	1.19	6.46E-06
H4TG	-0.03	-0.29	0.23	8.22E-01
H1CH	0.17	-0.11	0.46	2.34E-01
H2CH	0.75	0.45	1.05	1.28E-06
H3CH	0.10	-0.22	0.41	5.45E-01
H4CH	-1.25	-1.66	-0.85	1.13E-09
H1FC	0.08	-0.23	0.39	5.99E-01
H2FC	0.85	0.53	1.17	2.32E-07
H3FC	0.28	-0.05	0.61	9.84E-02
H4FC	-0.86	-1.21	-0.52	9.54E-07
H1PL	0.45	0.14	0.75	4.20E-03
H2PL	1.37	1.00	1.75	1.06E-12
H3PL	0.95	0.60	1.30	1.17E-07
H4PL	-0.64	-0.98	-0.31	1.38E-04
H1A1	0.39	0.08	0.69	1.23E-02
H2A1	1.10	0.73	1.46	3.74E-09
H3A1	0.41	0.10	0.72	9.87E-03
H4A1	-1.39	-1.81	-0.97	1.05E-10
H1A2	0.82	0.47	1.17	4.53E-06
H2A2	0.79	0.46	1.11	2.10E-06
H3A2	0.61	0.29	0.93	2.07E-04
H4A2	-1.00	-1.37	-0.63	1.38E-07

CHAPTER

7

Summary, general discussion, and future perspectives

Thromboinflammation, which is a main trigger for endothelial dysfunction, has emerged as a new term to describe the interconnection between the simultaneous activation of the coagulation pathway and immune response. In the present thesis, the role of thromboinflammation in different high-risk populations, such as women vs. men in the general Dutch population, patients with T2DM from different ethnicities, and COVID-19 patients are highlighted.

Thromboinflammation, gender differences, and cardiovascular disease

Thromboinflammation exhibits sex differences, contributing to the risk of cardiovascular disease. Endothelial glycocalyx, a key regulator of thromboinflammation, is also involved in various vascular complications.

In the present thesis, in **Chapter 2**, we observed an association between early (pre-clinical) microvascular health changes measured by SDF imaging and coagulation factor activation and discovered a striking sex difference in microvascular health, in which women showed a perturbed endothelial glycocalyx concomitant with a more procoagulable endothelial surface, and this association was not observed in men. Based on previous studies [1-3], specifically in women, an increase in endothelial glycocalyx is associated with an increased risk of CHD. These findings highlight the importance of sex differences in microcirculatory perturbation in CHD, suggesting the potential clinical utility of monitoring microcirculatory change specifically in women to prevent the development of CHD. In line with these findings are earlier studies revealing that women who were suspected of or had confirmed clinical ischaemic heart disease have less atherosclerosis than men and a lower prevalence of obstructive coronary artery disease (CAD), especially when they are young [4]. Additionally, more than 50% of women with angina tested negative for coronary angiography, further indicating sex differences in CHD development [5]. Therefore, based

on these previous findings, accumulating evidence shows that perturbation of the microcirculation is more evident to contribute to CHD in women [6].

Perturbation of the endothelial glycocalyx could lead to procoagulant status [7], and together with previous studies demonstrating that the underlying systemic presence of a hypercoagulable state was associated with the incidence of CHD [8-10], hints toward an association between endothelial glycocalyx health and CHD which is mediated by coagulation activation. From the Tromsø Study, a case-cohort design with 1495 participants included, revealed that Syndecan-4, one of the core proteins of endothelial glycocalyx, was associated with myocardial infarction incidence. The observed association was also stronger in women than men, indicating the link between endothelial glycocalyx and CHD as well as gender differences [11]. Interestingly, such a sex-dependent association between CHD and impaired sublingual microvascular glycocalyx barrier function in women was also found in a study by Brands et al. [12].

Thromboinflammation, diabetes in different ethnicities, and HDL function and dyslipidemia

HDL exhibits functions including anti-inflammatory and anti-thrombotic capacities, which can regulate thromboinflammation in pathophysiological conditions [13]. In chronic situations such as CHD, diabetes, and chronic kidney disease, HDL could lose its protective function and even gain adverse functionality further exacerbating the disease progression [14-17].

The mechanism of T2DM disease progression varies in different ethnicities [18] and recent studies showed that changes in HDL function may be one of the underlying mechanisms resulting in disease development and progression. Given that reduction of low-density lipoproteins (LDL) by statin use is associated with insulin resistance and an increased risk

of hyperglycemic complications in T2DM, particularly HDL functionality, may therefore be a better candidate to monitor diabetes progression [19-21].

A study comparing HDL function in Dutch South Asians to Dutch white Europeans within three age groups (neonates, adolescents, and adults), reported that in the absence of T2DM, only the ability of HDL to prevent LDL oxidation was decreased in overweight Dutch South Asians when compared to obese Dutch white Caucasians [22]. Another single-center study in Rotterdam assessing the relation between the development of dyslipidemia and glucose intolerance found that small HDL fractions were associated with insulin resistance and beta-cell dysfunction in South Asian families at risk of T2DM [15].

In **Chapter 3**, we compared HDL composition in healthy individuals and patients with T2DM of Dutch South Asian and Dutch white Caucasian ethnicity. Here we observed that between both ethnic groups, HDL composition differed. The impaired HDL functionality found in Dutch South Asians with T2DM might be because of loss of the smallest HDL subfractions; while in Dutch white Caucasians with T2DM, increased triglyceride content in the smallest HDL fraction contributes to HDL dysfunction. In line with these findings, small and dense HDL particles have been shown to play a vital role in multiple functions, such as cellular cholesterol efflux mediation, anti-oxidative, anti-thrombotic, anti-inflammatory, and anti-apoptotic capacities [16]. In our current study, we found that concentrations of the smallest HDL subfractions except triglyceride content were negatively associated with disease duration in Dutch South Asians with T2DM rather than in Dutch white Caucasian, suggesting a more vulnerable HDL composition phenotype. Moreover, T2DM patients in both ethnic groups showed significantly reduced anti-thrombotic capacity due to impaired HDL function. Consistent with an earlier finding, impaired HDL function in T2DM patients in terms of the capacity to suppress TNF-induced vascular cell adhesion molecule-1 (VCAM-1) expression in endothelial cells *in vitro* was observed [23]. According to our findings, HDL dysfunction induced thromboinflammation deregulation might contribute to a higher risk of disease development and progression in South Asians with T2DM.

In oxidative stress-induced cardiovascular disease, oxidized lipids can activate platelets via CD36, demonstrating a link between dysregulated lipoprotein metabolism, oxidative stress, and thrombus formation [24]. Lipids are involved in both the intrinsic and extrinsic pathways of prothrombin activation and dyslipidemia is one of the hallmarks of T2DM. In **Chapter 4**, using a novel targeted quantitative LC/MS-based Shotgun Lipidomics Assistant (SLA) platform, we generated a comprehensive mapping of the circulating lipidome in Dutch South Asians and Dutch white Caucasians with or without T2DM. Based on lipidomics phenotyping, we observed detailed insight into the complexity of lipid metabolism and the interindividual variations within the various ethnic groups. It is worth noting that there were distinct differences in the lipidome mainly related to the metabolism of cholesteryl esters (CEs), diacylglycerides (DGs), phosphatidylethanolamines (PEs), sphingomyelins (SMs), and triglycerides (TGs) between T2DM and healthy controls in our study population, which were consistent with previous findings observed in the case-cohort study nested within the PREDIMED trial [25] and the longitudinal METSIM study [26]. However, with conflicting results as reported in these two studies based on Chinese populations that FFA, SM, and LPC lipid species were higher in Chinese with T2DM, whereas we found opposite results in Dutch with T2DM, the high variability in lipidomics profile between ethnicities is further indicated.

Thromboinflammation and diabetes-related complications

Lipoprotein and lipid metabolism in patients with T2DM could lead to the deregulation of thromboinflammation and further affect the development or exacerbation of diabetes-related complications. Several studies discovered that dyslipidemia was linked to an increased risk of diabetes-related microvascular complications such as neuropathy and retinopathy [27-29]. South Asians have a higher prevalence of diabetic retinopathy than white Caucasians and a shorter aggravation time, and the diabetic retinopathy lesions [30] tend to be distributed more centrally [31]. In **Chapter 3**, we specifically observed that

lower ApoA2 and HDL-4 subclass concentrations in Dutch South Asian individuals with T2DM were associated with higher odds of having diabetes-related pan-microvascular complications such as retinopathy and neuropathy.

In addition to diabetic neuropathy and retinopathy, South Asian patients with T2DM are more likely to develop microvascular complications such as diabetic nephropathy, with a higher incidence of micro- and macroalbuminuria in South Asians as compared to white European Caucasians with T2DM and a faster progression to end-stage renal disease [32, 33]. This could be because these patients have a higher burden of systemic and glomerular inflammation. Additionally, South Asians have a unique body composition, with a more abdominally obese phenotype and a high percentage of visceral fat, which is dominant in the production and secretion of certain inflammatory cytokines, that contribute to the chronic low-grade inflammatory state [34]. Meanwhile, in **Chapter 4**, we identified a unique lipid species, DG, which was associated with diabetic nephropathy and renal functions. The DG- protein kinase C (PKC)/ protein kinase D (PKD) signaling network could regulate redox balance and induce oxidative stress [35]. In T2DM, DG concentration increases and the accumulation of DG further activates the PKC/PKD, thus resulting in diabetic nephropathy [36]. It was notable that DG 18:1_18:2 was higher in diabetic nephropathy, particularly in South Asians with T2DM, and had the most correlations with various clinical parameters. Even in an external cohort of Chinese subjects with IgA nephropathy, the correlations with renal function persisted. Future studies concerning diabetic nephropathy in multiple ethnic groups with large sample sizes are needed to verify our findings.

Thromboinflammation and COVID-19

Hyperinflammation is a hallmark of COVID-19, and the inflammatory response to SARS-CoV-2 infection frequently causes remarkable activation of the coagulation cascade. The

subsequent process called thromboinflammation is characterized by systemic endothelial damage and loss of proper anti-coagulant properties [37, 38].

Hyperinflammation induced by COVID-19 could disrupt vascular integrity. The glycocalyx is capable of regulating endothelial cell integrity and homeostasis through vascular barrier permeability protective function, anti-inflammation, and anti-coagulation capacity.

Buijssers et al. observed that the activity of endothelial glycocalyx-degrading enzyme heparanase, which was involved in vascular leakage and inflammation, was increased in COVID-19 patients and was associated with disease severity [39]. Additionally, Kümpers et al. revealed that non-anticoagulant heparin fragments could inhibit the activity of heparanase and prevent endothelial glycocalyx injury in response to COVID-19 serum [40]. Meanwhile, the MYSTIC study revealed that glycocalyx health, as measured by perfused boundary region (PBR), an inversed reflection of endothelial glycocalyx layer, was a prognostic predictor for COVID-19 and disease severity [41]. In **Chapter 5**, we showed that loss of endothelial glycocalyx in response to serum from ICU COVID-19 patients induced endothelial dysfunction through increased IL-6, ICAM1, ANG2, and HPSE1 gene expression and activation of the NF- κ B signaling pathway. In addition, damaged endothelial glycocalyx resulted in vascular leakage and disturbed cell-cell contact.

Inhibition of the protective ANG1/TIE2 signaling cascade by ANG2 is a central regulator in protecting the vasculature against thrombus formation and vascular stabilization [42, 43]. A number of studies indicated that circulating ANG2 levels were increased in COVID-19 and associated with a worse prognosis [44-46]. In line with these findings, we also found that ANG2 levels were increased in ICU COVID-19 patients (**Chapter 5**). The presence of endothelial glycocalyx is required for anti-coagulation property and maintenance of endothelial quiescence. We also showed that loss of endothelial glycocalyx in response to serum from ICU COVID-19 patients could form a pro-coagulant cell surface through increased tissue factor expression and increased secretion of ANG2 and vWF (**Chapter 5**). To further validate our hypothesis that glycocalyx damage contributed to thromboinflammation in COVID-19, we tested whether preservation of the endothelial

glycocalyx might be an effective intervention to improve vascular health. We found that the heparan sulfate mimetic fucoidan could restore endothelial functionality including restoration of the endothelial glycocalyx, ameliorating endothelial activation, and leading to protection of the endothelial barrier function and induced anti-thrombotic effects (**Chapter 5**).

Michalick et al. discovered that plasma mediators in patients with severe COVID-19 could lead to lung endothelial barrier failure [47]. Meanwhile, Stahl et al. showed that blood composition in critically ill COVID-19 patients could cause endothelial injury involving glycocalyx integrity loss and vascular destabilization [48]. A number of cytokines and chemokines were increased in COVID-19 patients; however, the observed cytokine storm in COVID-19 patients was lower than observed in non-COVID-19 severe cases with ARDS, sepsis, and influenza virus infection [49, 50]. The discrepancy suggests that other mediators such as oxidized lipids or dysfunctional lipoproteins might contribute to COVID-19 pathogenesis. Given that COVID-19, in the end, is an endothelial disease, in **Chapter 6**, we fulfill the missing puzzle of blood mediators leading to endothelial dysfunction in COVID-19. We found that increased levels of HDL triglyceride content and decreased levels of the smallest HDL subclass were associated with endothelial dysfunction and COVID-19 disease severity. Besides, dysfunctional HDL in COVID-19 patients had less anti-thrombotic capacity than healthy individuals, suggesting a higher risk of thromboinflammation. These findings were also in line with our previous observations that a disturbed endothelial glycocalyx in COVID-19 patients resulted in the formation of a pro-coagulant cell surface (**Chapter 5**).

Future perspectives and open questions

In this thesis, we emphasize thromboinflammation in high-risk populations such as females, South Asians, T2DM, and COVID-19 patients. We also show that perturbation of endothelial glycocalyx, dysfunction of HDL, and dysregulation of lipid metabolism can lead to thromboinflammation, which all can play a critical role in acute or chronic disease development.

In **Chapter 2**, we showed that glycocalyx function together with pro-coagulation factors could contribute to early CHD development in women. However, we still lack a detailed mechanism and follow-up information on non-obstructive CHD, which needs to be investigated. In **Chapter 3**, we showed the HDL compositional and functional changes in South Asians with T2DM. HDL function depended on both lipidome and proteome. Therefore, specific determination of the proteome in isolated HDL particles is the next step in unraveling the underlying mechanisms in HDL functional changes. In **Chapter 4**, we found a specific lipid that only appeared in renal diseases (diabetic nephropathy and IgA nephropathy). However, the concentration of this lipid is quite low, necessitating a more precise and in-depth measurement and analysis method on a renal disease cohort with a larger sample size. In **Chapter 5** and **Chapter 6**, we only compared healthy individuals with ICU COVID-19 patients; however, whether our findings were specifically characteristic of COVID-19 is still unknown, emphasizing the need for the inclusion of non-COVID-19 ICU patient samples.

We showed a reduction of HDL subfractions in diabetes and COVID-19. However, it is still unknown whether supplementation of HDL mimetic or HDL-raising agents could be a potential therapeutic strategy for COVID-19, diabetes, and diabetes-related complications, which needs to be explored further.

References

- 1 Olson NC, Cushman M, Judd SE, Kissela BM, Safford MM, Howard G, Zakai NA. Associations of coagulation factors IX and XI levels with incident coronary heart disease and ischemic stroke: the REGARDS study. *J Thromb Haemost*. 2017; **15**: 1086-94. 10.1111/jth.13698.
- 2 Fibrinogen Studies C, Danesh J, Lewington S, Thompson SG, Lowe GD, Collins R, Kostis JB, Wilson AC, Folsom AR, Wu K, Benderly M, Goldbourt U, Willeit J, Kiechl S, Yarnell JW, Sweetnam PM, Elwood PC, Cushman M, Psaty BM, Tracy RP, Tybjaerg-Hansen A, Haverkate F, de Maat MP, Fowkes FG, Lee AJ, Smith FB, Salomaa V, Harald K, Rasi R, Vahtera E, Jousilahti P, Pekkanen J, D'Agostino R, Kannel WB, Wilson PW, Tofler G, Arocha-Pinango CL, Rodriguez-Larralde A, Nagy E, Mijares M, Espinosa R, Rodriguez-Roa E, Ryder E, Diez-Ewald MP, Campos G, Fernandez V, Torres E, Marchioli R, Valagussa F, Rosengren A, Wilhelmsen L, Lappas G, Eriksson H, Cremer P, Nagel D, Curb JD, Rodriguez B, Yano K, Salonen JT, Nyyssonen K, Tuomainen TP, Hedblad B, Lind P, Loewel H, Koenig W, Meade TW, Cooper JA, De Stavola B, Knottenbelt C, Miller GJ, Cooper JA, Bauer KA, Rosenberg RD, Sato S, Kitamura A, Naito Y, Palosuo T, Ducimetiere P, Amouyel P, Arveiler D, Evans AE, Ferrieres J, Juhan-Vague I, Bingham A, Schulte H, Assmann G, Cantin B, Lamarche B, Despres JP, Dagenais GR, Tunstall-Pedoe H, Woodward M, Ben-Shlomo Y, Davey Smith G, Palmieri V, Yeh JL, Rudnicka A, Ridker P, Rodeghiero F, Tosetto A, Shepherd J, Ford I, Robertson M, Brunner E, Shipley M, Feskens EJ, Kromhout D, Dickinson A, Ireland B, Juzwishin K, Kaptoge S, Lewington S, Memon A, Sarwar N, Walker M, Wheeler J, White I, Wood A. Plasma fibrinogen level and the risk of major cardiovascular diseases and nonvascular mortality: an individual participant meta-analysis. *JAMA*. 2005; **294**: 1799-809. 10.1001/jama.294.14.1799.
- 3 Zakai NA, Judd SE, Kissela B, Howard G, Safford MM, Cushman M. Factor VIII, Protein C and Cardiovascular Disease Risk: The REasons for Geographic and Racial Differences in Stroke Study (REGARDS). *Thromb Haemost*. 2018; **118**: 1305-15. 10.1055/s-0038-1655766.
- 4 Reynolds HR, Bairey Merz CN, Berry C, Samuel R, Saw J, Smilowitz NR, de Souza A, Sykes R, Taqueti VR, Wei J. Coronary Arterial Function and Disease in Women With No Obstructive Coronary Arteries. *Circ Res*. 2022; **130**: 529-51. 10.1161/CIRCRESAHA.121.319892.
- 5 Lee BK, Lim HS, Fearon WF, Yong AS, Yamada R, Tanaka S, Lee DP, Yeung AC, Tremmel JA. Invasive evaluation of patients with angina in the absence of obstructive coronary artery disease. *Circulation*. 2015; **131**: 1054-60. 10.1161/CIRCULATIONAHA.114.012636.
- 6 Pries AR, Reglin B. Coronary microcirculatory pathophysiology: can we afford it to remain a black box? *Eur Heart J*. 2017; **38**: 478-88. 10.1093/eurheartj/ehv760.
- 7 Yuan L, Cheng S, Sol W, van der Velden AIM, Vink H, Rabelink TJ, van den Berg BM. Heparan sulfate mimetic fucoidan restores the endothelial glycocalyx and protects against

dysfunction induced by serum of COVID-19 patients in the intensive care unit. *ERJ Open Res.* 2022; **8**. 10.1183/23120541.00652-2021.

8 Song CJ, Nakagomi A, Chandar S, Cai H, Lim IG, McNeil HP, Freedman SB, Geczy CL. C-reactive protein contributes to the hypercoagulable state in coronary artery disease. *J Thromb Haemost.* 2006; **4**: 98-106. 10.1111/j.1538-7836.2005.01705.x.

9 Tantry US, Bliden KP, Suarez TA, Kreutz RP, Dichiaro J, Gurbel PA. Hypercoagulability, platelet function, inflammation and coronary artery disease acuity: results of the Thrombotic Risk Progression (TRIP) study. *Platelets.* 2010; **21**: 360-7. 10.3109/09537100903548903.

10 Bratseth V, Pettersen AA, Opstad TB, Arnesen H, Seljeflot I. Markers of hypercoagulability in CAD patients. Effects of single aspirin and clopidogrel treatment. *Thromb J.* 2012; **10**: 12. 10.1186/1477-9560-10-12.

11 Solbu MD, Kolset SO, Jenssen TG, Wilsgaard T, Lochen ML, Mathiesen EB, Melsom T, Eriksen BO, Reine TM. Gender differences in the association of syndecan-4 with myocardial infarction: The population-based Tromso Study. *Atherosclerosis.* 2018; **278**: 166-73. 10.1016/j.atherosclerosis.2018.08.005.

12 Brands J, Hubel CA, Althouse A, Reis SE, Pacella JJ. Noninvasive sublingual microvascular imaging reveals sex-specific reduction in glycocalyx barrier properties in patients with coronary artery disease. *Physiol Rep.* 2020; **8**: e14351. 10.14814/phy2.14351.

13 von Eckardstein A, Nordestgaard BG, Remaley AT, Catapano AL. High-density lipoprotein revisited: biological functions and clinical relevance. *Eur Heart J.* 2022. 10.1093/eurheartj/ehac605.

14 Li Y, Zhao M, He D, Zhao X, Zhang W, Wei L, Huang E, Ji L, Zhang M, Willard B, Fu Z, Wang L, Pan B, Zheng L, Ji L. HDL in diabetic nephropathy has less effect in endothelial repairing than diabetes without complications. *Lipids Health Dis.* 2016; **15**: 76. 10.1186/s12944-016-0246-z.

15 Yahya R, Jainandunsing S, Rashid M, van der Zee L, Touw A, de Rooij FWM, Sijbrands EJG, Verhoeven AJM, Mulder MT. HDL associates with insulin resistance and beta-cell dysfunction in South Asian families at risk of type 2 diabetes. *J Diabetes Complications.* 2021; **35**: 107993. 10.1016/j.jdiacomp.2021.107993.

16 He Y, Ronsein GE, Tang C, Jarvik GP, Davidson WS, Kothari V, Song HD, Segrest JP, Bornfeldt KE, Heinecke JW. Diabetes Impairs Cellular Cholesterol Efflux From ABCA1 to Small HDL Particles. *Circ Res.* 2020; **127**: 1198-210. 10.1161/CIRCRESAHA.120.317178.

17 Jia C, Anderson JLC, Gruppen EG, Lei Y, Bakker SJL, Dullaart RPF, Tietge UJF. High-Density Lipoprotein Anti-Inflammatory Capacity and Incident Cardiovascular Events. *Circulation.* 2021; **143**: 1935-45. 10.1161/CIRCULATIONAHA.120.050808.

- 18 Sattar N, Gill JM. Type 2 diabetes in migrant south Asians: mechanisms, mitigation, and management. *Lancet Diabetes Endocrinol*. 2015; **3**: 1004-16. 10.1016/S2213-8587(15)00326-5.
- 19 Mansi IA, Chansard M, Lingvay I, Zhang S, Halm EA, Alvarez CA. Association of Statin Therapy Initiation With Diabetes Progression: A Retrospective Matched-Cohort Study. *JAMA Intern Med*. 2021; **181**: 1562-74. 10.1001/jamainternmed.2021.5714.
- 20 Liew SM, Lee PY, Hanafi NS, Ng CJ, Wong SS, Chia YC, Lai PS, Zaidi NF, Khoo EM. Statins use is associated with poorer glycaemic control in a cohort of hypertensive patients with diabetes and without diabetes. *Diabetol Metab Syndr*. 2014; **6**: 53. 10.1186/1758-5996-6-53.
- 21 Sukhija R, Prayaga S, Marashdeh M, Bursac Z, Kakar P, Bansal D, Sachdeva R, Kesan SH, Mehta JL. Effect of statins on fasting plasma glucose in diabetic and nondiabetic patients. *J Investig Med*. 2009; **57**: 495-9. 10.2310/JIM.0b013e318197ec8b.
- 22 Bakker LE, Boon MR, Annema W, Dikkers A, van Eyk HJ, Verhoeven A, Mayboroda OA, Jukema JW, Havekes LM, Meinders AE, Willems van Dijk K, Jazet IM, Tietge UJ, Rensen PC. HDL functionality in South Asians as compared to white Caucasians. *Nutr Metab Cardiovasc Dis*. 2016; **26**: 697-705. 10.1016/j.numecd.2016.02.010.
- 23 Ebtehaj S, Gruppen EG, Parvizi M, Tietge UJF, Dullaart RPF. The anti-inflammatory function of HDL is impaired in type 2 diabetes: role of hyperglycemia, paraoxonase-1 and low grade inflammation. *Cardiovasc Diabetol*. 2017; **16**: 132. 10.1186/s12933-017-0613-8.
- 24 Jackson SP, Calkin AC. The clot thickens--oxidized lipids and thrombosis. *Nat Med*. 2007; **13**: 1015-6. 10.1038/nm0907-1015.
- 25 Razquin C, Toledo E, Clish CB, Ruiz-Canela M, Dennis C, Corella D, Papandreou C, Ros E, Estruch R, Guasch-Ferre M, Gomez-Gracia E, Fito M, Yu E, Lapetra J, Wang D, Romaguera D, Liang L, Alonso-Gomez A, Deik A, Bullo M, Serra-Majem L, Salas-Salvado J, Hu FB, Martinez-Gonzalez MA. Plasma Lipidomic Profiling and Risk of Type 2 Diabetes in the PREDIMED Trial. *Diabetes Care*. 2018; **41**: 2617-24. 10.2337/dc18-0840.
- 26 Suvitaival T, Bondia-Pons I, Yetukuri L, Poho P, Nolan JJ, Hyotylainen T, Kuusisto J, Oresic M. Lipidome as a predictive tool in progression to type 2 diabetes in Finnish men. *Metabolism*. 2018; **78**: 1-12. 10.1016/j.metabol.2017.08.014.
- 27 Rao H, Jalali JA, Johnston TP, Koulen P. Emerging Roles of Dyslipidemia and Hyperglycemia in Diabetic Retinopathy: Molecular Mechanisms and Clinical Perspectives. *Front Endocrinol (Lausanne)*. 2021; **12**: 620045. 10.3389/fendo.2021.620045.
- 28 Hukportie DN, Li FR, Zhou R, Zheng JZ, Wu XX, Zou MC, Wu XB. Lipid variability and risk of microvascular complications in Action to Control Cardiovascular Risk in Diabetes (ACCORD) trial: A post hoc analysis. *J Diabetes*. 2022; **14**: 365-76. 10.1111/1753-0407.13273.

- 29 Narindrarangkura P, Bosl W, Rangsin R, Hatthachote P. Prevalence of dyslipidemia associated with complications in diabetic patients: a nationwide study in Thailand. *Lipids Health Dis.* 2019; **18**: 90. 10.1186/s12944-019-1034-3.
- 30 van Niel J, Geelhoed-Duijvestijn P, Numans ME, Kharagjitsing AV, Vos RC. Type 2 diabetes in South Asians compared to Europeans: Higher risk and earlier development of major cardiovascular events irrespective of the presence and degree of retinopathy. Results from The HinDu The Hague Diabetes Study. *Endocrinol Diabetes Metab.* 2021; **4**: e00242. 10.1002/edm2.242.
- 31 He Y, Verma A, Nittala MG, Velaga SB, Esmailkhanian H, Li X, Su L, Li X, Jayadev C, Tsui I, Prasad P, Sadda SR. Ethnic Variation in Diabetic Retinopathy Lesion Distribution on Ultra-widefield Imaging. *Am J Ophthalmol.* 2022; **247**: 61-9. 10.1016/j.ajo.2022.10.023.
- 32 Chandie Shaw PK, Vandenbroucke JP, Tjandra YI, Rosendaal FR, Rosman JB, Geerlings W, de Charro FT, van Es LA. Increased end-stage diabetic nephropathy in Indo-Asian immigrants living in the Netherlands. *Diabetologia.* 2002; **45**: 337-41. 10.1007/s00125-001-0758-5.
- 33 Chandie Shaw PK, Baboe F, van Es LA, van der Vijver JC, van de Ree MA, de Jonge N, Rabelink TJ. South-Asian type 2 diabetic patients have higher incidence and faster progression of renal disease compared with Dutch-European diabetic patients. *Diabetes Care.* 2006; **29**: 1383-5. 10.2337/dc06-0003.
- 34 Bakker LE, Sleddering MA, Schoones JW, Meinders AE, Jazet IM. Pathogenesis of type 2 diabetes in South Asians. *Eur J Endocrinol.* 2013; **169**: R99-R114. 10.1530/EJE-13-0307.
- 35 Wang QJ. PKD at the crossroads of DAG and PKC signaling. *Trends Pharmacol Sci.* 2006; **27**: 317-23. 10.1016/j.tips.2006.04.003.
- 36 Noh H, King GL. The role of protein kinase C activation in diabetic nephropathy. *Kidney Int Suppl.* 2007: S49-53. 10.1038/sj.ki.5002386.
- 37 Ackermann M, Verleden SE, Kuehnel M, Haverich A, Welte T, Laenger F, Vanstapel A, Werlein C, Stark H, Tzankov A, Li WW, Li VW, Mentzer SJ, Jonigk D. Pulmonary Vascular Endothelialitis, Thrombosis, and Angiogenesis in Covid-19. *N Engl J Med.* 2020; **383**: 120-8. 10.1056/NEJMoa2015432.
- 38 Connors JM, Levy JH. Thromboinflammation and the hypercoagulability of COVID-19. *J Thromb Haemost.* 2020; **18**: 1559-61. 10.1111/jth.14849.
- 39 Buijssers B, Yanginlar C, de Nooijer A, Grondman I, Maciej-Hulme ML, Jonkman I, Janssen NAF, Rother N, de Graaf M, Pickkers P, Kox M, Joosten LAB, Nijenhuis T, Netea MG, Hilbrands L, van de Veerdonk FL, Duivenvoorden R, de Mast Q, van der Vlag J. Increased Plasma Heparanase Activity in COVID-19 Patients. *Front Immunol.* 2020; **11**: 575047. 10.3389/fimmu.2020.575047.

- 40 Drost CC, Rovas A, Osiaevi I, Rauen M, van der Vlag J, Buijssers B, Salmenov R, Lukasz A, Pavenstadt H, Linke WA, Kumpers P. Heparanase Is a Putative Mediator of Endothelial Glycocalyx Damage in COVID-19 - A Proof-of-Concept Study. *Front Immunol.* 2022; **13**: 916512. 10.3389/fimmu.2022.916512.
- 41 Rovas A, Osiaevi I, Buscher K, Sackarnd J, Tepasse PR, Fobker M, Kuhn J, Braune S, Gobel U, Tholking G, Groschel A, Pavenstadt H, Vink H, Kumpers P. Microvascular dysfunction in COVID-19: the MYSTIC study. *Angiogenesis.* 2021; **24**: 145-57. 10.1007/s10456-020-09753-7.
- 42 Lovric S, Lukasz A, Hafer C, Kielstein JT, Haubitz M, Haller H, Kumpers P. Removal of elevated circulating angiopoietin-2 by plasma exchange--a pilot study in critically ill patients with thrombotic microangiopathy and anti-glomerular basement membrane disease. *Thromb Haemost.* 2010; **104**: 1038-43. 10.1160/TH10-02-0138.
- 43 Higgins SJ, De Ceunynck K, Kellum JA, Chen X, Gu X, Chaudhry SA, Schulman S, Libermann TA, Lu S, Shapiro NI, Christiani DC, Flaumenhaft R, Parikh SM. Tie2 protects the vasculature against thrombus formation in systemic inflammation. *J Clin Invest.* 2018; **128**: 1471-84. 10.1172/JCI97488.
- 44 Price DR, Benedetti E, Hoffman KL, Gomez-Escobar L, Alvarez-Mulett S, Capili A, Sarwath H, Parkhurst CN, Lafond E, Weidman K, Ravishankar A, Cheong JG, Batra R, Buyukozkan M, Chetnik K, Easthausen I, Schenck EJ, Racanelli AC, Outtz Reed H, Laurence J, Josefowicz SZ, Lief L, Choi ME, Schmidt F, Borczuk AC, Choi AMK, Krumsiek J, Rafii S. Angiopoietin 2 Is Associated with Vascular Necroptosis Induction in Coronavirus Disease 2019 Acute Respiratory Distress Syndrome. *Am J Pathol.* 2022; **192**: 1001-15. 10.1016/j.ajpath.2022.04.002.
- 45 Maldonado F, Morales D, Diaz-Papapietro C, Valdes C, Fernandez C, Valls N, Lazo M, Espinoza C, Gonzalez R, Gutierrez R, Jara A, Romero C, Cerda O, Caceres M. Relationship Between Endothelial and Angiogenesis Biomarkers Envisage Mortality in a Prospective Cohort of COVID-19 Patients Requiring Respiratory Support. *Front Med (Lausanne).* 2022; **9**: 826218. 10.3389/fmed.2022.826218.
- 46 Schmaier AA, Pajares Hurtado GM, Manickas-Hill ZJ, Sack KD, Chen SM, Bhambhani V, Quadir J, Nath AK, Collier AY, Ngo D, Barouch DH, Shapiro NI, Gerszten RE, Yu XG, Collection MC-, Processing T, Peters KG, Flaumenhaft R, Parikh SM. Tie2 activation protects against prothrombotic endothelial dysfunction in COVID-19. *JCI Insight.* 2021; **6**. 10.1172/jci.insight.151527.
- 47 Michalick L, Weidenfeld S, Grimmer B, Fatykhova D, Solymosi PD, Behrens F, Dohmen M, Brack MC, Schulz S, Thomasch E, Simmons S, Muller-Redetzky H, Suttorp N, Kurth F, Neudecker J, Toennies M, Bauer TT, Eggeling S, Corman VM, Hocke AC, Witzenrath M, Hippenstiel S, Kuebler WM. Plasma mediators in patients with severe COVID-19 cause lung endothelial barrier failure. *Eur Respir J.* 2021; **57**. 10.1183/13993003.02384-2020.

48 Stahl K, Gronski PA, Kiyani Y, Seeliger B, Bertram A, Pape T, Welte T, Hoepfer MM, Haller H, David S. Injury to the Endothelial Glycocalyx in Critically Ill Patients with COVID-19. *Am J Respir Crit Care Med*. 2020; **202**: 1178-81. 10.1164/rccm.202007-2676LE.

49 Kox M, Waalders NJB, Kooistra EJ, Gerretsen J, Pickkers P. Cytokine Levels in Critically Ill Patients With COVID-19 and Other Conditions. *JAMA*. 2020; **324**: 1565-7. 10.1001/jama.2020.17052.

50 Leisman DE, Ronner L, Pinotti R, Taylor MD, Sinha P, Calfee CS, Hirayama AV, Mastroiani F, Turtle CJ, Harhay MO, Legrand M, Deutschman CS. Cytokine elevation in severe and critical COVID-19: a rapid systematic review, meta-analysis, and comparison with other inflammatory syndromes. *Lancet Respir Med*. 2020; **8**: 1233-44. 10.1016/S2213-2600(20)30404-5.

CHAPTER

8

**Nederlandse Samenvatting,
algemene discussie, en
toekomstperspectieven**

Thromboïnfammatie, een belangrijke trigger voor endotheliale dysfunctie, is een nieuwe term om de verbinding tussen de gelijktijdige activatie van de stollingsroute en immuunrespons te beschrijven. In dit proefschrift wordt de rol van thromboïnfammatie bij verschillende hoog risico populaties, zoals vrouwen versus mannen in de algemene Nederlandse bevolking, patiënten met type 2 diabetes mellitus (T2DM) van verschillende etniciteit en COVID-19-patiënten, belicht.

Thromboïnfammatie, gender verschillen en hart- en vaatziekten

Thromboïnfammatie vertoont geslachtsverschillen en draagt bij aan het risico op hart- en vaatziekten. De endotheliale glycocalyx, een belangrijke regulator van thromboïnfammatie, is ook betrokken bij verschillende vasculaire complicaties.

In **hoofdstuk 2** van dit proefschrift hebben we een verband waargenomen tussen vroege (preklinische) microvasculaire gezondheidsveranderingen, gemeten met sidestream dark-field (SDF)-imaging, en activatie van coagulatie factoren. We ontdekten een opvallend geslachtsverschil in microvasculaire gezondheid, waarbij vrouwen een verstoord endotheliale glycocalyx vertoonden in combinatie met een meer procoagulant endotheel oppervlak. Deze associatie niet werd waargenomen bij mannen. Op basis van eerdere studies [1-3], met name bij vrouwen, wordt een verstoring van de endotheliale glycocalyx geassocieerd met een verhoogd risico op cardiovasculaire hartziekten (CHD). Deze bevindingen benadrukken het belang van geslachtsverschillen in micro circulatoire verstoringen bij CHD, en suggereert dat het monitoren van microcirculatoire veranderingen specifiek bij vrouwen potentieel klinisch nuttig kan zijn om de ontwikkeling van CHD te voorkomen. In lijn met deze bevindingen zijn eerdere studies die aantoonen dat vooral premenopauzale vrouwen die verdacht werden van, of een bevestigde klinische ischemische hartziekte hebben, minder atherosclerose vertonen dan mannen met ook een lagere prevalentie van obstructieve coronaire hartziekte (CAD) [4]. Bovendien testte meer

dan 50% van de vrouwen met angina negatief voor coronaire angiografie, wat verdere aanwijzingen geeft voor geslachtsverschillen in de ontwikkeling van CHD [5]. Op basis van deze eerdere bevindingen toont toenemend bewijs aan dat verstoring van de microcirculatie duidelijk bijdraagt aan CHD bij vrouwen [6].

Verstoring van de endotheliale glycocalyx kan leiden tot een procoagulante toestand [7], en samen met eerdere studies die aantoonde dat de onderliggende systemische aanwezigheid van een hyper-coagulante toestand geassocieerd was met de incidentie van CHD [8-10], wijst dit op een verband tussen de gezondheid van de endotheliale glycocalyx en CHD welke is gemedieerd door coagulatie activatie. Vanuit de Tromsø Studie, een case-cohort studie design met 1495 geïncludeerde participanten, kwam naar voren dat Syndecan-4, een van de core-eiwitten waaraan heparaan sulfaat (HS) ketens verbonden zijn, in de endotheliale glycocalyx geassocieerd was met myocard infarct incidentie. Deze associatie was ook sterker in vrouwen dan in mannen, wat een link indiceert tussen de endotheliale glycocalyx en CHD als ook gender verschillen [11]. Een interessant gegeven zoals een seks-afhankelijke associatie tussen CHD en verminderde sublinguale microvasculaire glycocalyx barrière functie in vrouwen was ook gevonden in een studie van Brands et al. [12].

Thromboïnflematie, diabetes in verschillende etniciteiten, en HDL functie in dyslipidemie.

HDL heeft functies zoals ontstekingsremmende en antitrombotische eigenschappen, die thromboïnflematie kunnen reguleren in pathologische omstandigheden [13]. In studies naar chronische situaties zoals CHD, diabetes en chronische nierziekte kan HDL zijn beschermende functie verliezen en zelfs schadelijke eigenschappen krijgen, waardoor de progressie van de ziekte verergert [14-17].

Het mechanisme van T2DM-ziekteprogressie varieert bij verschillende etniciteiten [18] en recente studies hebben aangetoond dat veranderingen in de HDL-functie een van de onderliggende mechanismen kunnen zijn die leiden tot de ontwikkeling en progressie van de ziekte. Aangezien het verlagen van lipoproteïnen met een lage dichtheid (LDL) door het gebruik van statines geassocieerd is met insuline resistentie en een verhoogd risico op hypoglycemische complicaties bij T2DM, kan met name de functionaliteit van HDL een betere kandidaat zijn om de progressie van diabetes te monitoren [19-21].

Een studie die de HDL-functie vergeleek bij Zuid-Aziaten van Nederlandse afkomst en Nederlandse blanke Europeanen binnen drie leeftijdsgroepen (pasgeborenen, adolescenten en volwassenen), rapporteerde dat bij afwezigheid van T2DM alleen het vermogen van HDL om oxidatie van LDL te voorkomen verminderd was bij te zware Zuid-Aziaten van Nederlandse afkomst in vergelijking met obese Nederlandse blanke Europeanen [22]. Een andere single-center studie in Rotterdam die de relatie tussen de ontwikkeling van dyslipidemie en glucose-intolerantie onderzocht, vond dat kleine HDL-fracties geassocieerd waren met insulineresistentie en beta-cel dysfunctie bij Zuid-Aziatische families met risico op T2DM [14].

In **hoofdstuk 3** hebben we de HDL-samenstelling vergeleken tussen gezonde individuen en patiënten met T2DM van Nederlandse Zuid-Aziatische en Nederlandse blanke Kaukasische afkomst. Hier zagen we dat de HDL-samenstelling tussen beide etnische groepen verschilde. De verminderde HDL-functionaliteit die werd gevonden bij Nederlandse Zuid-Aziaten met T2DM kan worden verklaard door het verlies van de kleinste HDL-subfracties; terwijl bij Nederlandse blanke Kaukasiërs met T2DM een verhoogd triglyceridegehalte in de kleinste HDL-fractie een belangrijke rol speelt bij HDL-dysfunctie. In lijn met deze bevindingen hebben kleine en dichte HDL-deeltjes aangetoond dat ze een vitale rol spelen bij meerdere functies, zoals cellulair cholesterol-efflux, anti oxidatieve-, anti thrombotische-, anti inflammatoire- en anti apoptotische capaciteiten [15]. In onze huidige studie hebben we gevonden dat concentraties van de kleinste HDL-subfracties, behalve het triglyceridegehalte, negatief geassocieerd waren met de duur van de ziekte bij

Nederlandse Zuid-Aziaten met T2DM in plaats van bij Nederlandse blanke Kaukasiërs. Dit suggereert een kwetsbaarder HDL-samenstelling fenotype. Bovendien toonde de in-house HDL functionaliteitstest aan dat T2DM-patiënten in beide etnische groepen een significant verminderde antitrombotische capaciteit hadden als gevolg van een gestoorde HDL-functie. Consistent met een eerdere bevinding werd een gestoorde HDL-functie bij T2DM-patiënten waargenomen in termen van de capaciteit om TNF-geïnduceerde vasculaire cel adhesie molecule-1 (VCAM-1) expressie in endotheelcellen *in vitro* te onderdrukken [23]. Volgens onze bevindingen kan HDL-dysfunctie geïnduceerde thromboïnflectatoire deregulatie bijdragen aan een hoger risico op ziekteontwikkeling en -progressie bij Zuid-Aziaten met T2DM.

Bij door oxidatieve stress veroorzaakte cardiovasculaire ziekte kunnen geoxideerde lipiden via CD36 de activering van bloedplaatjes veroorzaken, wat een verband aantoont tussen ontregelde lipoproteïenmetabolisme, oxidatieve stress en thrombusvorming [24]. Lipiden zijn betrokken bij zowel de intrinsieke als extrinsieke routes van prothrombine-activatie en dyslipidemie is een van de kenmerken van T2DM. In **hoofdstuk 4** hebben we met behulp van een nieuwe gerichte kwantitatieve LC/MS-gebaseerde Shotgun Lipidomics Assistant platform een uitgebreide mapping van het circulerende lipidoom gegenereerd bij Nederlandse Zuid-Aziaten en Nederlandse blanke Kaukasiërs met of zonder T2DM. Op basis van lipidomics-fenotypering kregen we gedetailleerd inzicht in de complexiteit van het lipidenmetabolisme en de interindividuele variaties binnen de verschillende etnische groepen. Het is vermeldenswaardig dat er duidelijke verschillen waren in het lipidoom, voornamelijk gerelateerd aan het metabolisme van cholesteryl-esters (CEs), diacylglyceriden (DGs), fosfatidylethanolaminen (PEs), sfingomyelinen (SMs) en triglyceriden (TGs) tussen T2DM en gezonde controles in onze studie populatie. Dit was consistent met eerdere bevindingen die waren waargenomen in de case-cohortstudie die was ingebed in de PREDIMED-trial [25] en de longitudinale METSIM-studie [26]. Er waren echter ook tegenstrijdige resultaten gemeld in deze twee studies op basis van Chinese populaties waarbij FFA-, SM- en LPC-lipide soorten verhoogd waren bij Chinezen met

T2DM, terwijl wij tegengestelde resultaten vonden bij Nederlandse patiënten met T2DM, de hoge variabiliteit in de verschillende lipidoom profielen tussen de etniciteiten kan hierbij een rol spelen.

Thromboïnflematie en diabetes-gerelateerde complicaties

Lipoproteïne- en lipidenmetabolisme bij patiënten met T2DM kunnen leiden tot de ontregeling van thromboïnflematie en verder de ontwikkeling of verergering van diabetes-gerelateerde complicaties beïnvloeden. Verschillende studies ontdekten dat dyslipidemie geassocieerd was met een verhoogd risico op diabetes-gerelateerde microvasculaire complicaties zoals neuropathie en retinopathie [27-29]. Zuid-Aziaten hebben een hogere prevalentie van diabetische retinopathie dan witte Europeanen en een kortere verergeringstijd, en de diabetische retinopathie-laesies [30] hebben de neiging om meer centraal te worden verdeeld [31]. In **hoofdstuk 3** observeerden we specifiek dat lagere totale ApoA2- en HDL-4-subklasseconcentraties bij Nederlandse Zuid-Aziatische personen met T2DM geassocieerd waren met een hogere kans op diabetes-gerelateerde pan-microvasculaire complicaties zoals retinopathie en neuropathie.

Naast diabetische neuropathie en retinopathie hebben Zuid-Aziatische patiënten met T2DM meer kans op het ontwikkelen van microvasculaire complicaties zoals diabetische nefropathie, met een hogere incidentie van micro- en macroalbuminurie bij Zuid-Aziaten in vergelijking met witte Europese Kaukasiërs met T2DM en een snellere progressie naar eindstadium nierziekte [32, 33]. Dit zou kunnen komen doordat deze patiënten een hogere belasting hebben van systemische en glomerulaire ontstekingen. Bovendien hebben Zuid-Aziaten een unieke lichaamssamenstelling, met een meer abdominaal obesitas fenotype en een hoog percentage visceraal vet, dat dominant is in de productie en secretie van bepaalde inflammatoire cytokines die bijdragen aan de chronische laaggradige inflammatoire toestand [34]. Ondertussen hebben we in **hoofdstuk 4** een

unieke lipide soort, diacylglycerol (DG), geïdentificeerd die geassocieerd was met diabetische nefropathie en verslechterde renale functies. Het DG-proteïne kinase C (PKC) / proteïne kinase D (PKD) signaleringsnetwerk kan de redoxbalans reguleren en oxidatieve stress veroorzaken [35]. Bij T2DM neemt de concentratie DG toe en de ophoping van DG activeert het PKC / PKD, wat resulteert in diabetische nefropathie [36]. Het was opmerkelijk dat DG 18:1_18:2 hoger was bij diabetische nefropathie, vooral bij Zuid-Aziaten met T2DM, en correleerde met de meeste klinische parameters. Zelfs in een extern cohort van Chinese patiënten met IgA-nefropathie bleven deze correlaties met nierfunctie bestaan. Het verdient de aanbeveling om toekomstige studies over diabetische nefropathie bij meerdere ethniciteiten uit te voeren met grotere aantallen deelnemers om deze bevindingen te verifiëren.

Thromboïnflemmatie en COVID-19

Hyperinflammatie is een kenmerk van COVID-19 en de inflammatoire respons op SARS-CoV-2-infectie veroorzaakt vaak een opmerkelijke activering van de stollingscascade. Het daaropvolgende proces genaamd thromboïnflemmatie wordt gekenmerkt door systemische endotheliale beschadiging en verlies van antistolling eigenschappen [37, 38].

Hyperinflammatie veroorzaakt door COVID-19 kan de vasculaire integriteit verstoren. De endotheliale glycocalyx reguleert cel integriteit en homeostase door middel van de beschermende permeabiliteit functie van de vasculaire barrière, anti-inflammatie en antistolling capaciteit. Buijsers et al. merkten op dat de activiteit van het endotheliale glycocalyx-afbrekende enzym heparanase, dat betrokken was bij vasculaire lekkage en ontsteking, verhoogd was bij COVID-19-patiënten en geassocieerd was met de ernst van de ziekte [39]. Bovendien toonden Kümpers et al. aan dat niet-antistolling heparine fragmenten de activiteit van heparanase konden remmen en zo endotheliale glycocalyx beschadiging konden voorkomen in reactie op COVID-19-serum [40]. Ondertussen leverde

de MYSTIC-studie ook bewijs dat de gezondheid van de glycocalyx, gemeten door veranderingen in de perfusie grensregio op het endotheel oppervlak (PBR) in kleine bloedvaten, een voorspellende prognostische marker was voor COVID-19-septische patiënten [41]. In **hoofdstuk 5** hebben we aangetoond dat verlies van de endotheliale glycocalyx als reactie op serum van COVID-19-patiënten op de intensieve care (ICU) endotheliale disfunctie induceerde door verhoogde IL-6, ICAM1, ANG2 en HPSE1 genexpressie en activering van de NF- κ B signaal route. Bovendien leidde beschadiging van het endotheliale glycocalyx tot vasculaire lekkage en een verstoord cel-cel contact.

Remming van de beschermende ANG1/TIE2 signaal route door ANG2 is een centrale regulator bij de bescherming van de bloedvaten tegen thrombus vorming en reguleert vasculaire stabilisatie [42, 43]. Een aantal studies toonde aan dat circulerende ANG2-niveaus verhoogd waren bij COVID-19 en geassocieerd werden met een slechtere prognose [44-46]. In lijn met deze bevindingen vonden we ook dat ANG2-niveaus verhoogd waren bij ICU COVID-19-patiënten (**Hoofdstuk 5**). De aanwezigheid van het endotheliale glycocalyx is vereist voor antistolling eigenschappen en het normaal functionerend endotheel. We hebben ook aangetoond dat verlies van het endotheliale glycocalyx als reactie op serum van ICU COVID-19-patiënten een pro-coagulant cel oppervlakte vormt door verhoogde expressie van tissue factor en verhoogde secretie van ANG2 en vWF (**Hoofdstuk 5**). Om verder de hypothese te valideren dat een beschadigde glycocalyx bijdraagt aan thromboinflammatie in COVID-19, hebben we getest of preservatie van de endotheliale glycocalyx een effectieve interventie kan zijn en vasculaire gezondheid kan bevorderen. We hebben gevonden dat de aanwezigheid van het HS-mimeticum fucoidan endotheel functionaliteit kan herstellen, inclusief de endotheliale glycocalyx. Hierdoor wordt endotheliale activiteit vermindert wat leidt tot bescherming van de endotheliale barrière functie en herstel van de anti thrombotisch oppervlak (**Hoofdstuk 5**).

Michalick et al. ontdekten dat plasma mediators bij patiënten met ernstige COVID-19 konden leiden tot falen van de pulmonaire endotheel barrière [47]. Ondertussen toonde

Stahl et al. aan dat de bloed samenstelling bij ernstig zieke COVID-19 patiënten endotheel letsel kon veroorzaken, waaronder verlies van glycocalyx integriteit en vasculaire destabilisatie [48]. Naast verhoging van een aantal cytokines en chemokines bij COVID-19 patiënten blijkt de waargenomen cytokinestorm lager dan bij niet-COVID-19 patiënten met bijvoorbeeld ernstige gevallen met acuut nierfalen (ARDS), sepsis en influenza virusinfectie [49, 50]. Deze discrepantie suggereert dat andere mediators, zoals geoxideerde lipiden of dysfunctionele lipoproteïnen, mogelijk bijdragen aan COVID-19 pathogenese. Aangezien COVID-19 uiteindelijk een endotheel ziekte is, vullen we in **hoofdstuk 6** het ontbrekende puzzelstukje van bloedmediators die leiden tot endotheel disfunctie bij COVID-19 in. We vonden dat verhoogde niveaus van HDL-triglyceriden en verminderde hoeveelheden van de kleinste HDL-subklasse geassocieerd waren met endotheel disfunctie en de ernst van COVID-19. Bovendien had dysfunctioneel HDL bij COVID-19-patiënten minder antithrombotische capaciteit dan bij gezonde individuen, wat wijst op een hoger risico op thromboïnfinitie. Deze bevindingen waren ook in lijn met onze eerdere waarnemingen dat een verstoorde endotheliale glycocalyx bij COVID-19-patiënten leidde tot de vorming van een pro-coagulant celoppervlak (**Hoofdstuk 5**).

Toekomstperspectieven en open vragen

In dit proefschrift benadrukken we thromboïnfinitie bij hoog risico populaties zoals vrouwen, Zuid-Aziaten, T2DM patiënten en COVID-19 patiënten. We laten ook zien dat verstoring van de endotheliale glycocalyx, HDL disfunctie en ontregeling van het lipiden metabolisme kunnen leiden tot thromboïnfinitie, die allemaal een kritieke rol kunnen spelen bij acute of chronische ziekte ontwikkeling. In **hoofdstuk 2** toonden we aan dat verandering van de glycocalyx functie samen met pro-coagulatiefactoren kon bijdragen aan de vroege ontwikkeling van CHD bij vrouwen. We missen echter nog een gedetailleerd mechanisme en follow-up informatie over deze vorm van niet-obstructieve CHD, dat moet worden onderzocht. In **hoofdstuk 3** toonden we de veranderingen in HDL-compositie en -functie bij Zuid-Aziaten met T2DM aan. HDL-functie was afhankelijk van zowel het lipidoom als het proteoom. Daarom is de specifieke bepaling van het proteoom in

geïsoleerde HDL-deeltjes de volgende stap om het onderliggende mechanisme van HDL dysfunctie te ontdekken. In **hoofdstuk 4**, vonden we dat een specifiek lipide alleen te vinden was bij nierziekten (diabetische nefropathie en IgA-nefropathie). Alhoewel, de concentratie van dit lipide vrij laag is, dit maakt het noodzakelijk dat er preciezer en een meer in-depth metingen en analyse uitgevoerd moet worden in een groter nierziekte cohort om dit lipide als biomarker aan te kunnen merken. In **hoofdstuk 5** en **hoofdstuk 6** hebben we alleen gezonde controles met COVID-19 patiënten op de ICU getest. Om dit specifiek aan deze patiënten toe te schrijven is het noodzakelijk om in een vervolgstudie niet-COVID-19 patiënten op de ICU te includeren.

We hebben laten zien dat bepaalde HDL subfracties in diabetes en COVID-19 verlaagd zijn. Echter, weten we nog niet of HDL mimeticum HDL verhogende medicatie toediening een potentieel therapeutische strategie kan zijn voor patiënten met COVID-19, diabetes, of diabetes gerelateerde complicaties, dat zal nog verder onderzocht moeten worden.

Referenties

- 1 Zakai NA, Judd SE, Kissela B, Howard G, Safford MM, Cushman M. Factor VIII, Protein C and Cardiovascular Disease Risk: The REasons for Geographic and Racial Differences in Stroke Study (REGARDS). *Thromb Haemost.* 2018; **118**: 1305-15. 10.1055/s-0038-1655766.
- 2 Olson NC, Raffield LM, Lange LA, Lange EM, Longstreth WT, Jr., Chauhan G, Debette S, Seshadri S, Reiner AP, Tracy RP. Associations of activated coagulation factor VII and factor VIIa-antithrombin levels with genome-wide polymorphisms and cardiovascular disease risk. *Journal of thrombosis and haemostasis : JTH.* 2018; **16**: 19-30. 10.1111/jth.13899.
- 3 Fibrinogen Studies C, Danesh J, Lewington S, Thompson SG, Lowe GD, Collins R, Kostis JB, Wilson AC, Folsom AR, Wu K, Benderly M, Goldbourt U, Willeit J, Kiechl S, Yarnell JW, Sweetnam PM, Elwood PC, Cushman M, Psaty BM, Tracy RP, Tybjaerg-Hansen A, Haverkate F, de Maat MP, Fowkes FG, Lee AJ, Smith FB, Salomaa V, Harald K, Rasi R, Vahtera E, Jousilahti P, Pekkanen J, D'Agostino R, Kannel WB, Wilson PW, Tofler G, Arocha-Pinango CL, Rodriguez-Larralde A, Nagy E, Mijares M, Espinosa R, Rodriguez-Roa E, Ryder E, Diez-Ewald MP, Campos G, Fernandez V, Torres E, Marchioli R, Valagussa F, Rosengren A, Wilhelmsen L, Lappas G, Eriksson H, Cremer P, Nagel D, Curb JD, Rodriguez B, Yano K,

Salonen JT, Nyyssonen K, Tuomainen TP, Hedblad B, Lind P, Loewel H, Koenig W, Meade TW, Cooper JA, De Stavola B, Knottenbelt C, Miller GJ, Cooper JA, Bauer KA, Rosenberg RD, Sato S, Kitamura A, Naito Y, Palosuo T, Ducimetiere P, Amouyel P, Arveiler D, Evans AE, Ferrieres J, Juhan-Vague I, Bingham A, Schulte H, Assmann G, Cantin B, Lamarche B, Despres JP, Dagenais GR, Tunstall-Pedoe H, Woodward M, Ben-Shlomo Y, Davey Smith G, Palmieri V, Yeh JL, Rudnicka A, Ridker P, Rodeghiero F, Tosetto A, Shepherd J, Ford I, Robertson M, Brunner E, Shipley M, Feskens EJ, Kromhout D, Dickinson A, Ireland B, Juzwishin K, Kaptoge S, Lewington S, Memon A, Sarwar N, Walker M, Wheeler J, White I, Wood A. Plasma fibrinogen level and the risk of major cardiovascular diseases and nonvascular mortality: an individual participant meta-analysis. *JAMA : the journal of the American Medical Association*. 2005; **294**: 1799-809. 10.1001/jama.294.14.1799.

4 Reynolds HR, Bairey Merz CN, Berry C, Samuel R, Saw J, Smilowitz NR, de Souza A, Sykes R, Taqueti VR, Wei J. Coronary Arterial Function and Disease in Women With No Obstructive Coronary Arteries. *Circulation research*. 2022; **130**: 529-51. 10.1161/CIRCRESAHA.121.319892.

5 Lee BK, Lim HS, Fearon WF, Yong AS, Yamada R, Tanaka S, Lee DP, Yeung AC, Tremmel JA. Invasive evaluation of patients with angina in the absence of obstructive coronary artery disease. *Circulation*. 2015; **131**: 1054-60. 10.1161/CIRCULATIONAHA.114.012636.

6 Pries AR, Reglin B. Coronary microcirculatory pathophysiology: can we afford it to remain a black box? *European heart journal*. 2017; **38**: 478-88. 10.1093/eurheartj/ehv760.

7 Yuan L, Cheng S, Sol W, van der Velden AIM, Vink H, Rabelink TJ, van den Berg BM. Heparan sulfate mimetic fucoidan restores the endothelial glycocalyx and protects against dysfunction induced by serum of COVID-19 patients in the intensive care unit. *ERJ Open Res*. 2022; **8**. 10.1183/23120541.00652-2021.

8 Bratseth V, Pettersen AA, Opstad TB, Arnesen H, Seljeflot I. Markers of hypercoagulability in CAD patients. Effects of single aspirin and clopidogrel treatment. *Thromb J*. 2012; **10**: 12. 10.1186/1477-9560-10-12.

9 Tantry US, Bliden KP, Suarez TA, Kreutz RP, Dichiaro J, Gurbel PA. Hypercoagulability, platelet function, inflammation and coronary artery disease acuity: results of the Thrombotic Risk Progression (TRIP) study. *Platelets*. 2010; **21**: 360-7. 10.3109/09537100903548903.

10 Song CJ, Nakagomi A, Chandar S, Cai H, Lim IG, McNeil HP, Freedman SB, Geczy CL. C-reactive protein contributes to the hypercoagulable state in coronary artery disease. *Journal of thrombosis and haemostasis : JTH*. 2006; **4**: 98-106. 10.1111/j.1538-7836.2005.01705.x.

11 Solbu MD, Kolset SO, Jenssen TG, Wilsgaard T, Lochén ML, Mathiesen EB, Melsom T, Eriksen BO, Reine TM. Gender differences in the association of syndecan-4 with

myocardial infarction: The population-based Tromso Study. *Atherosclerosis*. 2018; **278**: 166-73. 10.1016/j.atherosclerosis.2018.08.005.

12 Brands J, Hubel CA, Althouse A, Reis SE, Pacella JJ. Noninvasive sublingual microvascular imaging reveals sex-specific reduction in glycocalyx barrier properties in patients with coronary artery disease. *Physiological reports*. 2020; **8**: e14351. 10.14814/phy2.14351.

13 von Eckardstein A, Nordestgaard BG, Remaley AT, Catapano AL. High-density lipoprotein revisited: biological functions and clinical relevance. *European heart journal*. 2022. 10.1093/eurheartj/ehac605.

14 Yahya R, Jainandunsing S, Rashid M, van der Zee L, Touw A, de Rooij FWM, Sijbrands EJG, Verhoeven AJM, Mulder MT. HDL associates with insulin resistance and beta-cell dysfunction in South Asian families at risk of type 2 diabetes. *Journal of diabetes and its complications*. 2021; **35**: 107993. 10.1016/j.jdiacomp.2021.107993.

15 He Y, Ronsein GE, Tang C, Jarvik GP, Davidson WS, Kothari V, Song HD, Segrest JP, Bornfeldt KE, Heinecke JW. Diabetes Impairs Cellular Cholesterol Efflux From ABCA1 to Small HDL Particles. *Circulation research*. 2020; **127**: 1198-210. 10.1161/CIRCRESAHA.120.317178.

16 Li Y, Zhao M, He D, Zhao X, Zhang W, Wei L, Huang E, Ji L, Zhang M, Willard B, Fu Z, Wang L, Pan B, Zheng L, Ji L. HDL in diabetic nephropathy has less effect in endothelial repairing than diabetes without complications. *Lipids in health and disease*. 2016; **15**: 76. 10.1186/s12944-016-0246-z.

17 Jia C, Anderson JLC, Gruppen EG, Lei Y, Bakker SJL, Dullaart RPF, Tietge UJF. High-Density Lipoprotein Anti-Inflammatory Capacity and Incident Cardiovascular Events. *Circulation*. 2021; **143**: 1935-45. 10.1161/CIRCULATIONAHA.120.050808.

18 Sattar N, Gill JM. Type 2 diabetes in migrant south Asians: mechanisms, mitigation, and management. *Lancet Diabetes Endocrinol*. 2015; **3**: 1004-16. 10.1016/S2213-8587(15)00326-5.

19 Mansi IA, Chansard M, Lingvay I, Zhang S, Halm EA, Alvarez CA. Association of Statin Therapy Initiation With Diabetes Progression: A Retrospective Matched-Cohort Study. *JAMA Intern Med*. 2021; **181**: 1562-74. 10.1001/jamainternmed.2021.5714.

20 Liew SM, Lee PY, Hanafi NS, Ng CJ, Wong SS, Chia YC, Lai PS, Zaidi NF, Khoo EM. Statins use is associated with poorer glycaemic control in a cohort of hypertensive patients with diabetes and without diabetes. *Diabetol Metab Syndr*. 2014; **6**: 53. 10.1186/1758-5996-6-53.

21 Sukhija R, Prayaga S, Marashdeh M, Bursac Z, Kakar P, Bansal D, Sachdeva R, Kesan SH, Mehta JL. Effect of statins on fasting plasma glucose in diabetic and nondiabetic patients. *Journal of investigative medicine : the official publication of the American Federation for Clinical Research*. 2009; **57**: 495-9. 10.2310/JIM.0b013e318197ec8b.

- 22 Bakker LE, Boon MR, Annema W, Dijkers A, van Eyk HJ, Verhoeven A, Mayboroda OA, Jukema JW, Havekes LM, Meinders AE, Willems van Dijk K, Jazet IM, Tietge UJ, Rensen PC. HDL functionality in South Asians as compared to white Caucasians. *Nutrition, metabolism, and cardiovascular diseases : NMCD*. 2016; **26**: 697-705. 10.1016/j.numecd.2016.02.010.
- 23 Ebtehaj S, Gruppen EG, Parvizi M, Tietge UJF, Dullaart RPF. The anti-inflammatory function of HDL is impaired in type 2 diabetes: role of hyperglycemia, paraoxonase-1 and low grade inflammation. *Cardiovascular diabetology*. 2017; **16**: 132. 10.1186/s12933-017-0613-8.
- 24 Jackson SP, Calkin AC. The clot thickens--oxidized lipids and thrombosis. *Nature medicine*. 2007; **13**: 1015-6. 10.1038/nm0907-1015.
- 25 Razquin C, Liang L, Toledo E, Clish CB, Ruiz-Canela M, Zheng Y, Wang DD, Corella D, Castaner O, Ros E, Aros F, Gomez-Gracia E, Fiol M, Santos-Lozano JM, Guasch-Ferre M, Serra-Majem L, Sala-Vila A, Buil-Cosiales P, Bullo M, Fito M, Portoles O, Estruch R, Salas-Salvado J, Hu FB, Martinez-Gonzalez MA. Plasma lipidome patterns associated with cardiovascular risk in the PREDIMED trial: A case-cohort study. *International journal of cardiology*. 2018; **253**: 126-32. 10.1016/j.ijcard.2017.10.026.
- 26 Suvitaival T, Bondia-Pons I, Yetukuri L, Poho P, Nolan JJ, Hyotylainen T, Kuusisto J, Oresic M. Lipidome as a predictive tool in progression to type 2 diabetes in Finnish men. *Metabolism: clinical and experimental*. 2018; **78**: 1-12. 10.1016/j.metabol.2017.08.014.
- 27 Hukportie DN, Li FR, Zhou R, Zheng JZ, Wu XX, Zou MC, Wu XB. Lipid variability and risk of microvascular complications in Action to Control Cardiovascular Risk in Diabetes (ACCORD) trial: A post hoc analysis. *Journal of diabetes*. 2022; **14**: 365-76. 10.1111/1753-0407.13273.
- 28 Rao H, Jalali JA, Johnston TP, Koulen P. Emerging Roles of Dyslipidemia and Hyperglycemia in Diabetic Retinopathy: Molecular Mechanisms and Clinical Perspectives. *Frontiers in endocrinology*. 2021; **12**: 620045. 10.3389/fendo.2021.620045.
- 29 Narindrarangkura P, Bosl W, Rangsin R, Hatthachote P. Prevalence of dyslipidemia associated with complications in diabetic patients: a nationwide study in Thailand. *Lipids in health and disease*. 2019; **18**: 90. 10.1186/s12944-019-1034-3.
- 30 van Niel J, Geelhoed-Duijvestijn P, Numans ME, Kharagjitsing AV, Vos RC. Type 2 diabetes in South Asians compared to Europeans: Higher risk and earlier development of major cardiovascular events irrespective of the presence and degree of retinopathy. Results from The HinDu The Hague Diabetes Study. *Endocrinol Diabetes Metab*. 2021; **4**: e00242. 10.1002/edm2.242.
- 31 He Y, Verma A, Nittala MG, Velaga SB, Esmaeilkhanian H, Li X, Su L, Li X, Jayadev C, Tsui I, Prasad P, Sadda SR. Ethnic Variation in Diabetic Retinopathy Lesion Distribution on

Ultra-widefield Imaging. *American journal of ophthalmology*. 2023; **247**: 61-9. 10.1016/j.ajo.2022.10.023.

32 Chandie Shaw PK, Baboe F, van Es LA, van der Vijver JC, van de Ree MA, de Jonge N, Rabelink TJ. South-Asian type 2 diabetic patients have higher incidence and faster progression of renal disease compared with Dutch-European diabetic patients. *Diabetes care*. 2006; **29**: 1383-5. 10.2337/dc06-0003.

33 Chandie Shaw PK, Vandenbroucke JP, Tjandra YI, Rosendaal FR, Rosman JB, Geerlings W, de Charro FT, van Es LA. Increased end-stage diabetic nephropathy in Indo-Asian immigrants living in the Netherlands. *Diabetologia*. 2002; **45**: 337-41. 10.1007/s00125-001-0758-5.

34 Bakker LE, Sleddering MA, Schoones JW, Meinders AE, Jazet IM. Pathogenesis of type 2 diabetes in South Asians. *European journal of endocrinology / European Federation of Endocrine Societies*. 2013; **169**: R99-R114. 10.1530/EJE-13-0307.

35 Wang QJ. PKD at the crossroads of DAG and PKC signaling. *Trends in pharmacological sciences*. 2006; **27**: 317-23. 10.1016/j.tips.2006.04.003.

36 Noh H, King GL. The role of protein kinase C activation in diabetic nephropathy. *Kidney international*. 2007: S49-53. 10.1038/sj.ki.5002386.

37 Connors JM, Levy JH. Thromboinflammation and the hypercoagulability of COVID-19. *Journal of thrombosis and haemostasis : JTH*. 2020; **18**: 1559-61. 10.1111/jth.14849.

38 Ackermann M, Verleden SE, Kuehnel M, Haverich A, Welte T, Laenger F, Vanstapel A, Werlein C, Stark H, Tzankov A, Li WW, Li VW, Mentzer SJ, Jonigk D. Pulmonary Vascular Endothelialitis, Thrombosis, and Angiogenesis in Covid-19. *N Engl J Med*. 2020. 10.1056/NEJMoa2015432.

39 Buijssers B, Yanginlar C, de Nooijer A, Grondman I, Maciej-Hulme ML, Jonkman I, Janssen NAF, Rother N, de Graaf M, Pickkers P, Kox M, Joosten LAB, Nijenhuis T, Netea MG, Hilbrands L, van de Veerdonk FL, Duivenvoorden R, de Mast Q, van der Vlag J. Increased Plasma Heparanase Activity in COVID-19 Patients. *Frontiers in immunology*. 2020; **11**: 575047. 10.3389/fimmu.2020.575047.

40 Drost CC, Rovas A, Osiaevi I, Rauen M, van der Vlag J, Buijssers B, Salmenov R, Lukasz A, Pavenstadt H, Linke WA, Kumpers P. Heparanase Is a Putative Mediator of Endothelial Glycocalyx Damage in COVID-19 - A Proof-of-Concept Study. *Frontiers in immunology*. 2022; **13**: 916512. 10.3389/fimmu.2022.916512.

41 Rovas A, Osiaevi I, Buscher K, Sackarnd J, Tepasse PR, Fobker M, Kuhn J, Braune S, Gobel U, Tholking G, Groschel A, Pavenstadt H, Vink H, Kumpers P. Microvascular dysfunction in COVID-19: the MYSTIC study. *Angiogenesis*. 2021; **24**: 145-57. 10.1007/s10456-020-09753-7.

- 42 Lovric S, Lukasz A, Hafer C, Kielstein JT, Haubitz M, Haller H, Kumpers P. Removal of elevated circulating angiopoietin-2 by plasma exchange--a pilot study in critically ill patients with thrombotic microangiopathy and anti-glomerular basement membrane disease. *Thromb Haemost*. 2010; **104**: 1038-43. 10.1160/TH10-02-0138.
- 43 Higgins SJ, De Ceunynck K, Kellum JA, Chen X, Gu X, Chaudhry SA, Schulman S, Libermann TA, Lu S, Shapiro NI, Christiani DC, Flaumenhaft R, Parikh SM. Tie2 protects the vasculature against thrombus formation in systemic inflammation. *The Journal of clinical investigation*. 2018; **128**: 1471-84. 10.1172/JCI97488.
- 44 Price DR, Benedetti E, Hoffman KL, Gomez-Escobar L, Alvarez-Mulett S, Capili A, Sarwath H, Parkhurst CN, Lafond E, Weidman K, Ravishankar A, Cheong JG, Batra R, Buyukozkan M, Chetnik K, Easthausen I, Schenck EJ, Racanelli AC, Outtz Reed H, Laurence J, Josefowicz SZ, Lief L, Choi ME, Schmidt F, Borczuk AC, Choi AMK, Krumsiek J, Rafii S. Angiopoietin 2 Is Associated with Vascular Necroptosis Induction in Coronavirus Disease 2019 Acute Respiratory Distress Syndrome. *The American journal of pathology*. 2022; **192**: 1001-15. 10.1016/j.ajpath.2022.04.002.
- 45 Maldonado F, Morales D, Diaz-Papapietro C, Valdes C, Fernandez C, Valls N, Lazo M, Espinoza C, Gonzalez R, Gutierrez R, Jara A, Romero C, Cerda O, Caceres M. Relationship Between Endothelial and Angiogenesis Biomarkers Envisage Mortality in a Prospective Cohort of COVID-19 Patients Requiring Respiratory Support. *Front Med (Lausanne)*. 2022; **9**: 826218. 10.3389/fmed.2022.826218.
- 46 Schmaier AA, Pajares Hurtado GM, Manickas-Hill ZJ, Sack KD, Chen SM, Bhambhani V, Quadir J, Nath AK, Collier AY, Ngo D, Barouch DH, Shapiro NI, Gerszten RE, Yu XG, Collection MC-, Processing T, Peters KG, Flaumenhaft R, Parikh SM. Tie2 activation protects against prothrombotic endothelial dysfunction in COVID-19. *JCI Insight*. 2021; **6**. 10.1172/jci.insight.151527.
- 47 Michalick L, Weidenfeld S, Grimmer B, Fatykhova D, Solymosi PD, Behrens F, Dohmen M, Brack MC, Schulz S, Thomasch E, Simmons S, Muller-Redetzky H, Suttrop N, Kurth F, Neudecker J, Toennies M, Bauer TT, Eggeling S, Corman VM, Hocke AC, Witzenrath M, Hippenstiel S, Kuebler WM. Plasma mediators in patients with severe COVID-19 cause lung endothelial barrier failure. *The European respiratory journal : official journal of the European Society for Clinical Respiratory Physiology*. 2021; **57**. 10.1183/13993003.02384-2020.
- 48 Stahl K, Gronski PA, Kiyani Y, Seeliger B, Bertram A, Pape T, Welte T, Hoepfer MM, Haller H, David S. Injury to the Endothelial Glycocalyx in Critically Ill Patients with COVID-19. *American journal of respiratory and critical care medicine*. 2020; **202**: 1178-81. 10.1164/rccm.202007-2676LE.
- 49 Kox M, Waalders NJB, Kooistra EJ, Gerretsen J, Pickkers P. Cytokine Levels in Critically Ill Patients With COVID-19 and Other Conditions. *JAMA : the journal of the American Medical Association*. 2020; **324**: 1565-7. 10.1001/jama.2020.17052.

50 Leisman DE, Ronner L, Pinotti R, Taylor MD, Sinha P, Calfee CS, Hirayama AV, Mastroiani F, Turtle CJ, Harhay MO, Legrand M, Deutschman CS. Cytokine elevation in severe and critical COVID-19: a rapid systematic review, meta-analysis, and comparison with other inflammatory syndromes. *Lancet Respir Med*. 2020; **8**: 1233-44. 10.1016/S2213-2600(20)30404-5.

Curriculum Vitae

Lushun Yuan was born in Shanghai, China in 1992. In September 2011, he began his study of clinical medicine at Wuhan University, China. Following this, he interned for six months as a trainee in CHU Brabois, Service d'Urologie, Université de Lorraine, Nancy, France, starting from September 2015. In the summer of 2016, he obtained his Bachelor degree of Clinical medicine. In the same year, he started the master study of Clinical medicine (Surgery) and research in the department of Urology, Zhongnan Hospital of Wuhan University, China. There he worked as an intern in the department of Urology and did the research on urological malignancies. In June 2018, he graduated from Wuhan University in China with a Master of Clinical Medicine (Surgery). Meanwhile, he received funding from the China Scholarship Council for his PhD studies at Leiden University Medical Center in the Netherlands. From October 2018, he worked as a PhD candidate in the Department of Internal medicine, Division of Nephrology at Leiden University Medical Center. Under the supervision of Prof. T.J. Rabelink and Dr. B.M. van den Berg, he started the work of thromboinflammation in high-risk human populations. The results of his research were published in peer-reviewed international scientific journals and are presented in this thesis. After receiving his PhD, he will begin his residency training at Shanghai General Hospital in China.

List of publications

1. **Lushun Yuan**, Shuzhen Cheng, Wendy M P J Sol, Anouk I M van der Velden, Hans Vink, Ton J Rabelink, Bernard M van den Berg. Heparan sulfate mimetic fucoidan restores the endothelial glycocalyx and protects against dysfunction induced by serum of COVID-19 patients in the intensive care unit. *ERJ Open Res.* 2022 May 3;8(2):00652-2021.
2. **Lushun Yuan**, Ruifang Li-Gao, Aswin Verhoeven, Huub J. van Eyk, Maurice B. Bizino, Patrick C.N. Rensen, Ingrid M. Jazet, Hildo J. Lamb, Ton. J Rabelink, Martin Giera, Bernard M. van den Berg. Altered HDL composition is associated with risk for complications in type 2 diabetes mellitus in South Asian descendants: a cross-sectional, case-control study on lipoprotein subclass profiling. *Diabetes Obes Metab.* 2023 Aug;25(8):2374-2387.
3. **Lushun Yuan**, Jihee Han, Anouk I.M. van der Velden, Hans Vink, Renée de Mutsert, Frits R. Rosendaal, Astrid van Hylckama Vlieg, Ruifang Li-Gao, T.J Rabelink, Bernard M. van den Berg. Sex-specific association between microvascular health and coagulation parameters: the Netherlands Epidemiology of Obesity (NEO) Study. *J Thromb Haemost.* 2023 Jun 8;S1538-7836(23)00442-7.
4. **Lushun Yuan**, Niek Blomberg, Aswin Verhoeven, Huub J. van Eyk, Maurice B. Bizino, Patrick C.N. Rensen, Ingrid M. Jazet, Hildo J. Lamb, Ton. J Rabelink, Martin Giera, Bernard M. van den Berg. Diacylglycerol abnormalities in diabetic nephropathy in Dutch South Asians and Dutch white Caucasians with type 2 diabetes mellitus: lipidomic phenotyping of plasma in a cross-sectional study. (under review)
5. **Lushun Yuan**, Aswin Verhoeven, Shuzhen Cheng, Wendy M P J Sol, Ton. J Rabelink, Martin Giera, Bernard M. van den Berg. High-density lipoprotein composition related to endothelial dysfunction is associated with disease outcome in COVID-19 patients. *Metabolites* (in preparation)

6. Shuzhen Cheng, Di Wu, **Lushun Yuan**, Hanxiong Liu, Hesham R Ei-Seedi, Ming Du. *Crassostrea gigas*-Based Bioactive Peptide Protected Thrombin-Treated Endothelial Cells against Thrombosis and Cell Barrier Dysfunction. *J Agric Food Chem.* 2022 Aug 10;70(31):9664-9673.
7. Gangqi Wang, Bram Heijs, Sarantos Kostidis, Rosalie G J Rietjens, Marije Koning, **Lushun Yuan**, Gesa L Tiemeier, Ahmed Mahfouz, Sébastien J Dumas, Martin Giera, Jesper Kers, Susana M Chuva de Sousa Lopes, Cathelijne W van den Berg, Bernard M van den Berg, Ton J Rabelink. Spatial dynamic metabolomics identifies metabolic cell fate trajectories in human kidney differentiation. *Cell Stem Cell.* 2022 Nov 3;29(11):1580-1593.e7.

Acknowledgement

I would like to thank everyone who played a role in making this thesis possible, including my supportive colleagues and collaborators. Your help throughout my entire Ph.D period has been invaluable, and I am grateful for all of your contributions.

I want to start by thanking my promoter, Prof. Dr. T.J. Rabelink, for giving me the opportunity to pursue my Ph.D here in 2018. It is an absolute privilege and joy to work under your guidance and supervision, and I will treasure the lessons you taught me on balancing life and work and being a good doctor and scientist for years to come.

A big thanks also goes out to my co-supervisor Dr. B.M. van den Berg for providing daily instructions and training me to become a better researcher through our many enlightening discussions.

To the members of the glyocalyx group: Gangqi, Wendy, Rosalie, Cristina, and Anouk, thank you for your encouragement, support, and friendship throughout our time together. I feel incredibly lucky to have worked with such a helpful and friendly team.

A special mention goes to Shuzhen, a visiting Ph.D student and dear friend, for being an incredible help in both my work and personal life. I especially appreciate the time he took to cook me night-meals during those late nights working in the lab.

I would also like to give a shoutout to Jacques Duijs, the loveliest guy I've had the pleasure of meeting in the Netherlands. Coffee breaks with you are always the highlight of my day, and I hope we remain friends forever.

I am also thankful for my colleagues from the Eindhoven Laboratory: Kelley, Araci, and Mieke, for their assistance and useful life advice.

My appreciation goes to colleagues from CPM: Martin, Aswin, and Niek, for collaborating with me on various projects and providing valuable data and techniques.

Thank you to colleagues from Epidemiology: Renée, Astrid, Ruifang, and Jihee, for helping me with the NEO study. I am particularly indebted to Ruifang who gave me kind encouragement and useful instruction in my other projects.

To my K5 roommates: Dianne, Franca, Gangqi, Gesa, Hayat, Jurriën, Loïs, Lotte, Marlon, Novella, Qiao, Rosalie, Rudmer, Sophie, Suzanne, Taya, and Wouter, thank you for making our time together so enjoyable!

Finally, I want to express my gratitude to my family members, especially my parents, for their unwavering support. To my lovely wife Zhou, thank you for being there for me every step of the way, you are my biggest motivator in becoming a better person. Now, with the arrival of our baby, I have even more reasons to strive for greatness.